

This electronic thesis or dissertation has been downloaded from the King's Research Portal at <https://kclpure.kcl.ac.uk/portal/>



Quiescence and cell fate regulation are essential for preserving adult stem cell number and function

Jones, Kieran Michael

Awarding institution:
King's College London

The copyright of this thesis rests with the author and no quotation from it or information derived from it may be published without proper acknowledgement.

END USER LICENCE AGREEMENT



Unless another licence is stated on the immediately following page this work is licensed

under a Creative Commons Attribution-NonCommercial-NoDerivatives 4.0 International

licence. <https://creativecommons.org/licenses/by-nc-nd/4.0/>

You are free to copy, distribute and transmit the work

Under the following conditions:

- Attribution: You must attribute the work in the manner specified by the author (but not in any way that suggests that they endorse you or your use of the work).
- Non Commercial: You may not use this work for commercial purposes.
- No Derivative Works - You may not alter, transform, or build upon this work.

Any of these conditions can be waived if you receive permission from the author. Your fair dealings and other rights are in no way affected by the above.

Take down policy

If you believe that this document breaches copyright please contact librarypure@kcl.ac.uk providing details, and we will remove access to the work immediately and investigate your claim.

**Quiescence and cell fate regulation are essential for
preserving adult stem cell number and function**

A thesis submitted for the degree of Doctor of Philosophy at King's College
London

2013

Kieran Michael Jones

King's College London

The Dental Institute

Department of Craniofacial Development and Stem Cell Biology

Contents

Quiescence and cell fate regulation are essential for preserving adult stem cell number and function	1
Contents	2
List of Figures	8
Abbreviations	12
Acknowledgements.....	15
Abstract	16
Chapter 1.....	17
Introduction.....	17
1.1. Stem cell function in embryonic development and adult tissue	18
1.2. Formation of vertebrate limb skeletal muscle.....	20
1.3. Satellite cells	21
1.3.1. Formation of a satellite cell pool.....	22
1.3.2. Satellite cells are stem cells in adult skeletal muscle.....	22
1.3.3. The satellite cell response to myotrauma	23
1.3.4. Heterogeneity of the satellite cell pool.....	32
1.4. The satellite cell niche	34
1.5. Ageing in skeletal muscle	38
1.5.1. Age-associated intrinsic changes in satellite cells	39
1.5.2. Age-associated changes in the satellite cell niche	41
1.6. Neurogenesis	44
1.6.1. Embryonic neurogenesis.....	45
1.7. Adult neurogenesis and adult neural stem cell properties.....	45
1.8. Subventricular zone - olfactory bulb neurogenesis	46
1.8.1. The neurogenic lineage in the adult subventricular zone.....	48
1.9. Adult hippocampal neurogenesis.....	51
1.9.1. The neurogenic lineage in the adult subgranular zone	53
1.10. Adult neural stem cell niches	55
1.10.1. Notch signalling in the neurogenic niches	56
1.11. Survival of neural stem cell progeny in the hippocampus	59

Contents

1.12. Survival of neural stem cell progeny in the SVZ-OB system	60
1.13. Heterogeneity of neural stem cells	61
1.13.1. Heterogeneity of SVZ NSCs	61
1.13.2. Heterogeneity of SGZ NSCs	64
1.14. Epigenetic control of adult neurogenesis	66
1.14.1. Chromatin structure and remodelling proteins	66
1.14.2. CHD proteins	72
1.14.3 CHD7	72
1.15. Aims and objectives	76
Chapter 2.....	77
Methods.....	77
2.1. Solutions and reagents.....	78
2.1.1. General reagents	78
2.1.2. Immunohistochemistry reagents	79
2.1.3. Plasmid linearisation and mRNA probe synthesis reagents	80
2.1.4. Section <i>in situ</i> hybridisation reagents.....	82
2.1.5. Wholemout <i>in situ</i> hybridisation reagents.....	85
2.1.6. Satellite cell isolation and culture reagents	86
2.1.7. Neural stem cell culture reagents.....	88
2.2. Animals	89
2.3. Methods for Chapter 3 and Chapter 4	90
2.3.1. Satellite cell <i>in vivo</i> cell division analysis.....	90
2.3.2. <i>In vivo</i> FGFR inhibition.....	90
2.3.3. Purified myofibre extract	91
2.3.4. Single muscle fibre isolation.....	92
2.3.5. Tibialis anterior muscle preparation	92
2.3.6. Myoblast isolation	92
2.3.7. Myogenic cell preparation	93
2.3.8. <i>In vitro</i> activation of Cre recombinase	94
2.3.9. <i>In vivo</i> activation of Cre recombinase.....	94
2.3.10. Fluorescence-activated cell sorting	94
2.3.11. SC and skeletal muscle histology and immunofluorescence	95
2.3.12. Analysis of satellite cells and their progeny	95
2.3.13. Whole-mount <i>in situ</i> hybridisation	96

Contents

2.3.14 Plasmid digestion and DNA extraction	97
2.3.15. Probe synthesis	97
2.3.16. RNA isolation and RT-qPCR.....	98
2.3.17. Antibodies and reagents	99
2.3.18. Genotyping	100
2.3.19. Statistics and data.....	102
2.4. Methods for Chapter 5 and Chapter 6	102
2.4.1. Isolation, growth, and differentiation of NSCs.....	102
2.4.2. Forebrain processing	103
2.4.3. Neural stem cell histology and immunofluorescence.....	103
2.4.4. Frozen section histology and immunofuorescence.....	104
2.4.5. Section <i>in situ</i> hybridisation.....	104
2.4.6. Probe synthesis from PCR reaction	106
2.4.7. RNA isolation and RT-qPCR.....	107
2.4.8. <i>In vivo</i> activation of Cre recombinase.....	108
2.4.9. NSC <i>in vivo</i> cell division analysis	108
2.4.10. Analysis of NSCs and their progeny.....	109
2.4.11. Antibodies and reagents	110
2.4.12. Genotyping	110
2.4.14. Image processing.....	112
2.4.15. Statistics and data.....	112
Chapter 3.....	113
Results Part I.....	113
3.1. Skeletal muscle and ageing.....	114
3.1.1. Satellite cells display a decline in number and function in aged skeletal muscle	116
3.1.2. Aged satellite cells cycle more frequently during homeostasis	120
3.2. Formation of a purified myofibre extract to determine age-associated changes in the satellite cell myofibre niche.....	122
3.3. Aged purified myofibre extract induces quiescent satellite cells to cycle	124
3.3.1. FGF2 is sufficient to drive satellite cells to cycle	127
3.3.2. FGF2 is upregulated in aged skeletal muscle fibres	129
3.3.3. Induction of aged niche-derived FGF2 disrupts satellite cell quiescence..	135
3.4. Discussion.....	139

Contents

Chapter 4.....	145
Results Part II.....	145
4.1. Sprouty proteins modulate FGF signalling.....	146
4.1.1. Loss of <i>Spry1</i> further enhances loss of satellite cell quiescence in response to the aged niche <i>in vitro</i>	147
4.1.2. <i>Spry1</i> inhibits FGF2-FGFR signalling.....	152
4.1.3. <i>Spry1</i> overexpression inhibits the mitogenic effect of the aged niche.....	154
4.2. Short-term loss of <i>Spry1 in vivo</i> causes increased satellite cell cycling and increased Pax7 cell number.....	157
4.3. Long-term loss of <i>Spry1 in vivo</i> leads to loss of stem cell number and impaired satellite cell function.....	159
4.4. Inhibition of FGF signalling in the aged satellite cell niche rescues stem cell number and function.....	163
4.5. The adult niche is inhibitory to satellite cell activation.....	166
4.6. Discussion.....	168
Chapter 5.....	173
Results Part III.....	173
5.1. Chromatin remodelling in adult neurogenesis.....	174
5.2. <i>Chd7</i> heterozygous mice display reduced olfactory bulb length and reduced number of tyrosine hydroxylase ⁺ interneurons.....	180
5.3. CHD7 is expressed in the dorso-lateral aspect of the subventricular zone and in the rostral migratory stream.....	188
5.3.1. CHD7 is expressed at high levels in transit-amplifying cells in the subventricular zone.....	191
5.4. Reduction in <i>Chd7</i> expression results in a decrease in immature neuron production in the subventricular zone.....	195
5.4.1. Loss of <i>Chd7</i> in NSCs blocks their differentiation.....	198
5.5. Restoration of <i>Chd7</i> function partially rescues the expression of tyrosine hydroxylase in the olfactory bulb.....	203
5.6. Discussion.....	206
5.6.1. The reduction in olfactory bulb size and number of tyrosine hydroxylase ⁺ interneurons may be progressive with age.....	208
5.6.2. A reduction in <i>Chd7</i> expression may result in a loss of cells of the tyrosine hydroxylase lineage, or a loss of tyrosine hydroxylase production.....	209
5.6.3. CHD7 regulates subventricular zone - olfactory bulb neurogenesis.....	212
5.6.4. Loss of <i>Chd7</i> results in a large reduction in olfactory bulb neurogenesis.....	213

Contents

5.6.5. CHD7 in adult subventricular zone neurogenesis.....	213
Chapter 6.....	215
Results Part IV.....	215
6.1. Quiescence of a somatic stem cell population is essential for maintenance of the stem cell pool	216
6.1.1. Maintenance of neural stem cell quiescence.....	216
6.1.2. Neural stem cell proliferation and ageing	217
6.1.3. Regulation of neural stem cell fate decisions	217
6.2. CHD7 is expressed in transit amplifying cells in the subgranular zone	220
6.3. The GLAST::CreERT2;Chd7 ^{fl/fl} mouse line allows for efficient deletion of <i>Chd7</i> in the dentate gyrus	226
6.4. Loss of <i>Chd7</i> in neural stem cells causes a reduction in neurogenesis	231
6.5. Loss of <i>Chd7</i> leads to a transient increase in neurogenesis	234
6.6. Loss of <i>Chd7</i> impairs mature neuron formation	237
6.7. CHD7 regulates neural stem cell quiescence	240
6.8. Loss of <i>Chd7</i> results in an increase in the number of neural stem cells.....	244
6.9. Loss of neural stem cell quiescence may be due to loss of Notch signalling...	249
6.10. A decrease in <i>Chd7</i> expression may be linked to intellectual disability in CHARGE syndrome	251
6.11. Discussion.....	254
6.11.1. Chd7 may regulate neural stem cell quiescence cell autonomously or non-cell autonomously.....	256
6.11.2. Decreased Notch signalling only accounts for some of the phenotypes seen after the loss of Chd7	257
6.11.3. Chd7 may have separate roles in the self-renewal, maintenance of quiescence, and differentiation of neural stem cells	257
6.11.4. <i>In vivo</i> clonal analysis of adult neural stem cells	260
6.11.5. Neural stem cell quiescence and maintenance of the stem cell pool	260
6.11.6. CHD7 and the regulation of apoptosis.....	261
6.11.7. CHD7 may regulate adult hippocampal and olfactory bulb neurogenesis in a similar fashion.....	262
6.11.8. CHD7 and human disease	262
6.11.9. CHD7 regulates adult hippocampal neurogenesis via SoxC transcription factors.....	263
6.12. CHD7 regulates different aspects of adult neurogenesis.....	264
Chapter 7.....	266

Contents

Discussion	266
7.1. Discussion.....	267
7.1.1. Quiescence is a property of many somatic stem cells essential for stem cell function and maintenance of the stem cell pool	267
7.1.2. Maintenance of the stem cell pool is essential for tissue function.....	269
7.1.3. Upregulation of FGF2 in the aged satellite cell niche may be due to accumulated myofibre damage	271
7.1.4. Ageing in the hippocampus is associated with altered neural stem cell function and cognitive decline.....	271
7.1.5. Ageing in the hippocampus is associated with changes in the chromatin landscape	272
7.1.6. CHD7 and the regulation of bHLH factors in neurogenesis and myogenesis	274
7.1.7. CHD proteins in adult neurogenesis.....	274
7.1.8. CHD7 may play a role in autism spectrum disorder and neurodegenerative disorders.....	275
7.1.9. Intrinsic and extrinsic changes affect somatic cell function.....	276
7.2. Future work	277
7.2.1. In vivo clonal lineage analysis.....	277
7.2.2. The long-term effect of a loss of <i>Chd7</i> on the neural stem cell pool	278
7.2.3. The role of CHD7 on neural stem cell quiescence	278
7.2.4. Chromatin immunoprecipitation of CHD7 in cultured neural stem cells	279
Bibliography.....	280

Enclosed in back cover:

Chakkalakal, J. V., Jones, K. M., Basson, M. A. & Brack, A. S. The aged niche disrupts muscle stem cell quiescence. *Nature* **490**, 355-360, doi:10.1038/nature11438 (2012).

List of Figures

Figure 1 - Schematic illustration of the myogenic lineage of satellite cells.....	21
Figure 2 - Schematic of FGF-ERK signalling.....	32
Figure 3 - Schematic illustration of the satellite cell niche.....	37
Figure 4 - Schematic illustration of impaired muscle regeneration in old age.	39
Figure 5 - Schematic illustration of adult subventricular zone neurogenesis.....	47
Figure 6 - Schematic illustration of the multipotency of adult neural stem cells in the subventricular zone.....	49
Figure 7 - Schematic illustration of the adult subventricular zone cell lineage	50
Figure 8 - Schematic illustration of adult subgranular zone neurogenesis.....	52
Figure 9 - Schematic illustration of the adult subgranular zone lineage.....	54
Figure 10 - Schematic illustration of Notch signalling in neural stem cells.....	59
Figure 11 - Schematic illustration of the regional specification of SVZ cells	63
Figure 12 - Schematic illustration of radial and horizontal neural stem cells in the subgranular zone.....	65
Figure 13 - Schematic illustration of the action of chromatin remodelling complexes. .	71
Figure 14 - Overview of the protein structure of CHD7.....	75
Table 1 - Mouse lines used.....	90
Table 2 - Details of PCR primers	101
Table 3 - RT-qPCR primer sequences	108
Table 4 - Details of PCR primers 2	111
Figure 15 - The number of satellite cells declines in aged skeletal muscle and their function is impaired.....	119
Figure 16 - Aged satellite cells cycle more frequently during homeostasis.....	121
Figure 17 - Purified myofibre extract represents soluble fractions from skeletal muscle fibres.....	123
Figure 18 - The aged niche induces the loss of satellite cell quiescence.....	126

List of Figures

Figure 19 - FGF2 acts as a potent mitogen to induce satellite cells to cycle in a dose-dependent manner.....	128
Figure 20 - Expression of Fgf2 from the muscle fibre increases in aged skeletal muscle	132
Figure 21 - Muscle fibre-derived FGF2 increases with age	134
Figure 22 - FGF2 is an aged niche-derived factor that induces satellite cells to cycle	138
Figure 23 - The systemic environment and the niche have opposing influences on satellite cells in adult and aged skeletal muscle	144
Figure 24 - Reduction in <i>Spry1</i> increases reserve cell cycling in response to the aged niche.....	149
Figure 25 - Loss of <i>Spry1</i> specifically from satellite cells in vivo causes increased sensitivity to the aged niche and impaired function.	151
Figure 26 - <i>Spry1</i> inhibits FGF2-FGFR signalling.....	153
Figure 27 - Overexpression of <i>Spry1</i> inhibits the mitogenic effect of the aged niche.	155
Figure 28 - <i>Spry1</i> overexpression in vivo inhibits the mitogenic effect of the aged niche	156
Figure 29 - Short-term increase in FGF signalling increases satellite cell cycling.....	158
Figure 30 - Chronic exposure to FGF signalling leads to depletion of the satellite cell pool and impaired satellite cell function.....	162
Figure 31 - Inhibition of FGF signalling rescues stem cell number and function	165
Figure 32 - The adult niche is inhibitory to satellite cell activation.	167
Figure 33 - Schematic illustration of the changes in satellite cells with ageing under homeostatic conditions	170
Figure 34 - Modulation of FGF signalling affects satellite cell outcome	172
Figure 35 - Reduced expression of <i>Chd7</i> leads to a decrease in tyrosine hydroxylase+ interneurons due to decreased olfactory epithelial stem cell proliferation.....	178
Figure 36 - A reduction in <i>Chd7</i> expression may cause a decrease in SVZ-OB neurogenesis leading to a loss of interneuron production	180
Figure 37 - Reduction in <i>Chd7</i> expression causes a decrease in olfactory bulb length	184

List of Figures

Figure 38 - Reduction in <i>Chd7</i> expression specifically affects tyrosine hydroxylase+ olfactory bulb interneurons.....	186
Figure 39 - Reduction in <i>Chd7</i> expression results in a decrease in TH-lineage cells.	187
Figure 40 - CHD7 is expressed in the subventricular zone, rostral migratory stream, and olfactory bulb	190
Figure 41 - CHD7 is expressed by proliferating cells and type C cells.....	193
Figure 42 - Schematic of CHD7 expression in the SVZ.....	194
Figure 43 - Reduction in <i>Chd7</i> expression affects SVZ neurogenesis.....	197
Figure 44 - Efficient recombination in the GLAST::CreERT2 mouse line.....	200
Figure 45 - Loss of <i>Chd7</i> in neural stem cells affects subventricular zone neurogenesis	202
Figure 46 - Restoration of <i>Chd7</i> function in neural stem cells partly rescues tyrosine hydroxylase production in the olfactory bulb	205
Figure 47 - Reduction in <i>Chd7</i> expression affects subventricular zone neurogenesis	207
Figure 48 - Regulation of <i>Er81</i> expression by CHD7.....	211
Figure 49 - Schematic diagram of the fate decisions of adult neural stem cells.....	220
Figure 50 - CHD7 is expressed in the subgranular zone of the dentate gyrus.....	222
Figure 51 - CHD7 is expressed by a subset of type 2a cells	224
Figure 52 - Schematic of CHD7 expression in the dentate gyrus	225
Figure 53 - Efficient recombination in the dentate gyrus of GLAST::CreERT2 mice. a,	229
Figure 54 - The GLAST::CreERT2; <i>Chd7</i> ^{f/f} mouse line allows for efficient deletion of <i>Chd7</i>	231
Figure 55 - <i>Chd7</i> regulates adult hippocampal neurogenesis	234
Figure 56 - Loss of <i>Chd7</i> results in a transient increase in neurogenesis.....	237
Figure 57 - CHD7 is essential for neurogenesis in vitro.....	240
Figure 58 - Loss of <i>Chd7</i> initially results in increased subgranular zone proliferation	242
Figure 59 - CHD7 regulates neural stem cell quiescence.....	243

List of Figures

Figure 60 - Loss of <i>Chd7</i> results in an increase in the number of neural stem cells ..	247
Figure 61 - The disposable stem cell hypothesis may account for an increase in the number of neural stem cells in <i>Chd7</i> mutants over time.....	248
Figure 62 - Loss of <i>Chd7</i> leads to a decrease in Notch signalling	250
Figure 63 - Reduction in <i>Chd7</i> expression affects hippocampal neurogenesis.....	253
Figure 64 - Schematic diagram of the role of CHD7 in adult hippocampal neurogenesis	256
Figure 65 - The role of CHD7 in adult hippocampal neurogenesis	258

Abbreviations

aCasp	Cleaved caspase 3
Ang1	Angiopoietin 1
AraC	Arabinoside
bHLH	Basic helix-loop-helix
BL	Basal lamina
BLBP	Brain lipid binding protein
Bmi1	B lymphoma Mo-MLV insertion region 1 homolog
BMP	Bone morphogenic protein
bp	Base pairs
BrdU	5-bromo-2'-deoxyuridine
BRG1	BRM/SWI2-Related Gene
BSA	Bovine serum albumin
BV	Blood vessel
CalB	Calbindin
CalR	Calretinin
CNS	Central nervous system
CTX	Cardiotoxin
CSF	Cerebrospinal fluid
ddH ₂ O	Double distilled water
DEPC	Diethyl pyrocarbonate
DG	Dentate gyrus
DII	Delta-like ligand
DMD	Duchenne muscular dystrophy
DMSO	Dimethyl sulphoxide
dpi	Days post injury
DTA	Diphtheria toxin A
DTR	Diphtheria toxin receptor
E	Embryonic day
ECM	Extracellular matrix
EDL	Extensor digitorum longus
EGF	Epidermal growth factor
EGFR	EGF receptor
ES cells	Embryonic stem cells
EtOH	Ethanol
FBS	Foetal bovine serum
FCS	Foetal calf serum
FACS	Fluorescence-activated cell sorting
FGF	Fibroblast growth factor
FGFR	FGF receptor
g	Relative centrifugal force
GFAP	Glial fibrillary acidic protein

Abbreviations

GL	Granular layer
GLAST	Glutamate aspartate transporter
gt	Gene trap
H	Histone
HGF	Hepatocyte growth factor
HGPS	Hutchinson-Gilford Progeria Syndrome
Hip	Hippocampus
His	High-stringency wash
HS	Horse serum
HSC	Haematopoietic stem cell
HSPG	Heparan sulfate proteoglycan
IGF	Insulin-like growth factor
I.P.	Intraperitoneal
Jag	Jagged
LRC	Label-retaining cells
MABT	Maleic acid buffer with Tween-20
MAPK	Mitogen-activated protein kinase
me3	Tri-methylated
ML	Molecular layer
MyoG	Myogenin
N.A.	Not attained
NCAM	Neural cell adhesion molecule
ND	Not detected
NGF	Nerve growth factor
NICD	Notch intracellular domain
N.S.	Not significant
NTMT	Sodium chloride-Tris-Magnesium-Tween-20 buffer
OB	Olfactory bulb
P	Postnatal day
PBAF	Polybromo-associated BRG1-associated factor
PBS	Phosphate buffered saline
PBSTw	PBS with Tween-20
PBSTx	PBS with Triton X
PcG	Polycomb group
PCP	Planar cell polarity
PCR	Polymerase chain reaction
PDGF	Platelet-derived growth factor-BB
PFA	Paraformaldehyde
PI	Propidium iodide
PME	Purified myofibre extract
PRC	Polycomb repressive complex
RG	Radial glia
RMS	Rostral migratory stream
ROS	Reactive oxygen species
RSC	Reserve cell

Abbreviations

RT-qPCR	Real-time reverse-transcription PCR
RTK	Receptor tyrosine kinase
S.E.M.	Standard error of means
SC	Satellite cell
SGZ	Subgranular zone
shRNA	Short hairpin RNA
siRNA	Short interfering RNA
Spry	Sprouty
SSC	Standard saline citrate
STAT	Signal transducer and activator of transcription
SVZ	Subventricular zone
TA	Tibialis anterior
TAE	Tris base, acetic acid, EDTA
TE	Tris-EDTA
TGF	Transforming growth factor
TH	Tyrosine hydroxylase
TNF	Tumour necrosis factor
TxG	Trithorax group
ub	Ubiquitin
VEGF	Vascular endothelial growth factor
w/v	Weight/volume
WT	Wild type

Acknowledgements

I would like to thank Dr. M. Albert Basson for all of his support and guidance throughout my time at King's College London, and for being a great source of inspiration which has shaped me as a scientist. I would like to thank Dr. Andrew Brack for all of the excellent training and support in Boston and for providing an incredible scientific environment. In particular, I would like to thank Dr. Joe Chakalakal who was great to work with. I am grateful to all of the lab mates that I've had the pleasure of working with in the Brack lab and HSCI, and in the Basson lab and CFD, especially Dr. Tian Yu, who has taught me so much over the years. I would also like to thank my fellow write-up person, Lara, who has been a great friend and colleague, and Leena, who has been brilliant throughout the years in CFD and even more so outside of CFD. Finally, I would like to thank all of my friends and family for their support.

Abstract

Somatic stem cell populations display a remarkable capacity to self-renew and generate specialised cell types throughout the life of the organism. In my thesis I examined extrinsic and intrinsic factors that regulate stem cell quiescence, a reversible state of growth arrest crucial to the preservation of somatic stem cell number and function in many systems. Skeletal muscle-specific stem cells, known as satellite cells (SCs) are responsible for skeletal muscle regeneration. The ability of skeletal muscle to regenerate declines with age. I identify fibroblast growth factor 2 (FGF2) as a potent mitogenic factor that is up-regulated in the aged muscle fibre and causes a loss of SC quiescence and depletion of the stem cell pool. Deletion of a negative regulator of FGF signalling, *Sprouty1* (*Spry1*), in SCs increases stem cell loss, whereas over-expression of *Spry1* partly prevents depletion. These experiments show that an age-associated change in the SC niche is partly responsible for stem cell depletion during ageing.

In the adult forebrain, new neurons produced from neural stem cells (NSCs) in the hippocampus play an important role in learning and memory formation. I show that deletion of the chromatin remodelling enzyme chromodomain helicase DNA-binding protein 7 (CHD7) in NSCs results in a severe reduction in neurogenesis. I identify CHD7 as an essential regulator of NSC quiescence and self-renewal. Collectively, my results suggest that the regulation of the intrinsic chromatin landscape and the extrinsic niche environment are essential for somatic stem cell function, and may contribute to ageing when disrupted.

Chapter 1

Introduction

1.1. Stem cell function in embryonic development and adult tissue

Stem cells are characterised by two essential properties:

1. The ability to generate daughter cells capable of differentiation into multiple cell types, known as multipotency, and
2. The ability to undergo numerous rounds of cell division whilst maintaining an undifferentiated pool, known as self-renewal.

During embryonic development, embryonic stem (ES) cells from the inner cell mass of blastocysts can proliferate extensively and can differentiate into ectoderm, mesoderm and endoderm [1]. ES cells form all the cell types of adult organisms indirectly through the generation of other stem cell populations. However, many embryonic cells lose their stem cell properties as differentiation ensues and the signals that promote growth decline. By adulthood, stem cells are no longer dispersed throughout the organism but, instead, exist in discrete niches in many tissues. Somatic stem cells retain the ability to self-renew and generate different specialised cell types [1, 2].

Generally, somatic stem cells divide infrequently under homeostatic conditions. Instead, they form lineage-restricted progenitors with a greater proliferative output. Progenitors then form an immature differentiated cell type, often with migratory capabilities, which mature into a new fully functional cell type [2, 3].

Quiescence is a reversible state of growth arrest crucial to the preservation of somatic stem cell number and function in many systems [4-6]. Limiting the proliferative output of somatic stem cells prevents the accumulation of DNA replication errors in stem cells, and also stops the depletion of the stem cell pool through replicative senescence [7]. The niche is a critical factor in the maintenance of somatic stem cell function and provides the proper cues needed for stem cell quiescence under homeostatic conditions [6, 8]. Aberrant changes in the niche can lead to a loss of stem cell quiescence and an alteration in stem cell function [6, 8].

Ageing is a physiological process whereby the composition of many somatic stem cell niches is disrupted and the stem cells display intrinsic changes [9]. An 'adult' stage of life is generally considered to be when stem cells become quiescent but before any large loss in the stem cell pool later in life. In mice, skeletal muscle is generally accepted as being in an adult stage between 3-8 months old [10, 11], and the adult forebrain is considered adult between 2-5 months old [12]. 'Aged' is considered to be a stage where stem cells exhibit an impaired function in the absence of any other diseases. Murine skeletal muscle is considered to be aged at around 24 months old [10, 11], based on a decrease in skeletal muscle function as assessed by contractile properties. The adult murine forebrain is considered aged as early as 12 months old as it exhibits a large decrease in stem cell self-renewal and proliferation which has been associated with cognitive defects [12-16].

Ageing leads to alterations in stem cell number and function, often having a negative impact on tissue homeostasis. In addition, the numbers of stem cells present in various tissues generally decline with age [17-20]. The notable exception to this general rule is the haematopoietic system, which exhibits an increase in the number of haematopoietic stem cells with age [21]. Despite this, aged haematopoietic stem cells display a loss in self-renewal potential and skewed fate decisions [21].

Very little is known about age-related changes in mammalian stem cell niches and how this impacts on stem cell number. Furthermore, the mechanisms controlling stem cell quiescence and fate decisions are not completely understood. Current literature indicates that intrinsic changes in somatic cells, such as epigenetic changes [22, 23], and extrinsic influences, such as the stem cell niche [12, 19, 24], clearly play an important role in the regulation of stem cell number and function.

This thesis examines fundamental properties of somatic stem cells in two well-characterised types of stem cells: skeletal muscle stem cells and neural stem cells. Specifically, influences on stem cell quiescence and differentiation will be

explored in the context of homeostasis and also in a state of physiological disease, such as ageing.

1.2. Formation of vertebrate limb skeletal muscle

Muscle is composed of elongated, multinucleated myofibres that are capable of contracting. Skeletal muscle is transversely striated and principally attached to bone to allow for skeletal movement. Skeletal muscle contraction is achieved through the interaction between myofibrillar proteins, which temporarily bind to each other and release, generating force [25].

In vertebrates, skeletal muscle forms from paraxial mesoderm, which segments and form pairs of transitory structures on either side of the neural tube called somites [26]. Somites differentiate into dermatome, myotome and sclerotome. Cells in the dermatome form the skin of the back, the sclerotome forms the vertebrae and rib cartilage, and cells in the myotome become specified as skeletal muscle progenitors. Cells migrating from the myotome begin to express myogenic determination genes, such as *MyoD* and *Myf5*, once they reach the limb [27]. These muscle progenitor cells undergo extensive proliferation in the limb and fuse to form the first multinucleated muscle fibres around embryonic day (E) 11-14 in mouse [28]. Throughout the first weeks of postnatal life in mice, skeletal muscle undergoes great muscle growth, with little addition of myonuclei to myofibres from postnatal day (P) 14, although the extensor digitorum longus (EDL) muscle of the hind limb continues to increase in weight up to 17 weeks of age [29].

1.3. Satellite cells

Somatic stem cells are present in adult skeletal muscle. These cells are referred to as satellite cells (SCs) by virtue of their distinct location on the surface of the myofibre, underneath the basal lamina. SCs are capable of producing proliferative myoblasts which can differentiate into myotubes. SCs are also able to maintain their own population through self-renewal, hence they fit the definition of stem cells (**Figure 1**).

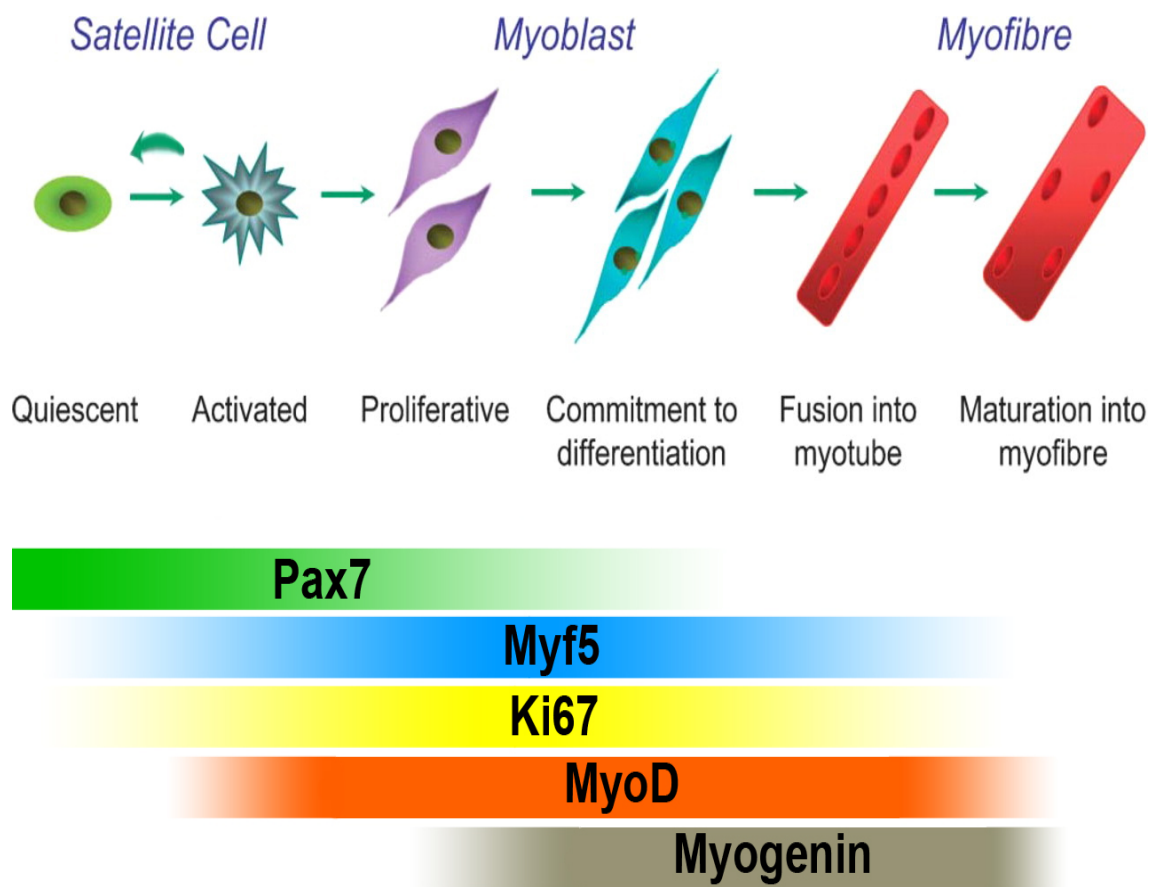


Figure 1 - Schematic illustration of the myogenic lineage of satellite cells. Under homeostatic conditions SCs are completely quiescent. However, in response to myotrauma they activate and proliferate to form myoblasts, becoming positive for markers of cell cycle entry such as Ki67 and upregulating MyoD and Myf5. As myoblasts become more committed to differentiation and form myotubes, they upregulate myogenin and mature into new myofibres. A subset of activated SCs are able to self-renew and maintain Pax7 expression. Adapted from [30].

1.3.1. Formation of a satellite cell pool

Most SCs are formed from the somites, with the notable exception of the head muscles, which have a distinct embryonic origin and form from the pre-chordal mesoderm and other cell lineages [31-33]. SCs are widely accepted as forming from a distinct subset of a large population of myogenic progenitors, which retain multipotency and self-renewal capacity throughout adulthood [34].

Tritiated thymidine labelling studies have shown that SCs are mitotically active and contribute to new myonuclei during postnatal growth before P21 [35]. After P21, most SCs become mitotically quiescent and do not contribute to new myonuclei [35-37]. Quiescent SCs express Pax7, which is essential for their proper function in growth of postnatal skeletal muscle and regeneration of adult muscle after myotrauma [34]. Collectively, these data indicate that the majority of developmental and postnatal myogenesis is completed by P21 as SCs enter a quiescent state.

1.3.2. Satellite cells are stem cells in adult skeletal muscle

The stem cell properties of SCs were first hypothesised in the 1960s as it was demonstrated that SCs underwent cell division in regenerating muscle [38, 39]. However, it was not until myofibres were isolated and cultured *ex vivo* that SCs were shown to generate myoblast progeny that could fuse and differentiate into myotubes [40, 41].

More recently, inducible genetic lineage tracing studies, taking advantage of Pax7 as a marker of SCs, have further demonstrated that SCs can generate myoblasts for muscle growth and repair *in vivo*. Using different Pax7^{CreER/+} mouse lines crossed with R26R^{lacZ/+} mice, activation of CreER^{T2} by tamoxifen administration confirmed β -galactosidase activity specifically in SCs. During muscle regeneration, however, β -galactosidase activity was readily detected in *de novo* muscle fibres, indicating differentiation and fusion of SC-derived myoblasts [42, 43]. In addition, after injury, β -galactosidase expression was

detected in a similar number of SCs as was seen prior to injury suggesting that the SC pool is replenished by self-renewal [42].

Transplantation into injured skeletal muscle has reinforced the stem cell nature of SCs. Donor-derived SCs are able to occupy a SC niche on the periphery of the myofibre and remain quiescent and undifferentiated whilst retaining the ability to activate and proliferate in response to myotrauma [44, 45]. Even after serial transplantations, grafted myogenic cells are able to contribute myonuclei and retain proliferative potential [46-52]. In addition, it has been observed that engraftment of a single myofibre, or a single isolated SC, can repopulate the host muscle with new myonuclei and SCs, firmly showing that SCs are a source of myogenic precursors with self-renewal capability [53, 54].

1.3.3. The satellite cell response to myotrauma

Adult skeletal muscle displays the remarkable capability to regenerate after injury, a phenomenon that relies on Pax7⁺ SCs. Indeed, even after severe myofibre necrosis, rat skeletal muscle is able to re-establish full contraction power potential as soon as three weeks after injury [55]. Muscle fibre regeneration involves the activation of SCs to form myoblasts with a concurrent upregulation of the basic helix-loop-helix (bHLH) myogenic determination factor MyoD. MyoD⁺ myoblasts continue to proliferate and amplify their population as they downregulate Pax7. Through fusing with each other and existing multinucleated cells, myoblasts are able to form immature myotubes, identified by myogenin (MyoG) expression. Myotubes continue to mature into new myofibres. A subset of activated SCs are able to retain Pax7 expression, downregulate MyoD expression and return to quiescence through a process of self-renewal, retaining the ability to undergo the same processes of muscle regeneration during subsequent traumas [56] (see **Figure 1**).

1.3.3.1. Pax7+ satellite cells are essential for muscle regeneration

SCs have been widely implicated as the main stem cell responsible for muscle regeneration. However, until recently, the necessity of SCs for regeneration had not been fully demonstrated. Utilisation of CreER driven by a Pax7 promoter has allowed for the genetic ablation of Pax7⁺ SCs in a specific and temporal manner when used in combination with alleles that express diphtheria toxin A (DTA) flanked by a floxed 'stop' signal. Upon tamoxifen-induced cre-mediated recombination of floxed stop sequences, the R26R^{DTA} mouse line constitutively expresses DTA, a potent inhibitor of protein synthesis that kills the cells in which it is produced [57]. Hence, crossing mice where CreER is driven by Pax7 with mice where DTA is flanked by floxed stop signals have allowed groups to analyse the contribution of SCs to homeostatic muscle function and muscle regeneration. Studies employing this technique have shown that skeletal muscle lacking SCs displayed no regenerating myofibres after injury [58-61]. Furthermore, the few cells which escaped Cre-mediated recombination were unable to regenerate the muscle, suggesting there may be a minimum threshold for the number of SCs in skeletal muscle, or per myofibre, required for proper regeneration [58-61]. These data show an absolute requirement for Pax7⁺ SCs in muscle regeneration. Without SCs, skeletal muscle is unable to form new myofibres after injury.

1.3.3.2. Signalling cascades in the satellite cell response to myotrauma

The process of repair and regeneration of adult skeletal muscle shares many similarities with developmental myogenesis. However, unlike in development, SCs are quiescent in adulthood and so they require an orchestrated set of cues to activate and proliferate, followed by signals to their progeny to differentiate into myotubes to form new muscle fibres. Various secreted growth factors have been shown to play an important role in the up and down-regulation of muscle specific genes and the sequence of growth factor release appears to be highly regulated in order to enable efficient muscle repair without activating SCs under homeostatic conditions [62].

Many growth factors play a stimulatory role in myogenic proliferation and differentiation. Hepatocyte growth factor (HGF), for example, is released from regenerating myotubes and activated SCs and can act in an autocrine manner to enhance SC proliferation [63]. Insulin-like growth factor (IGF) has a unique dual role in muscle regeneration, inducing both the proliferation of SCs (which express the IGF receptor) as well as their differentiation throughout the regenerative response [64-67]. Transforming growth factor β (TGF β) is released by platelets and myoblasts and acts to depress SC proliferation and differentiation *in vitro*, possibly to maintain a pool of undifferentiated progenitors in regenerating muscle [68, 69]. The effect of TGF β *in vivo*, however, is more varied, and can induce or inhibit SC proliferation depending on the presence of other growth factors [70, 71].

The immune system plays an essential role in muscle regeneration with inflammation being a key response to muscle damage. Tumour necrosis factor- α (TNF α) is a well-characterised cytokine partly responsible for the activation of the inflammatory response. TNF α is released by activated leukocytes, macrophages, and injured muscle fibres and acts not only as a chemoattractant and activator of other leukocytes, but is also involved in the degeneration and regeneration of damaged muscle fibres [72, 73]. By binding to TNF receptor, TNF α promotes the activation of the transcription factor nuclear factor κ B (NF κ B) in muscle fibres, leading to the catabolism of muscle proteins and induction of reactive oxygen species (ROS) [74, 75]. Additionally, TNF α has been shown to directly activate SCs and enhance expression of MyoD to aid muscle regeneration [73]. Interleukin-6 (IL-6) plays a similar role to TNF α , regulating muscle protein breakdown and activating SCs [73, 76]. Platelet-derived growth factor-BB (PDGF) is released from platelets, macrophages, and injured blood vessels, and can signal to myoblasts to stimulate their proliferation and inhibit their differentiation [68, 77]. By modulating angiogenesis, PDGF can also indirectly regulate skeletal muscle regeneration [68]. These studies show the immune system to be a key regulator of the SC-response to myotrauma.

Wnt proteins belong to a large family of secreted molecules that can signal through distinct canonical and non-canonical pathways. β -catenin, the downstream effector of canonical Wnt signalling, has been shown to be expressed by cultured rat and mouse myoblasts [78, 79] and by the mouse C2 cell line [80] where it interacts with cadherins to regulate the early steps of myoblast differentiation and fusion [78, 80-83]. Recent studies have shown that β -catenin can interact with the myogenic determination factor MyoD and this interaction is essential for muscle differentiation [84]. Furthermore, canonical Wnt signalling has been implicated in the regulation of SC proliferation after myotrauma, with induction of proliferation or quiescence dependent on the Wnt ligands present and the localisation of stabilised β -catenin [79].

Notably, not only secreted factors can modulate regenerative behaviour. Notch signalling involves the binding of a transmembrane ligand to the extracellular domain of a Notch receptor (see **Figure 10**). In mammals there are four Notch receptors (Notch1-4) which can interact with their ligands delta-like 1 (Dll1), dll3 and dll4, and jagged1 (Jag1) and Jag2. Ligand binding to Notch receptor leads to the proteolytic cleavage of the Notch intracellular domain (NICD) by γ -secretase. The NICD can then translocate to the nucleus and activate target gene transcription through interaction with the transcription factor RBPJ (see **Figure 10**). Notch signalling has been shown to aid the homing of SC precursors to a SC position [85] and prevent precocious differentiation of myogenic precursors during development [86, 87]. Notch signalling plays a similar role in adult SCs. SCs express Notch1-3 as well as Dll1 and Jag1 [88, 89]. Activation of Notch1 promotes the activation of postnatal and adult mouse SCs and prevents their differentiation, with mutant mouse models of increased Notch signalling showing compromised muscle regeneration [88, 90]. In agreement with these findings, loss of Notch signalling through loss of Rbpj function leads to the spontaneous differentiation of quiescent SCs and depletion of the stem cell pool [91].

The balance between proliferation and differentiation of myogenic cells is important for efficient muscle regeneration and this balance has been shown to

rely on crosstalk between Notch and Wnt signalling cascades [92]. Brack et al. showed that activation of postnatal myogenic precursors through Notch signalling is antagonised by Wnt3a to promote differentiation [92]. Crosstalk between the two pathways converge on glycogen synthase kinase 3 β , which is maintained in an active state by Notch signalling and inactivated by Wnt signalling [92]. Interestingly, asymmetric distribution of Numb, a negative regulator of Notch signalling, in some SC divisions has been hypothesised to lead to different transcriptional programs and cell fates [88, 93]. This suggests that localisation of Numb and abrogation of Notch signalling may alter the balance between an activated SC self-renewing or differentiating [88, 93].

1.3.3.3. Fibroblast growth factor signalling in muscle regeneration

Fibroblast growth factors (FGFs) are a large family of heparin-binding proteins, consisting of twenty-two members in vertebrates. They have diverse roles in regulating cell proliferation, migration and differentiation. FGF1-10 and FGF15-23 elicit their effect by binding to FGF receptors (FGFRs), and activating their receptor tyrosine kinase activity. So far, four genes encoding FGF receptors have been identified (*Fgfr1 - 4*). FGFRs consist of three domains: an extracellular ligand binding domain; a transmembrane domain; and an intracellular tyrosine kinase domain. FGF binding to FGFRs leads to the formation of a receptor complex composed of two FGF molecules linked by heparin sulphate proteoglycans (HSPG) and bound to the FGFR. Formation of this complex leads to receptor dimerisation and tyrosine phosphorylation on its intracellular domain. Receptor phosphorylation allows for the binding of adaptor proteins on the intracellular domain of the receptor, which become phosphorylated by the receptor heterodimers. Other intracellular signalling molecules bind the receptor and adaptor proteins and are phosphorylated themselves, leading to an intracellular signalling cascade. Activation of FGFRs engages several second messenger pathways, which include Protein Kinase C, Akt, and Ras – MAP Kinase (**Figure 2**).

The strength and type of pathway activated can be modulated by many different factors. These include the expression and levels of ligands and cognate receptors, and modifications of HSPGs which can differentially modulate ligand-receptor specificity [94]. Additionally, interactions of FGFRs with adhesion molecules, such as neural cell adhesion molecule (NCAM) and N-Cadherin [95, 96], and other receptors, can further modify downstream signalling events.

Skeletal muscle expresses all four FGFRs, with FGFR2 and 3 being expressed only at low or negligible levels [97-99]. Myoblast cultures express FGFR1 and 4, and tend to upregulate *Fgfr1* after mitogen addition [98]. *In vitro*, FGFs tend to stimulate myoblast proliferation. FGF2 has a potent mitogenic effect and stimulates SCs to enter the cell cycle [100-102]. FGF2 can maintain the proliferation of myoblast cultures whilst not altering the transition from proliferation to differentiation in isolated myofibres [100-102]. FGF1, 4, and 6 can also enhance SC proliferation on *ex vivo* myofibre cultures, and, additionally, FGF6 slows down the transition to differentiation in myogenic cells [97]. FGF6 is expressed in cultured isolated rat myofibres, suggesting that the myofibre can act as a source of FGFs under certain conditions [97].

Interestingly, rat myoblast cultures express *Fgf1* and *Fgf2* suggesting that myogenic precursors themselves can enhance their proliferation through an autocrine mechanism of action of these ligands *in vitro* [103, 104]. In addition, FGFs may elicit their effect by modulating the expression of other factors.

Rosenthal et al. showed that treatment of myoblasts with FGF2 resulted in a reduction of IGF-II expression, leading to the hypothesis that FGF2 inhibits muscle cell differentiation through inhibition of IGF-II expression [105].

Under normal homeostatic conditions in skeletal muscle fibres there is very little FGF present [106]. FGFs are associated with the extracellular matrix (ECM), outside of the basal lamina, and it is not until the muscle is damaged that the muscle fibre and SCs are exposed to FGFs in the surrounding area. A large amount of FGFs are released after muscle injury in the inflammatory phase of regeneration. These mitogenic factors act to induce the proliferation of SCs and also chemotactically recruit other muscle precursor cells [68]. In addition,

Husmann et al. showed that FGFs also possess potent angiogenic capabilities, which may aid their regenerative effects [68]. FGF2 protein is found in the perimysium and ECM surrounding muscle fibres [107], and has been shown to be produced by infiltrating macrophages of the inflammatory response and many mononuclear cells in regenerating rat muscle [68, 108]. Upregulation of FGF2 seen in mouse models of Duchenne muscular dystrophy (DMD), where skeletal muscle undergoes repeated rounds of degeneration and regeneration due to the lack of functional dystrophin protein, could partly explain the persistent skeletal muscle regeneration seen in these animals [68].

Concomitantly, inhibition of FGF signalling through the blockade of FGFR results in a large decrease in muscle mass and this has been attributed to premature terminal differentiation causing a depletion of the pool of myogenic progenitors [109-111]. Genetic overexpression of Sprouty (Spry) proteins, negative regulators of receptor tyrosine kinase (RTK) signalling, prevents embryonic myogenic progenitor cells from proceeding down the myogenic differentiation program and instead encourages self-renewal, further showing a role for FGF signalling in myogenesis [112].

The role of FGF2 *in vivo* after muscle injury appears to be mainly restricted to the initial activation and proliferation of SCs. The injection of neutralising antibodies to FGF2 at the time of muscle injury reduced the number and diameter of regenerating myofibres, suggesting a delay in the activation of SCs and / or myoblast fusion [113]. Taken together, these data show that FGF2 exhibits mostly a mitogenic role. FGF6 plays a prominent role in regeneration *in vivo* and is induced in response to muscle injury [114]. Mutant mice null for FGFR4, FGF6, and both FGF6 and FGF2, display severely impaired regeneration with increased fibrosis after injury, attributed to a lack of SC activation and defective migration to damaged areas [99, 114, 115].

Strict control of FGF signalling in the SCs of injured adult skeletal muscle is essential for efficient regeneration and the return to quiescence of myogenic progenitors [42]. Shea et al. showed that deletion of *Spry1*, which encodes for a negative regulator of FGF signalling (**Figure 2**) specifically in SCs, leads to

increased FGF signalling, causing a subset of myogenic progenitors to apoptose [42]. These data demonstrate a critical role for regulation of FGF signalling in SC proliferation and differentiation.

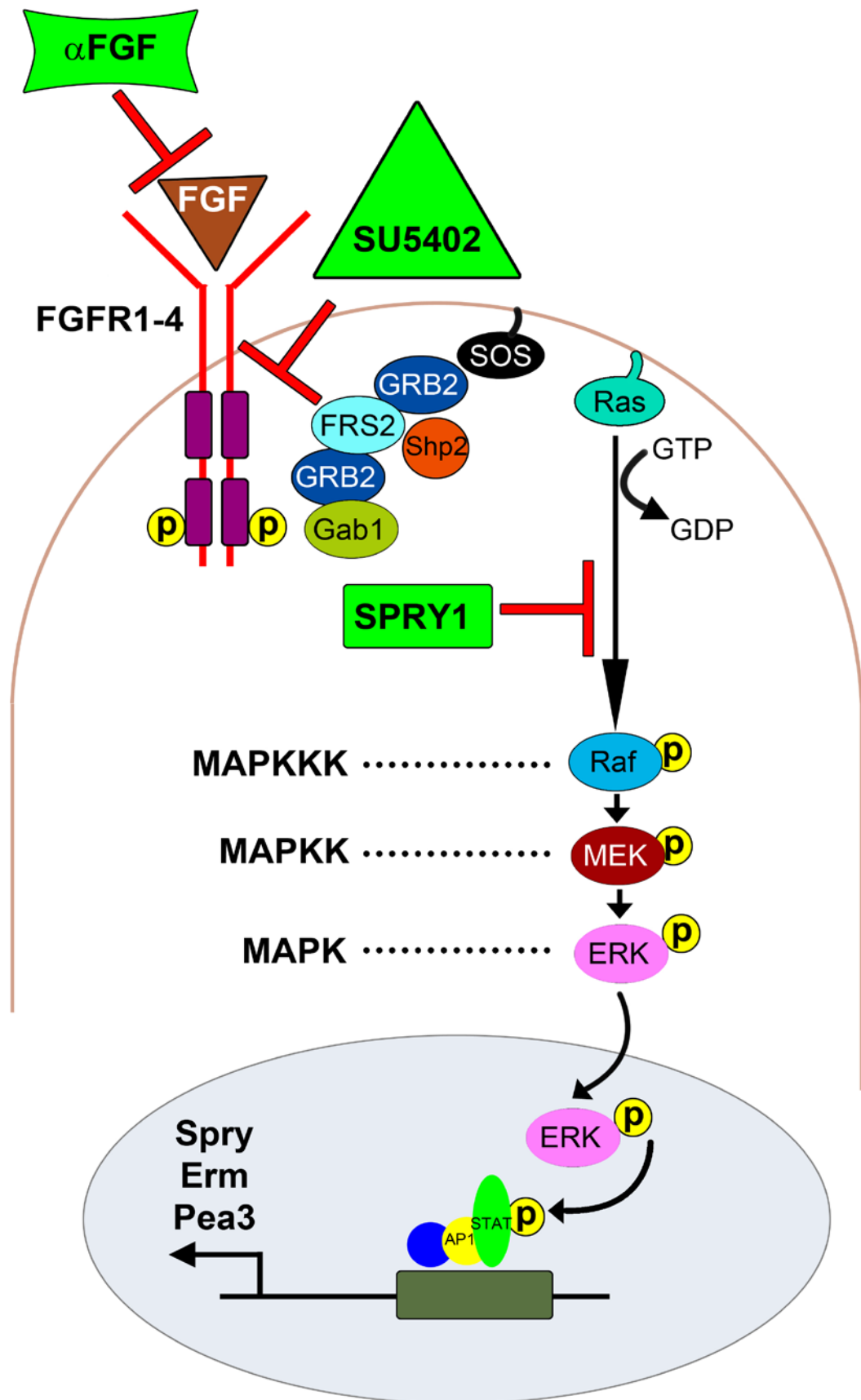


Figure 2 - Schematic of FGF-ERK signalling. FGF signalling is initiated by FGF ligand binding to FGFR. This leads to dimerisation of FGFRs and the cross phosphorylation of tyrosine residues intracellularly. These phosphorylated residues are then bound specifically by several intracellular signal transduction proteins such as GRB2 and FRS2. These initiate several signalling pathways such as PLC γ pathway (not shown), PI3K/PKB pathway (not shown) and the Ras/ERK pathway. After activation by addition of GTP, Ras initiates signal transduction through a series of 3 tyrosine-serine/threonine kinases (MAPKKK to MAPK) that culminates in the phosphorylation and activation of several transcription factors such as activating protein-1 (AP-1), and signal transducer and activator of transcription (STAT). The downstream effectors of Ras/ERK signalling include Erm, Pea3, and Sprouty. Sprouty proteins negatively regulate receptor tyrosine kinase signalling somewhere around the level of Ras or Raf. FGF signalling can be inhibited by the addition of a chemical inhibitor of FGFR called SU5402 which binds to the intracellular kinase domain of FGFR. The addition of a blocking antibody to FGFs (α FGF) can inhibit FGF-mediated FGFR signalling. ERK, extracellular-signal related kinase; FRS2, fibroblast growth factor receptor substrate 2; Gab, Grb2-associated protein; Grb2, growth factor receptor-bound protein 2; MEK, mitogen-activated protein kinase kinase; Raf, v-raf-leukaemia viral oncogene homologue 1; Ras, rat sarcoma; SHP2, SH2 domain-containing tyrosine phosphatase 2; SOS, son of sevenless.

1.3.4. Heterogeneity of the satellite cell pool

Many studies propose that the SC pool is functionally heterogeneous, suggesting that not all SCs have stem cell characteristics. For example, deletion of *Spry1* specifically in adult SCs caused the apoptosis of not all, but a subset of muscle progenitors after injury [42]. Indeed, in many adult stem cell populations there is growing evidence that stem cells with different proliferative kinetics, differentiation potentials and mitogenic responsiveness exist in the same tissue. In adult skeletal muscle there is clear evidence for heterogeneity in SC populations from different muscles and also between SCs within the same tissue. For example, SCs associated with extraocular muscles continue to proliferate and contribute myonuclei to the tissue in the absence of damage, unlike limb SCs, and, strikingly, these muscles are not affected in DMD [116, 117]. Comparing various limb muscles, SCs also present with different proliferation and differentiation kinetics [118], suggesting a large degree of heterogeneity in SC pools.

1.3.4.1. Self-renewal heterogeneity

In transplantation studies of irradiated mice, some transplanted SCs were able to give rise to many clones and new muscle whereas some grafts did not give rise to any, suggesting that a subset of SCs may have a limited capacity for self-renewal [53, 54]. This idea is supported by *ex vivo* studies. In isolated single muscle fibres MyoD is rapidly induced as SCs activate and proliferate. Most cells downregulate Pax7 expression and commit to differentiation through activation of MyoG. However, a subset of activated SCs are able to maintain Pax7 expression, downregulate MyoD expression, and return to quiescence [119, 120]. This progression suggests that all cells enter a Pax7 and MyoD co-expression stage before a subset self-renew.

Kuang et al. and Brack et al. proposed that a subset of SCs which did not express a reporter driven by the Myf5 promoter are the true stem cell of skeletal muscle as they have never activated the myogenic differentiation program [83, 121]. The cells which did express the reported gene, on the other hand, are their myoblast progeny [83, 121]. In support of these data, around 10% of SCs were found to have no Myf5 protein at all [122]. Further evidence for this heterogeneity come from studies which have noted that only a subset of SCs undergo asymmetric divisions [88, 93, 123, 124]. For example, asymmetric distribution of Numb, an inhibitor of Notch signalling, was found to take place in some but not all SC divisions [88, 93]. However, contradictory data came from Kanisicak et al. who used a MyoD^{iCre/+} mouse line to drive YFP or β -galactosidase expression [125]. The authors showed that all SCs were labelled with this mouse line, suggesting that all SCs have activated the myogenic differentiation program at some point [125]. Therefore, further study into heterogeneity based on the stage of differentiation of SC populations is needed.

Sacco et al. analysed heterogeneity based on the expression of certain genes of fluorescence-activated cell sorting (FACS)-isolated single SCs from the same muscle [54]. Whilst all cells expressed Pax7 and Myf5 transcript, 25% of SCs expressed MyoD, indicating a degree of differentiation commitment, and a small population expressed Pax3, a marker of progenitors intermediate between SCs

and myoblasts [54]. Collectively, these data show that there is heterogeneity within the SC pool with regards to gene transcription, degree of differentiation, and self-renewal capability.

1.3.4.2. Proliferative heterogeneity

Heterogeneity of cells in the SC position can be seen during postnatal growth, with cells separated into either a rapidly proliferative majority or slowly proliferative minority pool [126]. In these stages of postnatal myogenesis, the slow-dividing SCs are thought to be the self-renewing population [126]. The fast-dividing population, on the other hand, act as transit amplifying cells and undergo limited divisions before continuing through the myogenic program [126]. This is also seen in *ex vivo* systems in adult muscle with label retaining experiments [124]. Cells which proliferate slowly and retain a dye or DNA-replication label are known as label-retaining cells (LRCs), whereas cells which proliferate more rapidly and dilute the label to undetectable levels are known as non-LRCs. Shinin et al. demonstrated that LRCs have an increased tendency to self-renew rather than differentiate in *ex vivo* cultures and therefore appear to be more stem cell-like [124]. Ono et al. added to this concept and showed that transplantation of LRCs in injured muscle led to more efficient muscle regeneration than transplantation of non-LRCs [127]. Furthermore, the authors demonstrated that, upon a second injury, more newly regenerated fibres were only observed in the LRC-transplanted muscle compared to the primary engraftment [127]. These data suggest that the less proliferative SCs are true muscle stem cells, whilst the more proliferative SCs are progenitors with limited self-renewal capacity [127].

1.4. The satellite cell niche

SCs reside in a microenvironment that maintains stem cell quiescence during homeostasis but also allows for efficient activation, proliferation, and differentiation during skeletal muscle regeneration. The SC niche is composed

of ECM, the myofibre, vascular cells, neural cells, inflammatory cells, other surrounding cells such as adipocytes and fibroblasts, diffusible molecules, and the SC itself (**Figure 3**).

Experiments in the early 1990s identified the muscle fibre as an essential component of the SC niche. Upon destruction of the myofibre, whilst leaving the basal lamina intact, SCs rapidly entered the cell cycle and proliferated [128]. These experiments described a role for the myofibre in the maintenance of SC quiescence, a feature of many stem cells that allows for maintenance of the stem cell pool and proper function throughout life [128]. More recent studies have reported many SC regulatory factors to be expressed by myofibres. Myofibres secrete stromal cell-derived factor-1 which binds to chemokine receptor type 4 on the surface of SCs to stimulate their migration to areas of high chemokine gradients [129]. Furthermore, the Notch ligand Delta is expressed by myofibres and is upregulated following muscle injury [130]. Delta binds to Notch receptor on SCs and stimulates their proliferation [130].

Growth factors also constitute an important part of the SC niche and their effects are discussed in **Section 1.3.3.2** and **Section 1.3.3.3**. Many growth factors are associated with ECM proteins, in close contact with the basal lamina, and can be activated by proteolytic enzymes, enabling them to carry out the highly orchestrated processes of SC activation, proliferation and differentiation upon muscle injury [131-134]. Basal lamina components, including laminin and fibronectin, support SC proliferation and it has been proposed that the basal lamina functions as a scaffold for the formation of new myofibres [8].

Mononucleated interstitial cells and growth factor-secreting fibroblasts are major components of the stromal tissue in adult skeletal muscle. Tcf4⁺ fibroblasts and their interactions with SCs have recently been shown to be essential for efficient muscle regeneration and also affect the differentiation potential of myogenic precursors [59, 135].

The vasculature plays an important role in SC regulation, perhaps exemplified by the fact that many SCs are closely associated with capillaries [136, 137]. Endothelial cells promote proliferation of myoblasts by secreting a panel of growth factors such as vascular endothelial growth factor (VEGF), IGF-1, HGF, and PDGF. In addition, angiopoietin-1 (Ang-1) is secreted by perivascular cells and binds to its cognate receptor Tie-2 on SCs to promote a return to quiescence of a subset of SCs after activation [137, 138].

Under homeostatic conditions the immune system plays little or no role in the regulation of SC behaviour, and only a small number of immune cells reside within homeostatic skeletal muscle. However, upon muscle injury, immune cells are recruited and, in addition to removing necrotic tissue, they secrete factors that encourage SC activation, inhibit apoptosis, and remodel the ECM to allow for efficient muscle regeneration [139].

The SC niche is also subject to peripheral nervous input from the motor neuron. In the 1970s, Schultz et al. showed that acute denervation results in activation and proliferation of SCs, mimicking the proliferation seen after myotrauma [140]. Chronic denervation results in progressive skeletal muscle atrophy and a large decline in stem cell number, thought to be due to exhaustion of the satellite cell pool, decreased ability of SCs to enter the cell cycle, and increased apoptosis [141-144]. The mechanisms responsible for these phenotypes remain largely unknown, however it has been suggested that denervation may influence myofibre properties and have a secondary effect on SCs [145].

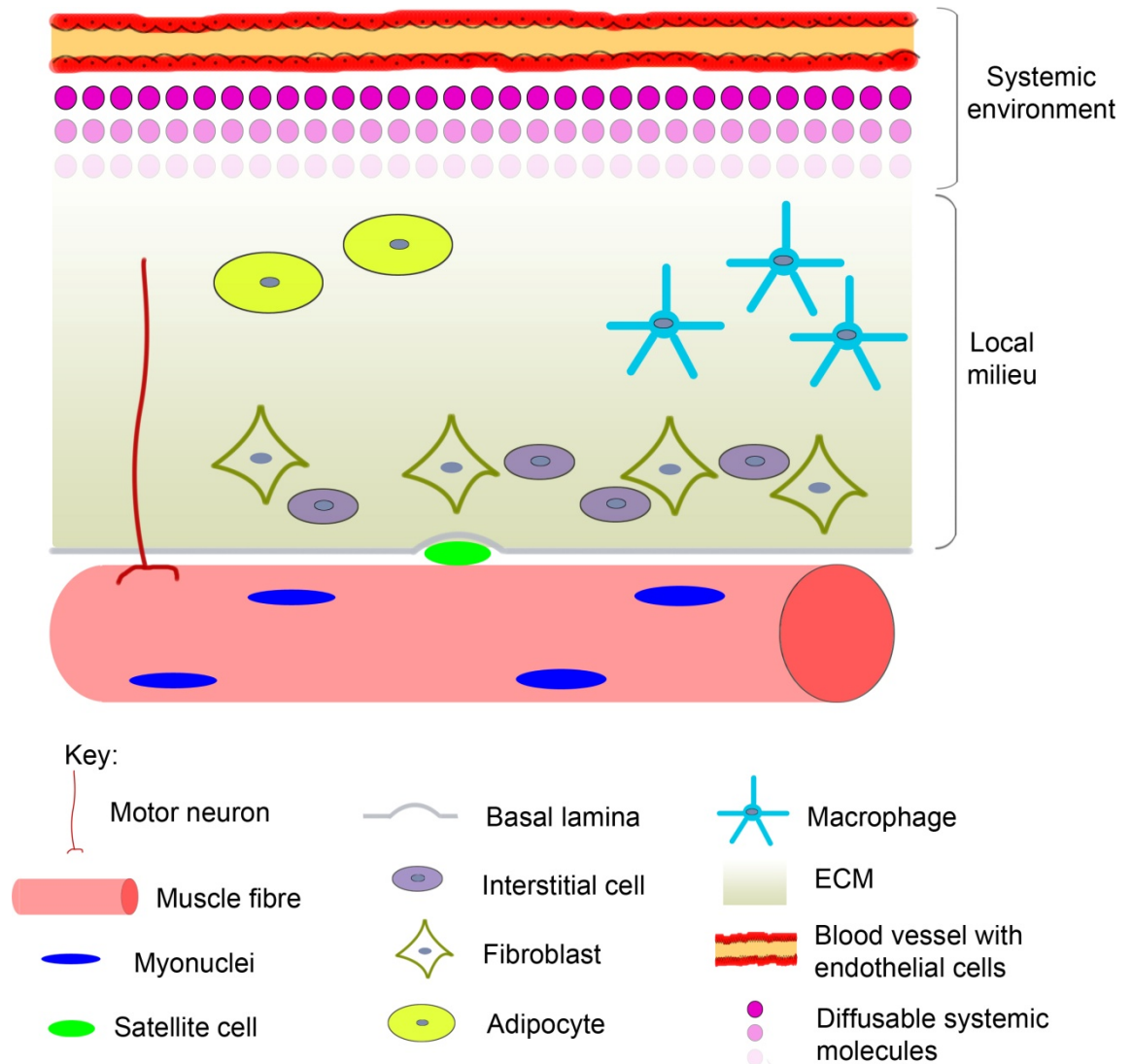


Figure 3 - Schematic illustration of the satellite cell niche. The SC is in close contact with the muscle fibre and the basal lamina. Under homeostatic conditions the SC is shielded from potent activatory stimuli such as factors in the ECM secreted by fibroblasts, interstitial cells, and macrophages. The systemic environment of blood vessels, endothelial cells, and associated cells such as pericytes (not shown) can influence SC function. The motor neuron can influence SC behaviour through activity on the muscle fibre. Adapted from [8].

1.5. Ageing in skeletal muscle

Ageing is associated with impairment of skeletal muscle regeneration following injury (**Figure 4**). Furthermore, as age progresses, there is a decrease in skeletal muscle mass (sarcopenia) and muscle fibres are replaced by fat and fibrous tissue, leading to reduced physiological function [146]. Because SCs appear to be solely responsible for skeletal muscle regeneration, these hallmarks of ageing are associated with a progressive loss of stem cell number and function. During regeneration of aged muscle, SCs exhibit a large decrease in activation and proliferation at the population level and generate fewer myoblasts compared with adult muscle [147, 148]. There is a large volume of evidence suggesting that the decline in SC function is attributable to both cell-intrinsic and cell-extrinsic factors. However, the issue of whether the number of SCs declines with age is still somewhat controversial, with studies documenting increased and decreased numbers of SCs depending on the species, muscle, and technique of observation [146]. Despite this, there is accumulating evidence that limb skeletal muscle exhibits a decline in the number of SCs present throughout ageing under homeostatic conditions [149-151]. Furthermore, what drives a change in SC number and whether a change in stem cell number results in an age-related decline in regenerative capacity has not been investigated. Regardless of changes in stem cell number, it has been shown that SCs in aged tissue are able to effectively participate in muscle regeneration given the appropriate signals.

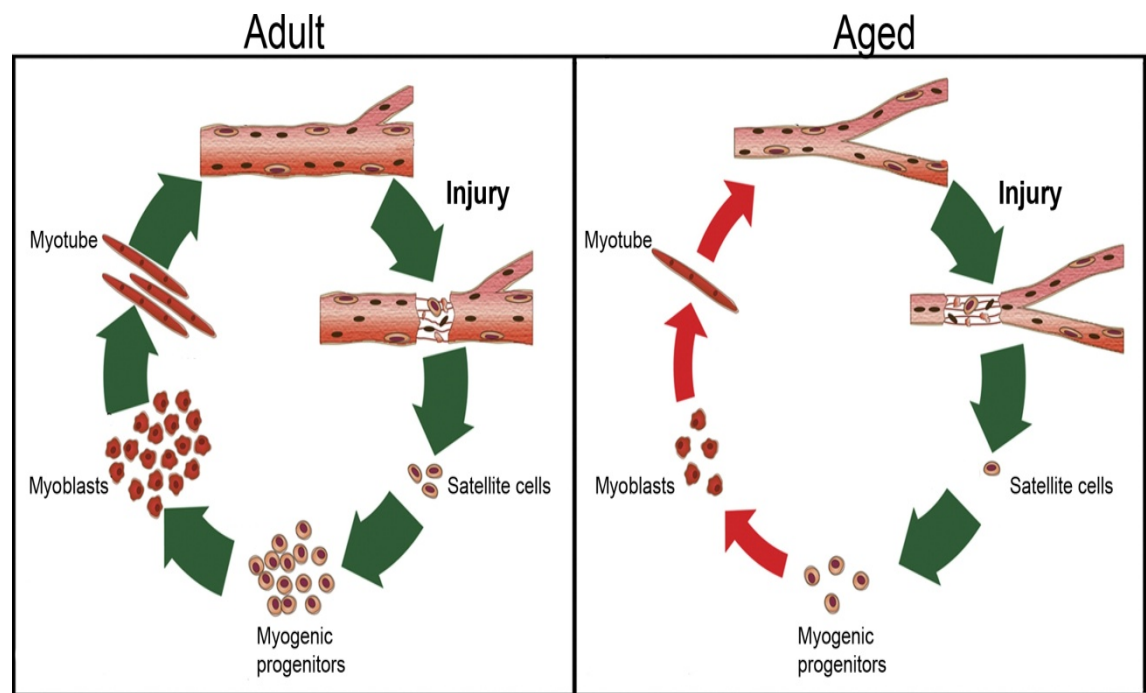


Figure 4 - Schematic illustration of impaired muscle regeneration in old age. In response to injury, SCs from adult skeletal muscle are able to rapidly activate and form myoblasts which then fuse to form new myofibres. However, as ageing progresses, SCs display an impaired ability to regenerate damaged myofibres due to impaired function. There may be fewer SCs present in the muscle which are less able to proliferate and form myoblast progeny and, furthermore, myoblasts fuse to form thinner, more fragile myotubes. Collectively this leads to a decline in skeletal muscle function. Adapted from [152].

1.5.1. Age-associated intrinsic changes in satellite cells

SCs, like other somatic stem cells, have a limited proliferative capacity and undergo replicative senescence after a finite number of divisions [153].

Telomeres are repetitive nucleotide sequences at the ends of chromatids and are implicated in cellular ageing and chromosome stability [154]. As cells divide their telomeres become slightly shorter, and so telomere length can be an indication of replicative history. *In vitro* studies using SCs of different ages, and from DMD patients, noted that cells isolated from older donors or DMD patients, where SCs would have been forced to proliferate more, have a decreased proliferative capacity and increased tendency to become senescent, and this was associated with telomere shortening [153, 155, 156]. Sacco et al. used a

mouse model of telomere shortening on a muscular dystrophy model background and noted that these mice presented with severe muscular dystrophy and impaired SC proliferation both *in vivo* and *in vitro* [152]. This suggested that shortened telomeres may caused impaired SC function [152, 157].

Experiments examining changes in gene expression in human cells have demonstrated that the transcriptional profile of SCs is altered during ageing [158]. However, this was performed at the population level and so it is unknown if some aged SCs retain transcriptional signatures of young SCs. Additionally, it is not known if these intrinsic changes are permanent or reversible. It is possible that the age-associated decline in SC function is from epigenetic changes which are reversible.

Aged myoblasts in culture display a slow response to mitogenic factors [159, 160]. However, over time in culture and after many passages, aged myoblasts proliferate at almost a similar rate to young myoblasts [151, 160]. This suggests that age-related cell-intrinsic changes in SCs are responsible for reduced proliferative output. Despite this striking result it is possible that passaging of the cells may select for a subpopulation of myoblasts with similar proliferative potential from both the young and aged animals. Alternatively, these data may suggest that reversible epigenetic changes may be responsible for the delayed activation of aged SCs.

Activation and lineage progression of SCs to myoblasts is dependent on Notch signalling. Insufficient upregulation of the Notch ligand Dll1 after muscle injury has been proposed to be one of the major factors implicated in impaired SC proliferation after muscle injury in aged animals [130]. Furthermore, forced expression of Notch signalling in aged homeostatic muscle restores regenerative potential to that of an adult muscle [130].

SCs have the ability to differentiate into non-myogenic cells, including fibroblasts and adipocytes, under certain conditions [161-164]. With ageing, myogenic cells tend to adopt a fibroblast fate due to elevated Wnt signalling,

and inhibition of Wnt signalling in progenitors blocked the increase in fibrosis that is usually seen after injury of aged skeletal muscle [164, 165]. Interestingly, this is different to the role of Wnt signalling in regeneration of adult skeletal muscle, where it promotes proliferation and the early phases of myogenic differentiation (See **Section 1.3.3.2**). These differences could be due to the effects of signalling through different Wnt proteins and receptors, or perhaps the SC response to Wnt signalling may change with age.

The differentiation of myogenic cells is also impaired with ageing as SCs fuse to form thinner, more fragile myotubes [155]. Furthermore, fewer aged myogenic cells expressed markers of more mature myofibres after being placed in differentiation conditions compared to adult cells, consistent with impaired differentiation [150, 166]. Interestingly, after multiple passages myoblasts were capable of efficient differentiation, suggesting that reversible cell-intrinsic changes in myogenic cells result in impaired differentiation capability [10].

1.5.2. Age-associated changes in the satellite cell niche

In invertebrate stem cell systems, age-associated changes in the niche have been shown to negatively impact on stem cell maintenance and function [167, 168]. The niche is an important regulator of stem cell quiescence, a reversible state of proliferative inactivity essential for maintenance of stem cell number and function in many mammalian systems [20]. The environment can reverse cell-intrinsic changes that occur with age, suggesting that the niche can influence SC function. Heterochronic transplantation studies, where aged or young whole muscle was transplanted into either aged or young hosts, demonstrated that the systemic environment can affect regeneration. Engraftment was successful when old muscle was transplanted into young hosts, whereas regeneration was impaired when young muscle was transplanted into aged hosts [148, 169]. Furthermore, the regeneration of a single aged fibre transplanted into a young irradiated host was comparable to the engraftment of a young fibre transplanted into a young host [150],

suggesting that the host environment affects stem cell function and regeneration.

Parabiotic studies have been used to examine the effect of the aged and adult environment on stem cell function in different systems, including skeletal muscle SCs. These experiments involve surgically joining together two animals so that they develop a single, shared circulatory system, followed by inflicting muscle injury to examine SC activation and differentiation. In heterochronic pairs, where aged mice were paired with adult mice, injury to the aged mice resulted in increased activation of their SCs and improved regeneration [10, 164]. Aged SCs exposed to an adult systemic environment were also less prone to adopt a fibrotic fate [10, 164]. These studies also showed that the aged systemic environment may inhibit muscle regeneration as regeneration of the skeletal muscle of adult heterochronic pairs was impaired compared to adult homochronic pairs and adult SCs had an increased tendency to adopt a fibrotic fate [10, 164]. Aged skeletal muscle also displays decreased capillarisation compared to young muscle, suggesting that the ability of systemic factors to contact the myofibre and SC may be decreased [170]. These studies show that the young systemic environment has a pro-proliferative effect on SCs, whereas the aged systemic environment is detrimental to SC function during regeneration.

Changes in the composition of the ECM with age may also have detrimental effects on skeletal muscle regeneration. A thickened basal lamina and an increase in connective tissue between muscle fibres have been noted in aged compared to young muscle [171-173]. A thicker basal lamina would result in more collagen surrounding the fibre, possibly changing the physical properties and stiffness of the niche and altering SC function [146].

As ageing progresses there are changes in the expression of circulating factors important for muscle regeneration. An increased level of TGF β occurs with age, and this has been suggested to impair SC activation [174-176]. Administration of neutralising antibodies to the downstream effector of TGF β signalling, phospho-SMAD3, restores regeneration in aged skeletal muscle [174]. TGF β

signalling also enhances the adoption of a fibrotic or adipogenic cell fate, possibly in part due to driving the expression of periostin, a protein produced by interstitial fibroblasts [164, 165, 177, 178]. Enhanced TGF β signalling combined with decreased Notch signalling (see **Section 1.5.1**) with ageing will collectively promote the expression of cell cycle inhibitors such as p15, p16, p21, and p27 in SCs, supporting the idea that the balance between signalling pathways is crucial to ensure proper stem cell function [174, 175].

A functional deficit in the immune response with age can affect SC function. *In vitro* studies suggest that many of the immune cells' key responses, such as phagocytosis and chemotaxis, are impaired with age [179]. This would hamper the regenerative response and SC activation as immune cells can influence SC behaviour through the release of cytokines, such as IL-6, and the removal of damaged tissue.

The neuromuscular junction also undergoes age-related changes, with electron microscope examination revealing decreases in nerve terminal area and occasional denervated postsynaptic regions in aged skeletal muscle [180]. The resulting activation and exhaustion of the stem cell pool may potentially be one of the causes of decreased SC number with age [141-143, 181].

These data demonstrate that it is possible to restore regenerative potential to aged SCs through modulation of the niche. However, although many of these studies have examined aged SCs in the context of muscle injury and regeneration, few studies have looked at the internal and external changes under homeostatic conditions. This analysis will be necessary to prevent, or even reverse, age-associated changes in muscle stem cell number and function.

1.6. Neurogenesis

Despite originating from different cell populations during embryonic development and serving different tissue systems, there are similarities in the regulation of adult skeletal muscle stem cells and neural stem cells. Both stem cell populations are relatively quiescent and form specified mature cell types through the generation of transit amplifying daughter cells [182, 183].

Furthermore, both stem cell populations reside in well-defined niches which can modulate their function under homeostatic conditions and under traumatic conditions [8, 183]. Interestingly, skeletal muscle stem cells and neural stem cells both exhibit a decline in number with ageing [8, 184]. Investigating the extrinsic and intrinsic mechanisms which regulate the maintenance and self-renewal of these two stem cell populations may therefore provide an insight into the common mechanisms by which somatic stem cell number and function are regulated.

Neurogenesis is the formation of new neurons that are able to functionally integrate into synaptic circuitry. In mammals, neurogenesis occurs throughout embryonic developmental stages to form the CNS. Neurogenesis also occurs in discrete regions of the postnatal and adult forebrain at a much lower level. Neural stem cells (NSCs) are multipotent cells capable of self-renewal, and are responsible for the generation of new neurons and glia during development and in adulthood.

1.6.1. Embryonic neurogenesis

During development, radial glia (RG) in the neuroepithelium form the neurons and glial cells of the entire CNS in a defined manner [185]. By the end of development most RG convert into mature astrocytes [185]. However, some RG cells form somatic NSCs instead, which retain many of the stem cell markers seen in RG cells. Adult NSCs have many morphological characteristics of RG cells and indeed serve a similar function as the primary progenitors of new neurons and glia [186].

1.7. Adult neurogenesis and adult neural stem cell properties

NSCs have been shown to persist in at least two specialised niches of the adult forebrain of many mammalian species: The subgranular zone (SGZ) of the dentate gyrus (DG), and the subventricular zone (SVZ) of the walls of the lateral ventricles [183]. NSCs in these regions continue to generate new neurons throughout life [187-189]. Although NSCs in the SGZ and SVZ are separated spatially and give rise to neurons that serve different systems and purposes, there are common themes that define the adult NSCs and their niches. Adult NSCs in both systems have a radial morphology [190] and express astrocytic markers such as glial fibrillary acidic protein (GFAP) [191, 192], brain lipid-binding protein (BLBP), vimentin, and glutamate aspartate transporter (GLAST), as well as expressing stem cell markers such as Sox2 and Nestin, much like RG cells [193]. In addition, there is some overlap between signalling pathways that modulate SGZ and SVZ systems, and also embryonic RG function [194].

Adult NSCs in both niches display the capacity for self-renewal throughout life, as well as the ability to generate neurons and glia [195]. This has been shown by *in vivo* labelling studies and *in vitro* culture assays in many mammalian species, including humans [189, 196-200]. However, unlike their embryonic counterparts, adult NSCs are relatively quiescent and divide infrequently under homeostatic conditions. Doetsch et al. demonstrated the quiescent nature of adult NSCs by using the anti-mitotic agent cytosine arabinoside (AraC), which

killed the rapidly-dividing NSC progeny in the SVZ, but did not affect the slowly-dividing NSCs [201]. Upon removal of AraC, the NSCs were able to generate immature precursors and new neurons [201]. These data show that radial astrocyte-like cells in the SGZ and SVZ are the true neural stem cells of the adult forebrain.

1.8. Subventricular zone - olfactory bulb neurogenesis

The SVZ is the layer of cells around the walls of the lateral ventricle, outside of the ependymal layer (**Figure 5a,b**). The SVZ is the major source of adult neurogenesis in the mouse and is responsible for short-term olfactory memory and long-term associative olfactory memory [202-204]. In addition, olfactory bulb neurogenesis regulates olfaction dependent sex responses and predator avoidance, implicating SVZ neurogenesis in pheromone-related behaviours and olfactory fear conditioning [202]. Cells born in the SVZ traverse a long distance anteriorly via chain migration through a well-defined pathway called the rostral migratory stream (RMS) towards the olfactory bulb (OB) [205, 206]. Once they reach the OB, the immature neurons then migrate radially to different OB layers and differentiate into new interneurons (**Figures 5a-c**) [205]. This process is functionally correlated with olfactory learning and it has been shown an increased number of newborn OB interneurons survive during olfactory behaviours [201, 207]. It is estimated that the number of newly formed interneurons that are added to the OB ranges from 10,000 to 30,000 per day in adult mice [208], to 80,000 in young adult rats [209]. This correlates to around 1% of the olfactory granule cell population per day in a young adult rodent [209, 210]. The size of the OB does not change substantially throughout life, suggesting that SVZ-OB neurogenesis must be accompanied by cell death [210-212]. Indeed, large levels of apoptosis are observed in the OB, which presumably maintains a constant OB cell number [210].

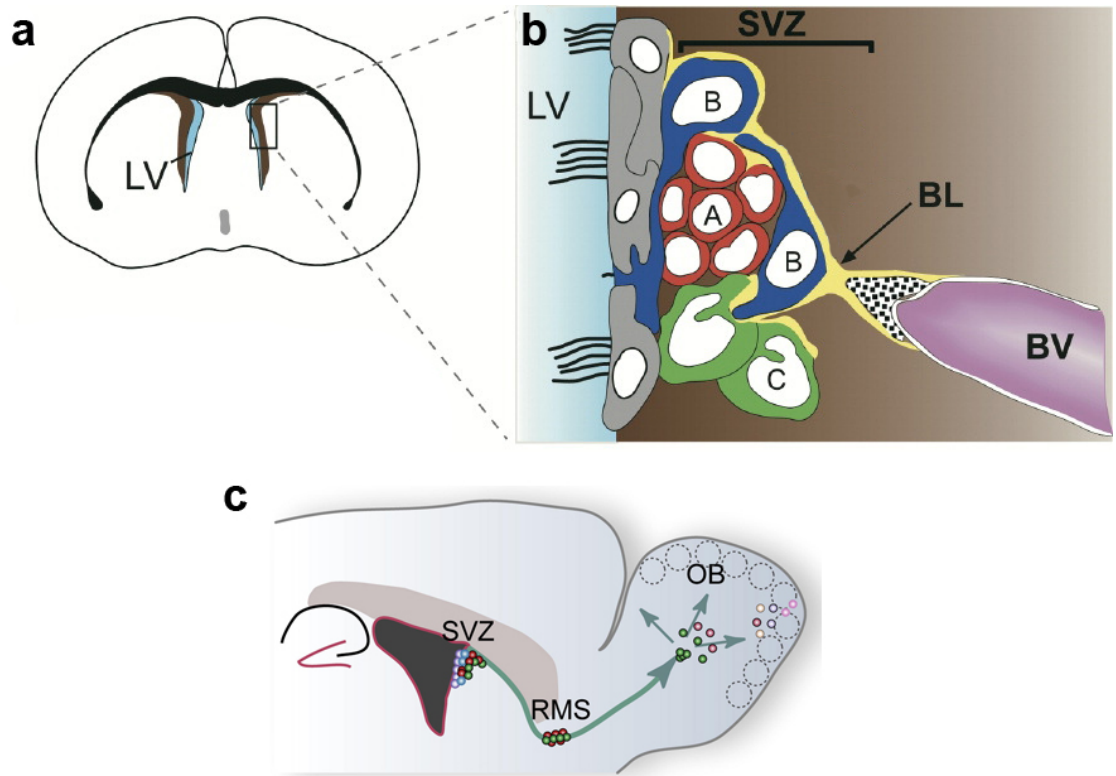


Figure 5 - Schematic illustration of adult subventricular zone neurogenesis. **a**, Illustration of a coronal section of the adult mouse brain showing the lateral ventricles (LV). The boxed area is shown enlarged in **b**. **b**, Composition of the SVZ niche. The LV is lined by ependymal cells (grey) and SVZ cells are ensheathed by a basal lamina (BL - yellow). Type B cells (dark blue) are the NSCs of the SVZ and have many features of astrocytes. Some contact the ventricle through a single cilium and may contact a blood vessel (BV). Type B cells give rise to type C cells (green) which are rapidly dividing. Type C cells give rise to type A cells (red). Type A cells migrate via chain migration through the rostral migratory stream (RMS) towards the olfactory bulb (OB; **c**). Once in the OB, type A cells migrate radially to different areas of the OB where they mature into new interneurons. Adapted from [213] and [214].

1.8.1. The neurogenic lineage in the adult subventricular zone

Different types of neurons are generated by SVZ cells. The vast majority newborn cells are GABAergic glomerular cells (**Figure 6**) [215-220]. A minority of newborn cells become GABAergic periglomerular cells [215, 216, 218-220], and one study also noted the formation of glutamatergic juxtglomerular neurons (see **Figure 11**) [221]. Parenchymous astrocytes and oligodendrocytes of the corpus callosal white matter are also produced to a limited extent by SVZ cells (**Figure 6**) [216]. The primary precursors for the generation of these cells are SVZ NSCs, also called type B cells [201]. These NSCs exist along the lateral, medial, and dorsal walls of the lateral ventricle in the SVZ, as well as in the RMS and corpus callosum [201, 222, 223]. Type B cells are relatively quiescent but divide infrequently to form transit-amplifying progeny, also known as type C cells [183]. Type C cells divide rapidly to amplify their population and they give rise to neuroblasts, also known as type A cells. Type A cells are ensheathed by astrocytes and migrate along the RMS to the OB [183]. Type A cells then mature into new granule or periglomerular neurons after arrival in the OB (see **Figure 5** and **Figure 7**) [183].

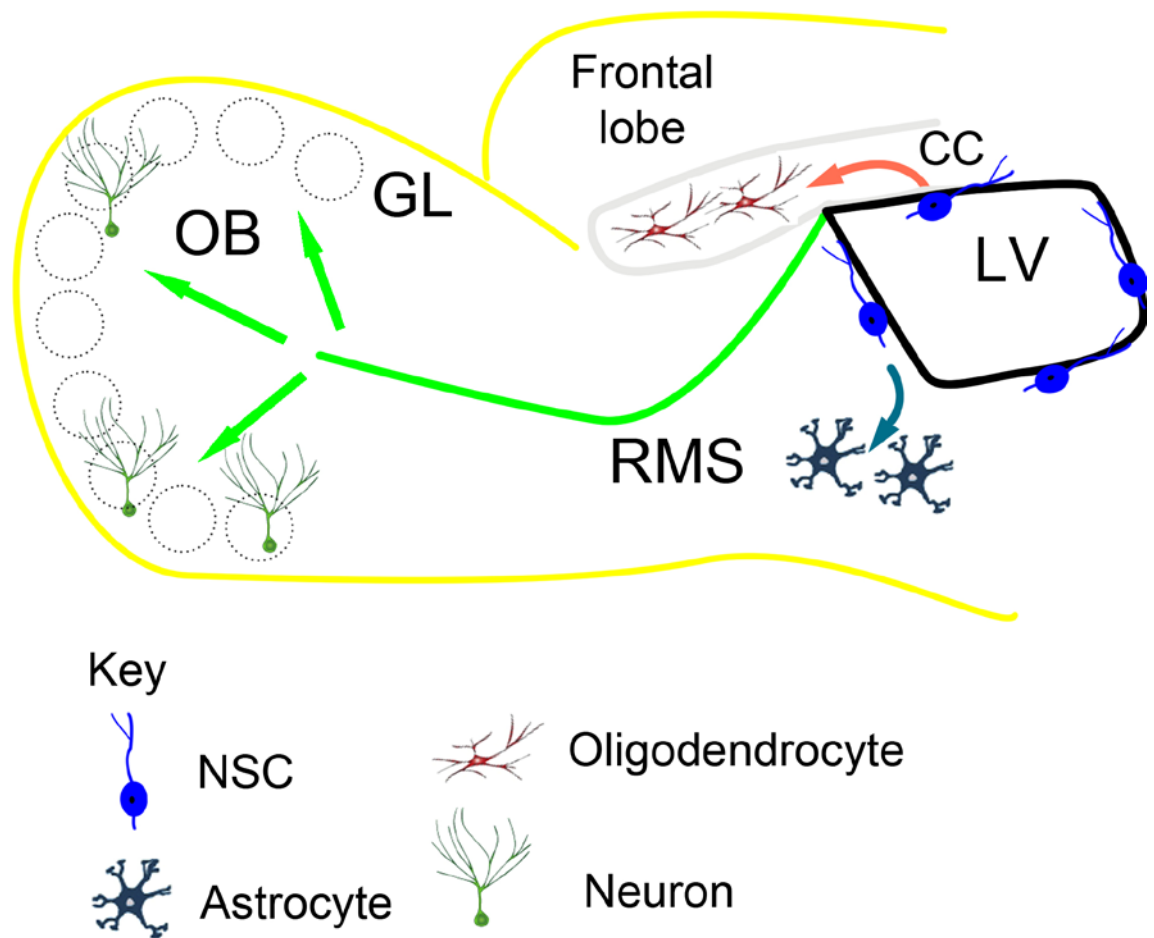


Figure 6 - Schematic illustration of the multipotency of adult neural stem cells in the subventricular zone. SVZ NSCs are capable of forming interneurons in the olfactory bulb (OB), mature astrocytes in the parenchyma, and oligodendrocytes in the corpus callosum (CC). GL, glomerular layer; LV, lateral ventricle; RMS, rostral migratory stream.

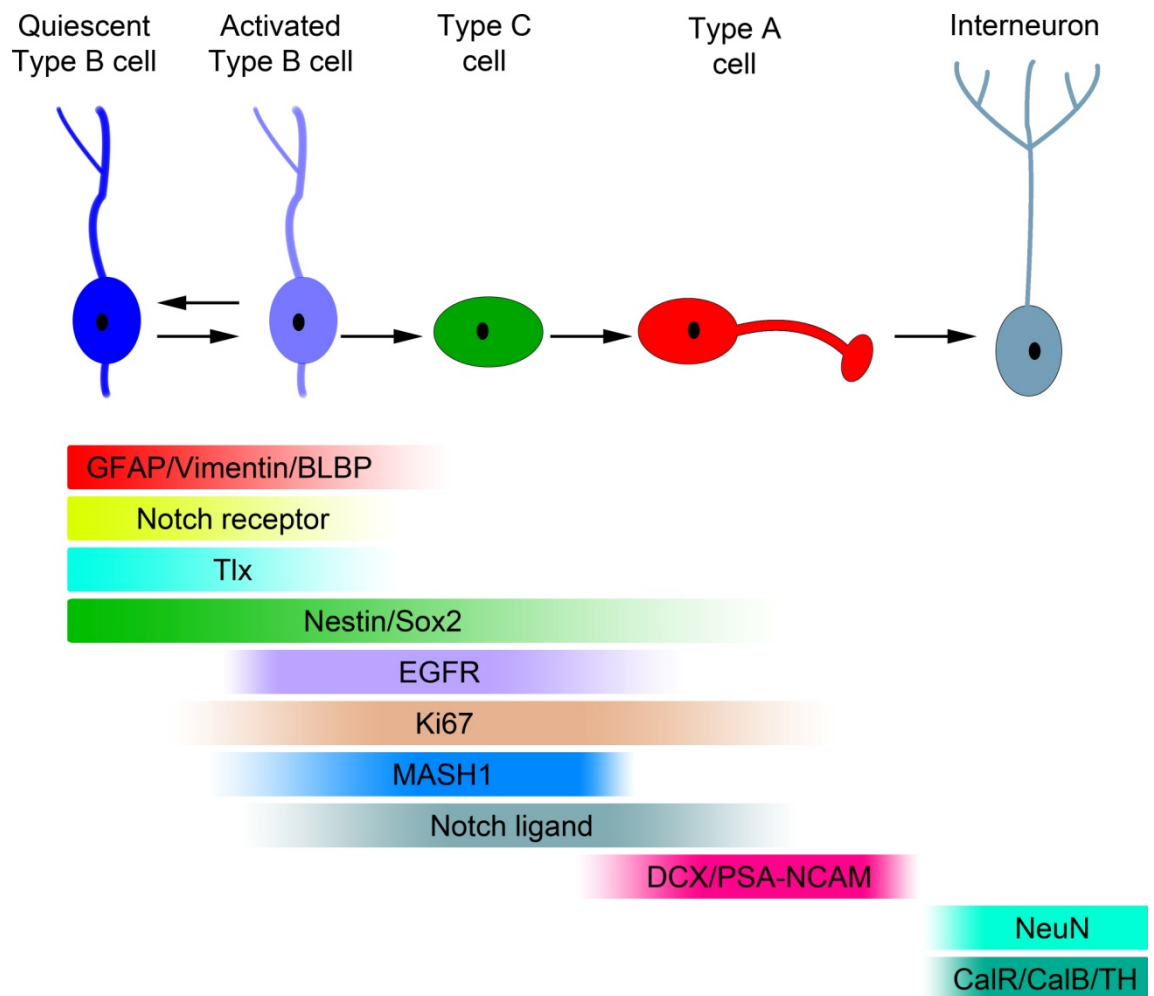


Figure 7 - Schematic illustration of the adult subventricular zone cell lineage. Type B cells are relatively quiescent and express astrocytic markers such as GFAP, vimentin and BLBP as well as Notch receptor, Tlx, Nestin, and Sox2. Upon activation, type B cells upregulate EGFR and become positive for cell cycle markers such as Ki67. MASH1 marks activated type B cells and their progression to type C cells. Type C cells downregulate astrocytic markers and Notch receptor and upregulate Notch ligand to induce Notch signalling in type B cells. Type C cells proliferate rapidly and form type A cells which express doublecortin (DCX) and polysialic acid neural cell adhesion molecule (PSA-NCAM). Type A cells downregulate stem cell markers such as Nestin and Sox2 as well as EGFR, MASH1 and Notch ligand. In addition they are much less proliferative than type C cells and few are positive for Ki67. Type A cells migrate to the OB where they form different types of interneurons. All interneurons are positive for NeuN but these can be further categorised into interneuron type by their expression of calretinin (CalR), calbindin (CalB), and tyrosine hydroxylase (TH).

1.9. Adult hippocampal neurogenesis

Neurogenesis in the DG plays an important role in hippocampus-dependent learning tasks and memory formation. Blocking hippocampal neurogenesis leads to decreased performance in various learning and memory tasks and, conversely, increasing neurogenesis in this region leads to improved performance [224-227]. Cells born in the SGZ migrate only a small distance through the granular layer (GL) and, unlike in the OB, cells mature and become only one type of neuronal population: granule neurons (**Figure 8**) [228]. Generation of astrocytes and, to a very limited extent, oligodendrocytes from SGZ cells have also been observed under certain conditions [229-233]. The production of new neurons in the hippocampus is much lower than in the SVZ-OB system, with the formation of new cells estimated to be around 9000 per day in an adult rat [232, 234], corresponding to 0.03% of the total hippocampal dentate neuronal population [235]. Interestingly, in the DG old neurons are not just replaced but SGZ neurogenesis contributes to the increase in the volume of the granular layer and the number of granule cells throughout life [224, 236, 237].

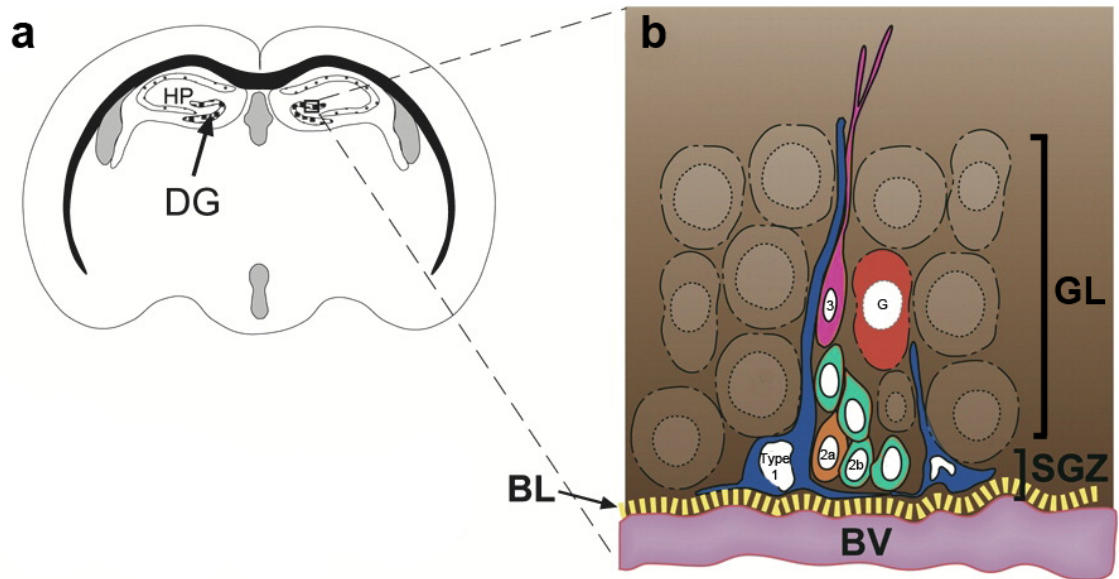


Figure 8 - Schematic illustration of adult subgranular zone neurogenesis. **a**, Illustration of a coronal section of the adult mouse brain showing the dentate gyrus (DG) of the hippocampus (HP). The boxed area is enlarged in **b**. **b**, Composition of the SGZ niche. Type 1 cells (dark blue) are the NSCs of the SGZ. They are usually in close contact with a blood vessel (BV) and a basal lamina (yellow stripes). Type 1 cells are relatively quiescent and give rise to type 2a cells (orange). Type 2a cells proliferate rapidly and form type 2b cells (light green) which are less proliferative and more committed to differentiation. Type 2b cells give rise to type 3 cells (purple) which migrate to deeper layers of the granular layer (GL) and divide infrequently. Type 3 cells form new mature granule neurons (G; red). Adapted from [213].

1.9.1. The neurogenic lineage in the adult subgranular zone

Dentate granule neurons are generated throughout life by SGZ cells in many species, including humans [189]. The primary precursors for adult born dentate cells are SGZ NSCs, also called type 1 cells. Type 1 cells have a unique morphology compared to other cells in the hippocampus as they have their cell body in the SGZ and extend astrocytic projections through the granular layer and into the molecular layer of the DG (see **Figure 8**) [228]. These cells share many similarities with type B cells in the SVZ, however, the two cell types are not identical. Type 1 cells and Type B cells serve different brain systems and functions, so the regulation of the NSCs in the different niches may be different.

NSCs in the SGZ divide very infrequently and can form transit amplifying progeny collectively known as type 2 cells [228]. Type 2 cells are divided into two subtypes corresponding to consecutive stages of cell development based on proliferative output and stage of differentiation and are called type 2a and type 2b cells. It is thought that type 2a cells are the primary daughter cells of type 1 cells as they have a relatively high proliferative output and express few differentiation markers [228]. Type 2a cells then form type 2b cells, which are more limited in their proliferative output and express markers consistent with a greater commitment to differentiation (**Figure 9**) [228]. Type 2b cells give rise to neuroblasts, also called type 3 cells, which migrate to deeper layers of the DG. Type 3 cells proliferate much less and exit the cell cycle and give rise to postmitotic immature granule cells which form nascent network connections (see **Figure 8 and Figure 9**) [233]. Some of these immature neurons eventually mature into new granule cells which project axons to the CA3 region of the hippocampus and receive input from the entorhinal cortex [203].

1: Introduction

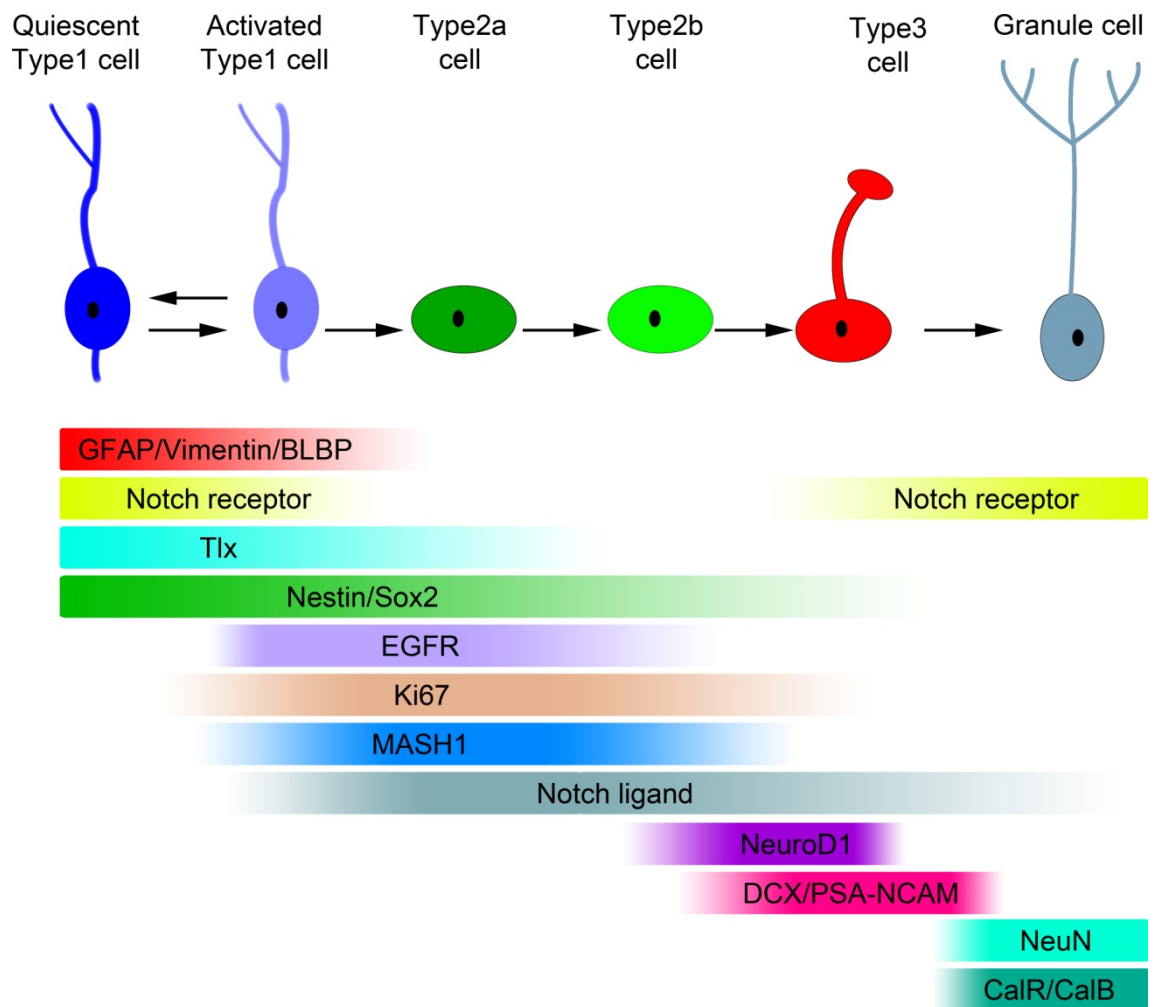


Figure 9 - Schematic illustration of the adult subgranular zone lineage. Type 1 cells are relatively quiescent and express astrocytic markers such as GFAP, vimentin and BLBP as well as Notch receptor, Tlx, Nestin, and Sox2. Upon activation, type 1 cells upregulate EGFR and become positive for cell cycle markers such as Ki67. MASH1 marks activated type 1 cells and their progression to type 2a cells. Type 2a cells downregulate astrocytic markers and Notch receptor and upregulate Notch ligand to induce Notch signalling in type 1 cells. Type 2a cells proliferate rapidly and form type 2b cells. As type 2b cells become more committed to the neural lineage they begin to upregulate NeuroD1 and downregulate EGFR. Type 2b cells form type 3 cells which express doublecortin (DCX) and polysialic acid neural cell adhesion molecule (PSA-NCAM). Type 3 cells downregulate stem cell markers such as Nestin and Sox2 as well as MASH1 and Notch ligand. Type 3 cells form new granule cells which express NeuN and low levels of Notch receptor. Immature granule cells initially express calretinin (CalR) and as the cell matures it downregulates CalR and upregulates calbindin (CalB).

1.10. Adult neural stem cell niches

The ability of SVZ and SGZ NSCs to act as the primary progenitors in the generation of new neurons is partly due to signalling that occurs in the NSC niche, and partly due to intrinsic differences between these stem cell astrocytes and non-stem cell astrocytes. When adult SVZ cells are transplanted to non-neurogenic regions they usually differentiate into parenchymous astrocytes [238]. Lim et al. discovered that transplantation of NSCs in the striatum accompanied by ectopic expression of an inhibitor of bone morphogenic protein (BMP) signalling, Noggin, promoted the cells to differentiate into neurons [239]. This suggests that the environmental signals around neurogenic astrocytes are essential for part of their function. However, when parenchymal tissue is transplanted to the SVZ of adult mice these astrocytes do not become neurogenic, suggesting that environmental signals, although important for NSC proliferation and differentiation, do not confer a neurogenic phenotype on astrocytes [240]. The adult NSC niches are thus able to instruct NSCs towards neurogenesis and gliogenesis. In addition to this, the hippocampal microenvironment has been shown to have an instructive role in stem cell fate. Studies by Shihabuddin et al showed that adult spinal cord stem cells transplanted into the hippocampus were instructed towards a neurogenic and gliogenic lineage characteristic of the hippocampus [241]. This suggests that common features may be present in the microenvironments of CNS stem cell niches [241].

Astrocytes, vascular cells, NSC progeny and mature neurons are the major cell types of the neurogenic niches, which can influence the behaviour of neural progenitors. Astrocytes have been shown to play roles in modulating NSC proliferation and differentiation as well as migration and differentiation of progenitors [242-245]. Mature neurons near the neurogenic site regulate neurogenesis in response to neuronal activity, and many neurotransmitters have been shown to play a role in regulating NSC proliferation [246-248]. Vascular cells are also thought to play a role in regulating proliferation of NSCs in the niches. Indeed, the SVZ has a unique specialised vasculature associated

with it, displaying a modified blood-brain barrier devoid of astrocyte end-feet and pericyte coverage [249-251]. The SGZ and SVZ niches therefore provide important signals to regulate neurogenesis.

1.10.1. Notch signalling in the neurogenic niches

NSCs are mostly quiescent and only certain subpopulations appear to be proliferating and forming transit-amplifying cells [252, 253]. Notch signalling has been shown to be an essential regulator of NSC quiescence and inhibition of NSC differentiation. Notch1-4, their cognate ligands, Jagged (Jag) 1, and Delta-like ligand (Dll) 1, and downstream effectors, Hes1 and Hes5, are expressed in the SVZ and SGZ [252, 254, 255]. Notch signalling is highly active in type B cells in the SVZ and type 1 cells in the SGZ [252, 253, 256]. Pro-neural gene products, such as the bHLH transcription factors Mash1 and Neurogenin 1 and 2, induce the expression of Notch receptor ligands as well as initiating the neuronal differentiating program [257, 258]. The downstream effectors of Notch signalling, Hes1 and Hes5, then repress the expression of pro-neural genes and *Dll1* thereby inhibiting neuronal differentiation (**Figure 10**) [259]. This lateral inhibition by a committed neural progenitor cell prevents neighbouring NSCs from differentiating [259]. Therefore, Notch signalling represents a mechanism by which the proliferation and differentiation of NSCs is regulated by the production of transit amplifying progeny.

Imayoshi et al. inhibited Notch signalling in the SVZ by deleting *RBPJk*, a DNA-binding protein that forms a complex with NICD to initiate Notch-dependent signalling (**Figure 10**), specifically from adult NSCs [256]. The authors showed that loss of Notch signalling resulted in a transient increase in SVZ proliferation and neurogenesis, followed by a depletion of the NSC pool [256]. This was caused by loss of NSC quiescence and exhaustion of the NSC pool due to premature conversion of type B cells to type C cells [256]. A similar phenotype was found by Ehm et al. in the hippocampus, where deletion of *RBPJ* in adult NSCs led to a loss of NSC quiescence and a transient increase in neurogenesis followed by a depletion of the stem cell pool [252]. Ables et al. found a slightly

different phenotype with the loss of *Notch1* receptor in adult hippocampal NSCs which resulted in the eventual loss of type 1 cells but without a transient increase in proliferation [260]. The reason for this difference is probably due to Notch signalling being inactivated to a greater level in *RBPJ* mutants, and also due to the fact that other Notch receptors are present in the SGZ [252, 261]. In addition, Androutsellis-Theotokis et al. demonstrated that NSCs are also regulated by RBPJ-independent Notch signalling [262]. The authors showed that Notch receptor activation can induce the expression of *Hes3* and *Shh* through rapid activation of STAT3, thereby promoting the survival of neural stem cells [252, 262]. These data depict an important role for Notch signalling in the regulation of NSC quiescence as well as progenitor differentiation.

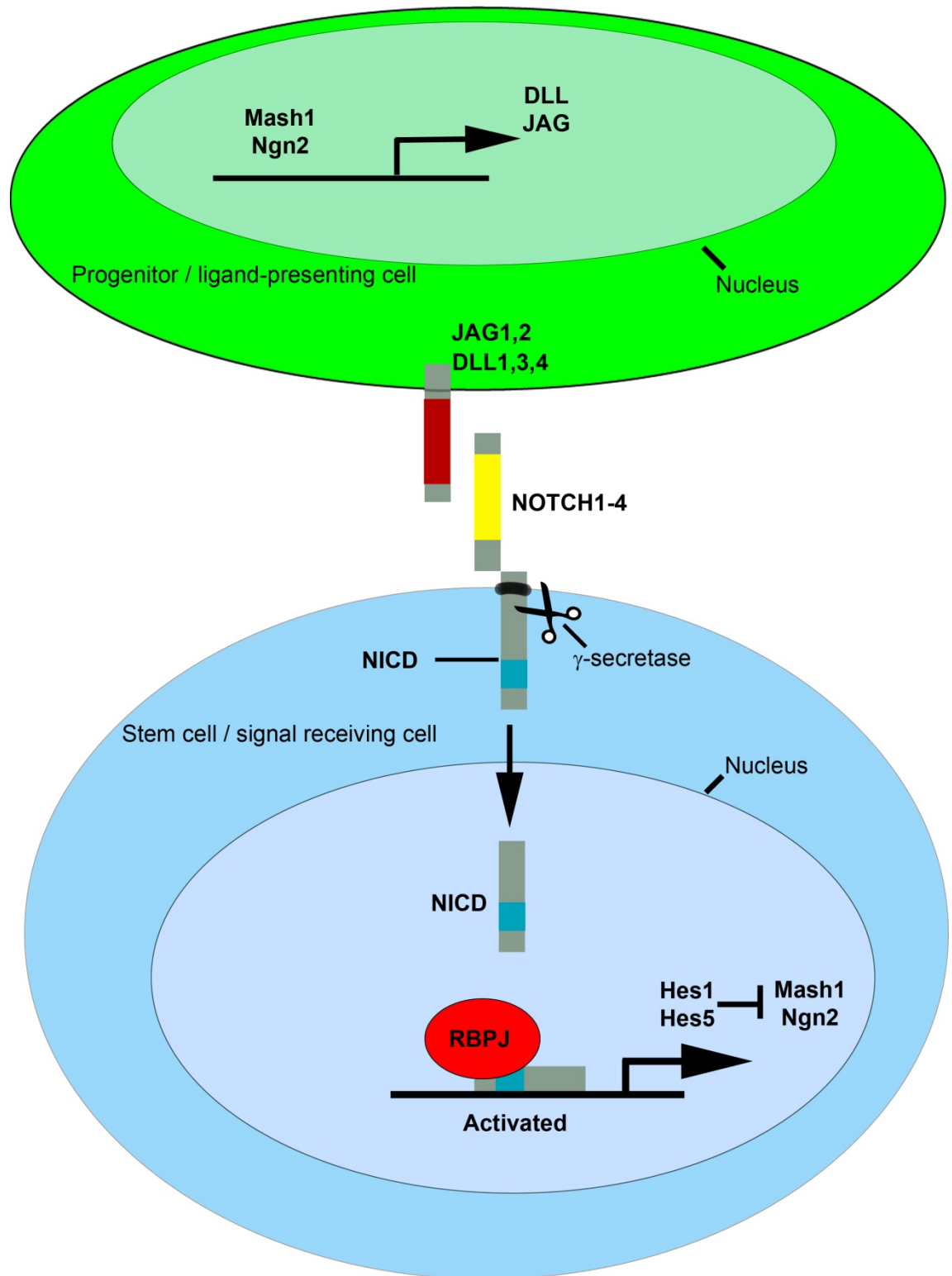


Figure 10 - Schematic illustration of Notch signalling in neural stem cells. The proneural proteins Mash1 and Ngn2 upregulate the expression of Notch ligands such as Dll1. Ligands activate Notch signalling in neighbouring cells. Upon Notch activation, Notch receptor is proteolytically cleaved by γ -secretase, freeing the Notch intracellular domain (NICD) from the cell membrane. The NICD then translocates to the nucleus where it forms a complex with RBPJ and induces the transcriptional activation of Notch target genes such as *Hes1* and *Hes5*. *Hes1* and *Hes5* repress proneural gene expression. Adapted from [263].

1.11. Survival of neural stem cell progeny in the hippocampus

The SVZ and SGZ produce a large number of immature neuroblasts, yet many do not go on to mature into new neurons and form stable synaptic contacts. In the hippocampus, programmed cell death is largely responsible for the numbers of new neurons formed and it has been shown that less than 30% of newborn cells in the hippocampus survive to be mature neurons [229, 233, 264]. There are two critical periods of survival of precursors and neurons, with most apoptosis taking place at the transit-amplifying to neuroblast stage, where newly born cells are between 2 and 4 days old, and a second period at the stage of maturation of immature neurons, where cells are between 1 and 3 weeks old [264]. The first period of survival is thought to limit the number of new neurons able to proceed down the neurogenic lineage, whereas the second period appears to be dependent on excitatory input, perhaps allowing for the selection of neurons with ideal electrophysiological properties [264, 265]. The few newborn neurons that do survive have been shown to remain integrated into the hippocampal synaptic circuitry for at least 11 months [266].

Just as there are mechanisms in place to limit the number of new neurons formed, there are also physiological stimuli that can increase the survival of newborn cells. Hippocampal dependent learning tasks can aid the survival of newborn cells up to one week old [267, 268]. Physical exercise has been shown to increase the proliferation and survival of type 2 and type 3 cells respectively, due, in part, to increased uptake of serum IGF1 in the brain parenchyma, leading to increased dentate neurogenesis [269-271]. In addition, exposing animals to an enriched environment can increase the survival of newborn

neurons in the SGZ without affecting SVZ neurogenesis [235]. Interestingly, these physiological stimuli only affect the behaviour of the progeny of NSCs and do not affect NSC behaviour. This suggests that NSCs are not responsive to acute fluctuations in changes in the environment, but are instead governed by NSC-specific genetic programs.

1.12. Survival of neural stem cell progeny in the SVZ-OB system

Between 15 and 45 days after being born approximately half of all newly generated SVZ cells undergo apoptosis, however, those that do survive are integrated into the OB for up to a year in mice [211, 219]. Hippocampal-dependent learning tasks, physical exercise, and an enriched environment all affect dentate neurogenesis but do not have any impact on OB neurogenesis. Instead, activity from the OB aids cell survival and causes an increase in proliferation of NSCs and their progeny in the SVZ [272-275]. Conversely, naris occlusion causes a decrease in neurogenesis by affecting the survival of new interneurons, mostly between two and four weeks after birth [273, 276]. Mice partaking in olfactory learning tasks show an increase in the survival of new interneurons involved with processing the odourants in the learning task [274]. Olfactory learning tasks involve training mice to associate a particular odour with a reward (a reinforced odour) as well as introducing a second odour that is not associated with a reward (non-reinforced odour). Interestingly, Alonso et al. showed that survival of newborn cells was also increased in the area of the OB responsive to the non-reinforced odour [274]. Additionally, exposure of animals to odourants without a learning paradigm (i.e. without a reward) did not affect new cell survival [274], suggesting there is an interplay between many factors in the physiological regulation of OB neurogenesis.

1.13. Heterogeneity of neural stem cells

Growing evidence suggests that the population of NSCs in both the SVZ and SGZ are heterogeneous in terms of their proliferative output and neurogenic potential. Due to inefficient lineage tracing however, it is not always possible to determine if activated NSCs represent a continuum in the neurogenic lineage or are instead discrete and separate populations. Instead, heterogeneity within the NSC pool is often inferred by morphological differences and surface marker expression.

1.13.1. Heterogeneity of SVZ NSCs

The morphology of SVZ B cells has been extensively studied to determine the ultrastructural characteristic differences between different types of stem cells, specifically activated and quiescent type B cells. A small subpopulation of B cells have an apical process that contacts the ventricle, and the number of cells contacting the ventricle appears to be increased when SVZ proliferation is stimulated, most probably allowing the stem cell to respond to activatory signals from the cerebrospinal fluid (CSF) [201]. Activation of SVZ stem cells is also associated with increased EGFR expression so that activated astrocytes are GFAP⁺EGFR⁺ [277]. Addition of EGF to NSC cultures increases the proliferation of progenitors, however there is a heterogeneous population of cells in these cultures and it is thought that type C cells are the main cells responding to EGF in these conditions [277].

Recent work shows that the plasticity of NSCs and progenitors in the SVZ is subject to regional specification. Postnatal RG and adult type B cells in different areas of the SVZ generate different types of OB neurons (**Figure 11**). This has been shown through the fate mapping of cells expressing different transcription factors in the SVZ and RMS in combination with lineage tracing of RG cells in restricted regions of the walls of the lateral ventricle in postnatal mice [278-282]. These data confirmed that NSCs from different regions of the SVZ ultimately gave rise to different types of periglomerular and glomerular interneurons. For

example, cells in the dorso-lateral aspect of the SVZ and RMS had a greater tendency to form tyrosine hydroxylase (TH)-positive interneurons in the glomerular layer of the OB (**Figure 11**) [207]. Thus, SVZ B cells have a regional limit to their plasticity as they inherit a regional pattern of gene expression from embryonic RG. Grafting experiments suggest that this specification is cell-autonomous and not dependent on the regional SVZ environment [223, 282, 283]. However, whether there is one stem cell population in the adult mammalian brain, which gives rise to this heterogeneous population, is still to be uncovered.

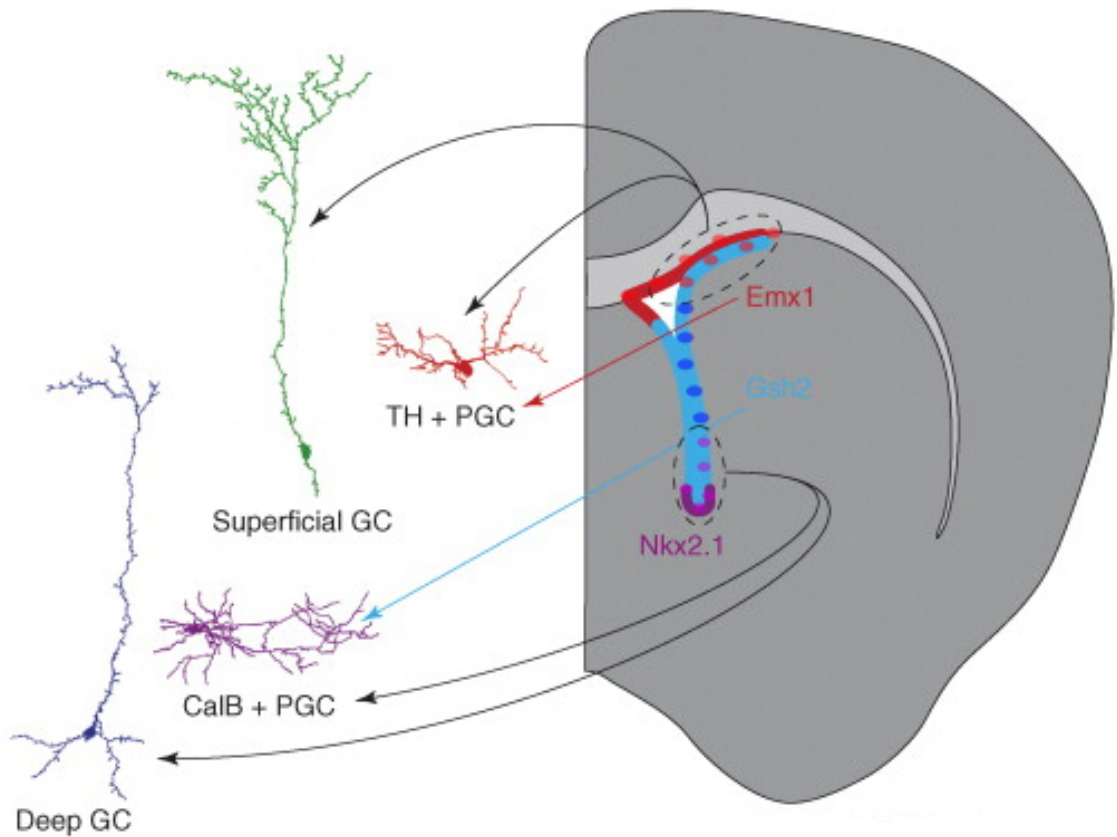


Figure 11 - Schematic illustration of the regional specification of SVZ cells. Labelling postnatal stem cells has shown that cells in the dorso-lateral aspect of the SVZ (dashed oval with red circles) produce mostly superficial glomerular cells (GCs; green) and TH⁺ glomerular cells (red). TH⁺ and some CalR⁺ periglomerular (PGC) OB interneurons are derived from Emx1-expressing progenitors (red arrow and red area). Deep GCs (blue) and CalB⁺ PGCs (purple) are produced primarily by lateral and ventral SVZ cells (dashed oval and purple circles). Some NSCs in this region express the transcription factors Gsh2 and Nkx2.1 (light blue and purple areas, respectively). Gsh2⁺ progenitors primarily produce CalB⁺ PGCs (light blue arrow). Adapted from [207].

1.13.2. Heterogeneity of SGZ NSCs

Two stem cell populations in the SGZ have been identified that possess different proliferative potentials and may be responsible for the neurogenic responses to different physiological stimuli. The quiescent NSC in the DG resides in the SGZ and extends processes perpendicularly through the granular layer and often into the molecular layer (**Figure 12**). In addition, a stem cell with horizontal astrocytic processes, running parallel to the SGZ, exists, and is much less quiescent (**Figure 12**) [233, 253, 284]. Studies by Lugert et al. have suggested that under homeostatic conditions, Notch-activated radial type 1 cells contribute very little to active dentate neurogenesis. Instead, Notch-activated horizontal NSCs are much more proliferative and may divide asymmetrically to form type 2 cells at a much greater rate than radial cells [253]. Whether horizontal astrocytes are derived from radial astrocytes is unknown, but during ageing this activated pool of NSCs is lost, resulting in decreased neurogenesis [253]. Despite both pools sharing a common dependence on Notch signalling, it is has yet to be uncovered whether they have different requirements for their maintenance and differentiation [253]. However, it has been shown that Notch-dependent radial NSCs respond to physical exercise and proliferate, without affecting the horizontal population [253]. In addition, seizures, a well documented stimulator of neurogenesis, increased proliferation of both Notch-dependent radial and horizontal NSCs (**Figure 12**) [253]. These findings are in contradiction with earlier studies, which suggests that radial SGZ NSCs do not respond to physical exercise [235, 267, 268]. Instead, these data indicate that Notch-activated NSCs may represent a distinct type of NSC, different from non-Notch-activated NSCs. Further study into these two populations with lineage tracing will uncover the true SGZ NSC lineage and their functional relevance.

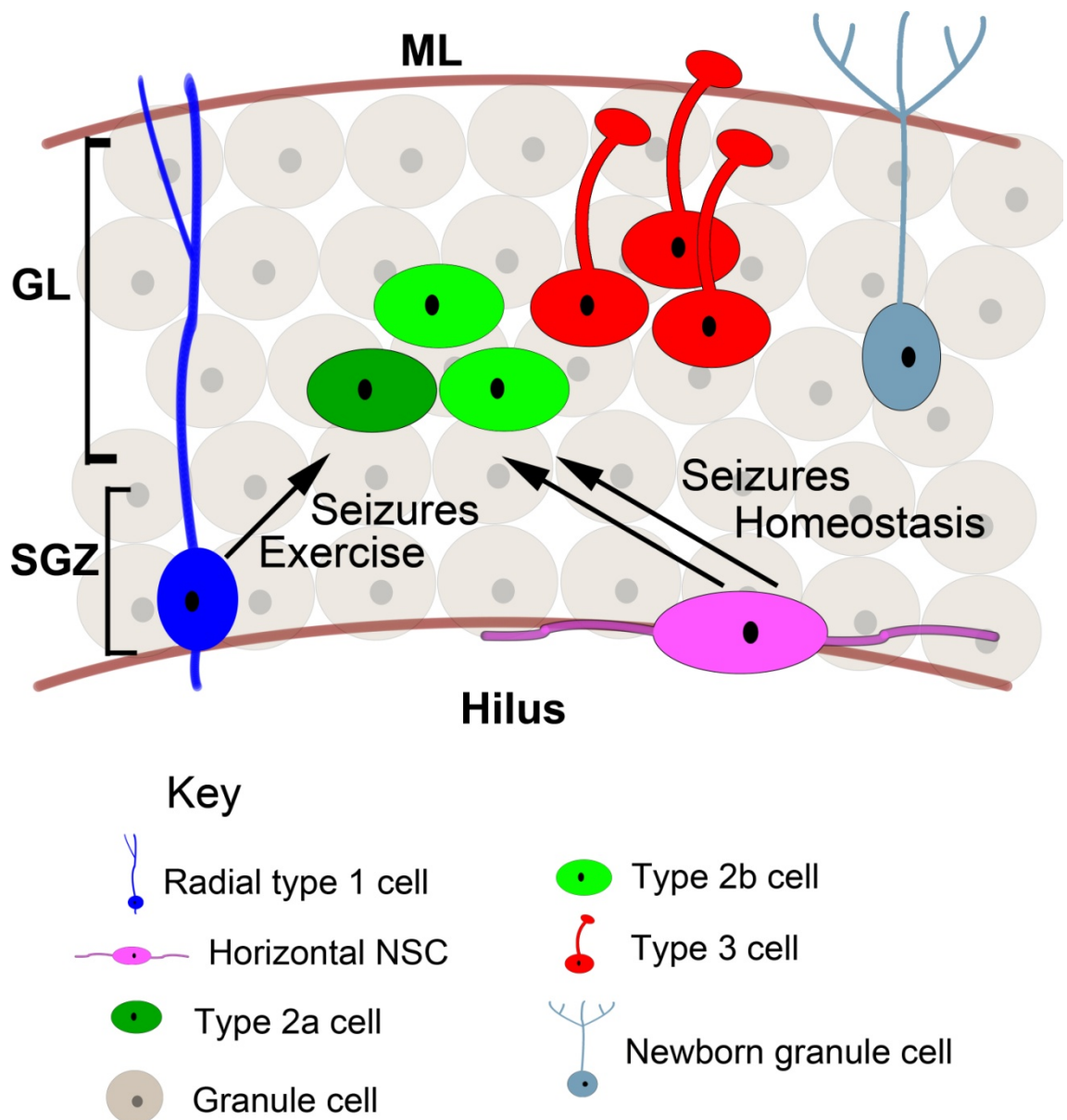


Figure 12 - Schematic illustration of radial and horizontal neural stem cells in the subgranular zone. Radial type 1 cells that have their cell body in the SGZ and extend astrocytic processes through the granular layer (GL) have long been proposed to be the NSC of the dentate gyrus. Under homeostatic conditions they are relatively quiescent. In response to physical exercise or seizures, Notch-dependent radial type 1 cells proliferate. Also in the SGZ resides a horizontal astrocyte, with astrocytic processes extending parallel to the SGZ. Under homeostatic conditions, Notch-dependant horizontal NSCs are relatively proliferative. They further increase their proliferative activity in response to seizures, but do not respond to physical exercise. ML, molecular layer.

1.14. Epigenetic control of adult neurogenesis

Epigenetic regulation of stem cell function is an emerging concept in the field of stem cell biology, and involves the regulation of gene transcription by DNA methylation, histone modifications, chromatin remodelling, and gene translation by microRNAs [285, 286]. These epigenetic changes permit cells to rapidly respond to internal and external physiological cues to coordinate the transition from one cellular state to another [286]. Chromatin remodelling has been shown to play a role in the differentiation and self-renewal of embryonic and postnatal neural stem and precursor cells [286], but there is now an emerging role for chromatin remodelling in the regulation of adult neurogenesis in both the SVZ and SGZ [287, 288].

1.14.1. Chromatin structure and remodelling proteins

Chromatin is structured in a way that not only allows great compaction of DNA within a nucleus, but also allows for the rapid activation and repression of potentially large sets of genes. Chromatin consists of DNA wrapped around histones to form nucleosomes and linker DNA in between nucleosomes (**Figure 13**). Tightly packed DNA in heterochromatic regions will generally be harder to access by transcription factors and polymerases (silenced chromatin regions), whereas DNA within linker regions and in a euchromatic state will generally be much easier to access (active chromatin regions). Chromatin can be silenced or activated through the action of proteins called chromatin remodellers. Some chromatin remodellers utilise energy from ATP hydrolysis to open up chromatin by evicting nucleosomes or inducing nucleosome sliding, as well as by mediating chromatin looping, and this can potentially have diverse effects on gene transcription (**Figure 13**).

There are two general groups for chromatin remodellers: trithorax group (TxG) proteins which usually cause the activation of their target loci, and polycomb group (PcG) proteins which tend to repress gene activation [289]. PcG and TxG proteins often form large multi-protein complexes that regulate chromatin

structure. PcG proteins usually belong to one of at least two complexes: Polycomb repressive complex (PRC) 1 and PRC2, whereas the composition of TxG complexes is heterogeneous. PcG and TxG proteins are antagonistic, evolutionary conserved chromatin complexes that can maintain gene expression states over many cell divisions [290] and often mediate gene expression through different histone modifications. For example, PRC2 contains Ezh2 (among other PRC2 components) which can catalyse histone H3 lysine 27 tri-methylation (H3K27me₃), leading to gene silencing. PRC1 can contain Ring1, an E3 ubiquitin ligase that mono-ubiquitylates histone H2A at lysine 119 (H2Aub₁), also resulting in gene silencing [291, 292]. The interplay between these two complexes can also lead to stable gene suppression [293, 294]. One model by which this happens involves the recruitment of PRC2 to specific loci where it catalyses H3K27me₃. The modified histones in turn recruit PRC1, which catalyses H2Aub₁ and thereby impedes gene transcription [295, 296]. In addition to these two complexes, other PcG complexes with different enzymatic activities can further regulate cellular biological processes [297].

TxG complexes can catalyse H3K4me₃ resulting in gene expression. However, it is unclear if TxG proteins cause gene activation by antagonising PcG function or by globally activating gene expression. The yeast SWI/SNF (switch/sucrose nonfermentable) subfamily was the first TxG chromatin remodelling complex to be discovered [298]. Mammalian SWI/SNF complexes comprise of the assembly of at least 14 subunits, allowing for an extensive diversity of complexes with specialised functions in specific tissues [299]. SWI/SNF complexes regulate the chromatin structure of a large number of genes involved in cell cycle regulation, cell signalling, and proliferation [299]. SWI-like ATP-dependent chromatin remodelling complexes are broadly divided into four main families based on the sequence and structure of the ATPase subunit: SWI/SNF, imitation-switch (ISWI), INO80, and CHD complexes. In addition, many predicted SWI-like proteins do not yet fit any of these classes and need further study [299]. Members of the SWI/SNF family are characterised by the presence of a bromodomain, which recognises acetylated lysine residues on histone tails [300]. The ISWI family of enzymes are characterised by a SANT domain, which

functions as a histone-binding module [301]. The INO80 member is the only chromatin remodelling enzyme in which DNA helicase activity has been observed [302]. Lastly, members of the CHD family are characterised by the presence of tandem N-terminal chromodomains and a central SNF2-like ATPase domain [303].

Many studies of histone modifications in ES cells have found that almost all sites of PcG activity not only carry the repressive H3K27me3 modification, but also carry the activating, TxG-associated H3K4me3 modification [304, 305]. These genomic regions are termed 'bivalent domains' and keep target loci in a silenced but poised state. Upon ES cell differentiation, many bivalent domains resolve. Induced genes become enriched for H3K4me3 and lose H3K27me3, while many non-induced genes retain H3K27me3 but lose H3K4me3 [305, 306]. These data show the dynamic modulation of histone modifications in stem cell maintenance and differentiation.

Chromatin remodelling can engage or maintain particular genetic programs and therefore likely plays a critical role in both stem cell maintenance as well as daughter cell differentiation. Maintaining stem cell properties involves the epigenetic suppression of pro-neural and glial genes and the activation of genes involved in self-renewal and quiescence. Conversely, NSC differentiation involves the removal of pro-neural gene suppression and instead involves the inhibition of genes involved in NSC maintenance. Recently, Lim et al. showed that the expression profiles of many epigenetic genes, such as genes encoding chromatin remodelling proteins, is altered along the adult neural lineage in the adult SVZ-OB system [287]. These data implicate the process of chromatin remodelling in playing a critical role in adult neurogenesis [287].

One of the most well studied PcG proteins in adult and postnatal neurogenesis is Bmi1 (B lymphoma Mo-MLV insertion region 1 homolog). Bmi1 is a member of the PRC1 complex and positively regulates H2Aub1 [307]. Mice deficient for *Bmi1* (*Bmi1*^{-/-}) displayed a loss of SVZ NSCs [308]. In contrast, lineage-restricted progenitors were not affected and this was shown to be mediated at least in part by p16 [308]. However, short hairpin-RNA (shRNA)-mediated

knockdown of *Bmi1* in the post-natal SVZ showed that *Bmi1* does negatively influence progenitor proliferation *in vitro* [288, 309]. This was shown to be partly due to elevated p21 levels, suggesting that NSC and progeny devoid of *Bmi1* throughout development may develop compensatory mechanisms to maintain neurogenesis, albeit to a much lesser extent [288, 309]. Furthermore, it has been found that loss of *Bmi1* leads to increased astrocyte formation both *in vivo* and *in vitro* [310, 311]. Conversely, lentiviral-mediated overexpression of *Bmi1* *in vitro* increased the self-renewal of NSCs, and increased SVZ proliferation and neurogenesis *in vivo* [312]. Interestingly, overexpression of *Bmi1* also led to the presence of large growths in the brain, indicating that prolonged expression of *Bmi1* could result in tumour formation [312]. Indeed, Cui et al. showed that *Bmi1* is expressed at high levels in several human neuroblastoma cell lines, but at very low levels in many glioblastoma lines [313]. When *Bmi1* levels were reduced via short interfering RNA (siRNA) in neuroblastomas, cells gave fewer tumour colonies, and formed a smaller number and size of tumours when injected into mice [313]. However, one study found no effect of *Bmi1* overexpression on NSC proliferation in either the SVZ or SGZ *in vivo*, suggesting that further analysis may be required [314].

Mixed-lineage leukemia 1 (*Mll1*) is a TxG member with H3K4 methyltransferase activity [315]. *Mll1* is expressed by cells in the SVZ and has been shown to play a role in postnatal neurogenesis [316]. Loss of *Mll1* from embryonic and postnatal NSCs revealed a role for *Mll1* in neuroblast migration and differentiation [316]. This was due to a direct effect of *Mll1* on suppressing the accumulation of repressive H3K27me3 at the locus of gene encoding the neuron-specific transcription factor *Dlx2* [316]. Loss of *Mll1* resulted in the accumulation of H3K27me3 and repression of *Dlx2*, causing impaired neuroblast differentiation and migration [316].

As well as regulating stem cell self-renewal and differentiation, chromatin remodelling enzymes and other epigenetic factors can also regulate cell fate choices [317-319]. BRG1 (brahma-related gene 1, also called SmarcaA2) is a TxG chromatin remodelling protein with helicase and ATPase activity that

belongs to the SWI/SNF family of complexes [289]. BRG1 has been shown to play a role in the regulation of the waves of neurogenesis and gliogenesis in embryonic development. Loss of *Brg1* caused premature neuronal differentiation and little gliogenesis, with cells being unable to respond to gliogenic cues [317]. This suggests that BRG1 is required to repress neuronal differentiation in NSCs as a means of permitting glial cell differentiation in response to gliogenic signals [317]. Taken together these data show that chromatin remodelling can potentially affect many areas of stem cell biology, such as stem cell maintenance, proliferation, and cell fate decisions.

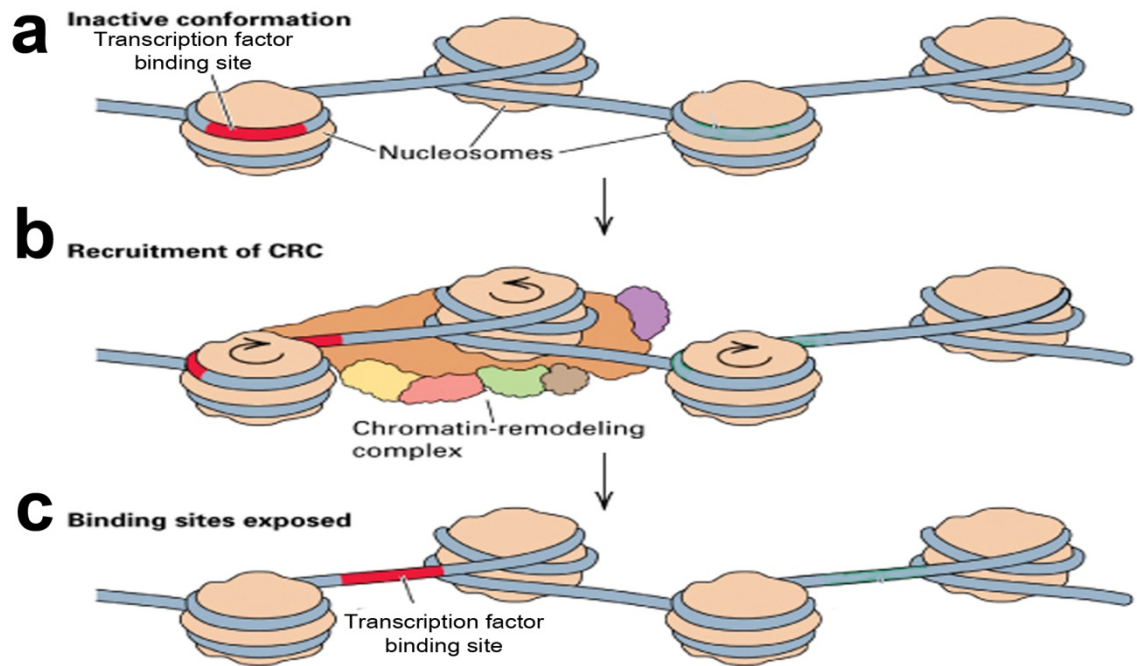


Figure 13 - Schematic illustration of the action of chromatin remodelling complexes.

Chromatin consists of DNA associated with histones to form nucleosomes and linker DNA in between nucleosomes. **a**, DNA and transcription factor binding sites associated with nucleosomes will generally be harder to access by transcription factors and polymerases compared to DNA in linker regions. Some large multi-subunit chromatin remodelling complexes can utilise the energy of ATP-hydrolysis to physically move nucleosomes or alter the structure of DNA within a nucleosome (**b**). This can lead to the exposure of previously inaccessible transcription factor binding sites and the silencing of others (**c**) leading to potentially diverse effects on gene transcription. Adapted from [320].

1.14.2. CHD proteins

The CHD (chromodomain-helicase-DNA-binding) family are SWI-like ATP-dependent chromatin remodelling proteins that have been predicted to act as part of large multi-subunit complexes [321, 322]. The CHD family consists of nine members divided into three subfamilies based on the presence of structural protein motifs [322]. The first subfamily includes CHD1 and CHD2, which contain a C-terminal DNA-binding domain. The second subfamily includes CHD3 and CHD4 which lack a DNA-binding domain and instead contain a pair of N-terminal PHD domains which may bind to nuclear proteins and nucleosomes [323]. The third subfamily includes CHD5 to CHD9. Members of this subfamily possess additional functional motifs such as SANT domains, BRK domains, CR domains, and a DNA-binding domain [303, 324-326]. However, these additional domains are not shared between subfamily members. Mutations in *CHD* genes have recently been implicated in human diseases. For example, mutations in *CHD8* has been shown to play a role in autism spectrum disorder, and may account for up to 0.4% of cases [327]. Additionally, mutations and deletions in *CHD5* have been associated with neuroblastoma development [328, 329].

1.14.3 CHD7

Mutations in *CHD7* have recently been implicated in human diseases. *De novo* mutations in *CHD7* is one of the leading causes of CHARGE syndrome, a congenital defect characterised by coloboma of the eye, heart defects, atresia of the nasal choanae, retardation of growth, genital and ear abnormalities and deafness [330]. Mutations in *CHD7* have also been implicated in Kallman syndrome, characterised hypogonadism and anosmia [331].

The CHD7 protein contains functional domains such as a chromodomain, SNF2-related helicase / ATPase and two tandem C-terminal BRK domains [321] (**Figure 14**). CHD7 binds to areas of methylated H3K4, with the majority of CHD7 sites overlapping with H3K4me1/2. CHD7 has been shown to bind to

regions distal to the transcription start site that show features of gene enhancer elements including hypersensitivity to DNase I digestion and colocalisation of the enhancer binding protein, p300 [332-335]. This interaction is predicted to be mediated by tandem N-terminal chromodomains and is thought to function to fine-tune cell type-specific gene expression (**Figure 14**) [332, 333].

ChIP-Seq data from mouse ES cells combined with global gene expression profiles obtained from *Chd7*^{+/+}, *Chd7*^{+/-}, and *Chd7*^{-/-} ES cells shows that CHD7 can either repress or stimulate gene expression, although negative regulation appears to be the more direct effect of CHD7 binding [332]. The *Chd7* Drosophila ortholog, *Kismet*, encodes a TxG protein [336-338]. Kismet stimulates transcriptional elongation by RNA polymerase II and may counteract PcG repression by recruiting the histone methyltransferases ASH1 and TRX to target loci [339]. Kismet itself is unable to bind methylated histone tails and was not found associated with methylated H3K4 [339]. Interestingly, Melicharek et al. showed that adult flies with decreased Kismet protein, displayed defects in gross motor coordination and defective learning and memory, and showed multiple neuronal populations to have defects in cell and axonal migration [340]. In mouse ES cells, CHD7 binding sites colocalise with binding sites of ES cell master regulators OCT4, Sox2, and NANOG, suggesting that CHD7 may have a wide variety of roles in ES cell maintenance and differentiation [332]. Indeed, in embryonic NSCs, CHD7 was shown to directly interact with Sox2 to regulate target gene expression, with common target genes including downstream effectors of the Notch and Sonic hedgehog (Shh) signalling pathways [341].

In addition to stem cell maintenance, CHD7 has been implicated in regulation of cell fate specification from adipogenesis to osteoblastogenesis of bone marrow mesenchymal stem cells during development [342]. CHD7 has also been shown to cooperate with PBAF (polybromo- and BRG1-associated factor-containing complex) to promote neural crest gene expression and cell migration during embryogenesis [343]. These data show that CHD7 has diverse roles in the regulation of fate specification, cell migration, and stem cell maintenance.

Mice homozygous for a *Chd7* loss-of-function allele die before E10.5 [344], thus the use of a conditional allele or heterozygous lines are necessary to study the effect of CHD7 later in development and in adulthood. Adult mice heterozygous for *Chd7* (*Chd7*^{+/-}) display a decreased brain size and decreased OB length [345, 346]. In addition, studies by Layman et al. showed that *Chd7*^{+/-} mice displayed a reduction in TH expression in the OB [345]. The authors showed that CHD7 was expressed by MASH1⁺ stem cells in the olfactory epithelium, and reduction in *Chd7* expression led to decreased proliferation of the epithelial stem cells [345]. This resulted in a decrease in the number of mature olfactory sensory neurons, which normally signal to dopaminergic interneurons [345]. Hence, a loss of signal to dopaminergic interneurons resulted in a decrease in TH-production (see **Figure 35**) [345]. These data implicate CHD7 in regulation of stem cells in adults. However, due to the role of postnatal and adult SVZ-OB neurogenesis in formation of OB interneurons, misregulation of olfactory epithelial stem cells may not be the sole cause of the OB defects seen in these mice (see **Figure 36**).

Collectively, these data strongly implicate a role for CHD7 in adult neurogenesis.

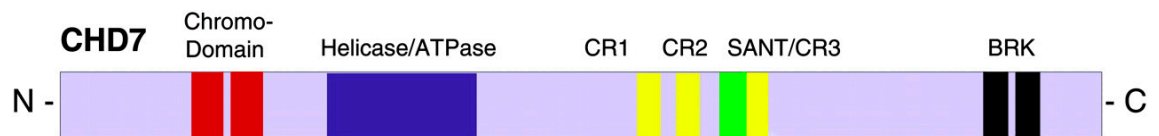


Figure 14 - Overview of the protein structure of CHD7. CHD7 is a large protein over 300kDa in size (CHD7_HUMAN, Q9P2D1). It contains tandem N-terminal chromodomains (red) that mediate binding to methylated histones, specifically all methylated forms of H3K4 [333]. It contains a helicase / ATPase domain (blue) that defines the ATP-dependent chromatin remodelling proteins and mediates chromatin remodelling [321]. It contains three conserved region domains (CR1-3; yellow) and a switching-defective protein 3, adaptor 2, nuclear receptor corepressor, transcription factor IIIB (SANT) domain (green) which is believed to function as a histone tail-binding module [301]. CHD7 has tandem N-terminal BRK domains (black), the function of which is still unknown, but may allow binding of CHD7 to certain proteins such as the transcriptional repressor CTCF [347]. Adapted from [348].

1.15. Aims and objectives

The maintenance and differentiation of somatic stem cells is strictly controlled. Extrinsic signals, such as from the niche, and intrinsic changes, such as from chromatin remodelling, can greatly impact stem cell function. Still many questions remain in understanding somatic stem cell function:

- What is the role of chromatin remodelling in somatic stem cells?
- How are the steps of activation and repression of key genes orchestrated with regards to stem cell activation, proliferation, differentiation and self-renewal?
- How does the niche influence somatic cell function under homeostatic conditions?
- How do age-related changes in mammalian stem cell niches drive changes in stem cell number, and how does this influence stem cell function?

This thesis aims to examine intrinsic and extrinsic regulators of two different somatic stem cell systems; skeletal muscle satellite cells and neural stem cells. This will help to better understand the regulation of stem cell quiescence and cell fate decisions, which are two fundamental properties of somatic stem cells and allow for the maintenance of a functional stem cell pool throughout life. I will examine the consequences of an altered stem cell niche on stem cell number and function. Additionally, I will analyse the effects of an altered intrinsic regulation of somatic stem cells.

Chapter 2

Methods

2.1. Solutions and reagents

Unless otherwise stated, all PBS and water solutions used in RNase-sensitive protocols were treated with 0.05% diethyl pyrocarbonate (DepC; Sigma) and autoclaved. All other stock solutions were sterilised by autoclaving. All water used was double distilled/deionised (ddH₂O).

2.1.1. General reagents

1x PBS	Phosphate buffered saline tablets (Sigma) were dissolved in ddH ₂ O
PBSTx	1ml TritonX (Sigma) was added to 1l of PBS prior to use to make 0.1%.

2.1.2. Immunohistochemistry reagents

Heat-inactivated goat serum	Goat serum (Sigma) heat inactivated at 50°C for 1 hour and stored in aliquots at -20°C
Blocking solution	10% heat-inactivated goat serum, 0.2% gelatin type A, made up with PBSTx
Antibody blocking solution (Ab block)	5% heat-inactivated goat serum, 0.2% gelatin type A, made up with PBSTx
Blocking solution for antibodies raised in goat	5% bovine serum albumin (BSA; Sigma) made up with PBSTx
Ab block for antibodies raised in goat	2% BSA made up with PBSTx
4% (w/v) PFA	Paraformaldehyde (PFA; Sigma) was dissolved in PBS with stirring and heating at 60°C. Aliquots were stored at -20°C
2N HCl	Made by diluting 11N HCl (Sigma) in ddH ₂ O
0.1M Borate buffer pH8.5	Made by dissolving sodium borate (Sigma) in ddH ₂ O and adjusting the pH to 8.5 with boric acid (Sigma)

2.1.3. Plasmid linearisation and mRNA probe synthesis reagents

Tris-EDTA (TE) buffer	1mM TRIS-HCl, pH 7.5 0.1mM EDTA Made in ddH ₂ O
Plasmid digestion reaction mix	Made according to manufactures specifications (NEB): 10µl plasmid (~5µg) 2µl restriction endonuclease; EcoR1, EcoRV, Spal 5µl 10x buffer 0.5µl BSA (if required) 33µl ddH ₂ O
Probe synthesis reaction mix	Made according to manufacturer's (Roche) specifications: 10µl sterile, distilled water 4µl 5x transcription buffer 2µl 0.1M DTT 2µl DIG nucleotide mix, pH8 1µl linearised plasmid at 1µg/µl 0.5µl Rnase inhibitor 1µl RNA polymerase enzyme; SP6 (Promega), T3 (Promega) or T7 (Promega) Made according to manufacturer's (Roche)

2: Methods

Probe synthesis from	specifications:
PCR primers	0.5ml sterile, distilled water
	4 μ l 5x transcription buffer
	2 μ l 0.1M DTT
	2 μ l DIG nucleotide mix, pH8
	10 μ l DNA
	0.5 μ l RNase inhibitor
	1 μ l RNA polymerase enzyme; SP6 (Promega), T3 (Promega) or T7 (Promega)

2.1.4. Section *in situ* hybridisation reagents

Acetylation solution	625µl trietholamine (Fluka) 130µl 11N HCl (Sigma) 125µl acetic anhydride (Fisher scientific) Made up to 50ml with DepC-treated sterile water immediately prior to use.
Proteinase K solution	20µg/ml proteinase K in PBS
Section hybridisation buffer	To make 100ml: 50ml formamide 20ml Dextran sulphate (Millipore) 1ml Denhardt's solution (Sigma) 2.5 ml 10mg/ml yeast tRNA (Invitrogen) 6ml 5M NaCl 2ml 1M Tris-HCl, pH8 1ml 0.5M EDTA 1ml 1M NaPO ₄ 5ml 20% Sarcosyl (Sigma) 11.5ml ddH ₂ O. Aliquots were stored at -20°C
5x standard saline citrate (SSC)	20xSSC (Sigma) was diluted 4 times in ddH ₂ O.

2: Methods

2xSSC	20xSSC was diluted 10 times in ddH ₂ O.
0.1xSSC	20xSSC was diluted 200 times in ddH ₂ O.
High stringency wash (His)	Formamide (Sigma) and 2xSSC were mixed in equal measures to produce the required volume of His.
RNase buffer	100ml 5M NaCl 10ml 1M Tris-HCl, pH7.5 10ml 0.5M EDTA Made up to 1L with ddH ₂ O and stored at room temperature.
RNaseA solution (10mg/ml)	100µl 1M Tris-HCl, pH7.5 30µl 5M NaCl 9.8ml distilled water 100mg RNaseA (Roche) Boiled for 15 minutes before aliquoting and storing at -20°C.
PBSTw	1ml Tween 20 (Sigma) in 1L PBS to make a 0.1% solution

2: Methods

Antibody block 10% heat inactivated goat serum in PBSTw

Sodium (Na) chloride- 1ml 5M NaCl

Tris-magnesium- 5ml 1M Tris-HCl, pH9.5

Tween20 buffer
(NTMT) 1.25ml 2M MgCl₂

5ml 10% Tween20

100µl 20mg/ml Levamisole

Made up to 50ml with water immediately prior to use.

2.1.5. Wholemount *in situ* hybridisation reagents

50% methanol	Methanol (Sigma) diluted in PBSTw
30% methanol	Methanol diluted in PBSTw
Hyb ⁻ pre-hybridisation mix	250ml Formamide 122.5ml ddH ₂ O 125ml 20x SSC 2.5ml 20% Tween 20
Hyb ⁺ pre-hybridisation mix	495ml Hyb ⁻ mix 2.5g yeast tRNA (Sigma) 5ml 50µg/ml Heparin (Sigma)
Hybridisation mix	4ml Hyb ⁺ mix with 2µg probe
Maleic acid buffer containing Tween 20 (MABT)	For a 5x stock: 500ml maleic acid pH 7.5 (Sigma) 750mM NaCl 0.5% Tween 20
Antibody block	10% BSA 2% Foetal calf serum (Sigma) Made in PBS

2.1.6. Satellite cell isolation and culture reagents

DMEM	Dulbecco's modified eagle's medium (Sigma) supplemented with 1% penicillin-streptomycin (Invitrogen)
Ham's F10	Ham's F10 nutrient mixture supplemented with 1% penicillin-streptomycin
Freezing medium	90% foetal calf serum (Invitrogen) 10% dimethyl sulfoxide (DMSO)
Cell dissociation solution	Non-enzymatic cell dissociation solution (Sigma)
Growth media	20% heat-inactivated foetal bovine serum (FBS) 5ng/ml FGF2 (R&D Systems) In Ham's F10 media
FACS-isolated SC basal media	DMEM + 5% Horse Serum (HS; Sigma)
Digest solution 1	0.2% Collagenase II (Invitrogen) 15ml total volume for up to 3 animals made in DMEM

2: Methods

Rinsing solution	10% HS 2mM HEPES In Ham's F10 media
Digest solution 2	0.015% Collagenase II 0.07% Dispase (invitrogen) In 7ml Rinsing solution
Single fibre digest solution	0.2% Collagenase I (Invitrogen) Made in DMEM
RSC generation media / SC differentiation media	3% HS Made in DMEM
Cell sorting media	10% HS Made in Ham's F10 media

2.1.7. Neural stem cell culture reagents

Euromed-N	Euromed-N (Euroclone) supplemented with 1% penicillin-streptomycin (Invitrogen)
Freezing medium	90% foetal calf serum (Invitrogen) 10% dimethyl sulfoxide (DMSO)
1x Trypsin-EDTA	1x Trypsin EDTA made by diluting 10x Trypsin-EDTA (Invitrogen) in DMEM
Growth media	20ng/ml human FGF2 (Peprotech) 20ng/ml human EGF (Peprotech) 1% N2 supplement (Invitrogen) In Euromed-N
3day Neuronal differentiation media	10ng/ml FGF2 0.5% N2 supplement 1% B27 supplement (Invitrogen) In Euromed-N
6day Neuronal differentiation media	After the 3day neuronal differentiation step: 10ng/ml FGF2 20ng/ml BDNF (Peprotech) 0.5% N2 supplement 1% B27 supplement In Euromed-N

2.2. Animals

Line	Description	Reference
<i>Pax7^{CreERT2/+}</i>	The CreERT2 cassette was placed within the 3' untranslated region of the Pax7 gene following the stop codon in exon 9.	[349]
<i>Spry1^{flox}</i>	The complete <i>Spry1</i> ORF is flanked with LoxP sites.	[350]
<i>CAG–GFP^{flox}; Spry1 (Spry1OX)</i>	Consists of chicken β -actin gene (CAG) promoter-loxP-GFP-loxP-Spry1ORF with a myc/his tag. The Spry1OX construct constitutively expresses GFP, and upon Cre-mediated recombination, Spry1 expression is induced, with concomitant loss of GFP marker expression.	[351]
<i>FgfR1/2^{flox/flox}</i>	For <i>FgfR2^{flox/flox}</i> , a 5' loxP site was inserted in the intron between exon 7 and 8, and a 3' loxP site was inserted in the intron downstream of exon 10. For <i>FgfR1^{flox/flox}</i> , exons 8–15 encoding the transmembrane domain, juxtamembrane domain and most of the tyrosine kinase domain of FGFR1, are flanked by loxP sites.	[352, 353]
<i>GLAST::CreERT2</i>	The CreERT2 expression cassette was inserted into a BAC with GLAST genomic DNA by homologous recombination at the transcription initiation site.	[354]
<i>Chd^{xk403/+}</i> (<i>Chd7^{gt/+}</i>)	The genetrapp construct contains a beta-geo cassette with a floxed splice acceptor. The Chdxk403 line has a genetrapp insertion site between exons 36 and 37, and produces a protein containing all exons, except 37 and 38, fused to the gene trap cassette. Cre-mediated recombination results in deletion of the splice acceptor site and loss of β -galactosidase activity.	[355, 356]

2: Methods

<i>Chd7^{fllox}</i>	Exon 3 of <i>Chd7</i> flanked by LoxP sites	EUCOMM ID: 35714
<i>NestinCre</i>	Transgenic mouse line.	[357]

Table 1 - Mouse lines used

2.3. Methods for Chapter 3 and Chapter 4

2.3.1. Satellite cell *in vivo* cell division analysis

To assess cell proliferation and label retention character, aged (24-28 months old) and adult (3-8 months old) C57BL/6, Ctrl, Spry1null and Spry1OX mice were fed BrdU (Sigma; 0.5 mg/ml supplemented with 5% sucrose) continuously for six weeks. For label retention studies, Spry1null mice were given three daily intraperitoneal (I.P.) injections of tamoxifen (see Section 2.3.9.) following BrdU loading and placed on regular drinking water to chase label. For cell proliferation and label retention studies, SCs were sorted, immediately fixed and processed for immunostaining with Pax7 and BrdU antibodies after sodium citrate antigen retrieval. For label retention studies, BrdU⁺ SCs were classified as label retaining on the basis of quantification of BrdU fluorescent intensity.

2.3.2. *In vivo* FGFR inhibition

Prolonged pharmacological inhibition of FGF activity *in vivo* was conducted as previously described [358]. Initially, anion exchange resin beads (AG1x2, 200-400, CL, CAT# 1401251, BioRad) were reconstituted at a beads/PBS ratio of 1:2. Half of the PBS-bead mixture was pelleted at 2,400g for 5 minutes. Pellets were then incubated with 500 μ M SU5402 (Calbiochem) or an equivalent volume of vehicle (DMSO) for 60 minutes on a nutator at room temperature. Loaded pellets were washed in PBS and reconstituted into 50% w/v PBS before I.P. injection of 300 μ l into aged and adult mice using a 25G5/8 1-ml insulin syringe (BD Biosciences). After injection, mice were fed BrdU continuously for six weeks before isolation of SCs. SCs were subsequently fixed and processed

for BrdU immunostaining via sodium citrate antigen retrieval. For quantification, 300–600 cells were counted per condition.

2.3.3. Purified myofibre extract

All reagents used to obtain purified myofibre extract are shown in **Section 2.1.6**. Initially, forelimb and hindlimb muscles were cut into smaller longitudinal pieces and digested into single or smaller groups of muscle fibres using digest solution 1 in a horizontal shaking water bath at 37 °C for 90 minutes [42]. Isolated muscle fibres were gently triturated and repeatedly washed in PBS (x6) to ensure removal of interstitial cells or other contaminating debris. Purified fibres were then incubated in a high-salt extraction buffer (400 mM NaCl, 1 mM EGTA, 1 mM EDTA, 10 mM Tris pH 7.5, 1mg/ml PMSF) to dissociate any ligands bound to receptors or the extensive basal lamina network of skeletal muscle fibres [359]. Dissected muscles in extraction buffer were further triturated with a glass Pasteur pipette to dissociate bound ligands. The muscle fibre mixture was centrifuged at 2,500g for 10 minutes to remove cytoskeletal and nuclear elements that compromise the majority of skeletal muscle fibre cytosol. The resultant supernatant was collected and spun at 375g for 5 minutes. Supernatant was then collected and transferred into Eppendorf tubes and spun at 16,500g for 30 minutes at 4 °C. The supernatant was pooled and subsequently drawn up into a 20-gauge syringe and filtered through a 0.45- μ m filter into Amicon Ultra centrifugal filter columns (10,000 relative molecular mass cut-off; UFC901008, Millipore). Exchanges with PBS were done at 2,050g for 20 minutes until the solution was translucent and concentrated into a volume of approximately 1 ml PBS. Protein concentration and purity was determined with a nanodrop analyser.

To assess cycling-inducing activity, cultures of RSCs and SCs in basal medium (3% HS for RSCs and 5% HS for satellite cells in DMEM) were incubated with 10 μ g total PME for 24 hr. For inhibition of FGF activity, RSCs and SCs were incubated with 10 μ M SU5402 (Calbiochem) or DMSO as carrier control for 1 hour before incubation with PME. For FGF2 neutralization, niche extracts were

incubated with 15 ng/ μ l FGF2 blocking antibody (Millipore) for 1 hour at 37°C before being added to RSC or SC cultures. Unless otherwise stated, three to five experiments were performed in triplicate and 300–600 RSCs or SCs were counted. PME were obtained from n = 5 different aged and adult mice and examined.

2.3.4. Single muscle fibre isolation

All reagents used for single muscle fibre isolation are shown in **Section 2.1.6**. Single fibres were isolated as previously described [360]. Briefly, EDL muscle was dissected and lightly digested in single fibre digest solution and incubated at 37°C shaking for 45 minutes to 1.5 hours. Following digestion, the muscle was transferred to a petri dish containing DMEM and triturated with a fire-polished Pasteur pipette pre-flushed in 10% HS to stop fibres from sticking to the pipette. Fibres were cleaned by transferring them to fresh petri dishes four times. Single fibre assays were performed using DMEM+3%HS and stated concentrations of FGF2 and/or PME.

2.3.5. Tibialis anterior muscle preparation

Dissected tibialis anterior (TA) muscle was fixed in 4% PFA for 20 minutes on ice and cryoprotected in 30% sucrose at 4°C overnight. Muscle was then frozen in OCT and sectioned in 10 μ m steps. For FGF2 immunohistochemistry, TA muscle was sectioned and stained immediately after cryoprotection and freezing without being fixed in PFA.

2.3.6. Myoblast isolation

All reagents used for myoblast isolation are shown in **Section 2.1.6**. SCs were isolated from bulk fibres as previously described [42] with modifications. Bulk skeletal muscle from hindlimbs, triceps and the lower back was digested in

digest solution 1 at 37°C for 75 minutes shaking. Contaminating adipose tissue was then removed through rinses in rinsing solution. Muscle was then physically dissociated by triturating with a jagged-edged glass Pasteur pipette in rinsing solution. To further remove any contaminating cells, the solution was centrifuged at 375g for 5 minutes and washed in rinsing solution 3 times. To remove individual fibres and associated SCs from the muscle tissue, the solution was resuspended in Digest solution 2 and incubated at 37°C for 30 minutes. Cells were dislodged from fibres by drawing and releasing the solution through a 20g needle 5 times. The solution was then centrifuged at 375g for 5 minutes and washed in rinsing solution 3 times. Cells were resuspended in 20% foetal bovine serum (FBS; Sigma), 5ng/ml FGF2 (Peprotech) with 1% Pen/Strep (Invitrogen) in Ham's F-10 (Growth media) and plated on uncoated tissue culture dishes for 5 minutes to remove fibroblasts. SCs in the supernatant were collected, centrifuged at 375g for 5 minutes, resuspended in growth medium and strained through a 20µm filter. To further remove fibroblasts, the Easy Sep Kit (Invitrogen) was used in combination with a Biotin-tagged anti-Sca1 antibody (BD Pharmingen; 1:400). Cells were then grown in growth media on 1:1000 ECM-coated tissue culture dishes (Nunc) with media changed every 1.5 days and passaged at 80% confluency using 1x cell dissociation solution (Sigma).

2.3.7. Myogenic cell preparation

To generate RSC cultures [361], low-passage primary myoblasts were plated in 1:500 ECM-coated eight-well Permanox chamber slides (Lab-Tek) at 80–90% confluency and maintained in growth medium (20% FBS, 5 ng/ml FGF2 in Ham's F-10). Subsequently, cells were switched to differentiation medium (3% HS in DMEM) for two to three days to allow for the formation of myotubes and SC-like RSCs expressing Pax7 that had escaped differentiation and returned to a quiescent state [361]. RSC cultures were then treated with appropriate PME for 24 hours. For adenovirus experiments, cells were infected after formation of myotubes and RSCs and allowed to recover for 24 hours before treatment with extracts unless otherwise stated.

2.3.8. *In vitro* activation of Cre recombinase

Cultures of RSCs were infected with either Ad5CMVCre-eGFP or Ad5CMV-eGFP-control adenovirus (Gene Transfer Vector Core, University of Iowa) (diluted 1:1000 in growth media from a stock titer of 1×10^{10} pfu/ml) with 1:1000 Polybrene Transfection Reagent (Chemicon) for 1.5 hours at 37 °C. Cells were washed in PBS and incubated in fresh differentiation medium for an additional 48 hours.

2.3.9. *In vivo* activation of Cre recombinase

Aged and adult mice were given one I.P. injection of 300µl of 10mg/ml tamoxifen (Sigma) diluted in corn oil (Sigma) daily for 3 days [42].

2.3.10. Fluorescence-activated cell sorting

All reagents used for fluorescence activated cell sorting (FACS) are shown in **Section 2.1.6**. To obtain highly purified myogenic cells, mononucleated cells were isolated from muscle as described previously [42] with modifications. After incubating cells in Digest solution 2 in **Section 2.3.6**, cells were dislodged from fibres by drawing and releasing the solution through a 20g needle 5 times. The solution was centrifuged at 375g for 5 minutes and washed in rinsing solution 3 times. Cells were incubated in sorting medium (10% HS, in Ham's F-10) for 10 minutes and then incubated in biotin-conjugated anti-VCAM1 (Novus) and anti-mouse integrin- α 7 (1:200; MBL) for 30 minutes. Cells were washed in sorting medium and spun at 375g for 5 minutes. Cells were stained in CD31-PE (BD Biosciences), CD45-PE (BD Biosciences), Pacific Blue (Invitrogen) and streptavidin-647 (Invitrogen), all at 1:200, for 30 minutes. Propidium iodide (PI) was added at 1:500 before sorting to enable the identification of dead cells. Myogenic cells had the following profile: VCAM1+, integrin- α 7+, CD31-, CD45-, PI-. Cells were sorted with FACS Aria (BD Biosciences).

2.3.11. SC and skeletal muscle histology and immunofluorescence

All reagents used for immunohistochemistry are shown in **Section 2.1.2**.

Cultures of RSCs, satellite cells and tibialis anterior tissue sections were fixed in 4% PFA for 5 minutes, washed and processed for immunohistochemistry as previously described [42]. Briefly, samples were washed in PBS followed by 2x10 minute washes in PBSTx to permeabilise samples. Non-specific antibody binding was blocked by incubating samples with blocking solution for 30 minutes. Primary antibody was diluted in Ab block and incubated with samples at 4°C overnight. The next day, unbound antibody was washed off with PBS washes and fluor-labelled secondary antibody (1:1500), diluted in Ab block, was incubated with samples for 1 hour at room temperature. Dapi (1:3000, Sigma) was also added. After secondary antibody incubation, samples were washed in PBS and mounted with Fluormount G (Fisher Scientific). For detection of FGF2 in transverse orientation, sections were not fixed. For longitudinal sections, samples were processed for primary FGF2 antibody before fixation. For BrdU detection, cultures of SC, RSCs and tissue sections were fixed in 4% PFA, washed in PBS and then antigen-retrieved with sodium citrate buffer (10 mM, 0.05% Tween in PBS) at 95 °C for 30 minutes before immunostaining as described above.

2.3.12. Analysis of satellite cells and their progeny

Muscles sections were stained with a cocktail of antibodies to determine the number of Pax7⁺ SCs that were quiescent (Pax7⁺, Ki67⁻) or cycling (Pax7⁺, Ki67⁺) underneath the basal lamina (laminin⁺). The total number of Pax7⁺ cells was quantified in a minimum of ten serial sections per muscle in three separate regions from the mid-belly of the muscle [42]. The number of Pax7⁺ cells was quantified on freshly isolated single EDL muscle fibres. A minimum of 20–30 muscle fibres were counted per animal [42]. Cultures of RSCs and SCs in eight-well Permanox chamber slides (Nunc) were stained with a panel of antibodies to characterise myogenic cells with self-renewal potential (Pax7⁺), cycling (Pax7⁺, Ki67⁺), apoptosis (activated caspase-3⁺) and differentiation (myogenin⁺)

[42]. For fate analysis, quantification of three to five experiments was performed in triplicate and 300–600 cells were counted per condition. To assess cell growth, satellite cells were plated at clonal density (10–12 cells per well, Nunc eight-well Permax chamber slides) and the number of cells present in each individual well was determined after four days in culture (10% HS in DMEM). For cell growth experiments, 21–28 clonal density cultures were examined per condition. Wells with no cells present after four days of culture were not included in quantification.

2.3.13. Whole-mount *in situ* hybridisation

RNA *in situ* hybridisation and riboprobe synthesis were performed as previously described [362]. Briefly, Digoxigenin-labelled anti-sense and sense riboprobes of *Fgf2* were synthesised from a plasmid preparation [363]. All details of the *Fgf2* plasmid can be found in **Section 2.3.15**. Purified isolated myofibres were fixed in PFA and washed in 100% methanol. Fibres were rehydrated in a series of methanol / PBS + 0.2% Tween 20 (PBSTw) washes, starting with 50% methanol for 5 minutes, then 30% methanol for 5 minutes, and then fibres were taken into PBSTw. For pre-hybridisation, muscle fibres were rinsed in PBSTw and then incubated with Hyb⁻ mix for 5 minutes at 70 °C, and then Hyb⁺ for 4 hours at 70°C. For hybridisation, fibres were incubated with 5µg/ml of either anti-sense or sense (control) *Fgf2* riboprobe in Hyb⁺ mix overnight at 70°C. The following day, any unbound probe was removed in a series of formamide / SSC washes and maleic acid buffer containing 0.2% Tween 20 (MABT) washes. These washes consisted of 55% formamide / 2x SSC containing 0.2% Tween 20 (SSCTw) for 30 minutes, then; 55% formamide / 1x SSCTw for 30 minutes, then; 1x SSCTw for 30 minutes, then; 2 washes of 0.2x SSCTw for 30 minutes each, then; 4 washes in MABT for 30 minutes each. Unspecific antibody binding was blocked using a solution of MABT with 2% Blocking Reagent (Roche) for 4 hours at room temperature. Bound riboprobe was then detected by staining fibres with anti-Digoxigenin antibody (1:5000 in blocking solution; Roche) at 4°C overnight. The following day, fibres were rinsed twice for 15 minutes in MABT +

10% FCS, followed by 6 washes in MABT for 15 minutes each. Fibres were then washed twice for 5 minutes each in NTMT and signal was detected using NBT/BCIP solution (Roche). After a signal appeared, fibres were washed 3 times for 5 minutes in PBSTw and then fixed in 4% PFA for 10 minutes. Following two further PBS washes, fibres were mounted onto coverslips. In some cases, after fixation and before mounting, muscle fibres were further processed for Pax7 immunostaining as described above.

2.3.14 Plasmid digestion and DNA extraction

Plasmid digests were carried out according to the manufacturer's recommendations (New England Biolabs) using the reaction mix detailed in **Section 2.1.3**. Plasmids were typically digested at 37°C overnight, unless the manufacturer's specification suggested otherwise.

After digestion, the linearised DNA was precipitated from the digest solution by centrifugation with an equal volume of phenol chloroform, and incubated at -20 °C for 1 hour with 0.1 volumes of 3M sodium acetate and 2.5 volumes of ethanol. The solution was centrifuged at max speed for 30 minutes to produce a DNA pellet which was washed with ethanol then stored in solution with 0.1 volumes of TE or DepC water. Linearised DNA was stored at -70°C until required for RNA probe synthesis.

2.3.15. Probe synthesis

Probes were synthesised using the reaction mix detailed in **Section 2.1.3**. The probe synthesis mix was left for 2 hours at 37°C. 1µl of the mix was then resolved on a 1.5% agarose gel to check for an RNA band, and to estimate the concentration of the probe against a 1µl sample of the linearised plasmid. If a RNA band was observed, 2µl of DNase I was added to the remaining mix, and the reaction left at 37°C for 15 minutes in order to digest any DNA still present. Finally, the probe was purified by spinning down the solution in SigmaSpin post-

reaction Cleanup columns (Sigma) according to the manufacturer's recommendations.

For *Fgf2*, antisense probe was made by linearising plasmid with NotI and synthesising probe with T3 [363]. Sense probe was made by linearising plasmid with EcoRI and synthesising probe with T7 [363].

2.3.16. RNA isolation and RT-qPCR

RNA extraction from approximately 10,000 FACS-isolated satellite cells and 50 single muscle fibres was done with Trizol (Invitrogen) according to the manufacturer's recommendations. Briefly 1ml of Trizol was added to samples and samples were homogenised by vortexing. 200µl of chloroform (Sigma) was added and mixed by vortexing. The solution was left to settle on ice for 5 minutes before phases were separated through centrifugation at 13000g for 15 minutes at 4°C. The aqueous phase containing RNA was transferred to a new Eppendorf tube and RNA was precipitated by adding 500µl isopropanol (Sigma), and 20-40µg of Ultrapure Glycogen (Invitrogen). RNA was left to precipitate at -80°C overnight. The following day, the RNA suspension was centrifuged at 13000g for 20 minutes. Any contaminants were then removed by washing the RNA pellet in ice-cold 75% ethanol and centrifuging at 13000g for 10 minutes. This step was performed twice. All traces of ethanol were removed and the RNA pellet was left to air dry for around 5 minutes. RNA was resuspended in RNase-free water and stored at -80°C. RNA concentration was determined using a nanodrop.

Purified RNA was then prepared for RT-qPCR analysis or array analysis. First-strand complementary DNA was synthesised from 4 µl (200 ng) of RNA using the SuperScript First-Strand cDNA Synthesis Kit (Invitrogen) according to manufacturer's recommendations. RT-qPCR was performed on a Step One Plus Real Time PCR machine (Applied Biosystems), with Platinum SYBR Green qPCR SuperMix-UDG and ROX master mix (Invitrogen) using primers

2: Methods

against *Pax7*, *Fgf2*, *Stat1*, and *Gapdh* as a housekeeping control. Primer sequences are as follows:

Fgf2 forward - 5'-CGGCTTCTTCCTGCGCATCC-3'

Fgf2 reverse - 5'-GGTACCGGTTGGCACACACTCC-3'

Pax7 forward - 5'-GTGGAATCAGAACCCGACCTC-3'

Pax7 reverse - 5'-GTAGTGGGTCCTCTCAAAGGC-3'

Gapdh forward - 5'-AGGTCGGTGTGAACGGATTTG-3'

Gapdh reverse - 5'-TGTAGACCATGTAGTTGAGGTCA-3'

All reactions for RT-qPCR were performed using the following thermal cycler conditions: 50 °C for 2 minutes, 95 °C for 2 minutes, 40 cycles of a two-step reaction, denaturation at 95 °C for 15 seconds, annealing at 60 °C for 30 seconds. Analysis of FGF ligands was conducted with the mouse growth factor RT2Profiler PCR array system (SABiosciences) according to the manufacturer's recommendations, with the exception that RNA was extracted by the Trizol method. Unless otherwise stated, data are from three separate reactions performed in triplicate from n = 4–6 mice per condition.

2.3.17. Antibodies and reagents

The antibodies used are as follows: rat anti-BrdU (1/500, Abcam), rabbit anti-Ki67 (1/500, Abcam), mouse anti-Pax7 (1/100, DSHB), rabbit anti-myogenin (1/250, Santa Cruz), rabbit anti-cleaved caspase-3 (1/500, Cell Signaling Technologies), chick anti-laminin (1/5,000, Abcam), VCAM (1/100), mouse anti-integrin- α 7 (1/200, MBL), CD31-PE and CD45-PE (1/200, BD), and rabbit anti-FGF2 (1/500, Abcam). The corresponding species-specific Alexa-conjugated (Pacific Blue, 488, 546, 647) secondary antibodies (Molecular Probes) were used at 1:1500 for immunohistochemistry and 1:200 for FACS.

2.3.18. Genotyping

Details of all primer sequences and the sizes of products produced from polymerase chain reaction (PCR) amplification can be found in **Table 2**.

Genotyping was carried out by PCR amplification using a FastStart Taq DNA polymerase kit (Promega), according to the manufacturer's recommendations.

PCR reactions were carried out in 20 μ l reactions using Promega reagents as follows:

4 μ l 5x transcription buffer

1.2 μ l MgCl₂ solution

1 μ l primer solution, containing 10 μ M of each primer

1 μ l DNA sample to be amplified

0.15 μ l dNTPs (25mM)

0.15 μ l Hot Start taq

12.5 μ l sterile water

All samples were amplified using the following program:

95°C for 10 minutes

40 cycles of: 94°C for 45 seconds

 57°C for 45 seconds

 72°C for 1 minute

Followed by 72°C for 7 minutes.

After PCR amplification, samples were resolved by electrophoresis, using a 1.5% agarose gel with 0.05% ethidium bromide in 1xTAE buffer.

2: Methods

Gene of interest	Primers
<i>Cre</i>	Primer A: CCTGGAAAATGCTTCTGTCCG Primer B: CAGGGTGTATAAGCAATCCC Cre: Primer pair A+B = 390bp Wildtype: No product
<i>Spry1flox</i>	Primer A: GGGAAAACCGTGTCTAAGGAGTAGC Primer B: GTTCTTTGTGGCAGACACTCTTCATTC Primer C: CTCAATAGGAGTGGACTGTGAAACTGC Spry1flox: Primer pair A+C = 342 bp Wildtype: Primer pair A+C = 311 bp Null: Primer pair A+B = 150 bp
<i>Spry1OX</i>	Primer A: GAGGAAATGCTGCGCACAAATGTATACTCGG Primer B: GGATACTGACACATTGTGCCTCAGCCTTTC Spry1OX : Primer pair A+B = 920bp Wildtype: No product
<i>FgfR1flox</i>	Primer A: GTATTGCTGGCCCACTGTTC Primer B: CTGGTATCCTGTGCCTATC Primer C: CAATCTGATCCCAAGACCAC FgfR1flox : Primer pair B+C = 387 bp Wildtype: Primer pair B+C = 327 bp Null: Primer pair A+C = 300 bp
<i>FgfR2flox</i>	Primer A: TGCAAGAGGCGACCAAGTCAG Primer B: ATAGGAGCAACAGGCGG FgfR2flox: Primer pair A+B = 207 bp Wildtype: Primer pair A+B = 142 bp

Table 2 - Details of PCR primers

2.3.19. Statistics and data

Unless otherwise stated, all data are represented as mean \pm s.e.m.; *P < 0.05 **P<0.01 ***P<0.001, student's t-test. For multiple comparisons, analysis of variance with Bonferroni's multiple-comparison post hoc test was used.

2.4. Methods for Chapter 5 and Chapter 6

2.4.1. Isolation, growth, and differentiation of NSCs

All reagents used for NSC cultures are shown in **Section 2.1.7**. Foetal-derived NSCs were isolated, grown, and differentiated as previously described [364, 365] with modifications. Briefly, the cortex and striatum from E16.5 embryos generated from a mating between NestinCre;Chd7^{f/+} and Chd7^{f/f} mice were dissected and put in to ice-cold PBS. Tissue pieces were centrifuged at 800g for 3 minutes, the supernatant was removed and the tissue was dissociated by incubating on ice for 10 minutes, flicking the side of the tube every 3 minutes to aid dissociation. 1ml of PBS was added and cells were then dissociated by triturating with a pipette tip and centrifuged at 375g for 5 minutes. Cells were then plated on laminin-coated (1:100; Sigma) tissue culture plates and grown in growth media containing 1% N2 supplement (Invitrogen), 20ng/ml EGF (Peprotech), 20ng/ml FGF2 (Peprotech), 1% Pen/Strep (Invitrogen) in Euromed-N (Euroclone). Growth media was changed every 1.5 days and cells were passaged at 70-80% confluency using 1x Trypsin EDTA (Sigma) which was neutralised with Trypsin inhibitor (Sigma). After genotyping, any NestinCre;Chd7^{f/f} cultures were pooled and Chd7^{f/f} control cultures were pooled.

Differentiation into neurons was performed as previously described [365] with modifications. Briefly, cells were plated onto laminin-coated (1:100) glass 8-well chamber slides pre-treated with poly-L-ornithine (Sigma) in neuronal differentiation media containing 1% B27 supplement (Invitrogen), 0.5% N2, and 10ng/ml FGF2 in Euromed-N. Cells were maintained in these conditions for 3 days (3d neuro diff) changing the media once throughout the period. After the 3

day period, cells were put into media containing 0.5% N2, 1%B27, 10ng/ml FGF2 and 20ng/ml BDNF (Peprotech) in Euromed-N. Cells were maintained in these conditions for a further 3 days (6d neuron dff) changing the media once throughout the period.

2.4.2. Forebrain processing

Mice were given a lethal dose of Euthanal (pentobarbital sodium; Merial) and perfused with 10ml of ice-cold PBS followed by 10ml ice-cold 4% PFA. Brains were then dissected and further fixed in 4% PFA overnight at 4°C. For section *in situ* hybridisation experiments, fixed brains were dehydrated in 70% ethanol and equilibrated into paraffin wax using a Leica ASP300 Tissue Processor. Brains were then embedded in paraffin wax, sectioned in 10µm steps, and placed on to Superfrost+ slides.

For immunohistochemistry, fixed brains were cryoprotected in 15% sucrose (Sigma) at 4°C overnight followed by 15% sucrose and 7.5% gelatine type B (Sigma) at 37°C overnight. Brains were then embedded in 15% sucrose and 7.5% gelatine type B and frozen in methylbutane (Sigma) with dry ice. Frozen brains were sectioned in 20µm steps and placed on to Superfrost+ slides.

2.4.3. Neural stem cell histology and immunofluorescence

All reagents used for immunohistochemistry are shown in **Section 2.1.2**. Cells on 8-well glass chamberslides were fixed in 4%PFA for 5 minutes followed by 2x 10 minute PBS washes. Cells were permeabilised with a 10 minute wash in PBSTx and non-specific antibody binding was blocked by incubating slides in blocking solution for 1 hour. Primary antibody was diluted in Ab block at 4°C overnight. The following day, unbound antibody was washed off with 3x 10 minute PBS washes and a 10 minute PBSTx wash. Slides were incubated with fluor-labelled secondary antibody (1:500) and Dapi (1:5000) in Ab block for 1

hour. Unbound secondary antibody was then washed off with 3x 10 minute PBS washes and mounted using Citifluor (Citifluor Ltd.).

2.4.4. Frozen section histology and immunofluorescence

Sections of the DG, SVZ, or OB on Superfrost+ slides were incubated in PBS at 37°C for 45mins to wash away the gelatine. Sections were then fixed with 4% PFA for 10 mins followed by 2x 10 minute PBS washes. Cells were permeabilised with a 10 minute wash in PBSTx and non-specific antibody binding was blocked by incubating slides in blocking solution for 1 hour. Primary antibody was diluted in Ab block at 4°C overnight. The following day, unbound antibody was washed off with 3x 10 minute PBS washes and 2x 10 minute PBSTx wash. Slides were incubated with fluor-labelled secondary antibody (1:200) and Dapi (1:5000) in Ab block for 1 hour. Unbound secondary antibody was then washed off with 3x PBS washes and slides were mounted using Citifluor. For BrdU, Ki67 and PCNA detection, tissue sections were antigen-retrieved with 2N HCl for 15 mins at 37°C prior to blocking sections. Acid was then neutralised with 2x 5 minute washes in 0.1M borate buffer pH 8.5.

2.4.5. Section *in situ* hybridisation

RNA *in situ* hybridisation and riboprobe synthesis were performed as described previously [363]. Briefly, Digoxigenin-labelled anti-sense and sense riboprobes of *Er81* were synthesised from a plasmid preparation as shown in **Section 2.3.14** and **Section 2.3.15**. *Er81* plasmid was linearised with *SpeI* and probe was synthesised using T7. *Chd7* was synthesised from PCR reaction. Probe synthesis from PCR reaction is shown in **Section 2.4.6**.

All reagents used for *in situ* hybridisation on tissue sections are shown in **Section 2.1.4**. All section *in situ* hybridisations were performed on wax section. Sections were rehydrated in a coplin jar through a series of xylene and ethanol washes: 3x3 minute washes in xylene followed by 2x2 minute washes in 100%

2: Methods

ethanol, 95% ethanol and 70% ethanol in water, then rinsed twice in water. Sections were then fixed in 4% PFA for 10 minutes at room temperature, then rinsed for 5 minutes in PBS. To permeabilise cell membranes, slides were washed for 10 minutes at 37°C in 50ml PBS with 50µl proteinase K. Slides were then rinsed again in PBS followed by incubation with acetylation solution for 10 minutes to minimise background. Following acetylation, slides were washed 3 times for 5 minutes each in PBS, then dehydrated through 70% and 95% ethanol washes before being left to air dry. Meanwhile, the chosen probe was added to hyb at a concentration of 1µg/ml, and then heated at 80°C for at least two minutes. Following dehydration, slides were transferred into a preheated humid (50% formamide / water solution) chamber. Once in the chamber, 300µl of probe/hyb solution was added to each slide and the slide was covered with parafilm. Hybridisation was performed at 65°C overnight.

The following day, slides were washed in 5xSSC solution to gently float off the parafilm coverslips. Slides were then washed for 30 minutes at 65°C in a high stringency wash to ensure that all the unbound or weakly bound probe was washed off the sections. Slides were washed 3 times for 10 minutes in RNase buffer at 37°C before undergoing a 30 minute wash in RNase A in RNase buffer (100µl of enzyme in 50 ml of buffer) at 37°C, to digest any unbound RNA. Slides were washed one last time in RNase buffer at 37°C for 15 minutes followed by two high stringency washes at 65°C for 20 minutes. Sides were then washed in 2xSSC and 0.1xSSC for 15 minutes at 37°C and a PBSTw wash for 15 minutes. Any non-specific antibody binding was then blocked by incubating slides in blocking solution (10% heat inactivated goat serum in PBSTw) for one hour at room temperature. Blocking solution was then replaced with antibody solution (anti-digoxigenin-AP diluted 1/5000 in 1% heat inactivated goat serum in PBSTw) and left overnight at 4°C.

After antibody incubation, slides were washed 4 times in PBSTw for 15 minutes each to ensure any unbound antibody was washed away. The slides were then washed in NTMT. Slides were then stained in BM purple with 25ng/ml

levamisole to minimise background staining. Slides were stained at room temperature in the dark until any signal was detected

Once sections were adequately stained, the BM purple was removed and slides were washed twice in PBS, fixed briefly in 4% PFA, then rinsed once more in PBS, before counterstaining in 20% nuclear fast red solution for 10 minutes. Finally, sections were dehydrated through a series of brief ethanol washes (2x70%, 95% and 100%), and washed 3 times for 3 minutes in Xylene before mounting with DPX.

2.4.6. Probe synthesis from PCR reaction

PCR reactions were carried out using a FastStart Taq DNA polymerase kit (Promega) according to the manufacturer's recommendations. PCR reactions were carried out in 20µl reactions using Promega reagents using the mix described in **Section 2.1.3**.

All samples were amplified using the following program:

95°C for 10 minutes

40 cycles of: 94°C for 45 seconds

 55°C for 45 seconds

 72°C for 1 minute

Followed by 72°C for 7 minutes.

PCR product was then purified using a QiaQuick PCR purification kit (Qiagen) according to the manufacturer's recommendations. Probe was then synthesised using the reaction mix detailed in **Section 2.1.3**. The probe synthesis mix was left for 2 hours at 37°C. 1µl of the mix was then removed and resolved on a 1.5% agarose gel to check for an RNA band, and to estimate the concentration of the probe against the DNA ladder. If an RNA band was observed, 2µl of

DNase I was added to the remaining mix, and the reaction left at 37°C for 15 minutes in order to digest any DNA still present. Finally, the probe was purified by spinning down the solution in SigmaSpin post-reaction Cleanup columns (Sigma) according to the manufacturer's recommendations.

For *Chd7*, primer sequences span exon 3 and are as follows:

Chd7 forward - 5' TTGGTAAAGATGACTTCCCTGGTG 3'

Chd7 reverse - 5' ATTGTAATACGACTCACTATAGGGGTTTTG 3'

Probe was synthesised using T7 polymerase.

2.4.7. RNA isolation and RT-qPCR

RNA extraction from approximately 1×10^6 foetal-derived NSCs was done with Trizol (Invitrogen) according to the manufacturer's suggested modifications, by the addition of ultrapure glycogen (Invitrogen), and prepared for RT-qPCR analysis as in **Section 2.3.16**.

First-strand complementary DNA was synthesised from 4 μ l (200 ng) of RNA using the Precision Nanoscript Reverse Transcriptase kit (PrimerDesign) according to manufacturer's recommendations. RT-qPCR was performed on a Stratagene Mx3000p Real Time PCR machine (Aglient Technologies), with Precision 2 x real-time PCR MasterMix (PrimerDesign) using primers against *Er81*, *Hes5*, *Chd7*, *Stk25*, *Prkca*, *Nrarp*, *Wnt9a*, *Cd24a*, *Ring1*, *Chd4*, *Bcan*, *Reln*, *Smarca2*, *NeuroD2*, *Spred1*, *Trp53*, *Arid1b*, and *Gapdh* as a housekeeping control. Primer sequences are shown in **Table 3**.

All reactions for RT-qPCR were performed using the following thermal cycler conditions: 95 °C for 10 minutes, 40 cycles of a two-step reaction, denaturation at 95 °C for 15 seconds, annealing at 60 °C for 1 minute, followed by a 50°C step for 30 seconds at the end. Unless otherwise stated, data are from two separate reactions performed in duplicate.

2: Methods

Target	Forward primer (5'-3')	Reverse primer (5'-3')
<i>Er81</i>	TCCATACCAGACAGCACCTAC	GTCGGCAAAGGAGGAAAAGAA
<i>Hes5</i>	AGTCCCAAGGAGAAAAACCGA	GCTGTGTTTCAGGTAGCTGAC
<i>Chd7</i>	TCACCAGCCTTGGGCACAACCTC	TAGCTGAGCGTTCTGTGCGCTG
<i>Stk25</i>	ATATCACCCGCTACTTCGGCT	GGTGGCAATATAGGTCTCTTCCA
<i>Prkca</i>	AGAGGTGCCATGAGTTCGTTA	GGCTTCCGTATGTGTGGATTTT
<i>Nrarp</i>	TTCAACGTGAACTCGTTCGGG	TTGCCGTCGATGACTGACTG
<i>Wnt9a</i>	TACAGCAGCAAGTTTGTCAAGG	ATTTGCAAGTGGTTTCCACTCC
<i>Cd24a</i>	CTTCTGGCACTGCTCCTACC	GGTAGCGTTACTTGGATTTGGG
<i>Ring1</i>	TCTGCCTGGACATGCTGAAG	CGTAGGGACCGCTTGGATAC
<i>Chd4</i>	GAGGAGGATATGGACGCACTTC	TGAGCTTTGGAGTCTCTGCTTC
<i>Bcan</i>	TCTGGAAGAAGTGTCTGGC	CTCCTCCAAGCATGTCCCAC
<i>Reln</i>	TACTCGCACCTTGCTGAAAT	CAGTTGCTGGTAGGAGTCAAAG
<i>Smarca2</i>	TCACGGACGGGTCTGAGAAA	CCCAGGTGTTCCAGCAAAGG
<i>NeuroD2</i>	CTCGCATGGCGCTCTGAAG	GAACAGGCGGGTCAGCATGG
<i>Spred1</i>	GAGATGACTCAAGTGGTGGATG	TCTGAAAGGTAAGGCCAAACTTC
<i>Trp53</i>	GCGTAAACGCTTCGAGATGTT	TTTTTATGGCGGGAAGTAGACTG
<i>Arid1b</i>	CAACAAAGGAGTCACCCGGC	CCCATCCCATACTGAGGTC
<i>Gapdh</i>	AGGTCGGTGTGAACGGATTTG	TGTAGACCATGTAGTTGAGGTCA

Table 3 - RT-qPCR primer sequences

2.4.8. *In vivo* activation of Cre recombinase

Unless otherwise stated, adult mice were given one I.P. injection of 120µl of 20mg/ml tamoxifen (Sigma) diluted in corn oil (Sigma) daily for 5 days.

2.4.9. NSC *in vivo* cell division analysis

For analysing SVZ or SGZ proliferation, animals were given one I.P. injection of BrdU (Sigma) dissolved in isotonic saline (0.9% NaCl) at a concentration of 75mg/kg. For the analysis of new cell formation, animals were administered BrdU in their drinking water for 3 weeks at a concentration of 1mg/ml, supplemented with 5% sucrose.

2.4.10. Analysis of NSCs and their progeny

In vitro cultures of foetal-derived NSCs were stained with antibodies to determine their stage of differentiation from immature neuron (DCX⁺) to mature neuron (MAP2⁺). The number of DCX⁺ or MAP2⁺ cells was counted per field of view and the percentage of cells positive for each marker was calculated by counting the total number of cells (Dapi⁺) per field of view. A minimum of 4 fields of view were counted at 20x magnification per culture. A minimum of 1000 cells were counted per culture. Each experiment was performed twice with duplicate cultures.

The number of BrdU⁺, DCX⁺, PCNA⁺, Sox2⁺, CHD7⁺, GFAP⁺ or MASH1⁺ cells per dentate gyrus section was calculated by counting the number of cells on each dentate gyrus on a minimum of 10 sections at least 40µm apart from the anterior to posterior DG. The number of animals used is shown by each experiment. The total number of cells per dentate gyrus was then averaged.

The number of BrdU⁺, PCNA⁺, or DCX⁺ cells in the subventricular zone was calculated by counting the number of cells on each SVZ on a minimum of 10 sections at least 40µm apart from the anterior SVZ. The number of animals used is shown by each experiment. The total number of cells per SVZ was then averaged.

The number of TH⁺, CalR⁺, or CalB⁺ cells in the olfactory bulb was calculated by counting the number of cells in several 10,000µm² areas throughout the glomerular layer. A minimum of 6 areas were counted per OB for a minimum of 8 sections at least 40µm apart in the bulk of the OB. The number of animals used is shown by each experiment. The total number of cells per defined area in the OB was then averaged.

For analysis of OB sizes, pictures of the forebrain and OB of *Chd7^{gt/+}* and WT mice were taken after perfusion fixing and prior to preparation for embedding. Measurements were then performed using Adobe Photoshop CS5 software.

2.4.11. Antibodies and reagents

The antibodies used are as follows: rat anti-BrdU (1/50, Abcam), mouse anti-Ki67 (1/50, Abcam), mouse anti-PCNA (1/200, Abcam), mouse anti-Sox2 (1/800, Abcam), rabbit anti-Chd7 (1/80, Abcam), rabbit anti-tyrosine hydroxylase (1/1000, Abcam), rabbit anti-GFAP (1/500, Sigma), mouse anti-GFAP (1/1000, Abcam), mouse anti-MASH1 (1/200, BD Biosciences), rabbit anti-DCX (1/500, Abcam), mouse anti-NeuN (1/100, Chemicon), goat anti-Calretinin (1/5000, Chemicon), rabbit anti-Calbindin (1/2000 Swant), rabbit anti-GFP (1/200, Invitrogen), mouse anti-PSA-NCAM (1/100, Sigma). The corresponding species-specific Alexa-conjugated (488, 568, 647) secondary antibodies (Invitrogen) were used at 1:200 for immunohistochemistry on tissue sections and 1:500 for immunohistochemistry on cultured cells. Dapi (Sigma) was used at 1:5000.

2.4.12. Genotyping

All genotyping was performed as in **Section 2.3.18**. Details of all primer sequences and the sizes of products produced from PCR amplification can be found in **Table 4**.

2: Methods

Gene of interest	Primers
Cre	Primer A: CCTGGAAAATGCTTCTGTCCG Primer B: CAGGGTGTATAAGCAATCCC Cre: Primer pair A+B = 390bp Wildtype: No product
Chd7gt	Primer A: CAGGAGAAGAAAGGGTTCCTG Primer B: GGCAGGTCCTTCATTGGA Primer C: TTTCCCAGTCACGACGTTG Chd7gt: Primer pair B+C = 1000bp Wildtype: Primer pair A+B - 280bp
Chd7flox	Primer A: GAAGGAGAAGAAAGAGCCCAAGAC Primer B: TGAGTTACGGAGAGAACCAAGCAC Chd7flox : Primer pair A+B - 392bp Wildtype: Primer pair A+B - 423bp
RYFP	Primer A: GCGAGGAGGCGCTCCCAGGTTCCG Primer B: CTTTAAGCCTGCCCAGAAGACTCC Primer C: GAGGCAGGAAGCACTTGCTCTCC Primer D: CATCAAGGAAACCCTGGACTACTG RYFP : Primer pair C+D =300bp Wildtype: Primer pair A+B = 500 bp

Table 4 - Details of PCR primers 2

2.4.14. Image processing

All images were processed using NIS Elements Viewer 4.0 and Adobe Photoshop CS5 software.

2.4.15. Statistics and data

Unless otherwise stated, all data are represented as mean \pm s.e.m.; *P < 0.05 **P < 0.01 ***P < 0.001, student's t-test. For multiple comparisons, analysis of variance with Bonferroni's multiple-comparison post hoc test was used.

Chapter 3

Results Part I

3.1. Skeletal muscle and ageing

Under normal homeostatic conditions, SCs are completely quiescent [35]. However, in response to muscle damage they are capable of rapidly activating and proliferating to generate myoblasts [182]. Myoblasts cycle quickly and are able to fuse with each other to form new myotubes [182]. Nascent myotubes mature into new myofibres to regenerate damaged muscle [182]. Pax7⁺ SCs are essential for the response to skeletal muscle injury and efficient regeneration [58, 59, 61]. In addition, SCs are capable of extensive self-renewal to retain a stem cell pool, with the ability to undergo the regenerative response upon successive myotraumas [53, 54]. However as ageing progresses, the regenerative ability of skeletal muscle declines due, at least in part, to impaired SC function (see **Figure 4**) [146, 147]. Activation of aged SCs is delayed in response to injury compared with their young counterparts, and their proliferative potential is reduced [159, 160]. Thus, aged SCs are less able to generate myoblast progeny. In addition, the differentiation capacity of aged SCs and their progeny is reduced, with cells fusing to form thinner myotubes which are delayed in upregulating mature fibre markers [150, 155, 166]. Furthermore, the self-renewal potential of aged SCs may be reduced, leading to further declines in regenerative capability following subsequent injuries [153, 155, 156]. These changes lead to a loss of skeletal muscle mass and age-associated sarcopenia, resulting in impaired skeletal muscle function in aged animals [146]. Whether the number of SCs declines with age is still somewhat controversial, with studies documenting increased and decreased numbers of SCs depending on the species, muscle, and technique of observation [146]. However, it is generally accepted that the number of Pax7⁺ SCs present in skeletal muscle undergoes a notable decline in ageing under homeostatic conditions [149-151].

Across different species and organ systems the stem cell niche has a critical role in the maintenance of stem cell number and function. In invertebrates, age associated changes in the niche have been shown to cause a decline in stem cell number and function [167, 168]. In mammals, the stem cell niche is a critical

factor in the maintenance of quiescence, a reversible state of growth arrest crucial to the preservation of adult stem cell number and function [20, 366].

Changing the aged SC niche can partly restore the proliferation and differentiation of aged SCs. For example, exposure to a young systemic environment promotes the proliferative expansion and myogenic progression of aged SCs in regenerative conditions [10, 148, 150, 164, 169]. Manipulation of growth factors and signalling pathways, such as Wnt signalling and Notch signalling, can also aid the regeneration of aged skeletal muscle [130, 164, 174]. The signalling cascades responsible for the decline in SC function in regenerating aged muscle have been intensively investigated, yet, in contrast, the mechanisms driving SC depletion under homeostatic conditions with age remain unknown.

The following experiments were conducted to investigate how age-associated changes in the niche impact SC number and function under homeostatic conditions:

1. Numbers of SCs present in skeletal muscle were determined in adult and aged animals and their function was assessed using an *in vitro* fate assay.
2. The cycling status of SCs was determined in adult and aged animals with 5-bromo-2'-deoxyuridine (BrdU) studies to determine if impaired function could be due to altered quiescence.
3. Age-associated changes in the SC niche were investigated through the use of a purified myofibre extract (PME) in combination with *in vitro* quiescence assays.
4. The possibility that deregulated FGF expression from the niche was responsible for skeletal muscle ageing was investigated through the use of pharmacological and genetic inhibitors of FGF signalling in combination with PME and *in vitro* quiescence assays.

3.1.1. Satellite cells display a decline in number and function in aged skeletal muscle

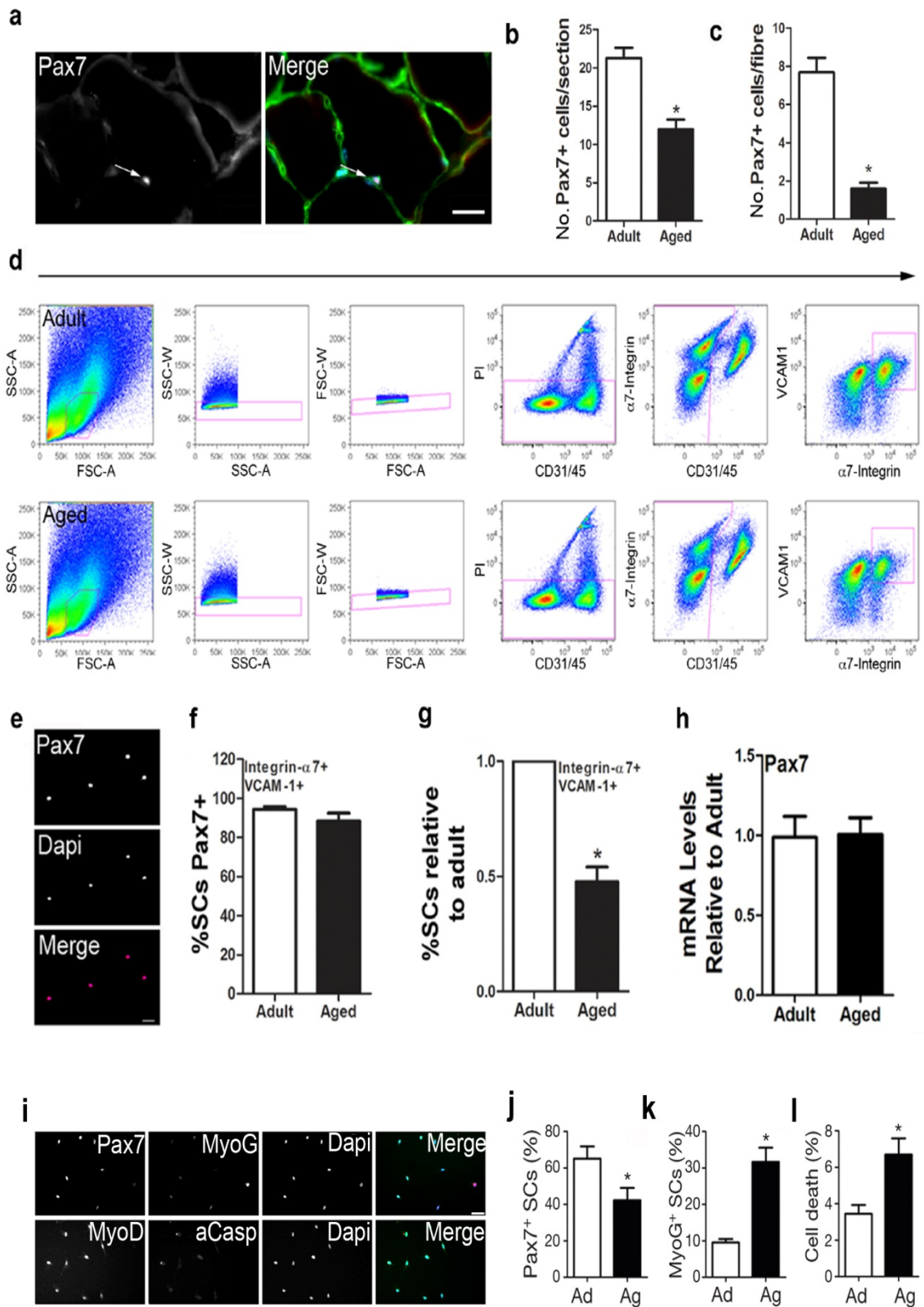
To first determine if there was any change in the SC pool with age, TA sections of adult (3-8 months old) and aged (24-28 months old) mice were stained with antibodies raised against the SC marker, Pax7, and laminin to mark the basal lamina (**Figure 15a**). SCs were identified as Pax7⁺ cells outside of the myofibre but underneath the basal lamina (**Figure 15a**). The number of Pax7⁺ SCs per section was reduced by almost 50% in aged skeletal muscle compared to adults (**Figure 15b**). The reduction in SC number was also confirmed by isolating single muscle fibres from EDL muscle and staining them with antibodies raised against Pax7 (**Figure 15c**). As a further method of confirmation, SCs from aged and adult skeletal muscle were FACS-isolated (**Figure 15d**). Cells were positively selected for VCAM-1 and α 7-integrin, and negatively selected for CD31, CD45, and propidium iodide (PI) to remove endothelial cells, immune cells, and dead cells respectively (**Figure 15d**). This sorting method allowed for the isolation of a 95% pure population of Pax7⁺ SCs, which were all quiescent (Ki67⁻), after staining for Pax7 and Ki67 immediately after sorting (**Figure 15e,f** and data not shown). FACS profiles of VCAM-1⁺, α 7-integrin⁺, CD31/45⁻, PI⁻ events showed that the percentage of SCs present in aged skeletal muscle was reduced by 50% compared to adult (**Figure 15d,g**). Furthermore, RT-qPCR analysis for the expression of *Pax7* revealed no difference in aged compared to adult FACS-isolated SCs, showing that a reduction in the number of Pax7⁺ cells is not due to a decrease in levels of *Pax7* transcript in aged cells (**Figure 15h**).

SCs in aged skeletal muscle display impaired regenerative capability [147]. To determine the exact cell-autonomous changes in SC function a fate assay was performed. FACS-isolated SCs were plated at clonal density in culture (DMEM+10%HS) and then stained with antibodies to determine self-renewal potential (Pax7), differentiation (MyoG), and apoptosis (cleaved caspase 3; aCasp) (**Figure 15i**). After four days in culture, aged SCs tended to lose markers of self-renewal potential (**Figure 15j**) as the percentage of Pax7⁺ cells

was decreased, and instead became more prone to differentiate (**Figure 15k**) and apoptose (**Figure 15l**).

Collectively, these data show that the number of SCs is decreased with age and the few that remain display a loss of self-renewal potential and increased tendency to differentiate or apoptose.

3: Results Part I



3: Results Part I

Figure 15 - The number of satellite cells declines in aged skeletal muscle and their

function is impaired. a, Representative image of Pax7 (white), laminin (green) and Dapi (blue) staining of 10µm thick skeletal muscle cross-sections (scale bar, 50µm). **b,** Quantification of the number of Pax7⁺ cells / muscle cross-section averaged from 30 cross-sections / mouse (n=5-6 animals / age group). **c,** Quantification of the number of Pax7⁺ cells / single muscle fibre from adult and aged skeletal muscle. 20-30 single muscle fibres / animal (n=5-6 animals / age group). **d,** FACS profiles for the isolation of purified SCs from adult and aged muscle. Cells were positively selected for VCAM-1 and α7-integrin and negatively selected for CD31, CD45 and propidium iodide (PI). Note the decrease in double-positive cells in aged muscle compared to adult muscle (far right panels). **e,** Representative image of freshly isolated SCs obtained by FACS, plated, immediately fixed and immunostained for Pax7 and Dapi. Scale bar, 20µm. **f,** Quantification of the percentage of Pax7⁺ cells from the selected gate. Note ~95% of sorted SCs from both adult and aged skeletal muscle are Pax7⁺ (100% were Myogenin-negative). **g,** Relative proportion of SCs sorted from live (PI⁻) cells derived from adult and aged muscles. **h,** RT-qPCR analysis for the expression of *Pax7* in aged relative to adult sorted SCs. **i,** Representative images of sorted SCs cultured for 4 days and stained with anti-Pax7, MyoG, MyoD, and cleaved caspase 3 (aCasp). **j,** Quantification of the percentage of Pax7⁺, MyoG⁺ (**k**) and cleaved caspase 3⁺ (aCasp; **l**) adult (Ad) and aged (Ag) cells after 4 days in culture. 21–28 clonal density cultures were examined per condition, performed in triplicate. Scale bar, 20µm. All individual experiments were performed in triplicate. All data represented as mean ±s.e.m.; *P<0.05 student's t test.

3.1.2. Aged satellite cells cycle more frequently during homeostasis

Preservation of the quiescent state is a fundamental process that maintains the number and function of self-renewing stem cells [367]. Loss of stem cell quiescence has been shown to cause a decline in stem cell number and impair stem cell function in many systems, including somatic NSCs [252, 259, 260]. Therefore, having shown that there is a depletion of the SC pool with age (see **Figure 15**), I sought to investigate whether the cycling status of SCs was altered in aged animals under homeostatic conditions. To determine if SC quiescence was disrupted under homeostatic conditions during ageing, BrdU was administered in the drinking water of adult and aged mice to label proliferating cells (**Figure 16a**). After 6 weeks of BrdU administration, SCs were FACS-isolated and immediately fixed and stained with antibodies raised against BrdU and Pax7 (**Figure 16a**). The percentage of aged SCs that were BrdU⁺ was nearly 3-fold greater compared to adult SCs. To further confirm this, sections of TA muscle from adult and aged animals were stained with antibodies raised against Pax7, laminin, and Ki67 to determine the number of SCs that had exited quiescence (**Figure 16c**). The percentage of Ki67⁺ SCs was increased 4-fold in aged animals compared to adults (**Figure 16d**), therefore showing that aged SCs lose their ability to retain a quiescent state *in vivo*.

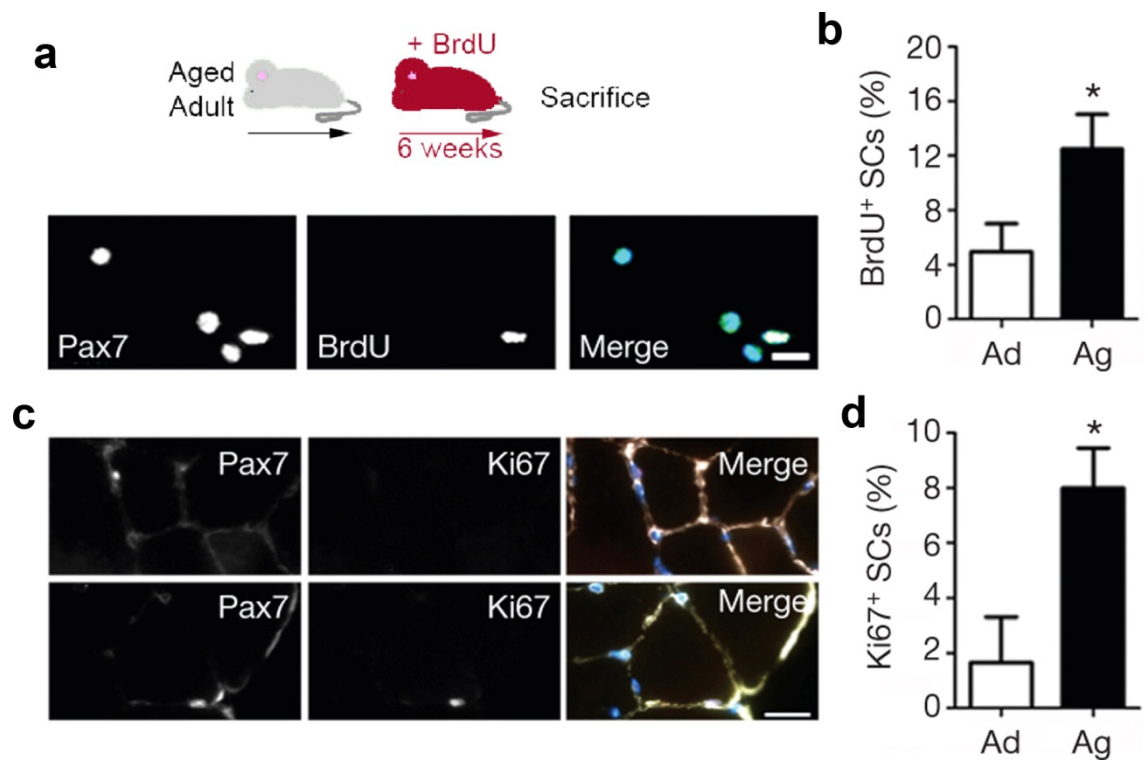


Figure 16 - Aged satellite cells cycle more frequently during homeostasis. **a**, BrdU feeding schematic and representative images of freshly isolated SCs obtained by FACS after 6 weeks of BrdU feeding, immediately fixed and immunostained for Pax7 and BrdU (Dapi in merge). **b**, Quantification of the percentage of BrdU⁺ SCs immediately after plating. 300-600 cells were assessed per experiment, performed in triplicate. n=4-6 animals / age group. **c**, Representative images of sections from aged muscle stained with anti-Pax7 (red in merge) and Ki67 (green in merge; Dapi, blue, in merge) showing a Pax7⁺Ki67⁻ cell (top panel) and a Pax7⁺Ki67⁺ cell (bottom panel). **d**, Quantification of the percentage of Ki67⁺ Pax7⁺ SCs per section (n = 4-6 animals per age group). All scale bars, 20 μ m. All data represented as mean \pm s.e.m.; *P<0.05 student's t test.

3.2. Formation of a purified myofibre extract to determine age-associated changes in the satellite cell myofibre niche

The stem cell niche is essential for quiescence and maintenance of the stem cell pool [168, 366]. Skeletal muscle stem cells are located along the length of the muscle fibre in close contact with the fibre and basal lamina. The association of SCs with a healthy mature muscle fibre is of vital importance to maintain adult SCs in a relatively quiescent state during homeostasis [128]. Hence, the differentiated progeny of SCs, the muscle fibre, functions as a niche cell for its own stem cell. To determine if changes in the niche of the SC with age account for loss of quiescence under homeostatic conditions and a decline in function, all soluble fractions produced by the muscle fibre were extracted (purified myofibre extract; PME). Firstly, skeletal muscle of adult and aged mice was digested and all contaminating mononucleated cells, including interstitial cells and fibroblasts, were washed away. After this step, the presence of any contaminating mononuclear cells in the fibre fraction were rare compared to the fraction of mononucleated cells that were excluded (**Figure 17a-d**), showing that the myofibre fraction was pure. Purified myofibres were then incubated in a high-salt protein extraction buffer (see **Section 2.3.3.**) to extract all soluble components of the niche.

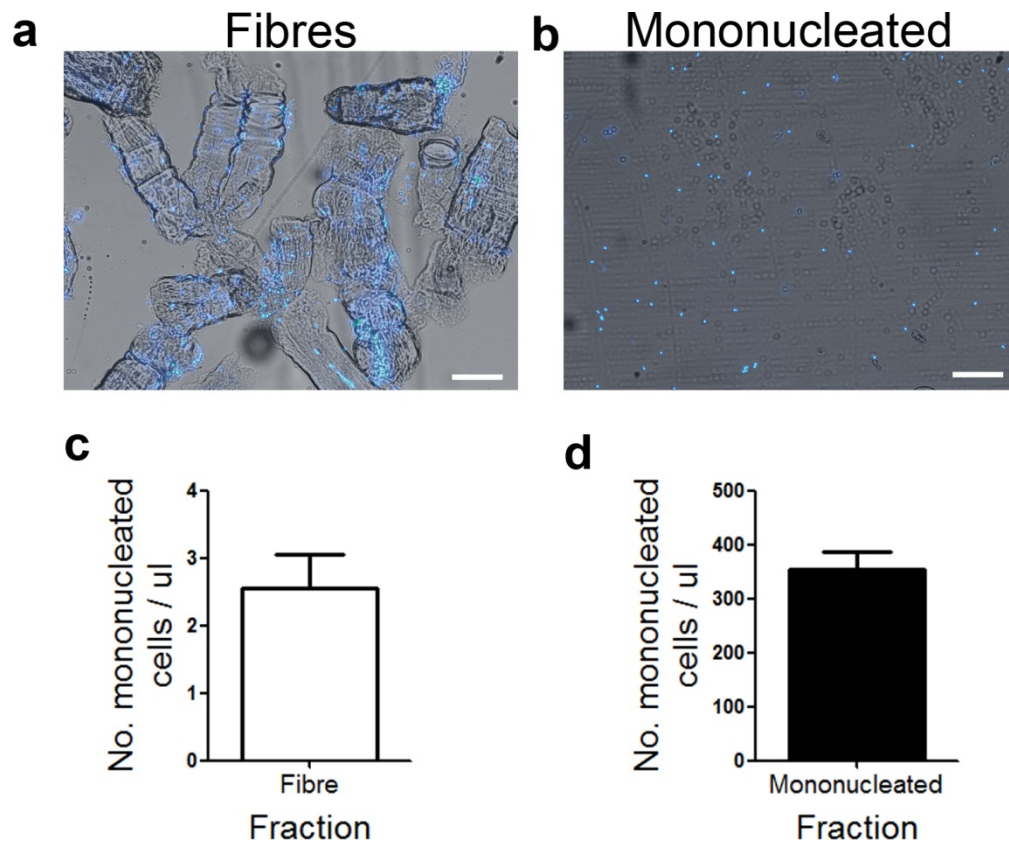


Figure 17 - Purified myofibre extract represents soluble fractions from skeletal muscle fibres. **a**, Representative image from the contents of the fibre fraction or the mononucleated fraction (**b**) of PME prior to the extraction of soluble fractions. Merge of brightfield and Dapi shown. Note very few mononucleated cells were present in the fibre fraction, and very few fibre fragments were present in the mononucleated fraction. Scale bars, 100 μ m. **c**, Quantification of the number of mononucleated cells present in the fibre fraction and the mononucleated fraction (**d**). Note that there are over 100-fold fewer mononucleated cells in the fibre fraction than the mononucleated fraction, showing efficient removal of contaminating cells. $n=1000$ cells per condition. Data are from 3 experiments conducted in triplicate. All data represented as mean \pm s.e.m.

3.3. Aged purified myofibre extract induces quiescent satellite cells to cycle

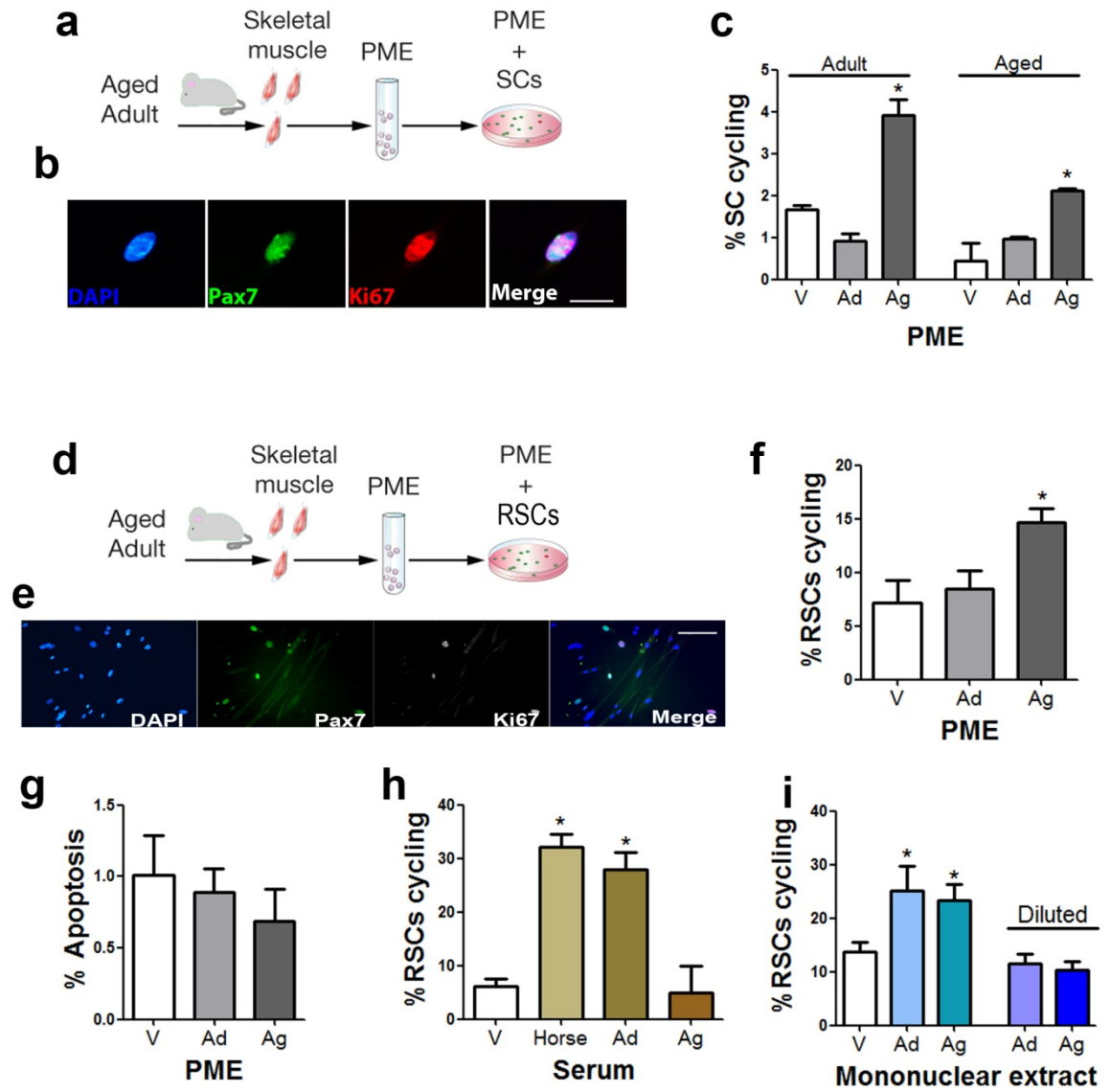
To identify if any soluble muscle-derived factors signal to SCs, PME was incubated with sorted SCs in basal media (DMEM+5%HS) for 48 hours and assayed for cell cycle entry (**Figure 18a,b**). In comparison with adult PME, aged PME increased the fraction of adult and aged quiescent cells that began to cycle (**Figure 18c**), suggesting that there are pro-mitogenic factor(s) in the aged fibre which are absent in the adult fibre.

Under differentiation conditions *in vivo* (DMEM+3%HS) myoblasts fuse to form myotubes, however, some myoblasts retain Pax7 expression and enter a quiescent state and these are termed reserve cells (RSCs) [182]. RSCs are an *in vitro* model of reversible SC quiescence [182]. To further confirm that aged PME induces a loss of quiescence, PME was incubated with RSCs and cells were assayed for cell cycle entry (**Figure 18d,e**). Like in sorted SCs, aged PME, but not adult PME, caused the loss of RSC quiescence (**Figure 18f**) and did not affect apoptosis (**Figure 18g**). In contrast to aged PME, aged serum did not induce cell cycle entry (**Figure 18h**) whereas adult serum did, in agreement with previous findings on the effect of adult and aged systemic system on SC activation [10].

Adult and aged mononuclear extract caused the activation of RSCs (**Figure 18i**). However, in adult and aged PME there are roughly 2.5 contaminating mononuclear cells / μl PME (see **Figure 17c**). When adult and aged mononuclear extract was diluted to a level close to what is present in the contaminating PME fraction it had no effect on RSC quiescence (**Figure 18i**), further showing the purity of adult and aged PME.

Collectively, these results demonstrate that the proliferative activity of SCs is induced by aged muscle fibre-derived factors.

3: Results Part I



3: Results Part I

Figure 18 - The aged niche induces the loss of satellite cell quiescence. **a**, Strategy to assess the mitogenic activity of PME with sorted SCs. Adult and aged PME was incubated with adult and aged sorted SCs for 48 hours prior to analysing cell cycle entry. **b**, Representative image of an activated SC stained for anti-Pax7, Ki67 and Dapi. Scale bar, 10 μ m. **c**, Quantification of the percentage of cycling (Ki67⁺) adult and aged SCs incubated with vehicle control (V), adult PME (Ad) or aged PME (Ag). **d**, Schematic of the experimental strategy to assess cycling reserve cells (RSCs) after exposure to adult or aged PME. PMEs were incubated with RSCs for 24 hours in basal media (DMEM+3%HS). **e**, Representative image of RSCs stained with anti-Pax7, Ki67 and Dapi. Scale bar, 100 μ m. **f**, Quantification of the percentage of cycling (Ki67⁺) RSCs incubated with vehicle control (V), adult PME (Ad) or aged PME (Ag). **g**, Quantification of the percentage of RSC apoptosis (aCasp⁺) after exposure to vehicle control (V), adult PME (Ad) or aged PME (Ag). Note apoptosis is less than 1% under all conditions. **h**, Quantification of the percentage of cycling RSCs after exposure to negligible amounts of serum (V, less than 3%), 10% horse serum (Horse), adult (Ad) and aged (Ag) serum directly isolated from mice. Note both 10%HS and adult serum can induce RSCs into cycle whereas aged serum is less effective. **i**, Quantification of the percentage of cycling RSCs after exposure to vehicle control (V), adult (Ad), or aged (Ag) mononuclear cell protein extract at a 20 μ g/ml concentration or diluted to contaminating concentrations found in adult and aged PMEs. Note no significant difference in the ability of diluted Ad and Ag mononucleated protein extract to induce RSCs into cycle. For all experiments, n=500-1000 cells per condition conducted in triplicate. All data represented as mean \pm s.e.m.; *P<0.05 student's t test.

3.3.1. FGF2 is sufficient to drive satellite cells to cycle

Members of the FGF family of ligands are well-characterised growth factors that are known to possess potent SC mitogenic activity (see **Section 1.4.3.3.** and **Figure 2**). In particular, FGF2 can effectively drive cycling of myogenic precursors [100-102]. FGF2 induced SCs on isolated single muscle fibres to cycle in a dose dependent manner (**Figure 19a**) and had a similar effect on RSCs (**Figure 19b**). Addition of FGF2 to sorted adult and aged SCs in basal media caused them to lose quiescence (**Figure 19c**). Furthermore, addition of FGF2 to adult PME caused isolated SCs and RSCs to cycle (**Figure 19d,e**). To further demonstrate the sensitivity of the quiescence assay and the potent mitogenic capabilities of FGF2, adult and aged sorted SCs were incubated with FGF2 or vehicle control for 24, 48, or 72 hours and then assayed for cell cycle entry. At 24 and 48 hour time points, SCs in basal media were relatively quiescent in the absence of FGF2, and aged and adult SCs lost quiescence in response to FGF2 addition (**Figure 19f**). At a 72 hour time point, many SCs were cycling, yet FGF2 still increased the number of cycling SCs (**Figure 19f**). These data show that sorted SCs are relatively quiescent in basal media up to 48 hours after isolation, and FGF2 can cause a loss of quiescence in a dose-dependent manner.

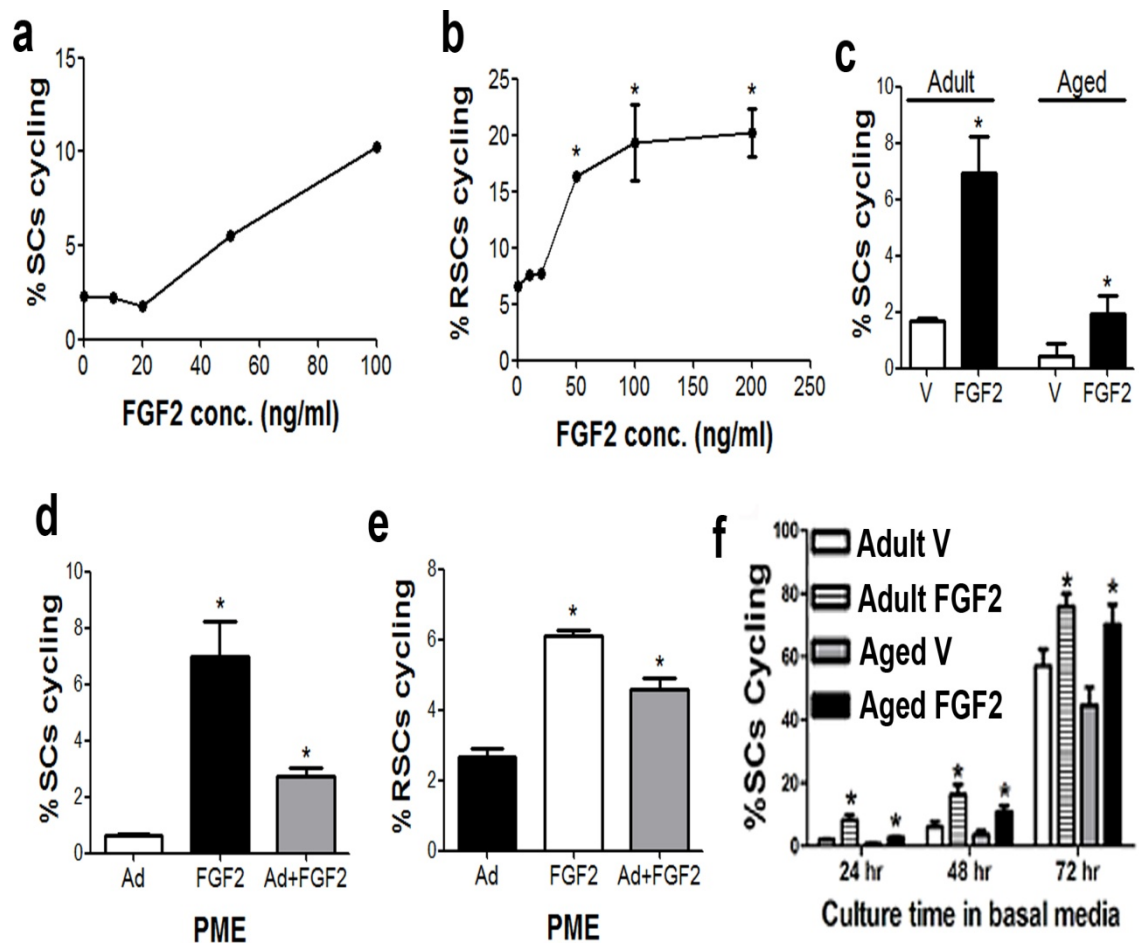


Figure 19 - FGF2 acts as a potent mitogen to induce satellite cells to cycle in a dose-dependent manner. **a**, Quantification of the percentage of cycling SCs (Ki67⁺) on isolated single muscle fibres. Fibres were incubated with different concentrations of FGF2 in basal media (DMEM+5%HS) for 24 hours and stained for anti-Pax7 and Ki67. n=30 fibres per condition. **b**, Quantification of the percentage of cycling RSCs after incubation with different concentrations of FGF2 in basal media (DMEM+3%HS) for 24 hours. n=500 cells performed in triplicate. **c**, Quantification of the percentage of aged and adult sorted SCs cycling after addition of 40ng/ml FGF2 for 48 hours of culture in basal media (DMEM+5%HS). n =300 cells performed in triplicate. **d**, Quantification of the percentage of cycling sorted SCs and RSCs (**e**) after exposure to Ad PME with or without prior treatment with 40ng/ml FGF2. Note addition of FGF2 to Ad PME caused the cycling of SCs and RSCs, whereas Ad PME on its own did not. n= 1000 cells / condition performed in triplicate. **f**, Quantification of the proportion of cycling sorted SCs cultured in basal media (DMEM+5%HS) with or without incubation with 100ng/ml FGF2 for 24, 48 and 72 hours. Data are from 2 experiments conducted in triplicate. n=1000 cells / experiment. All data represented as mean \pm s.e.m.; *P<0.05 student's t test.

3.3.2. FGF2 is upregulated in aged skeletal muscle fibres

To determine if FGF2 is a niche-derived factor which is upregulated in ageing, RNA from purified single skeletal muscle fibres from adult and aged mice was extracted and changes in the expression of *Fgf* ligands were determined by a targeted growth factor array. The expression of *Fgf1,2,6,13* and *18* was altered in aged muscle fibres compared to adult fibres (**Figure 20a**). Of these, *Fgf2* had the greatest fold change, being upregulated between 1.5 and 2 fold (**Figure 20a**). An increase in the expression of *Fgf2* was confirmed by RT-qPCR (**Figure 20b**). Furthermore, *in situ* hybridisation of an anti-sense probe to *Fgf2* on isolated adult and aged single fibres showed large areas, or 'hotspots', of *Fgf2* expression along the length of aged fibres which were not present in adult fibres (**Figure 20c,d**). Performing immunohistochemistry for Pax7 after *in situ* hybridisation using an anti-sense *Fgf2* probe showed that many of these *Fgf2* 'hotspots' were close to, but unlikely to be produced by, SCs (**Figure 20e**).

To determine if the expression of *Fgf2* is altered in aged myofibres compared to adult, RT-qPCR for *Fgf2* was performed on purified myofibres prior to extracting the soluble fraction. *Fgf2* was upregulated approximately 2-fold in aged PME compared to adult PME (**Figure 20f**).

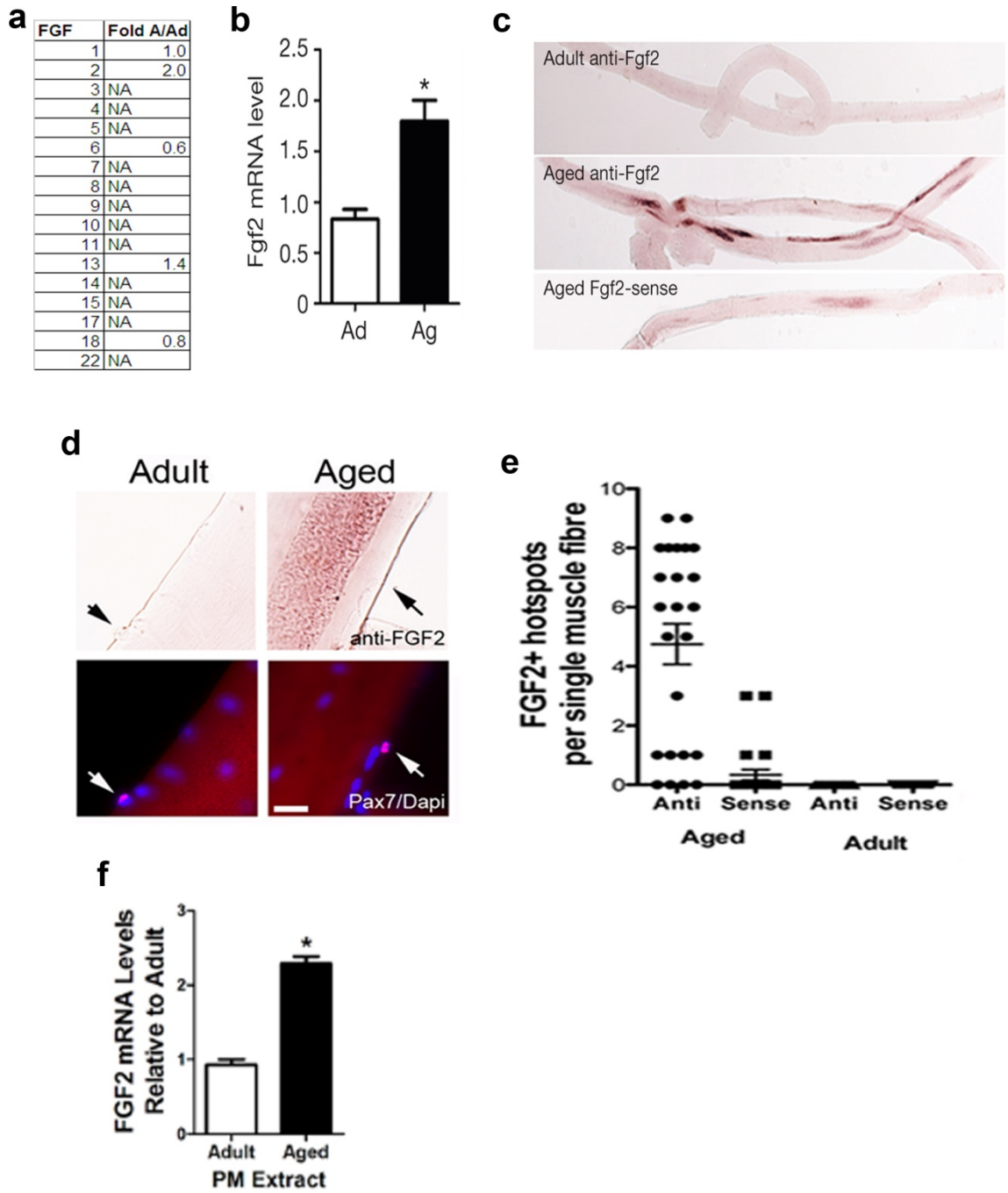
To determine if FGF2 protein was upregulated in aged PME, fibre fragments obtained to generate PMEs were immunostained for Pax7 and FGF2 (**Figure 21a**). A greater number of aged fibre fragments expressed FGF2 protein (**Figure 21b**), and FGF2 could be seen close to Pax7⁺ SCs (**Figure 21a**). Interestingly, the number of mononucleated cells expressing FGF2 in the mononucleated fraction was slightly decreased (**Figure 21c,d**). Although this was not significant, it argues against an increase in FGF2 outside of the myofibre being responsible for a loss of SC quiescence under homeostatic conditions.

To determine if FGF2 increased in aged skeletal muscle under homeostatic conditions, adult and aged TA sections were stained with antibodies raised against FGF2 and the number of FGF2⁺ areas were counted. Even though no *Fgf2* 'hotspots' were found on adult single fibres by *in situ* hybridisation, FGF2⁺

areas were found associated with adult skeletal muscle by immunostain (**Figure 21e**). This suggests that either the FGF2 antibody is more sensitive than the *Fgf2* anti-sense probe, or alternatively it may indicate a degree of non-specific antibody binding. Regardless, aged skeletal muscle displayed a 2-fold increase in the number of FGF2⁺ areas associated with muscle fibres (**Figure 21e,f**). Interestingly, the number of interstitial FGF2⁺ areas was decreased, further arguing against an increase in FGF2 expression outside of the myofibre causing a loss of SC quiescence. To determine if the areas of FGF2 protein on muscle fibres were close to SCs, adult and aged TA sections were stained with antibodies raised against FGF2, Pax7, and laminin. Of note, FGF2 protein was not detected on SCs (**Figure 21f**), further suggesting that they do not produce a significant amount of FGF2 under homeostatic conditions. However, the percentage of SCs found close to a source of FGF2 was increased 2-fold in aged skeletal muscle (**Figure 21g**).

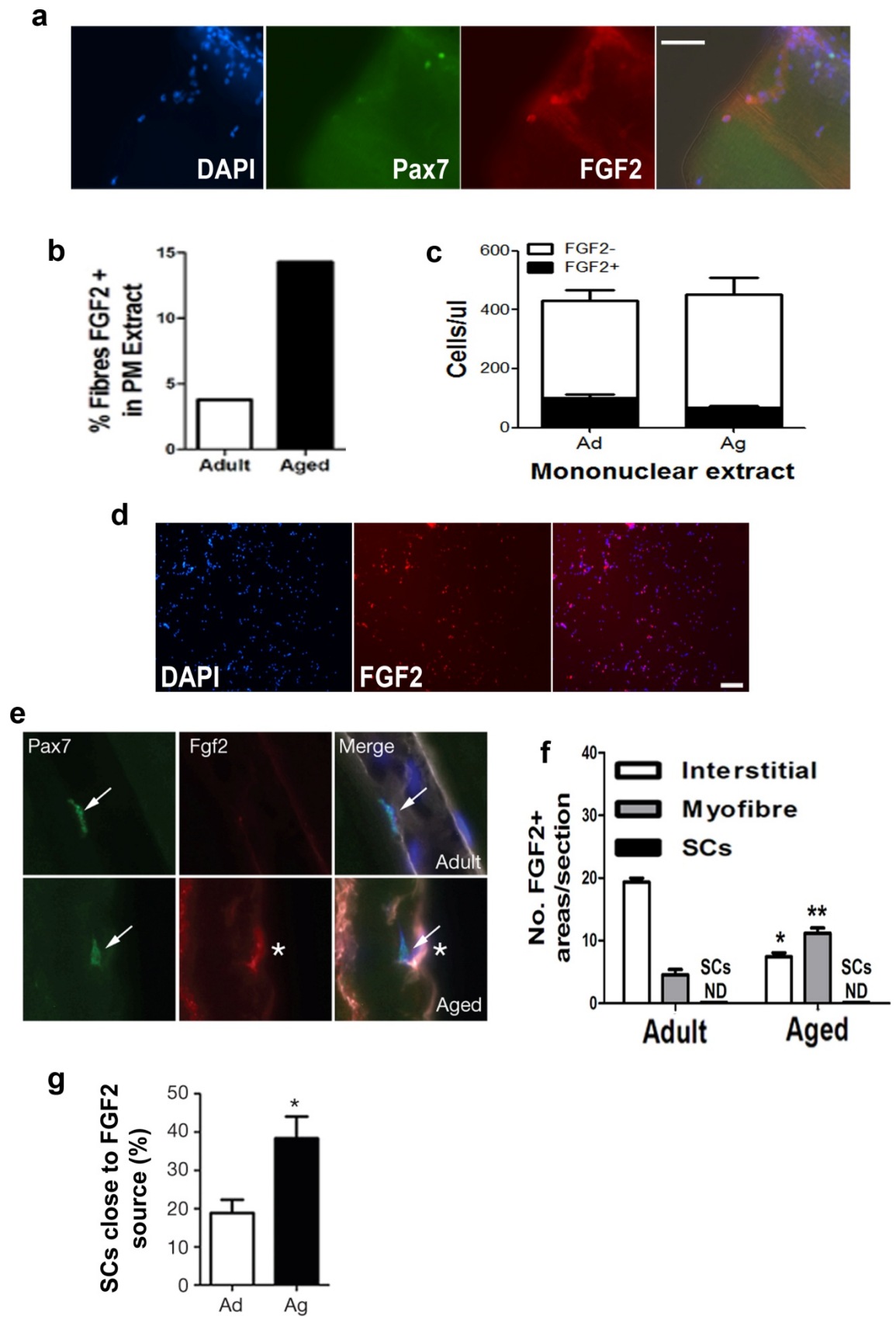
Together these results show that FGF2 is upregulated in aged skeletal muscle under homeostatic conditions and that the aged SC niche, the muscle fibre, is the principal source of FGF2.

3: Results Part I



3: Results Part I

Figure 20 - Expression of Fgf2 from the muscle fibre increases in aged skeletal muscle. a, Table of expression for 17 different FGF ligands from aged relative to adult isolated single muscle fibres (Fold A/Ad) from duplicate RT-qPCR based array kits (SAbiosciences). N.A. (not attained) designates whereby Cq values were greater than controls provided by the kit. **b,** Quantification of *Fgf2* expression in aged relative to adult single muscle fibres by RT-qPCR. Data are from 3 reactions conducted in triplicate. **c,** Representative images of *Fgf2 in situ* hybridisations on adult and aged single muscle fibres. A sense probe was used as a background negative control (lower panel). **d,** Representative image of *Fgf2 in situ* hybridisation on aged single muscle fibres shows increased *Fgf2* (brown) in close proximity to Pax7⁺ (red) SCs. Dapi (blue). Scale bar, 20µm. **e,** Quantification of the number of *Fgf2* 'hotspots' along the length of single muscle fibres. n>30 fibres / animal, n=3 mice / group. **f,** Expression of *Fgf2* in adult and aged fibres obtained to generate PME as assessed by RT-qPCR. Note the fold difference in *Fgf2* expression is similar to that observed for purified single muscle fibres (see **Figure 20b**). Data are from 3 reactions conducted in triplicate. All data represented as mean ± s.e.m.; *P<0.05.



3: Results Part I

Figure 21 - Muscle fibre-derived FGF2 increases with age. **a**, Representative image of aged fibres obtained to generate PME immunostained for Pax7, FGF2 and Dapi. Merge with brightfield. Scale bar, 50µm. Note FGF2 protein close to Pax7⁺ SCs. **b**, Quantification of the percentage of muscle fibres that contain FGF2⁺ regions in aged or adult fibres used to generate PME. Data are from 3 separate experiments. n=100 fibres / experiment. **c**, Quantification of FGF2⁺ cells in isolated skeletal muscle mononucleated cells. Note a decrease in the expression of FGF2 in aged compared to adult mononucleated compartments. Data are from 3 experiments conducted in triplicate. n=1000 cells per condition. **d**, Representative image of FGF2 expression in isolated skeletal muscle mononucleated cells. Scale bar, 100µm. **e**, Representative longitudinal sections of adult and aged skeletal muscle stained with anti-Pax7 (green), laminin (white) and FGF2 (red). A white arrow shows a Pax7⁺ satellite cell close to FGF2 (asterisk). Dapi (blue) in merge. **f**, Quantification of FGF2⁺ areas in transverse muscle sections showing increased muscle fibre-associated, and decreased interstitial-associated, FGF2 in aged muscle fibre sections. Note FGF2 protein was not detected (ND) on SCs. n = 5-6 mice / age group. **g**, Quantification of the percentage of SCs near (<20 µm) FGF2⁺ regions. n = 3 animals / age group. All data represented as mean ± s.e.m.; *P<0.05, **P<0.01 student's t test.

3.3.3. Induction of aged niche-derived FGF2 disrupts satellite cell quiescence

I have shown that FGF2 is a niche-derived factor which is upregulated in the aged SC niche (see **Figure 21**). Through *in vitro* assays, I have shown that the aged niche can drive the loss of quiescence of SCs (see **Figure 18**). From these data, I hypothesised that FGF2 was the potent mitogenic factor which was causing the loss of SC quiescence with age, leading to altered stem cell number and function. To test if FGF2 is directly responsible for the loss of SC quiescence, I inhibited FGF signalling genetically and by using chemical inhibitors, and I also blocked FGF2 activity directly.

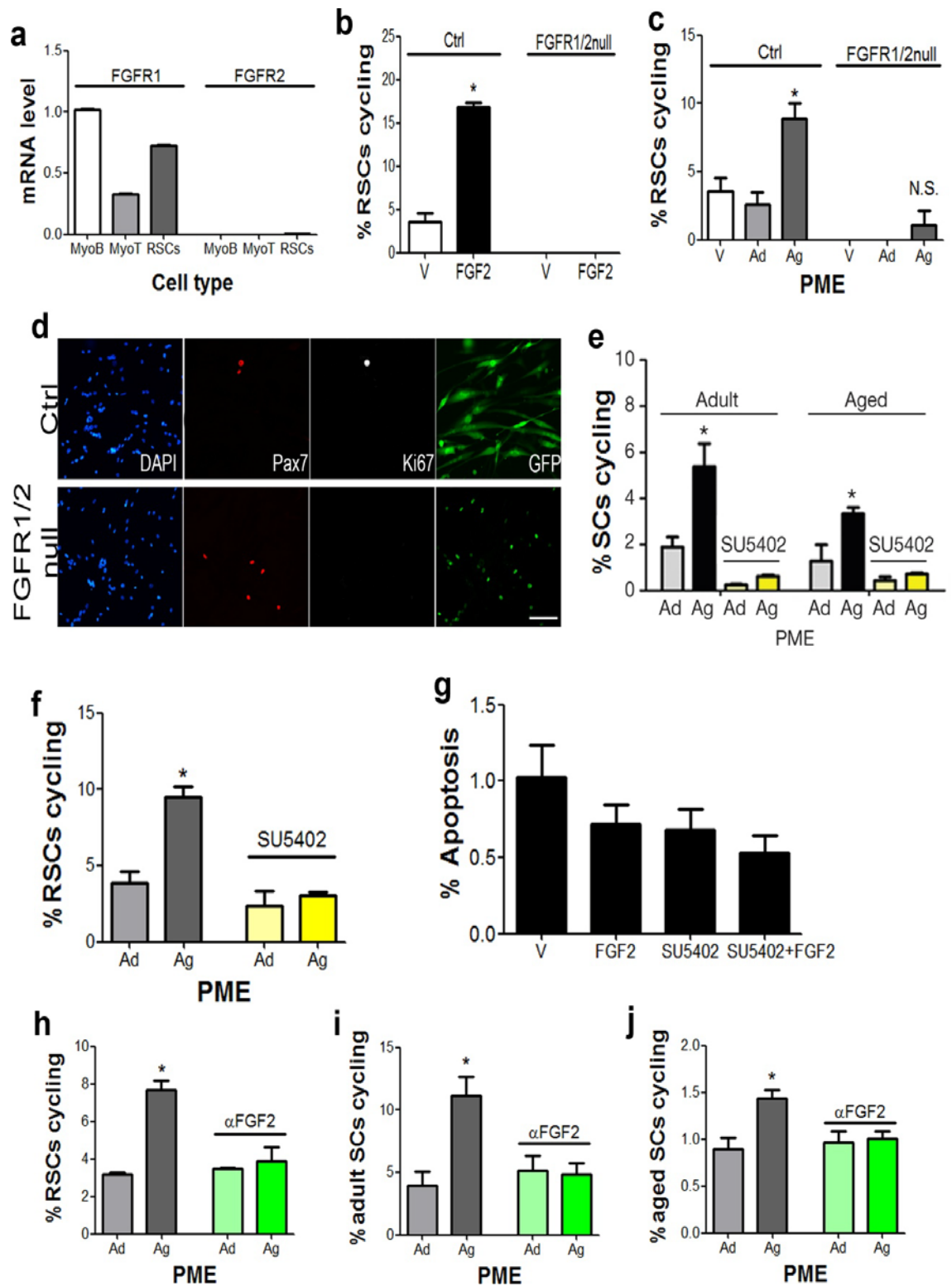
To investigate whether FGF2 is the factor in the aged niche which is causing SC activation, myoblasts from mice where both *FgfR1* and *FgfR2* alleles are floxed (*FgfR1/2^{flox/flox}*) were generated. Myoblasts were then treated with either GFP adenovirus (Ctrl) or Cre-GFP adenovirus (FGFR1/2null) to cause a loss of *FgfR1* and *FgfR2* function. RSCs were then generated to determine the effect of the loss of *FgfR1/2* on RSC quiescence. *FgfR2* is not expressed by myoblasts, myotubes, or reserve cells (**Figure 22a**), so any effects seen from *FgfR1/2* deletion is solely due to abrogation of signalling through FGFR1. Deletion of *FgfR1/2* completely inhibited the proliferative effect of FGF2 and aged PME in transfected cells (**Figure 22b-d**), suggesting that FGFR1 signalling is necessary for RSC activation. Furthermore, incubation of adult and aged sorted SCs with the FGFR-specific inhibitor, SU5402 (see **Figure 2**), prior to addition of adult or aged PME completely blocked aged-PME-induced stem cell activation (**Figure 22e**) and a similar effect was seen in RSCs treated with SU5402 (**Figure 22f**). Notably, incubation with SU5402 did not affect apoptosis (**Figure 22g**). These results show that signalling through FGFR is responsible for the loss of SC quiescence in the aged niche.

To directly test whether FGF2 was responsible for the altered biological activity of aged PME, the extract was treated with a blocking antibody against FGF2 (α FGF2; see **Figure 2**) prior to incubating it with RSCs or sorted SCs. Neutralisation of FGF2 activity prevented aged PME-induced cell cycle entry in

RSCs (**Figure 22h**) and adult (**Figure 22i**) and aged SCs (**Figure 22j**).

Therefore, the increased abundance of soluble muscle-fibre-derived FGF2 in aged muscle leads to a loss of quiescence in aged satellite cells.

3: Results Part I



3: Results Part I

Figure 22 - FGF2 is an aged niche-derived factor that induces satellite cells to cycle. **a**, Expression of *FgfR1* and *FgfR2* in myoblasts (MyoB), Myotubes (MyoT), and reserve cells (RSCs) as assessed by RT-qPCR. Data are from 3 reactions conducted in triplicate. **b**, Quantification of cycling RSCs after adenoviral Cre-mediated deletion of *FgfR1* and *FgfR2* from RSCs (FGFR1/2null) or control adenovirus (Ctrl) and upon incubation with vehicle (V), 40µm FGF2, or adult (Ad) or aged (Ag) PME (**c**). N.S., Not significant. n=300-600 cells / condition, 4-5 separate experiments. **d**, Representative image of myoblasts from *FgfR1/2^{flox/flox}* mice treated with Cre-GFP adenovirus (FGFR1/2null) or GFP adenovirus (Ctrl) and induced to form RSCs. Scale bar, 100µm. **e**, Quantification of the percentage of cycling adult and aged sorted SCs or RSCs (**f**) treated with adult or aged PME and SU5402. n=1000 cells per condition; n=5 animals per group. **g**, Quantification of the percentage of apoptotic RSCs (aCasp⁺) after incubation with SU5402 or FGF2. Note less than 1% of cells undergo apoptosis in all conditions. Data are from 3 experiments conducted in triplicate. n=500 cells per condition. **h**, Quantification of the percentage of cycling RSCs or adult (**i**), or aged (**j**) sorted SCs treated with adult or aged PME and FGF2-blocking antibody (αFGF2). n=1000 cells per condition; n=5 animals per group. All data represented as mean ± s.e.m.; *P<0.05, student's t test.

3.4. Discussion

I sought to investigate the influence of ageing on the SC niche and its impact on stem cell homeostasis. The data presented here identify a specific and functionally important change in the molecular composition of the aged stem cell niche. These data show that SCs are relatively dormant during homeostasis. By contrast, aged SCs become mitotically active, leading to a loss of self-renewal potential and this is a likely mechanism causing the eventual diminution of the SC pool with age (**Figure 23**). I have demonstrated that the aged SC niche, the muscle fibre, is pro-mitogenic and capable of driving a subset of SCs to break quiescence and lose self-renewing capacity under homeostatic conditions. I have identified FGF2 as a key niche-derived mitogenic factor that is increased in the aged niche.

Proliferative exhaustion of stem cell populations is marked by the failure to maintain quiescence, impaired self-renewal and eventual loss in numbers [367]. Loss of SC quiescence under homeostatic conditions was surprising considering their proliferative disadvantage in high-mitogen regenerative contexts [88]. Instead, it may have been expected that aged SCs would be even more quiescent than their adult counterparts. However, in support of a loss of quiescence with age, aged HSCs are more active in the aged niche [368, 369]. It is tempting to speculate that a consequence of ageing across stem cell niches is their inability to retain stem cells in a quiescent state.

These data are consistent with a key role for a niche-derived factor, FGF2, that is low in the adult SC niche and increases during ageing to drive cells out of quiescence and contribute to stem cell loss. SCs in the adult niche do not proliferate under homeostatic conditions, indicating that there are no pro-mitogenic factors in the adult niche. Alternatively SCs could be kept quiescent through the expression of *Spry1*, or quiescence-inducing factors such as Ang1 / Tie2 signalling [138], or by certain cell-to-cell contacts such as association with a healthy myofibre [128]. Aged SCs cycle, suggesting that the aged niche induces the loss of stem cell quiescence. Reducing the level of FGFR signalling, through deletion of *Fgfr1/2* and through chemical inhibitors of FGFR

and FGF2, altered the degree of cell cycle entry. Therefore, SCs are clearly responsive to changes in niche-initiated signalling and altering the level of FGF signalling can change stem cell outcome.

Loss of quiescence is consistent with the impaired function of aged SCs. Recent experiments examining the proliferative heterogeneity of SCs has uncovered two pools of SCs exist; a quiescent pool (LRC), and a more proliferative pool (non-LRC) [124, 127]. The non-LRC SC pool had a decreased ability to self-renew and reconstitute the niche after transplantation, whereas the LRC pool had an increased tendency to self-renew and were able to generate more new myofibres after multiple injuries [124, 127]. These data suggest that loss of quiescence can lead to impaired function and a loss of SC number over time.

I have shown that the expression of five Fgfs are altered in ageing (see **Figure 20a**). It is possible that the change in the expression of Fgfs other than FGF2 may account for other aspects of skeletal muscle ageing. For example, *in vitro*, FGF6 slows down the transition to differentiation in myogenic cells [97]. A decrease in *Fgf6* expression from the myofibre may increase the tendency for SCs to prematurely differentiate and contribute to the impaired regenerative capability of aged skeletal muscle. It would be interesting to investigate the effect of the changes in other Fgf ligands and see how they contribute to skeletal muscle ageing alone and in combination with other changes.

The systemic environment plays a significant role in SC proliferation *in vitro* and during repair. The young systemic environment stimulates SC proliferation, whereas the aged systemic environment inhibits SC proliferation (see **Figure 18h**) [10, 164]. These data show that the aged niche becomes stimulatory, suggesting that the systemic environment and the niche have opposing influences on SCs in both adult and aged muscle (**Figure 23**). During homeostasis, adult SCs remain quiescent when in a pro-mitogenic systemic environment, and aged SCs respond to the stimulatory myofibre niche when surrounded by an inhibitory systemic environment (**Figure 23**). These data suggest that the niche is dominant. In the context of injury, the relationship

between niche and systemic environment is disrupted due to breakdown of the myofibre after injury, leaving a permissive systemic environment to exert its influence on SCs. However, many factors are known to change in muscle during ageing including systemic factors, neuromuscular integrity and fibrosis (see **Section 1.6.2**). It will be of interest to determine how these changes may act either alone or collectively to affect SC function either directly or indirectly through niche modulation and maintenance with age.

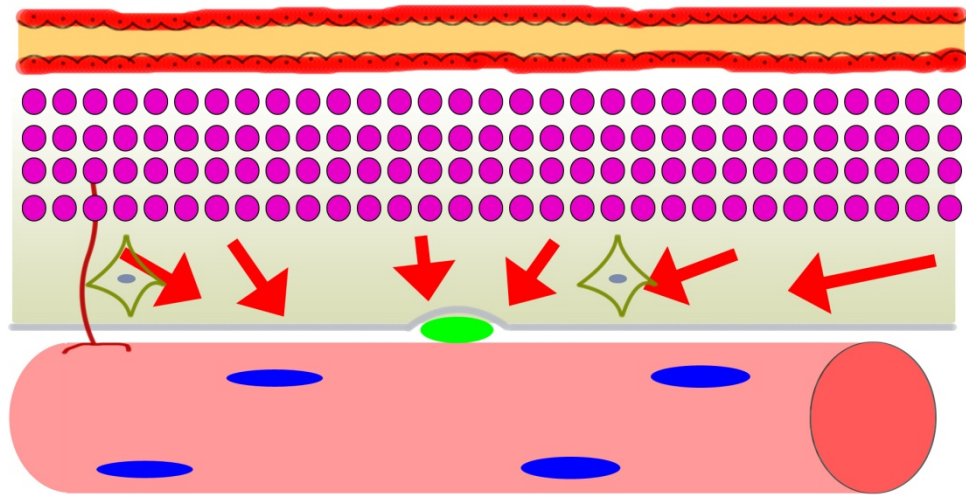
I have partially characterised the muscle stem cell niche during ageing, focusing on the elements that control stem cell quiescence and number during homeostasis. The reasons behind the increased FGF2 are not known, however, based on mRNA distribution, *Fgf2* mRNA appears to be located at many sites along the fibre (see **Figure 20c**), rather than localised to discrete regions such as the SC microenvironment, muscle-tendon connections or neuromuscular junction. I propose that the induction of this potent mitogen is an attempt to repair the aged muscle fiber. Since muscle fibres are not regenerated under homeostatic conditions there may be an accumulation of low-level chronic myofibre damage with age. This may cause the myofibre to upregulate FGF2 after a certain threshold has been reached in aged skeletal muscle. This upregulation of FGF2 is akin to the induction of FGFs during development to promote myogenic commitment and differentiation [102, 109, 370-373]. However, unlike during development, upregulation of FGF2 occurs at the expense of the stem cell number and function in aged skeletal muscle. Therefore, strategies to prevent chronic FGF2 production from the aged niche, or repress FGF signalling at the level of the aged SC, or prevent damage to the aged niche, may reduce stem cell loss during ageing.

These data suggest that increased niche-derived FGF2 and loss of quiescence may be detrimental to stem cell number and function. In order to determine if increased FGF2 expression from the niche negatively impacts SC number and function with age, I sought to modulate FGF signalling *in vivo* by altering the levels of the negative regulator of FGF signalling, *Spry1* (see **Figure 2**).

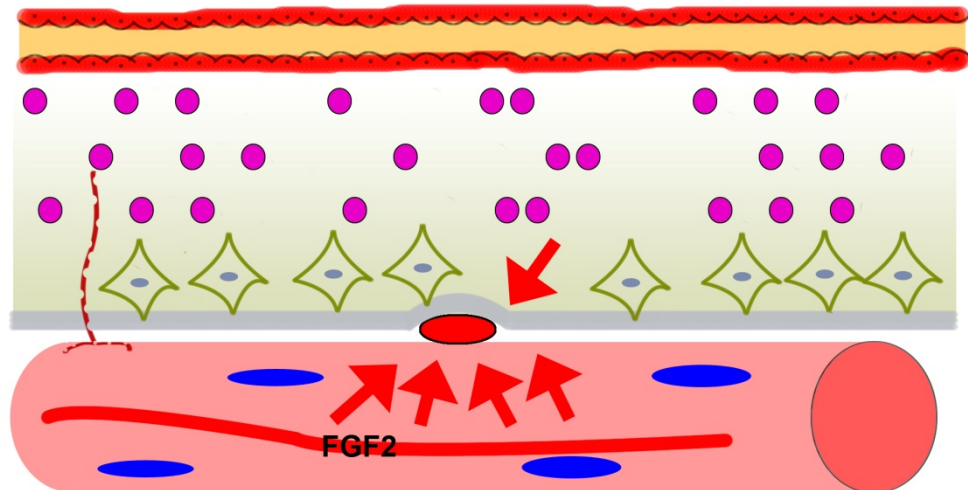
3: Results Part I

Furthermore, I sought to investigate if the loss of stem cell number with age can be halted by inhibiting FGF signalling specifically in SCs.

Adult



Aged



Key:











- | | | | | | |
|---|--------------------------|---|-------------------------------------|---|----------------------------------|
|  | Motor neuron |  | Cycling satellite cell |  | Pro-mitogenic systemic molecules |
|  | Muscle fibre |  | Basal lamina |  | Fibroblast |
|  | Myonuclei |  | ECM | | |
|  | Quiescent satellite cell |  | Blood vessel with endothelial cells | | |

Figure 23 - The systemic environment and the niche have opposing influences on satellite cells in adult and aged skeletal muscle. The systemic environment in adult skeletal muscle is pro-mitogenic and can enhance the activation of aged SCs [10, 164]. However, under homeostatic conditions, the basal lamina acts as a barrier to these mitogenic stimuli and SCs are maintained in a quiescent state (top panel). The aged SC systemic environment does not instruct SCs to cycle and is detrimental to regeneration [10, 164]. The aged SC niche, however, upregulates FGF2 and this causes SCs to cycle (bottom panel). This suggests that the niche is the dominant signal to SCs. Aged skeletal muscle also displays increased fibrosis, a thickened basal lamina and breakdown of the neuromuscular junction, which may all interact to modulate aged SC function.

Chapter 4

Results Part II

4.1. Sprouty proteins modulate FGF signalling

Sprouty (*Spry*) proteins are negative regulators of FGF signalling, specifically inhibiting Ras-ERK MAPK signalling, leaving phosphoinositide 3-kinase (PI3K) and other MAPK pathways unaffected (see **Figure 2**) [374, 375]. In mammals there are four *Spry* proteins (*Spry1-4*). The transcription of *Spry* genes is induced by Ras-ERK MAPK signalling (see **Figure 2**) [376]. However, the expression of *Spry* genes is not always induced by RTK signalling and their induction may be controlled differently in various cell types. For example, in NIH3T3 fibroblast cells and endothelial cells, the expression of *Spry2* is upregulated by growth factor addition, and, in contrast, *Spry1* is downregulated [374, 377]. Tissue-specific transcription factors may also regulate the spatiotemporal expression patterns of *Spry* genes. For example, in mouse kidney development, the transcription factor Wilms tumor-suppressor gene 1 induces the expression of *Spry1* by directly binding to the *Spry1* promoter [378]. This suggests that the different *Spry* proteins may play distinct roles in these cell types.

Spry proteins have recently been shown to play a role during embryonic myogenesis. Studies by Lagha et al. showed that *Spry1* is directly regulated by Pax3 [370]. The authors identified a role for *Spry* proteins in forming immature myogenic precursors at the expense of more differentiated cells [370]. This suggests that modulation of *Spry* levels may affect myogenic stem cell fate decisions.

Spry1 is robustly expressed in adult quiescent SCs under homeostatic conditions with the other *Spry* family members expressed at much lower levels [42, 89]. This suggests that growth factors may be present in uninjured muscle and can actively signal to SCs. It is possible that the growth factors present may induce SC quiescence rather than activation, or hold them in a state allowing for rapid activation upon injury. Alternatively, expression of *Spry1* may be controlled via transcription factor activity independent of RTK signalling, like in kidney development and embryonic myogenesis [370, 378].

Spry1 has recently been shown to be an essential regulator of adult SC function after myotrauma. Studies by Shea et al. have shown that *Spry1* expression is downregulated as SCs proliferate in response to injury and re-induced as SCs return back to quiescence [42]. Deletion of *Spry1* specifically in adult SCs led to an increase in the apoptosis of SCs after injury and, therefore, a reduction in the SC pool [42]. Collectively, these studies suggest a model whereby *Spry1* normally inhibits the RTK signals required for SC proliferation in homeostasis [42].

So far, I have shown that FGF2 is upregulated in the aged SC niche and this drives a loss of stem cell quiescence (see **Figure 23**). To investigate the role of FGF signalling in adult and aged SCs under homeostatic conditions, I sought to manipulate FGF signalling levels in SCs *in vivo*. This was achieved through the conditional deletion and overexpression of *Spry1* which allowed for the non-invasive manipulation of FGF signalling with endogenous regulators. The aims for this chapter are to:

1. Delete *Spry1* specifically in Pax7⁺ SCs to determine if increased FGF signalling further disrupts SC quiescence and function, and
2. Overexpress *Spry1* specifically in Pax7⁺ SCs to determine if blockade of FGF signalling under homeostatic conditions can rescue age-related changes in SC number and function.

4.1.1. Loss of *Spry1* further enhances loss of satellite cell quiescence in response to the aged niche *in vitro*

To increase the sensitivity of SCs to RTK signalling, *Spry1* levels were reduced using a *Spry1*^{flox/+} myoblast line. *Spry1*^{flox/+} myoblasts were induced to form RSCs and then cells were treated with either GFP adenovirus (Ctrl-AdV; WT) or Cre-GFP adenovirus (Cre-AdV; S1flx) to reduce *Spry1* levels (**Figure 24a,b**). Reduction in *Spry1* levels increased RSC sensitivity to FGF2 (**Figure 24c**) and aged PME (**Figure 24d**) and increased their cycling. These results suggested

that reducing *Spry1* levels would further increase stem cell responsiveness to the aged niche.

To determine if SCs are more sensitive to FGF2 in the aged niche, *Spry1*^{flox/flox} mice were crossed with *Pax7*^{CreERT2/+} mice to remove *Spry1* specifically in SCs. Adult and aged *Pax7*^{CreERT2/+}; *Spry1*^{flox/flox} (*Spry1*null) and Cre-negative control (WT) mice were given tamoxifen and SCs were isolated four weeks later (**Figure 25a**). Adult and aged *Spry1*null isolated SCs displayed an increased sensitivity to FGF2 (**Figure 25b,c**) and aged PME (**Figure 25d,e**) compared to WT controls. Interestingly, *Spry1*null isolated SCs also cycled more in vehicle control and adult PME compared to WT controls (**Figure 25d,e**). This could be explained by cells generally becoming more prone to activate after deletion of *Spry1* for 4 weeks.

I have previously shown that aged SCs are more prone to differentiate or apoptose compared to adult SCs (see **Figure 15k,l**). To determine if *Spry1*null SCs have an even greater tendency to apoptose or differentiate, *Spry1* was deleted specifically from adult and aged SCs for four weeks and isolated cells were plated at clonal density in culture. Their fate was determined by staining with antibodies to determine differentiation (MyoG) and apoptosis (aCasp). After four days in culture, *Spry1*null aged SCs became more prone to differentiate (**Figure 25f**) and apoptose (**Figure 25g**) compared to WT aged cells, whereas *Spry1*null adult SCs were not significantly different from adult WT cells (**Figure 25f,g**). These data suggest that increasing SC sensitivity to RTK signalling, through the loss of *Spry1*, increases SC cycling in the aged niche and further exaggerates age-associated changes in SC function.

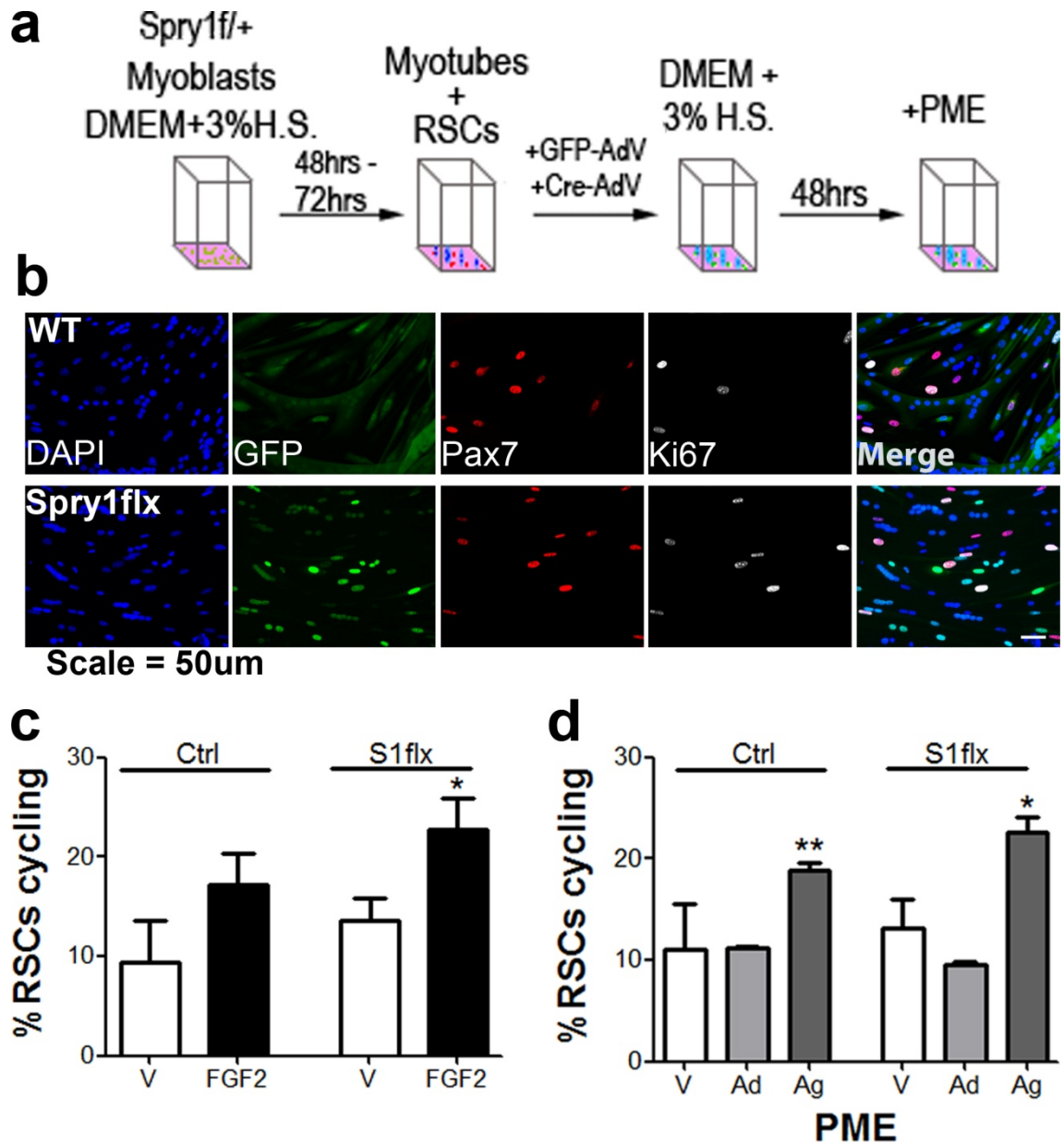


Figure 24 - Reduction in *Spry1* increases reserve cell cycling in response to the aged niche. **a**, Schematic of the experimental strategy to reduce *Spry1* levels *in vitro*. *Spry1*^{flx/+} myoblasts were put into differentiation media (DMEM+3%HS) and then treated with Cre-GFP adenovirus to reduce *Spry1* levels (S1flx) or GFP control (Ctrl). **b**, Representative image of RSCs and myotubes stained with GFP, Pax7, and Ki67. Scale bar, 50µm. **c**, Quantification of the percentage of cycling (Ki67⁺) RSCs after incubation with vehicle control (V), FGF2 or adult (Ad) or aged (Ag) PME (**d**). For all experiments, n=500-1000 cells per condition conducted in triplicate. All data represented as mean ± s.e.m.; *P<0.05, **P<0.01 student's t test.

4: Results Part II

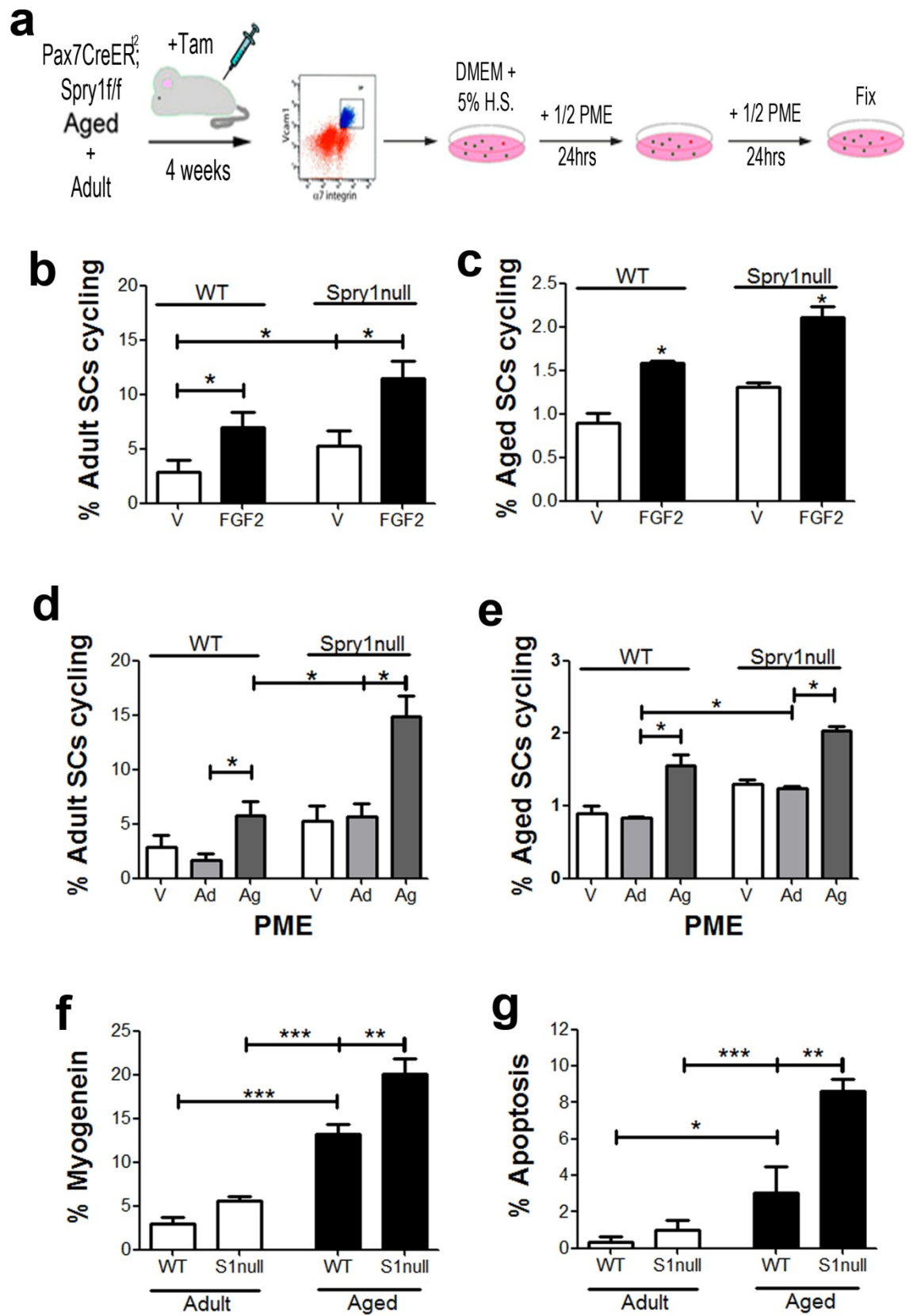


Figure 25 - Loss of *Spry1* specifically from satellite cells in vivo causes increased sensitivity to the aged niche and impaired function. **a**, Schematic of the experimental strategy to delete *Spry1* from adult and aged SCs and assess cell cycle entry after incubation with PME. **b**, Quantification of the percentage of cycling adult and aged (**c**) SCs after incubation with FGF2. **d**, Quantification of the percentage of cycling adult and aged (**e**) sorted SCs after incubation with vehicle control, adult PME, or aged PME. **f**, Quantification of the percentage of Myogenin⁺ (differentiated) and apoptotic (cleaved caspase 3⁺; **g**) cells from *Spry1* null (S1null) and WT adult and aged cells cultured for 4 days in DMEM+10%HS. 21-28 clonal density cultures were examined per condition, performed in triplicate. Note aged S1null cells display a much greater tendency to differentiate or apoptose compared to aged WT cells. For **b-e**, n=500-1000 cells per condition conducted in triplicate. All data represented as mean \pm s.e.m. ; *P<0.05, **P<0.01, ***P<0.001 student's t test.

4.1.2. *Spry1* inhibits FGF2-FGFR signalling

The *Spry* family of proteins inhibit RTK signalling. The data shown so far indicate that loss of *Spry1* increases SC cycling, differentiation and apoptosis in response to the aged niche. To determine if this effect of *Spry1* loss was through increasing FGF2-FGFR signalling, RSCs from *Spry1*^{flox/+} mice were generated and *Spry1* levels were reduced as in **Figure 24a**. Cells were treated with SU5402 prior to incubation with adult and aged PME to block FGFR signalling. Inhibition of FGFR blocked the increased sensitivity to aged PME in RSCs with reduced *Spry1* levels (**Figure 26a**). Furthermore, in cells from *Pax7*^{CreERT2/+}; *Spry1*^{flox/flox} mice treated as in **Figure 25a**, incubation of isolated cells with SU5402 prior to addition of PMEs had a similar effect and inhibited increased cell cycle entry in response to aged PME in *Spry1* null adult (**Figure 26b**) and aged (**Figure 26c**) SCs. To show that *Spry1* blocks FGF2-induced FGFR signalling, cells from *Pax7*^{CreERT2/+}; *Spry1*^{flox/flox} mice treated as in **Figure 25a** were isolated and incubated with adult and aged PME that had been treated with a blocking antibody to FGF2 (α FGF2). Block of FGF2 inhibited the effect of aged PME in WT and *Spry1* null adult (**Figure 26d**) and aged SCs (**Figure 26e**). Collectively, these results show that expression of *Spry1* is essential to maintain the quiescence of SCs in the aged niche by inhibiting FGF2 signalling.

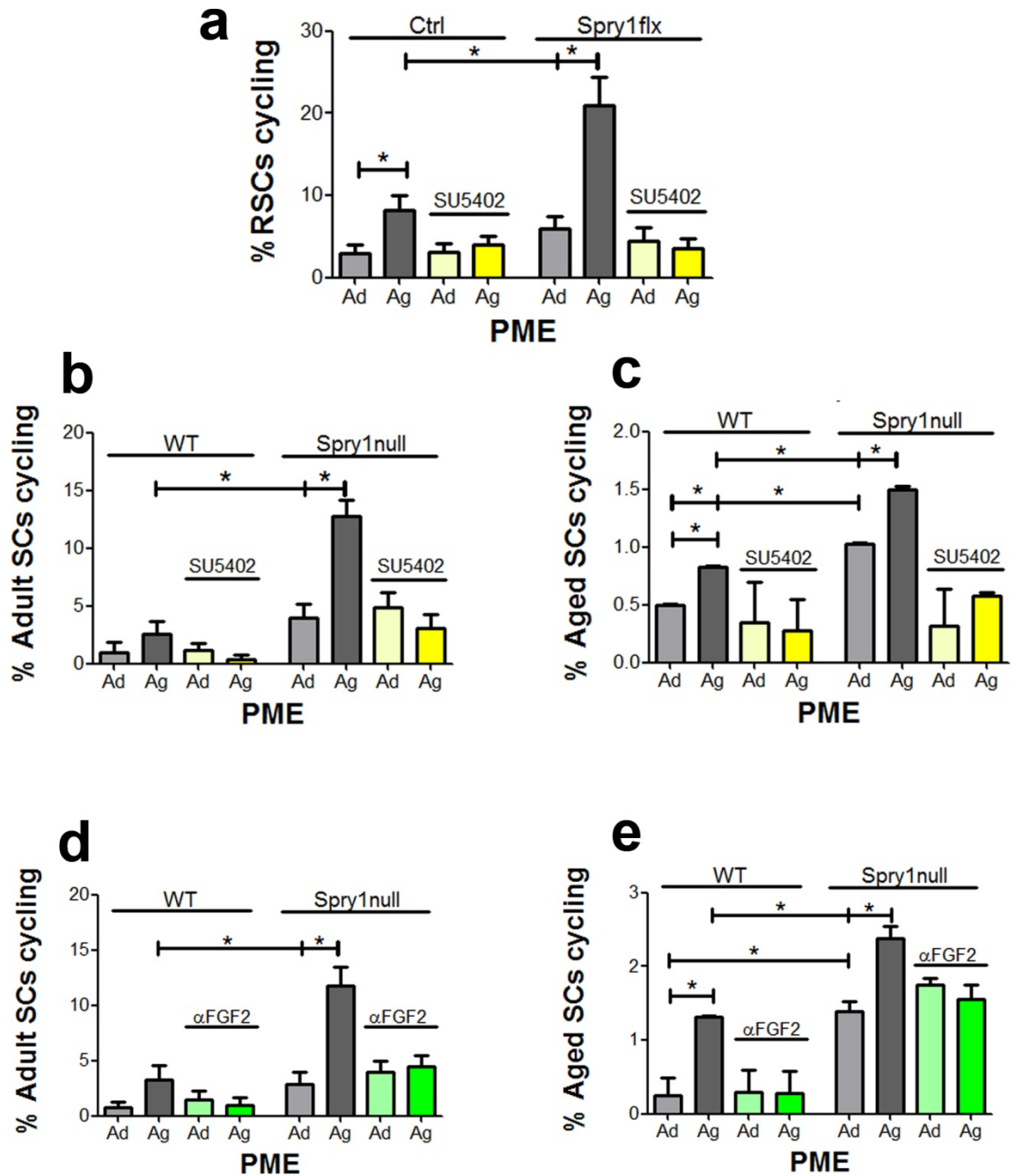


Figure 26 - Spry1 inhibits FGF2-FGFR signalling. **a**, Quantification of the percentage of cycling RSCs from Spry1flx or control cells incubated with adult (Ad) or aged (Ag) PME with or without the prior treatment with SU5402. **b**, Quantification of the percentage of cycling sorted SCs from Spry1null or control adult or aged (c) mice incubated with adult or aged PME with or without the prior treatment with SU5402. **d**, Quantification of the percentage of cycling sorted SCs from Spry1null or control adult or aged (e) mice incubated with adult or aged PME that had been treated with a blocking antibody to FGF2 (α FGF2) or vehicle control. n=500-1000 cells per condition conducted in triplicate. All data represented as mean \pm s.e.m.; *P<0.05, **P<0.01, ***P<0.001 student's t test.

4.1.3. *Spry1* overexpression inhibits the mitogenic effect of the aged niche

I have shown that loss of *Spry1* further increases mitogenic responsiveness of SCs to the aged niche (see **Section 4.1.1.**). Thus, I hypothesised that increasing levels of *Spry1* in SCs would inhibit cell cycle entry in response to FGF2 in the aged niche. To test this, myoblasts were generated from mice carrying a transgene encoding a Cre-inducible expression construct for *Spry1* controlled by a chicken β -actin gene (CAG) promoter (CAG–GFP^{flox}; *Spry1*; *Spry1OX*). *Spry1OX* myoblasts were treated with GFP adenovirus (Ctrl) or Cre adenovirus (*Spry1OX*) to cause an increase in *Spry1* expression (**Figure 27a**). RSCs were then generated to determine the effect of increased *Spry1* expression on RSC quiescence (**Figure 27a,b**). Overexpression of *Spry1* inhibited the activation of RSCs in response to FGF2 (**Figure 27c**) and aged PME (**Figure 27d**).

To further show that overexpression of *Spry1* can inhibit the effect of FGF2 in the aged niche, SCs from adult *Pax7*^{CreERT2/+}; *Spry1OX* (*Spry1OX*) and cre-negative control (WT) mice were isolated 10 days after tamoxifen administration, incubated with adult and aged PME and assayed for cell cycle entry (**Figure 28a**). *Spry1OX* SCs did not enter the cell cycle in response to aged PME (**Figure 28b**), showing that overexpression of *Spry1* in SCs inhibits the mitogenic effect of the aged niche.

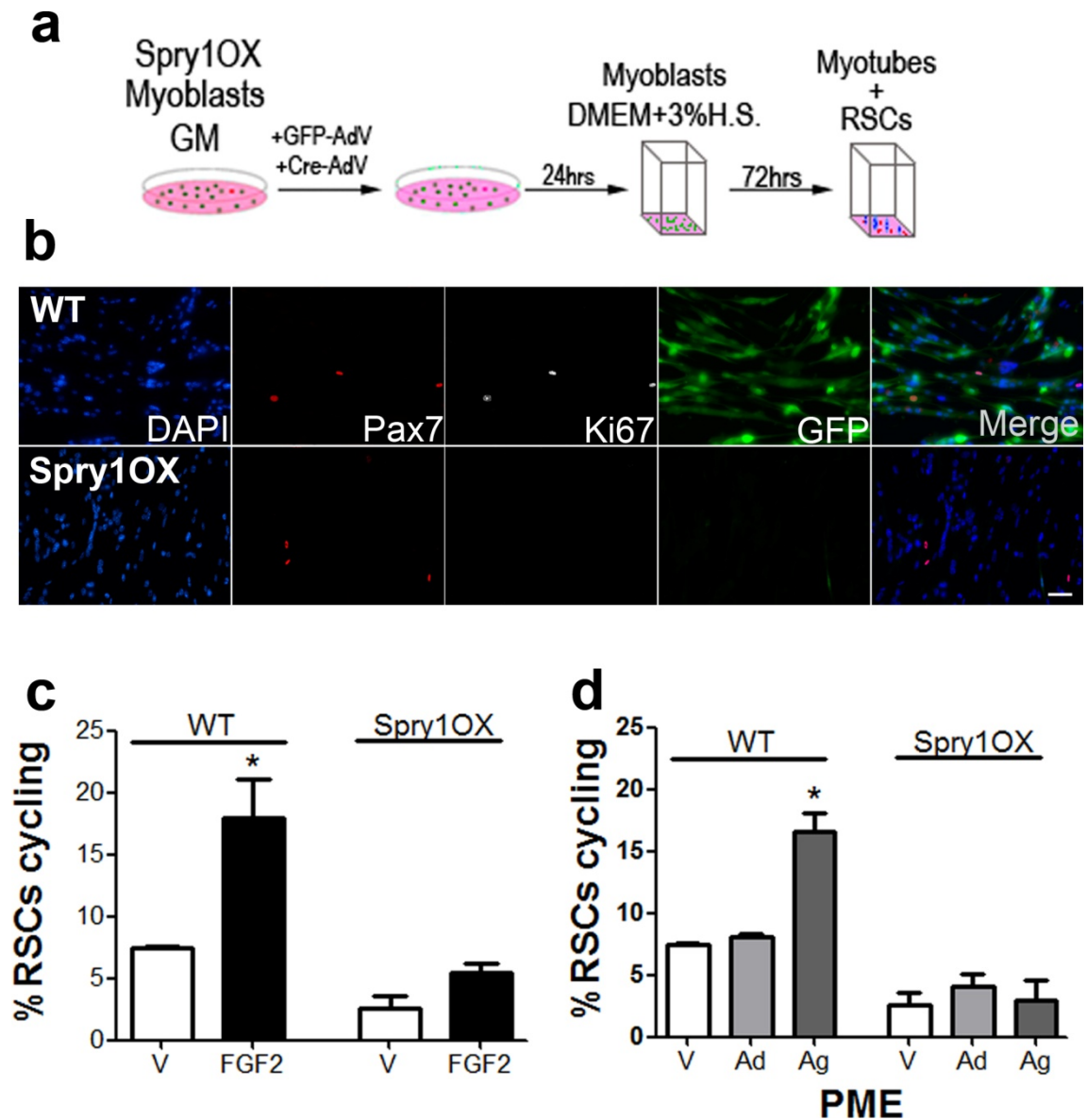


Figure 27 - Overexpression of *Spry1* inhibits the mitogenic effect of the aged niche. a, Schematic of the experimental strategy to overexpress *Spry1* levels *in vitro*. *Spry1*^{OX/OX} myoblasts were treated with Cre adenovirus to overexpress *Spry1* levels (Spry1OX) or GFP adenovirus as a control (WT) under growth conditions (GM). Cells were then put into differentiation media (DMEM+3%HS) to form RSCs and incubated with PME or FGF2. **b,** Representative image of RSCs and myotubes stained with GFP, Pax7, and Ki67. Scale bar, 50µm. Note, the Spry1OX line constitutively expresses GFP and recombination results in Cre-mediated deletion of GFP. **c,** Quantification of the percentage of cycling (Ki67⁺) RSCs after incubation with vehicle control (V), FGF2 or adult (Ad) or aged (Ag) PME (**d**). For all experiments, n=500-1000 cells per condition conducted in triplicate. All data represented as mean ± s.e.m.; *P<0.05, student's t test.

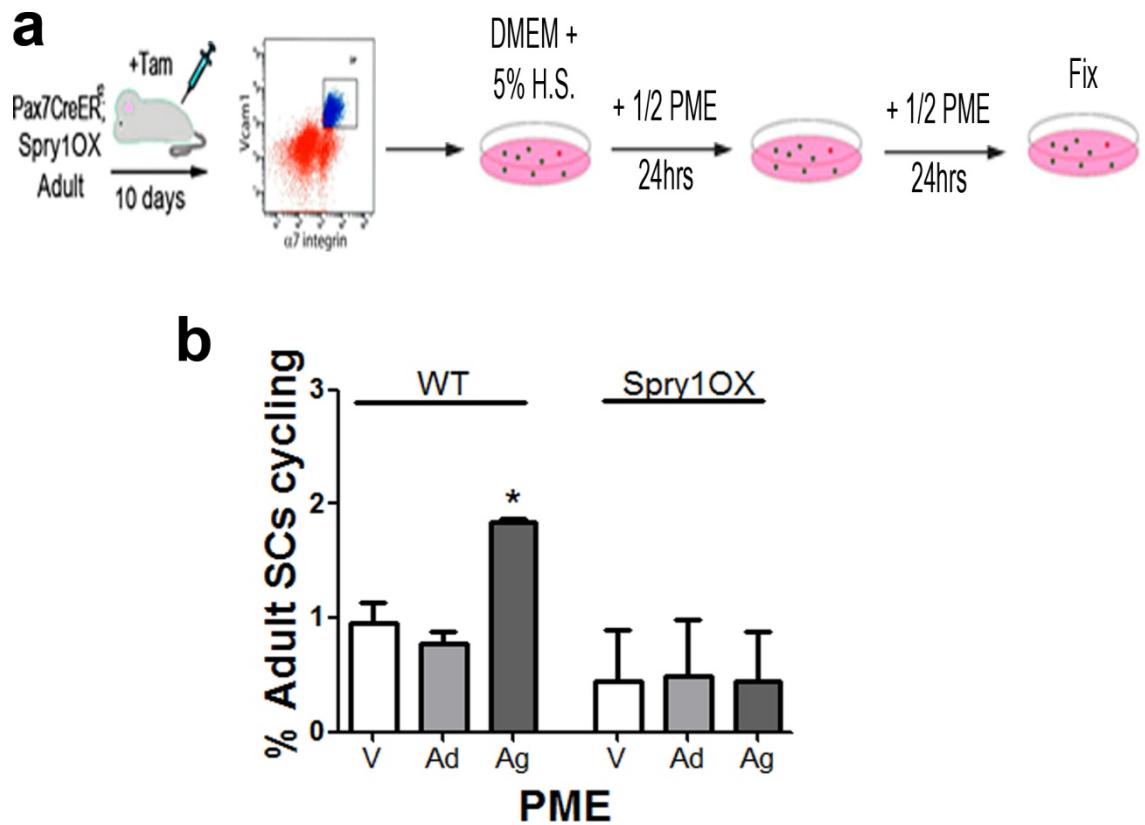


Figure 28 - *Spry1* overexpression in vivo inhibits the mitogenic effect of the aged niche.
a, Schematic of the experimental strategy to overexpress *Spry1* (*Spry1OX*) from adult SCs and assess cell cycle entry after incubation with PMEs. **b**, Quantification of the percentage of adult cycling sorted SCs after incubation with vehicle control, adult PME, or aged PME. $n=500-1000$ cells per condition conducted in triplicate. Data represented as mean \pm s.e.m.; * $P<0.05$, student's t test.

4.2. Short-term loss of *Spry1* *in vivo* causes increased satellite cell cycling and increased Pax7 cell number

Loss of *Spry1* in SCs causes increased FGF signalling and increased cycling in response to the aged niche in *in vitro* quiescence assays (see **Section 4.1.1.**). To test the requirement of *Spry1* for maintaining SC quiescence *in vivo*, tamoxifen was administered to adult and aged *Pax7*^{CreERT2/+}; *Spry1*^{flox/flox} mice (*Spry1*null) and Cre-negative controls (WT). Mice were sacrificed 10 days later and TA sections were stained with antibodies raised against Pax7 and Ki67 to determine the number of cycling SCs (**Figure 29a**). Loss of *Spry1* in adult mice caused no change in the number of cycling SCs (data not shown), consistent with there being no or very little FGF2 present in the adult niche. However, loss of *Spry1* increased the number of cycling SCs 1.5 fold in aged mice (**Figure 29b**). Furthermore, the number of Pax7⁺ cells on purified single myofibres was increased almost 4 fold after short-term deletion of *Spry1* in aged SCs, consistent with a loss of SC quiescence (**Figure 29c**). The number of Pax7⁺ cells was not changed in adult single fibres after loss of *Spry1*, further showing that a negligible level of FGF2 is present in the adult niche (**Figure 29c**).

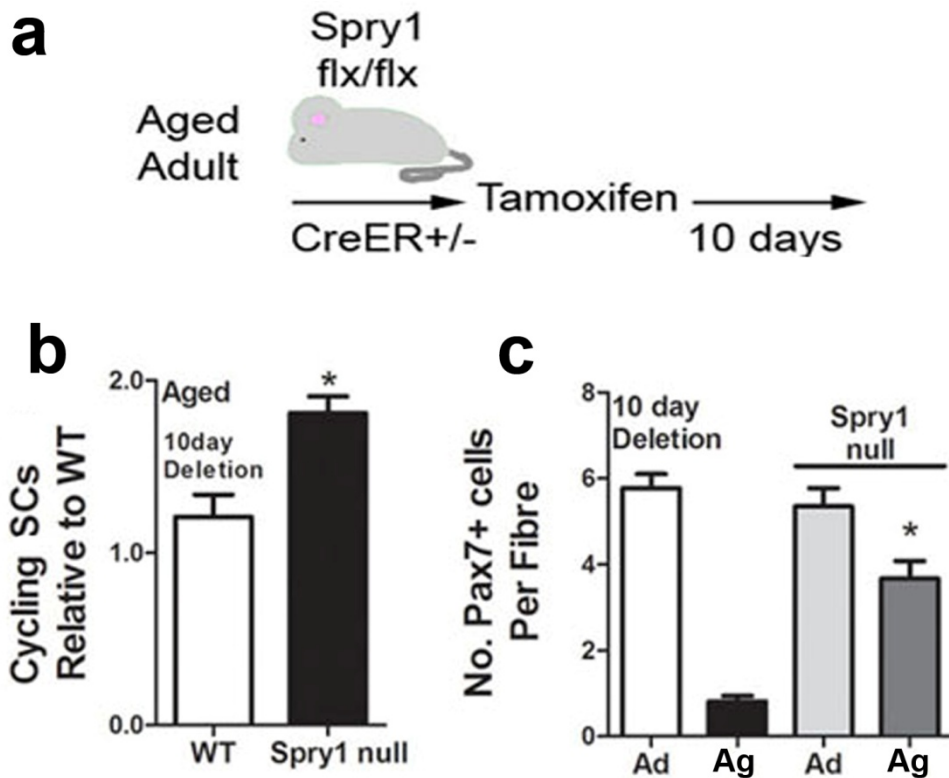


Figure 29 - Short-term increase in FGF signalling increases satellite cell cycling. a, Schematic of the experimental strategy to delete *Spry1* from adult and aged SCs. **b,** Quantification of the number of cycling (Ki67⁺) *Spry1* null and WT SCs in aged skeletal muscle cross-sections. Data are from 4-6 animals / condition. **c,** Quantification of the number of WT and *Spry1* null Pax7⁺ cells per isolated myofibre in adult (Ad) and aged (Ag) mice. Note, deletion of *Spry1* has no effect on adult SCs. Data are from 20-30 single muscle fibres / animal (n=5-6 animals / condition). All data represented as mean \pm s.e.m.; *P<0.05, student's t test.

4.3. Long-term loss of *Spry1* *in vivo* leads to loss of stem cell number and impaired satellite cell function

I have shown that acutely increasing the sensitivity of SCs to FGF2 in the aged niche further drives their cycling. Loss of quiescence is associated with depletion of the stem cell pool and impaired stem cell function [20, 366]. I hypothesised that further driving the loss of quiescence in SCs leads to an even greater loss of stem cell number and function under homeostatic conditions. To test this, BrdU was administered in the drinking water of adult and aged *Pax7^{CreERT2/+}; Spry1^{flox/flox}* mice (*Spry1* null) and Cre-negative controls (WT) for six weeks (**Figure 30a**). Mice were then injected with tamoxifen and put back on normal drinking water for six more weeks (chase period; **Figure 30a**). SCs were then FACS-isolated and immediately fixed and stained with antibodies raised against BrdU and Pax7 to determine loss of quiescence. Any cells that rapidly proliferated would have diluted the BrdU label to undetectable levels during the chase period (non-LRCs), whereas any cells which did not proliferate would have retained the BrdU label (LRCs). Adult *Spry1* null SCs did not lose quiescence and retained the BrdU label, consistent with a negligible amount FGF2 being present in the adult niche (**Figure 30b**). However, aged *Spry1* null cells further lost quiescence over the six week period and diluted the BrdU label (**Figure 30c**). These data show that aged SCs cycle extensively over six weeks after loss of *Spry1*.

To determine the effect of a further loss of quiescence on SC number and function, aged *Pax7^{CreERT2/+}; Spry1^{flox/flox}* (*Spry1* null) and Cre-negative control (WT) mice were injected with tamoxifen and sacrificed six weeks later (**Figure 30d**). The number of Pax7⁺ SCs was reduced by 50% in aged *Spry1* null mice compared to WT (**Figure 30e**), consistent with a loss of quiescence further driving SC depletion. To examine the effect of long-term *Spry1* loss on SC function, SCs were isolated from mice treated as in **Figure 30d** and plated at clonal density in culture and stained with antibodies to determine apoptosis (aCasp). After four days in culture the percentage of cells undergoing apoptosis was almost 3 fold higher in *Spry1* null cells compared to WT (**Figure 30f**). To

further show that long-term loss of *Spry1* leads to loss of the SC pool, adult *Pax7^{CreERT2/+}; Spry1^{flox/flox}* mice and WT controls were injected with tamoxifen and sacrificed 18 months later (termed a life-long deletion; **Figure 30g**). TA sections were then stained with antibodies raised against Pax7 and laminin to determine SC number. Life-long overexposure to FGF signalling caused a 50% decline in the number of SCs present in aged skeletal muscle (**Figure 30h**). These data show that prolonged FGF signalling drives SC depletion and impairs function under homeostatic conditions. Collectively, these data demonstrate that aged-niche-induced FGF signalling leads to an initial loss of quiescence followed by a depletion of the stem cell pool.

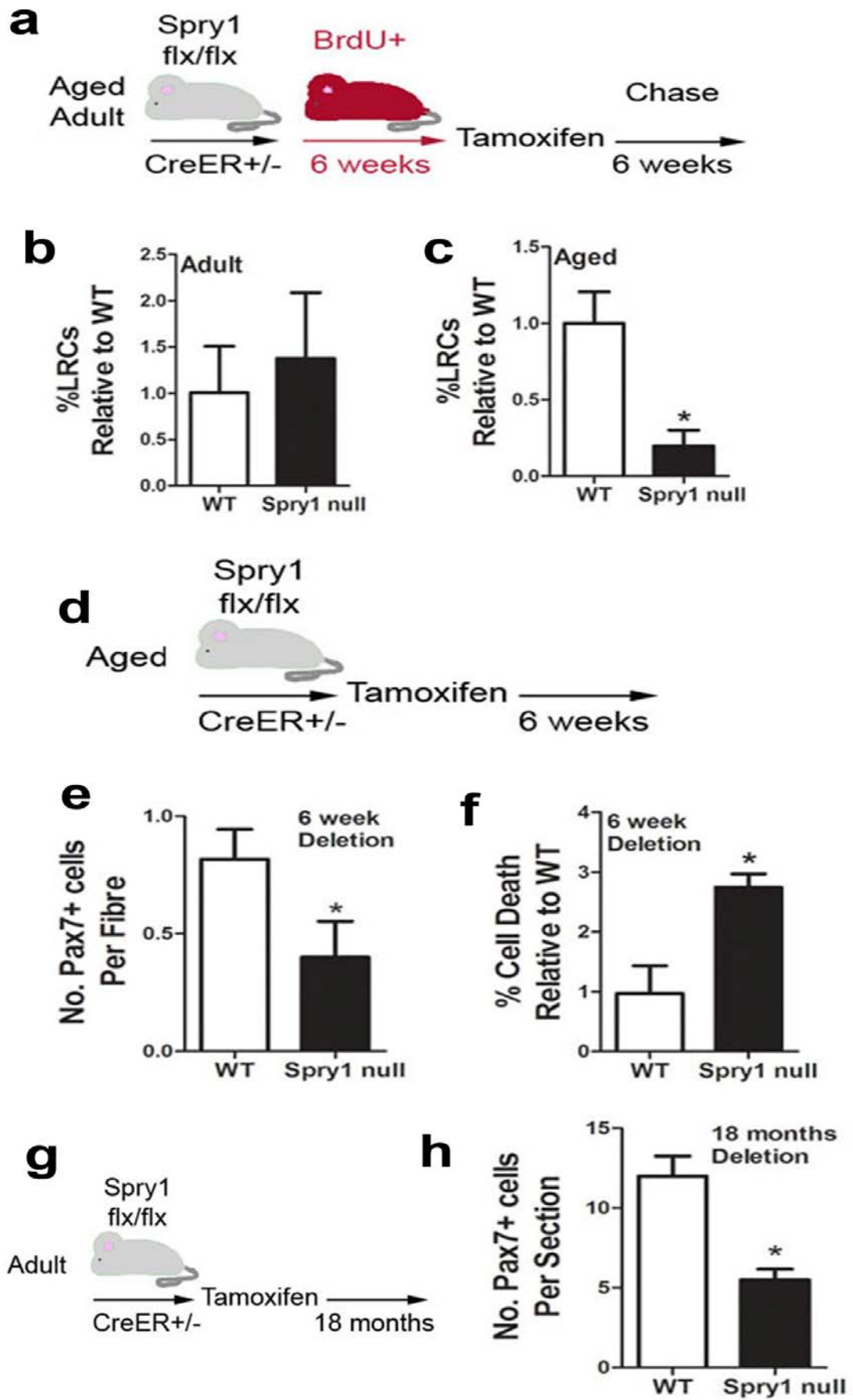


Figure 30 - Chronic exposure to FGF signalling leads to depletion of the satellite cell pool and impaired satellite cell function. **a**, BrdU pulse-chase schematic to determine loss of quiescence in *Spry1* null mice. Note, all mice were administered BrdU in their drinking water as wild types, before injection of tamoxifen. **b**, Quantification of the relative percentage of Pax7⁺BrdU⁺ cells (label retaining cells; LRCs) in adult and aged (**c**) *Spry1* null mice relative to WT, stained immediately after isolation. n=300-600 cells / experiment performed in triplicate. **d**, Schematic of the experimental strategy to delete *Spry1* from aged SCs for 6 weeks. **e**, Quantification of the number of Pax7⁺ SCs per isolated myofibre in WT mice and in long-term deleted *Spry1* mice (*Spry1* null). n=30-40 fibres / animal. **f**, Quantification of the percentage of Pax7⁺aCasp⁺ cells (cell death) in WT mice and in long-term deleted *Spry1* null mice after 4 days in culture (DMEM+10%HS). **g**, Schematic of the experimental strategy for a life-long deletion of *Spry1*. **h**, Quantification of the number of Pax7⁺ cells per muscle section in WT and life-long deleted *Spry1* mice (*Spry1* null). For all experiments n = 4-6 animals per condition. All data represented as mean ±s.e.m.; *P<0.05 student's t test.

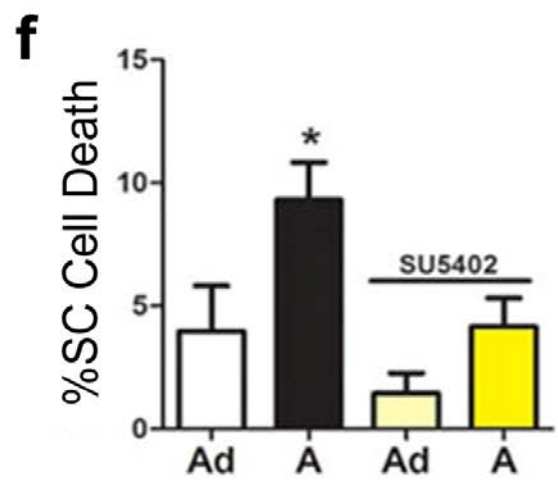
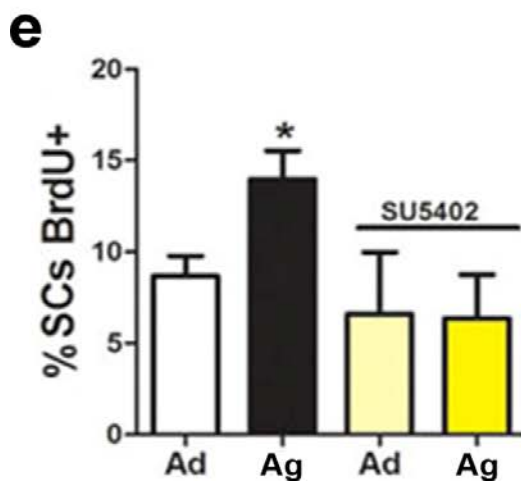
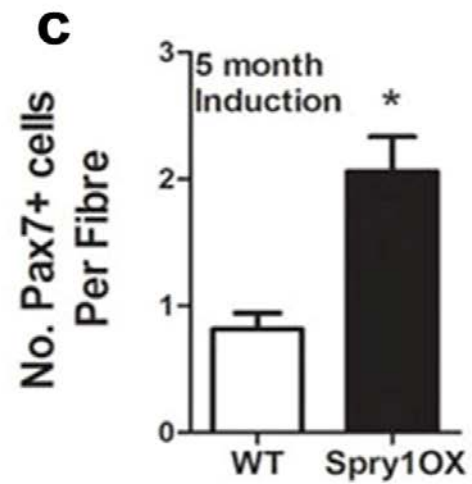
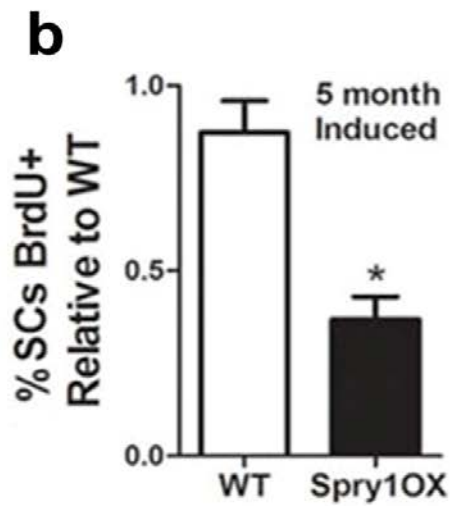
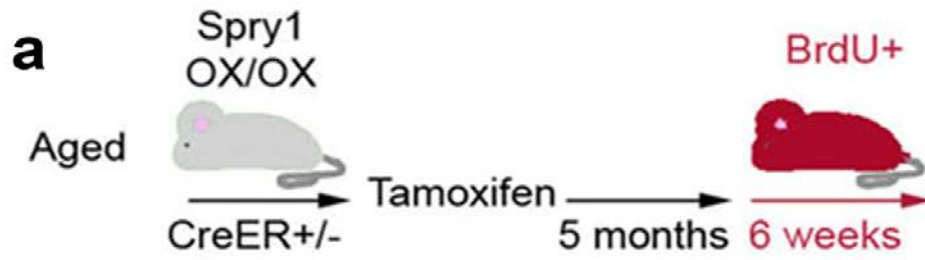
4.4. Inhibition of FGF signalling in the aged satellite cell niche rescues stem cell number and function

Upregulation of FGF2 in the aged niche causes a loss of SC quiescence. This leads to impaired SC function and a loss of the stem cell pool. I have shown that SCs in the aged niche are acutely sensitive to *Spry1* levels and the level of FGF signalling. Therefore, I hypothesised that inhibiting FGF signalling will prevent the age-associated loss of stem cell number and will antagonise the decline in SC function. To test this, 18 month old *Spry1*OX and WT mice were injected with tamoxifen and sacrificed 6.5 months later (**Figure 31a**). BrdU was administered in their drinking water in the last 6 weeks of life to determine the effect of inhibition of FGF signalling on SC quiescence (**Figure 31a**).

Remarkably, the percentage of SCs that had entered the cell cycle was reduced by half (**Figure 31b**). In addition, the number of SCs associated with purified single myofibres was increased two fold (**Figure 31c**). These data show that inhibition of FGF signalling in aged SCs partly inhibits the loss of SC quiescence and depletion of the stem cell pool.

To determine if prolonged FGF signalling could be inhibited pharmacologically, adult and aged mice were injected with a suspension of 500 μ M SU5402 or vehicle control adsorbed onto beads (to allow slow SU5402 release)[358]. Mice were then administered BrdU in their drinking water for six weeks and sacrificed (**Figure 31d**). Remarkably, the percentage of cycling aged SCs was reduced to adult levels after *in vivo* treatment with SU5402 (**Figure 31e**). Furthermore, after four days in culture, aged SCs that were treated with SU5402 *in vivo* were less prone to apoptosis (**Figure 31f**).

Collectively, these data show that inhibition of FGF signalling partly retains SC quiescence and this leads to maintenance of SC number and function.



4: Results Part II

Figure 31 - Inhibition of FGF signalling rescues stem cell number and function. **a**, BrdU feeding schematic of aged (18 month old) Spry1OX and WT mice after 5 months of overexpression. **b**, Quantification of the percentage of Pax7⁺BrdU⁺ isolated SCs from WT and Spry1OX mice stained immediately after isolation. **c**, Quantification of the number of SCs on isolated single myofibres from WT and Spry1OX mice. **d**, SU5402 (or vehicle control) injection and BrdU feeding schematic of adult and aged WT mice. **e**, Quantification of the percentage of BrdU⁺ SCs and aCasp⁺ **(f)** SCs (% SC cell death) isolated from adult (Ad) and aged (Ag) mice and stained immediately. For all experiments n = 4-6 animals per condition. All data represented as mean \pm s.e.m.; *P<0.05 student's t test.

4.5. The adult niche is inhibitory to satellite cell activation

The aged SC niche is pro-mitogenic and drives SCs out of quiescence causing depletion of the stem cell pool. I have shown that incubation of RSCs and isolated SCs with FGF2 added to adult PME causes SCs to cycle (see **Figure 19d,e**). However, addition of FGF2 to adult PME did not cause as many SCs to cycle compared to FGF2 alone. To confirm this, RSCs were incubated with different concentrations of FGF2 added to 20µg/ml adult PME and assayed for cell cycle entry. Although addition of FGF2 to adult PME induced RSC cycling, more RSCs remained quiescent with FGF2 incubated with adult PME compared to adult PME alone (**Figure 32a**). These data indicate that the adult niche is inhibitory to FGF2-induced SC activation, suggesting that the loss of SC quiescence in aged animals may be due to the increase in the production of FGF2 from the niche, and a decrease in the expression of inhibitory factors.

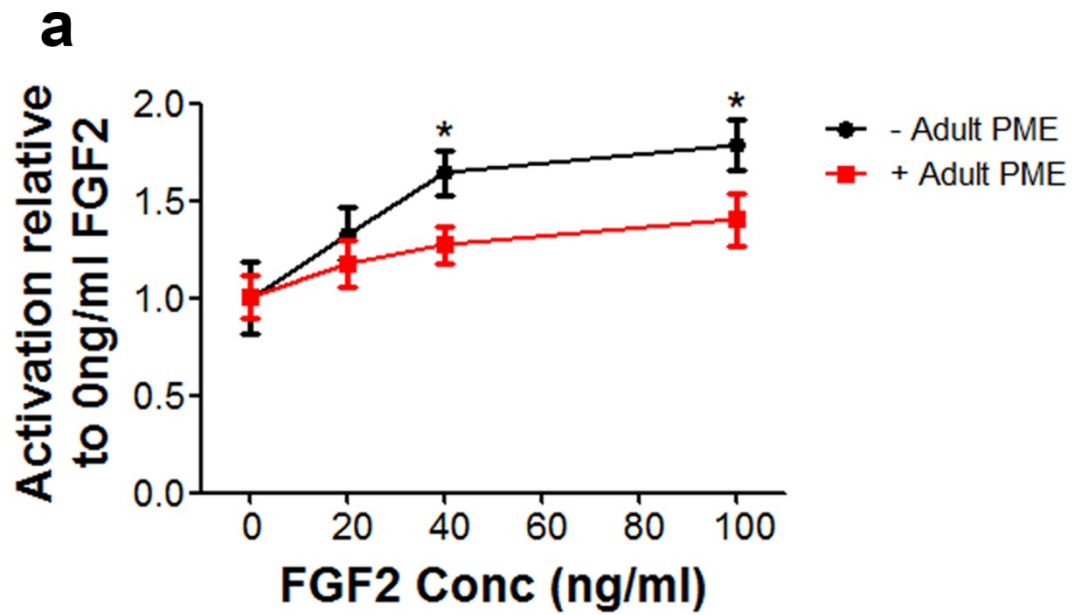


Figure 32 - The adult niche is inhibitory to satellite cell activation. a, Quantification of the relative percentage of activated RSCs (Pax7⁺Ki67⁺) after incubation with 40 μ g/ml adult PME (red line) or vehicle control (black line) and different concentrations of FGF2. n=500-800 cells per condition conducted in triplicate. Data represented as mean \pm s.e.m.; *P<0.05 student's t test.

4.6. Discussion

The data shown here support a model where FGF2 increases in the aged SC niche, the muscle fibre, which causes SCs to break quiescence and proliferate, leading to a loss of self-renewal function and eventual SC depletion (**Figure 33**). Manipulating *Spry1* levels, a negative feedback inhibitor of the FGF pathway, in SCs, altered the degree of cell cycle entry and stem cell loss (**Figure 34**). Therefore, a balance between excitatory and inhibitory signals is clearly essential to stem cell outcome.

Remarkably, conditional over-expression of *Spry1* in aged Pax7⁺ SCs was able to retain stem cell quiescence and prevent losses in SC number observed with age. These observations suggest that cell intrinsic mechanisms, at the level of feedback inhibition of niche-derived signalling, manipulated under conditions of homeostasis, can promote SC maintenance with age. Furthermore, administration of a chemical inhibitor of FGFR, SU5402, also attenuated the loss of SC number and inhibited apoptosis of SCs. These results suggest that it may be possible to prevent age-related sarcopenia in humans through the use of pharmacological inhibitors.

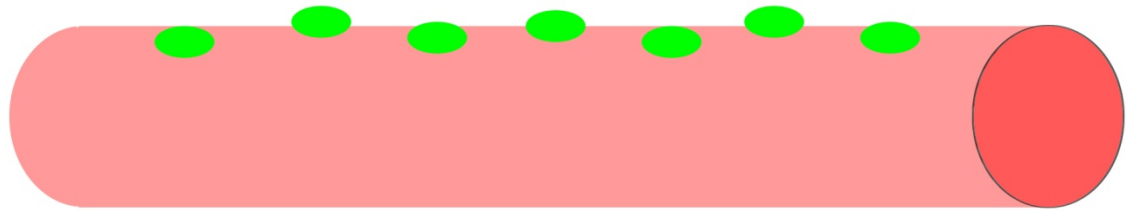
I have shown that inhibition of FGF signalling is important for the maintenance of SC number and function in the aged niche. However, the expression of FGF2 is also essential for efficient muscle regeneration [68, 100-102, 107, 108]. Inhibition of FGF signalling through blockade of FGFR has been shown to result in a large decrease in muscle mass and this has been attributed to premature terminal differentiation causing a depletion of the pool of myogenic progenitors [109-111]. This suggests that in order to maintain functional skeletal muscle, aged SCs would have to be unresponsive to FGF2 in the niche under homeostatic conditions, but then responsive to FGF2 under regenerative conditions. Thus, a temporal switch in sensitivity to FGF signalling would be needed to maintain SC number under homeostatic conditions, and regenerative capability after myotrauma.

RSCs generated from *Spry1*flx myoblasts displayed an increased sensitivity to FGF2 from the aged niche (see **Figure 24d**). However, *Spry1*null myoblasts (myoblasts from *Spry1*^{flx/flx} mice treated with Cre adenovirus) were unable to form RSCs (data not shown). These data further confirm previous findings that *Spry1* is required for a subset of activated SCs to return to quiescence [42]. Interestingly, the number of reserve cells formed from *Spry1*OX myoblasts was no different to controls, and, furthermore, the differentiation index for *Spry1*OX myoblasts was also no different to controls (data not shown). These data suggest that just the presence of *Spry1* is needed for the formation of quiescent RSCs and the level of *Spry1* does not play a role in specifying which cells will return to quiescence.

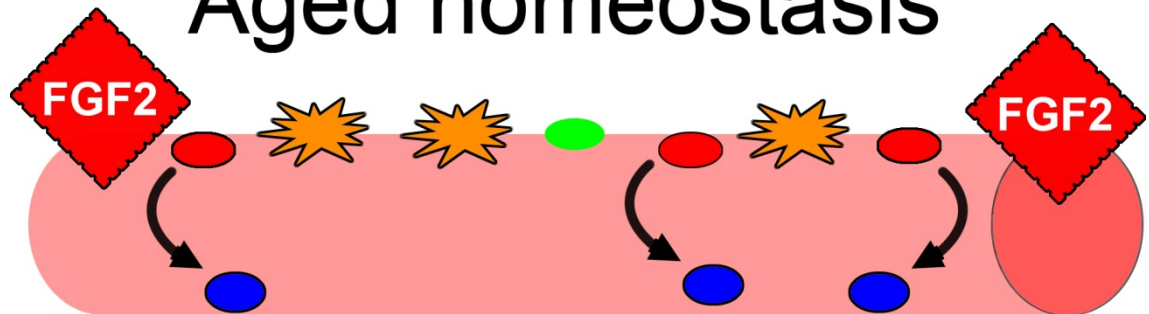
I have shown that the adult niche is inhibitory to FGF2-induced SC activation (see **Figure 32a**). Whether inhibitors of FGF signalling are present in the adult niche, or whether inhibitors of SC activation are present is unknown. The Ang1 / Tie2 signalling pathway is one of the main inhibitors of SC activation [138]. Ang1 / Tie2 signalling has been involved in various biological activities, including cell survival, proliferation, migration, chemotaxis, and quiescence [379, 380]. In skeletal muscle, Ang1 and Tie2 are expressed by quiescent SCs and their signalling acts to maintain SC quiescence [138]. However, it has not been shown if mature muscle fibres express Ang1 and, therefore, Ang1-Tie2 signalling may not be the inhibitor of SC activation in adult PME. It is interesting to speculate that ageing is associated with an increase in FGF2 expression from the niche and a concomitant decrease in inhibitory signalling molecules.

In this chapter I have identified inhibition of FGFR, either by overexpression of *Spry1* or by pharmacological methods, as a novel mechanism to maintain the number and function of SCs in aged mammals (**Figure 34**). Collectively these data show that inhibition of FGF signalling under homeostatic conditions is essential for maintenance of the SC pool during ageing.

Adult homeostasis



Aged homeostasis



Key



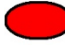
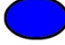
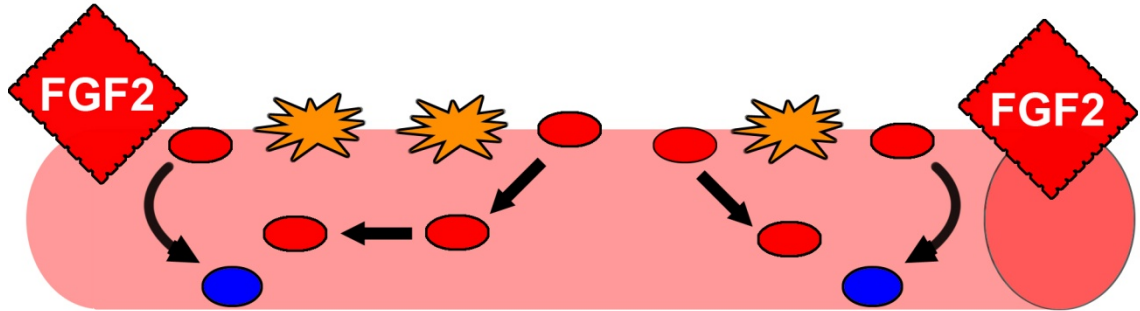
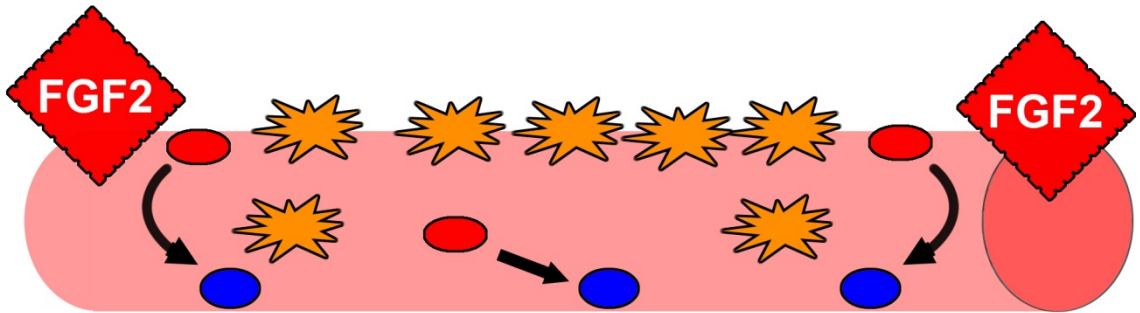
-  Quiescent SC
-  Apoptotic SC
-  Cycling SC
-  Differentiated SC

Figure 33 - Schematic illustration of the changes in satellite cells with ageing under homeostatic conditions. Under homeostatic conditions SCs are quiescent (top panel). However, in aged mice, the SC niche upregulates FGF2 (bottom panel). This drives a loss of stem cell quiescence and depletion of the stem cell pool as SCs have a decreased tendency to self-renew, and an increased tendency to apoptose or differentiate.

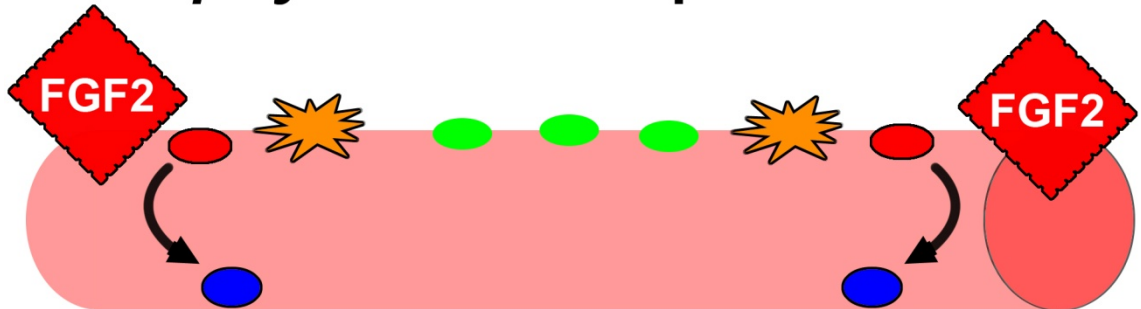
Short-term *Spry1* deletion



Long-term *Spry1* deletion



Spry1 overexpression



Key

 Quiescent SC

 Apoptotic SC

 Cycling SC

 Differentiated SC

Figure 34 - Modulation of FGF signalling affects satellite cell outcome. Short-term loss of *Spry1* in aged SCs (top panel) causes a further loss of SC quiescence and an increase in the number of Pax7⁺ cells. Long-term loss of *Spry1* in aged SCs (middle panel) causes a further loss of SC quiescence and depletion of stem cell pool as cells are more prone to differentiate or apoptose. The effects of the aged niche can be partly inhibited by pharmacological inhibition of FGF signalling or through overexpression of *Spry1* in SCs (bottom panel). Inhibition of FGF signalling in the aged niche maintains SC quiescence and causes an increase in SC number compared to WT and cells are less prone to apoptose. Modulation of *Spry1* in adult SCs under homeostatic conditions does not affect SCs (not shown).

Chapter 5

Results Part III

5.1. Chromatin remodelling in adult neurogenesis

Chromatin remodelling can engage or maintain particular genetic programs and therefore likely plays a critical role in stem cell maintenance as well as daughter cell differentiation [286]. Different cellular states may be defined at least in part by differential allocation of genomic regions to euchromatic or heterochromatic domains [381]. During development, an open chromatin state largely devoid of heterochromatin is a hallmark of stem cells, and this has been proposed to contribute to the pluripotency of ES cells [382, 383]. As ES cells differentiate they accumulate more areas of heterochromatin [382, 383]. CHD1 is a chromatin remodelling enzyme that has recently been shown to be required for ES cell self-renewal and pluripotency by maintaining a euchromatic state [384]. Knockdown of *Chd1* in ES cells caused the accumulation of large areas of heterochromatin and an increased propensity of cells to differentiate [384], showing that chromatin remodelling is essential for pluripotency.

Chromatin remodelling also plays a role in the maintenance and differentiation of somatic stem cell populations. For example, the chromatin remodelling enzyme CHD4 was shown to positively regulate HSC-specific transcriptional signatures, such as the expression of receptors important for HSC niche interaction, and negatively regulate genes involved with HSC differentiation, such as the cyclin-dependent kinase *Ccnd2* [385]. Deletion of CHD4 in HSC populations caused the loss of HSC quiescence and skewed their differentiation potential to generate mainly erythroid cells [385]. These data show that chromatin remodelling is a process which can potentially modulate many areas of somatic stem cell function.

The mRNA expression levels of many genes encoding chromatin remodelling proteins are changed as cells progress along the SVZ-OB adult neural lineage, from the SVZ to the RMS to the OB [287]. Furthermore, transcriptional profile analysis has revealed that the expression of genes encoding chromatin remodelling proteins are different between NSCs and non-neurogenic cells

[287]. These data suggest that chromatin remodelling is an active process in adult neurogenesis.

Chromatin remodelling proteins are generally categorised into one of two groups; trithorax group (TxG) proteins, which usually cause the activation of their target loci, and polycomb group (PcG) proteins which tend to repress gene activation [289]. Mixed lineage leukemia 1 (Mll1) is a TxG chromatin remodelling enzyme with H3K4 methyltransferase activity and is associated with epigenetic transcriptional activation. Lim et al showed that Mll1 is required in postnatal neurogenesis to suppress the accumulation of repressive H3K27me3 at the locus of gene encoding the neuron-specific transcription factor *Dlx2* in postnatal SVZ cells [316]. Loss of *Mll1* resulted in the accumulation of H3K27me3 and repression of *Dlx2*, causing impaired neuroblast differentiation and migration [316]. Bmi1 is a PcG protein and a member of the PRC1 complex which positively regulates H2Aub1 [307]. Bmi1 has been shown to be required for embryonic and post-natal NSC self-renewal [288, 308, 309]. *Bmi1* overexpression increased the self-renewal of embryonic NSCs and maintained their ability to produce neurons in culture after many passages [312]. These data suggest that chromatin remodelling plays a critical role in embryonic and postnatal neurogenesis. However, the role of chromatin remodelling in adult neurogenesis is unknown.

The chromatin remodelling enzyme CHD7 has been implicated in the regulation of embryonic brain development as *Chd7*^{-/-} mice exhibit severe brain defects [344]. *Chd7*^{-/-} mice die before E10.5 [344], but adult mice heterozygous for *Chd7* (*Chd7*^{+/-}) display a decreased brain size and decreased olfactory bulb (OB) length [345, 346]. In addition, studies by Layman et al. showed that *Chd7*^{+/-} mice displayed a reduction in tyrosine hydroxylase (TH) expression in the OB (**Figure 35**) [345]. The authors showed that CHD7 was expressed by MASH1⁺ stem cells in the olfactory epithelium, and reduction in *Chd7* expression led to decreased proliferation of the epithelial stem cells [345]. This resulted in a decrease in the number of mature olfactory sensory neurons, which normally signal to dopaminergic interneurons [345]. Hence, a loss of

signal to dopaminergic interneurons resulted in a decrease in TH-production (**Figure 35**) [345]. These data implicate CHD7 in regulation of stem cells in adults. However, due to the role of postnatal and adult SVZ-OB neurogenesis in formation of OB interneurons, misregulation of olfactory epithelial stem cells may not be the sole cause of the OB defects seen in these mice (**Figure 36**). The authors did not address the contribution of SVZ-OB neurogenesis to the formation of new OB interneurons in *Chd7*^{+/-} mice and so the role of CHD7 in adult neurogenesis remains unknown (**Figure 36**). In support for CHD7 playing a role in adult neurogenesis, CHD7 has been shown to directly interact with Sox2, a protein important in the maintenance and differentiation of NSCs [386-389].

I hypothesised that CHD7 plays a role in adult SVZ-OB neurogenesis and that loss of *Chd7* results in impaired formation or differentiation of OB interneurons (**Figure 36**).

The aims for this chapter are to:

1. Characterise gross changes in brain sizes and analyse the changes in OB interneuron number in *Chd7* heterozygous mice.
2. Determine the expression profile of CHD7 in SVZ-OB neurogenesis.
3. Determine changes in SVZ-OB neurogenesis by analysing the proliferation of cells in the SVZ and generation of immature neurons in *Chd7* heterozygous mice.
4. Establish whether CHD7 expression in adult NSCs is necessary for the production of OB interneurons by restoring *Chd7* function specifically in NSCs to rescue OB defects.

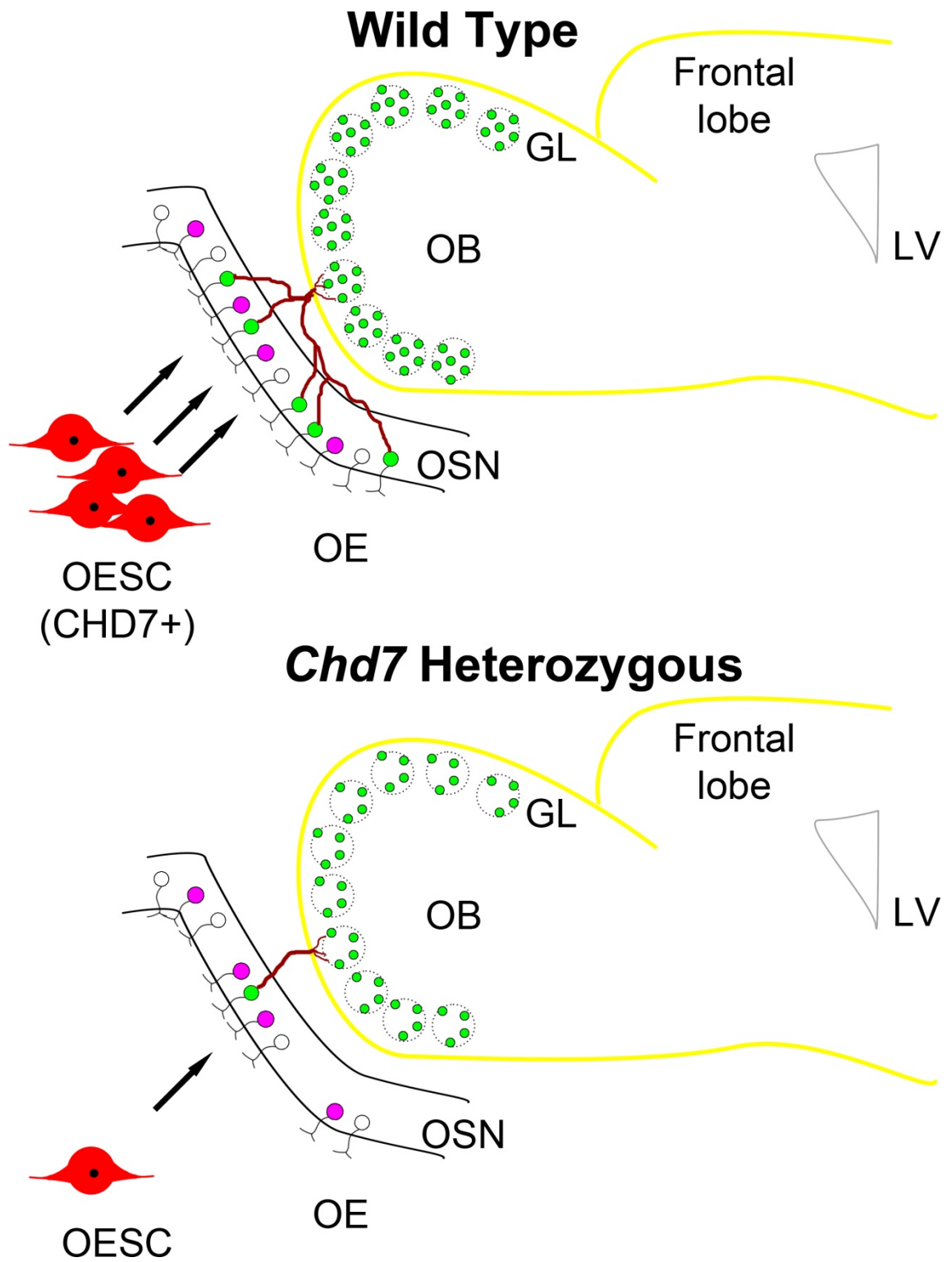
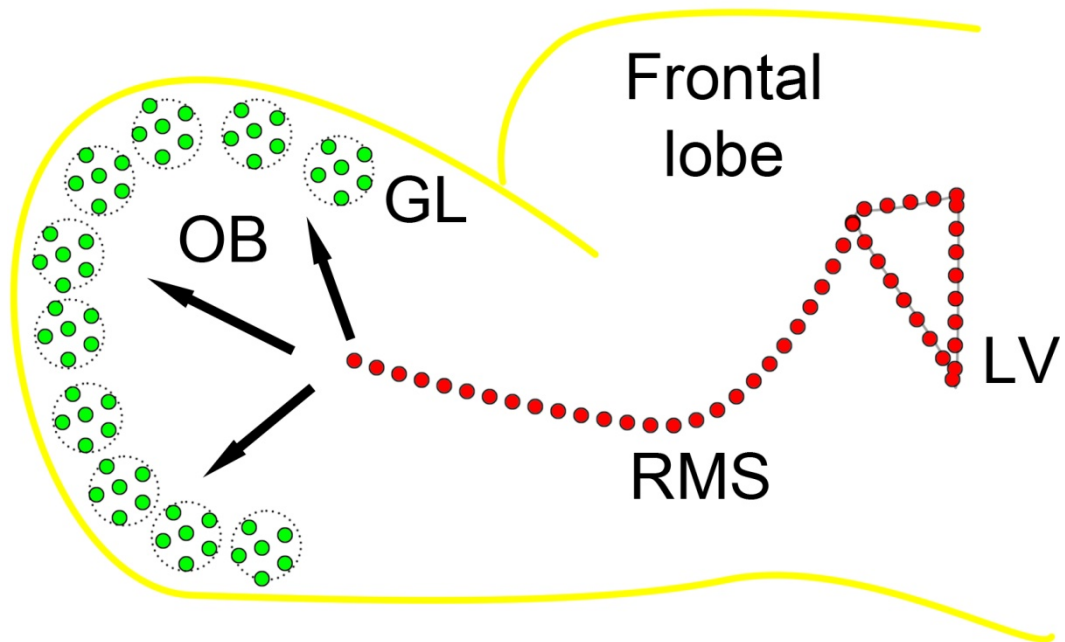


Figure 35 - Reduced expression of *Chd7* leads to a decrease in tyrosine hydroxylase+ interneurons due to decreased olfactory epithelial stem cell proliferation. CHD7 is expressed in olfactory epithelial stem cells (OESC) in the olfactory epithelium (OE) [345]. OESCs form olfactory sensory neurons (OSN). OSNs signal to dopaminergic interneurons (green circles) in the glomerular layer (GL) of the olfactory bulb (OB) to maintain their activity and production of tyrosine hydroxylase (TH; top panel). Layman et al. proposed that a reduction in *Chd7* expression led to the decreased proliferation of OESCs (bottom panel) [345]. This led to a decreased formation of OSNs and loss of signal to dopaminergic interneurons, resulting in either a decreased production of TH, or a loss of these interneurons (bottom panel) [345]. LV, lateral ventricle.

Wild Type



Reduced neurogenesis

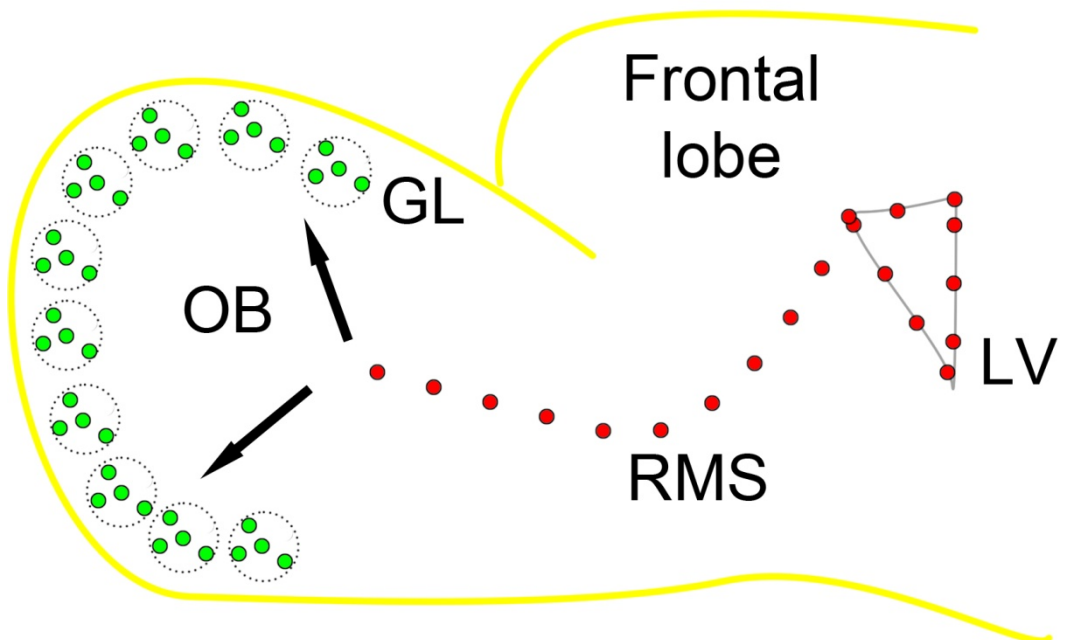


Figure 36 - A reduction in *Chd7* expression may cause a decrease in SVZ-OB neurogenesis leading to a loss of interneuron production. Neurogenic cells in the SVZ and rostral migratory stream (RMS; red dots) contribute to new interneuron formation in the olfactory bulb (OB), including the formation of tyrosine hydroxylase⁺ dopaminergic interneurons (green dots; top panel). Reduced SVZ-OB neurogenesis can lead to a decrease in the production of OB interneurons (bottom panel).

5.2. *Chd7* heterozygous mice display reduced olfactory bulb length and reduced number of tyrosine hydroxylase⁺ interneurons

Loss of *Chd7* function is embryonic lethal and is associated with defects in many developing tissues [344]. Therefore, to determine if there were any gross changes in adult forebrain size, mice heterozygous for a genetrap *Chd7* allele were utilised (**Figure 37a**; *Chd7^{gt/+}*) [356]. The genetrap allele contains a beta-geo fusion cassette with a floxed splice acceptor inserted into intron 36 of *Chd7*, presumably resulting in the translation of an unstable, truncated, non-functional protein which is rapidly degraded (**Figure 37a**) [356]. Mutations in *CHD7* have been implicated in the development of CHARGE syndrome [330]. Mice carrying the *Chd7^{gt}* allele have been previously shown to display phenotypes associated with *Chd7* haploinsufficiency such as abnormalities in pharyngeal arch arteries and other phenotypes associated with CHARGE syndrome [356]. Therefore, the *Chd7^{gt/+}* mouse line is presumed to have a reduced *Chd7* expression in all tissues. Furthermore, RT-qPCR analysis of dissected OB showed that *Chd7* expression is significantly reduced in adult (10-12 weeks old) *Chd7^{gt/+}* mice compared to WT (**Figure 37b**). Hence, adult *Chd7^{gt/+}* mice will be described as having a decrease in *Chd7* expression. Adult *Chd7^{gt/+}* mice display a very slight reduction in forebrain size (data not shown), but most notably display a 20% reduction in OB length (**Figure 37c,d**), with no change in OB width compared to WT littermates (data not shown). These data are in agreement with previous findings [345].

To determine if the reduction in OB length was progressive from postnatal stages to adulthood, the brain sizes of P21 *Chd7^{gt/+}* mice and WT littermates were analysed. A slight reduction in OB length could be seen in P21 *Chd7^{gt/+}* mice compared to WT (**Figure 37e**), suggesting that the reduction in OB length is progressive with age. Importantly, the overall brain size of *Chd7^{gt/+}* mice at P21 was not significantly different to WT littermates (**Figure 37f**), arguing against a decrease in *Chd7* expression causing a general developmental delay. Collectively, these data show that a reduction in *Chd7* expression mostly affects the OB size, and a decrease in the length of the OB is reduced from postnatal stages through to adulthood.

The olfactory bulb is composed of three main types of interneurons: TH⁺ (dopaminergic), CalR⁺ (GABAergic), and CalB⁺ (GABAergic) interneurons [223]. Cells born in the adult SVZ are capable of differentiating into one of these three types of interneuron in the OB [223]. The integration of these interneurons presumably contributes to proper OB formation, and the size of the OB is normally maintained throughout life through the turnover of OB interneurons [210]. To determine if a reduction in OB size was due to a reduction in the production of TH⁺, CalR⁺, or CalB⁺ interneurons, sections of OB from *Chd7^{gt/+}* and wildtype littermates (WT) were stained with antibodies raised against TH, CalR, and CalB (**Figure 38a,c,d**). The OB of *Chd7^{gt/+}* mice displayed a reduction in the number of cells expressing TH in the glomerular layer compared to WT (**Figure 38a,b**), in agreement with findings by Layman et al. [345]. Interestingly, reduction in *Chd7* expression had no effect on the expression of CalR (**Figure 38c,d**) and CalB (**Figure 38e,f**) in the glomerular layer. These data show that CHD7 specifically regulates TH-producing interneurons, leaving other OB interneuron populations unaffected.

To confirm that the production of cells in the TH-lineage is impaired, I performed an *in situ* hybridisation using an anti-sense *Er81* probe on OB sections of adult *Chd7^{gt/+}* and WT mice. *Er81* is a transcription factor that is required for TH-expression in the mouse OB and is used as an early marker of TH-lineage cells [390, 391]. Expression of *Er81* was decreased in the RMS and in areas of the

OB of *Chd7^{gt/+}* mice compared to WT, including in the glomerular layer where TH⁺ interneurons are found (**Figure 39a**). Furthermore, RT-qPCR analysis of dissected OB from *Chd7^{gt/+}* and WT mice confirmed that *Er81* expression was reduced by 33% in *Chd7^{gt/+}* mice (**Figure 39a**). These data show that a reduction in *Chd7* expression results in a decrease in the formation of cells of the TH⁺ interneuron lineage.

Alternatively, a decrease in *Er81* expression may lead to a decrease in TH expression from interneurons in the OB, rather than a loss of the interneurons themselves and this will be discussed in **Section 5.6.2**.

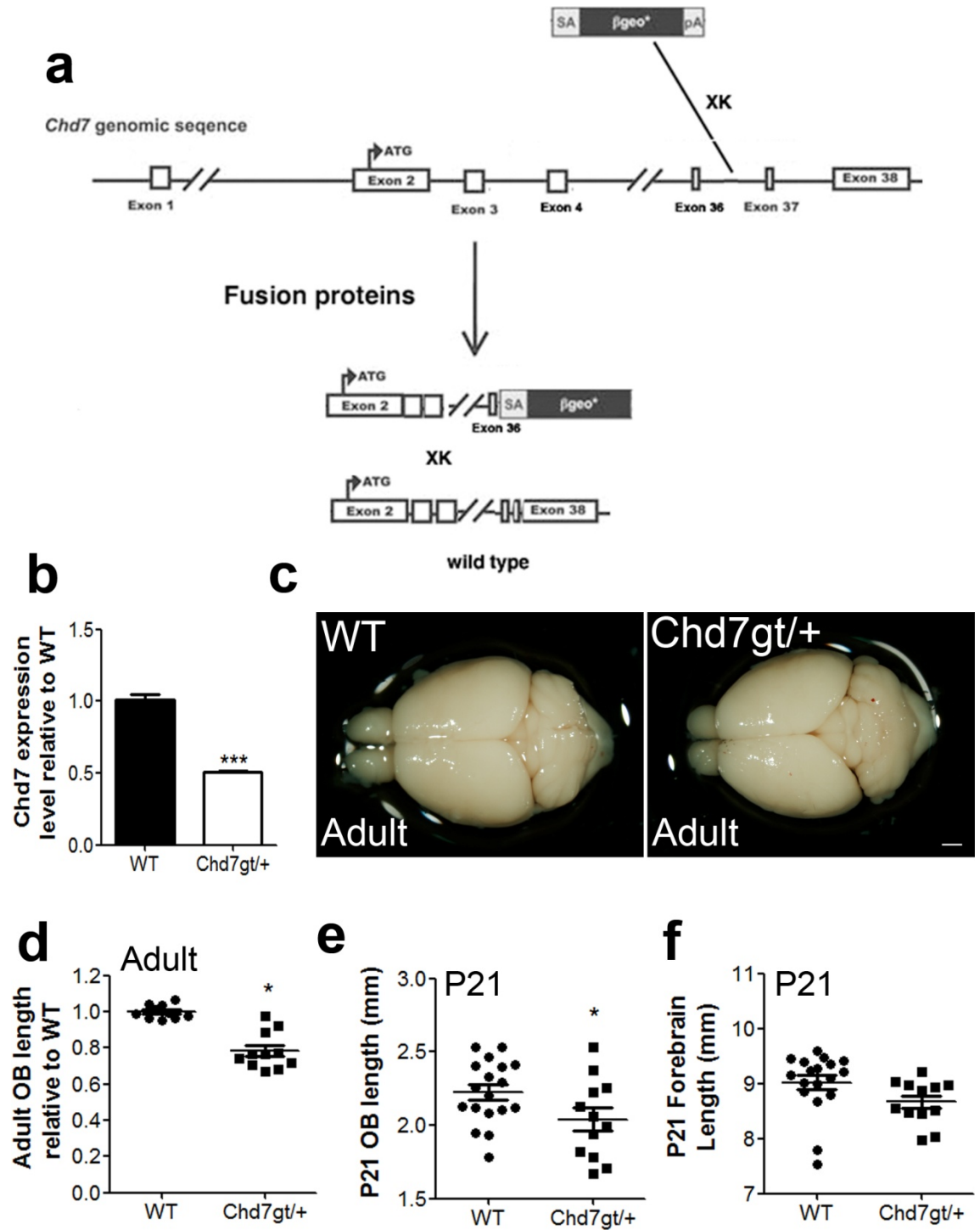


Figure 37 - Reduction in *Chd7* expression causes a decrease in olfactory bulb length. a, Schematic diagram of the *Chd7*^{Δk403} allele. The genetrap construct contains a beta-geo cassette with a floxed (not shown) splice acceptor (SA). The *Chd7*^{Δk403} line has a genetrap insertion site between exons 36 and 37, and produces a protein containing all exons, except 37 and 38, fused to the gene trap cassette. Adapted from [356]. **b,** RT-qPCR expression level of *Chd7* from dissected OB of adult *Chd7*^{gt/+} relative to wild type (WT) mice. n=2 animals / condition. Data are from 2 reactions conducted in duplicate. Note that *Chd7* expression is around 50% of WT levels in *Chd7*^{gt/+} OB. **c,** Representative image of brains from adult *Chd7*^{gt/+} and control mice (WT). Scale bar, 1mm. **d,** Quantification of OB lengths from adult *Chd7*^{gt/+} and WT mice. Each mark represents the length of 1 OB. n=6-8 animals / condition. **e,** Quantification of the OB length and forebrain length (**f**) of P21 *Chd7*^{gt/+} and WT mice. Each mark represents the length of 1 OB or forebrain hemisphere. n=8-11 animals / condition. All data represented as mean ± s.e.m.; *P<0.05 student's t test.

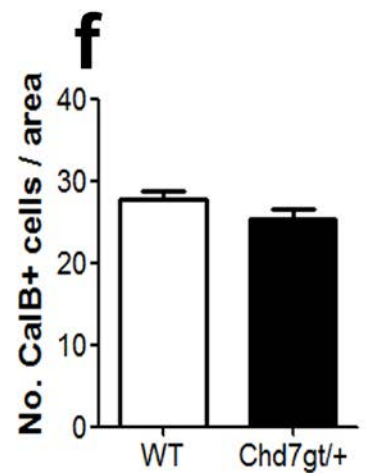
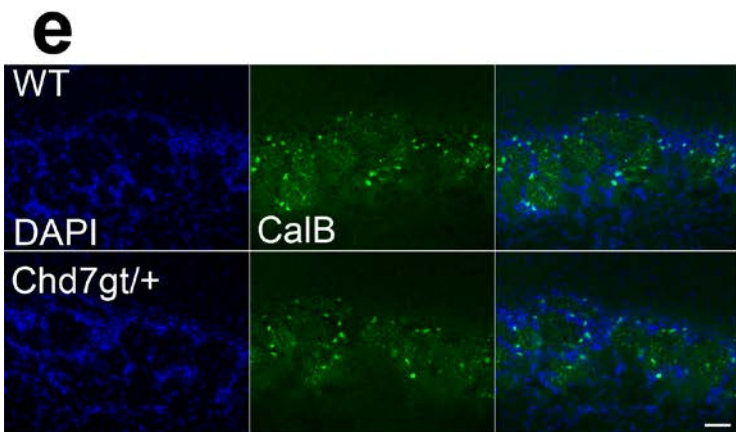
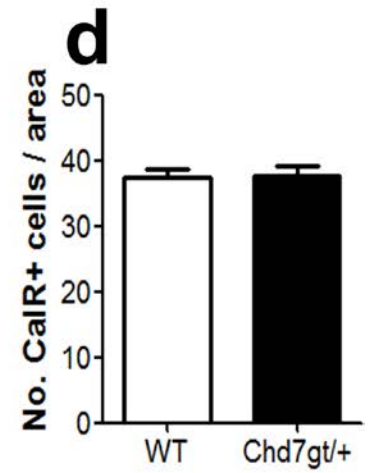
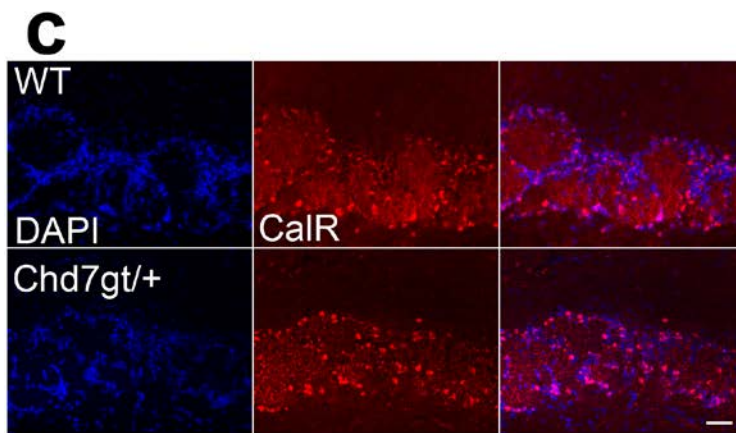
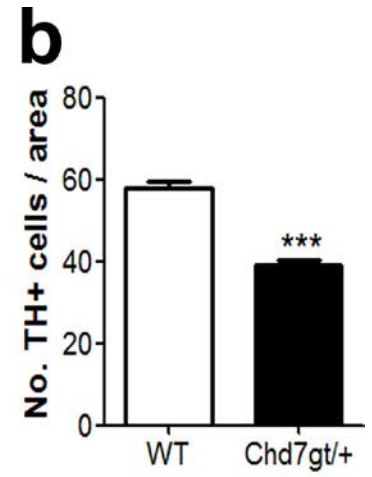
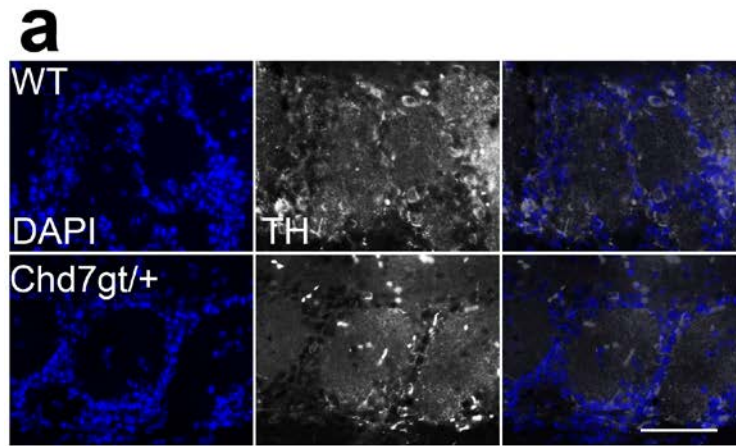


Figure 38 - Reduction in *Chd7* expression specifically affects tyrosine hydroxylase+ olfactory bulb interneurons. **a**, Representative image of a 10µm thick coronal section of OB glomerular layer stained with antibodies raised against TH, CalR (**c**), and CalB (**d**). Scale bar, 50µm. **b**, Quantification of the number of TH⁺, CalR⁺ (**d**), and CalB⁺ (**f**) cells / defined area in *Chd7^{gt/+}* and WT mice per 10µm section. n=3-4 animals / condition. All data represented as mean ± s.e.m.; ***P<0.001 student's t test.

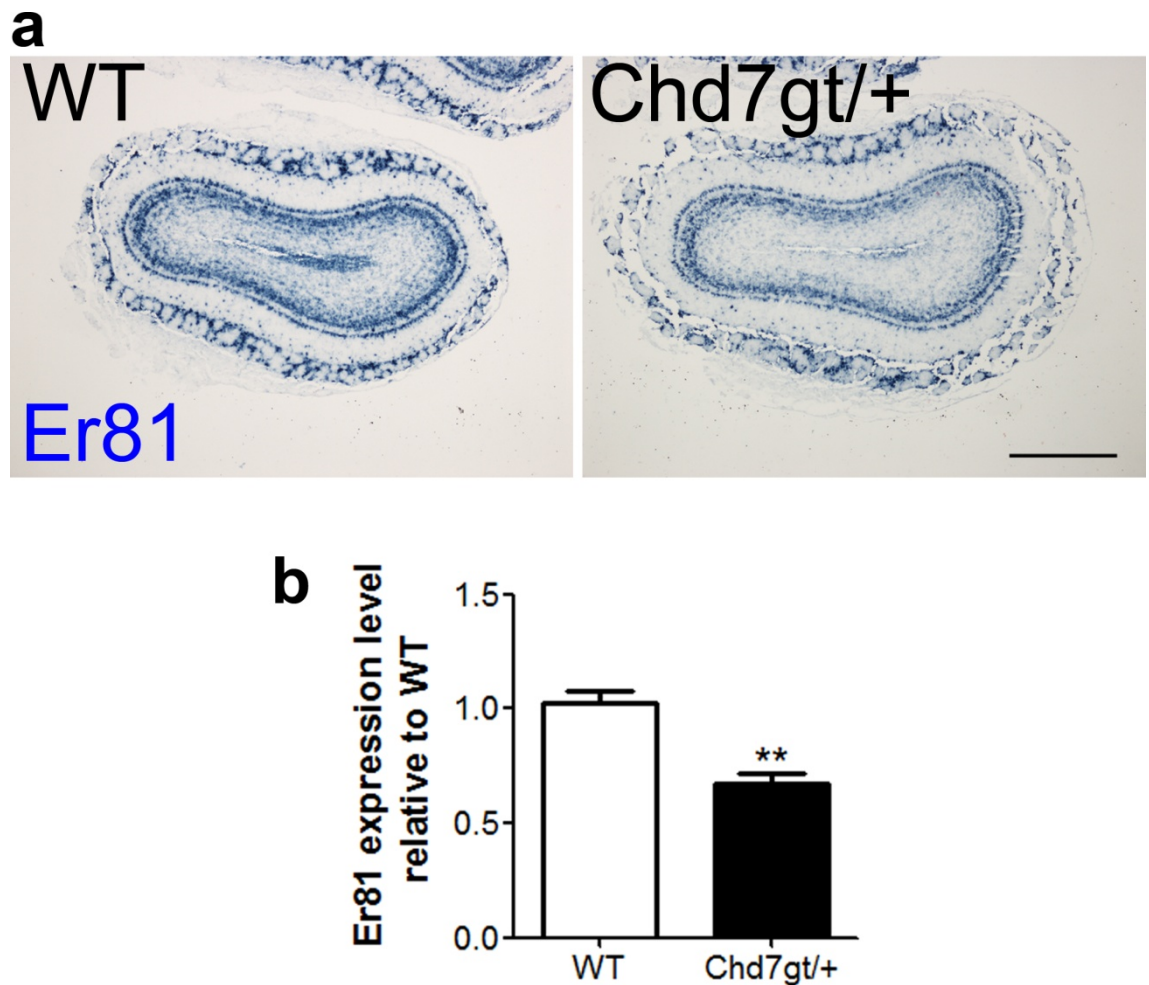


Figure 39 - Reduction in *Chd7* expression results in a decrease in TH-lineage cells. a, Representative image of an *in situ* hybridisation using an anti-sense *Er81* probe on OB sections of *Chd7^{gt/+}* and WT mice. Note a decrease in *Er81* expression in *Chd7^{gt/+}* OB compared to WT. Scale bar, 1mm **b,** Quantification of *Er81* expression from RT-qPCR experiments in *Chd7^{gt/+}* relative to WT OB. Data are from 3 reactions conducted in duplicate. Data represented as mean \pm s.e.m.; ** $P < 0.01$ student's t test.

5.3. CHD7 is expressed in the dorso-lateral aspect of the subventricular zone and in the rostral migratory stream

SVZ-OB neurogenesis is critical for the formation of new OB interneurons throughout life [183]. It is estimated that the number of newly formed interneurons that are added to the OB from cells born in the SVZ ranges from 10,000 to 30,000 per day in adult mice [208]. Adult NSCs residing in different areas of the SVZ give rise to different types of periglomerular and glomerular OB interneurons [223]. Of note, cells in the dorso-lateral aspect of the SVZ and RMS have a greater tendency to form tyrosine hydroxylase-positive interneurons in the glomerular layer of the OB (see **Figure 11**) [207]. My data so far shows that a reduction in *Chd7* expression is associated with a specific decrease in the number of TH-expressing cells in the OB (see **Section 5.2.**). Therefore, I hypothesised that a reduction in *Chd7* expression results in a loss of TH-producing interneurons in the OB due to abnormalities in SVZ-OB neurogenesis. To first determine if *Chd7* was expressed in cells in the SVZ neurogenic lineage, an *in situ* hybridisation using an anti-sense *Chd7* probe was performed on coronal sections of adult WT (CD1 mouse strain) brains. *Chd7* was expressed in the dorso-lateral aspect of the SVZ and in the RMS (**Figure 40a**), which is the area of the SVZ associated with the production of TH⁺ OB interneurons (see **Figure 11**) and this was confirmed by antibody staining (**Figure 40b**). *In situ* hybridisation using an anti-sense *Chd7* probe on coronal sections of the RMS and OB showed that *Chd7* was expressed in the RMS and glomerular layer of the OB, as well as in the granular cell layer to a lesser extent (**Figure 40c,d**). This was confirmed by staining sagittal sections of WT adult brains with an anti-CHD7 antibody (**Figure 40e**). These data show that CHD7 is expressed in the area of the SVZ associated with production of TH⁺ OB interneurons, as well as in the RMS and glomerular layer of the OB.

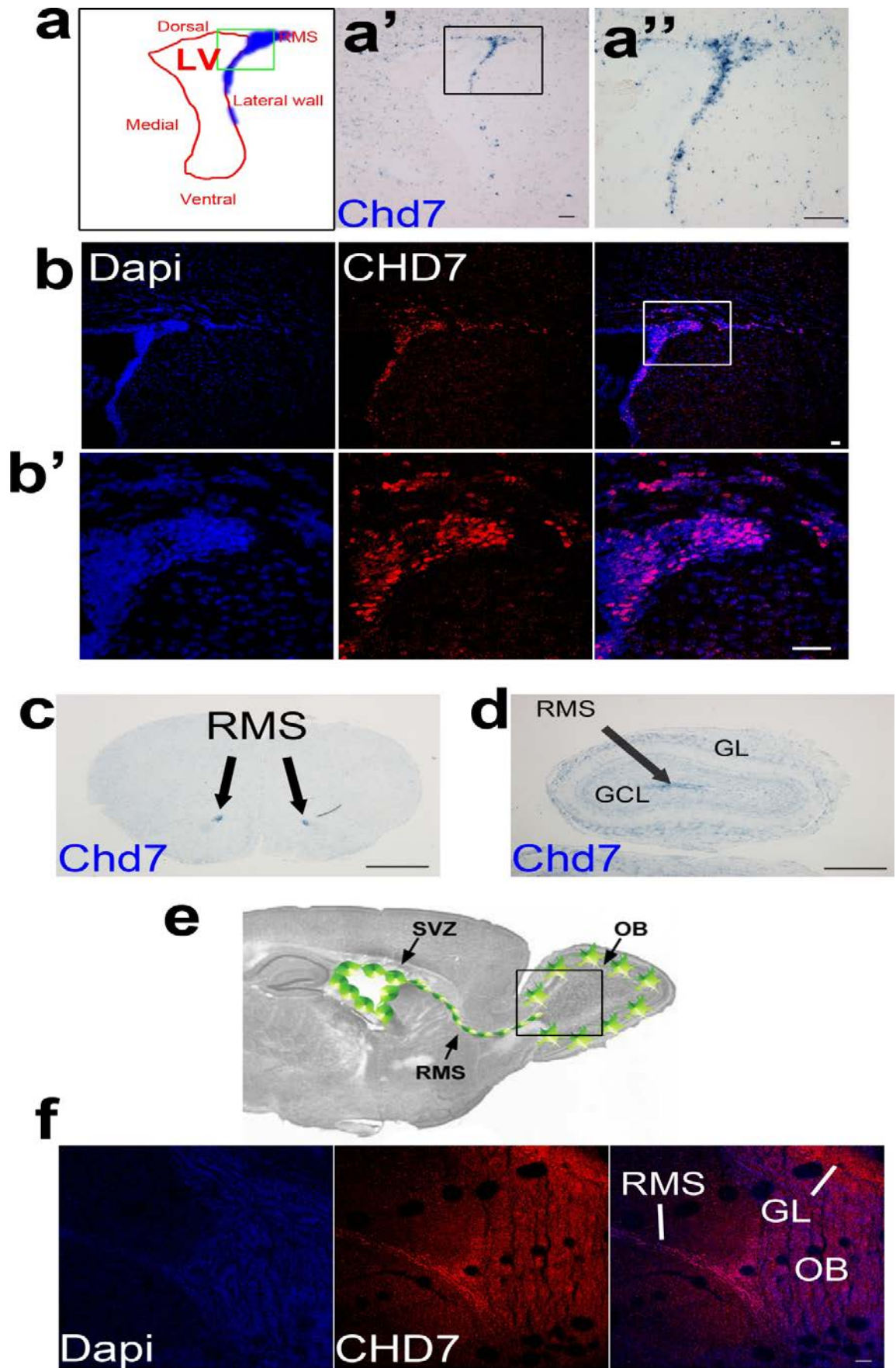


Figure 40 - CHD7 is expressed in the subventricular zone, rostral migratory stream, and olfactory bulb. **a**, Diagram of an *in situ* hybridisation using an anti-sense *Chd7* probe (blue) in the SVZ from **a'**. **a'** *In situ* hybridisation using an anti-sense *Chd7* probe (blue) in the SVZ. The boxed area is enlarged in **a''**. Scale bars, 100µm. **b**, Coronal adult SVZ section stained with an anti-CHD7 antibody and Dapi. The boxed area is enlarged in **b'**. Scale bars, 50µm **c**, *In situ* hybridisation using an anti-sense *Chd7* probe (blue) in a coronal section of the RMS and OB (**d**). Scale bars, 1mm. **e**, Diagram of a sagittal adult mouse brain showing the SVZ, RMS, and OB (adapted from http://neurochirurgie.charite.de/forschung/arbeitsgruppen/ag_endogene_neuronale_stammzellen/). Green areas represent where neurogenic cells can be detected. The boxed area depicts the area shown in **f**. **f**, Sagittal adult RMS and OB section stained with an anti-CHD7 antibody and Dapi. Scale bars, 100µm GCL, granule cell layer; GL, glomerular cell layer.

5.3.1. CHD7 is expressed at high levels in transit-amplifying cells in the subventricular zone

My data so far demonstrate that CHD7 is expressed in the SVZ-OB neurogenic niche (see **Section 5.3.**). To determine which cell types in the SVZ express CHD7, a series of co-localisation experiments were performed by staining SVZ sections with antibodies raised against CHD7 and various markers of cells in the neurogenic lineage (see **Figure 7**). Around 10% of GFAP⁺ NSCs and astrocytes expressed CHD7 (**Figure 41a,b**), suggesting that CHD7 may be expressed in a subset of NSCs. However, GFAP⁺ astrocytes were not the primary cell type that expressed CHD7 (**Figure 41a,c**). Sox2 is expressed by NSCs and type C cells (see **Figure 7**). CHD7 was expressed in nearly 40% of Sox2⁺ cells (**Figure 41d,e**), and the majority of CHD7⁺ cells were Sox2⁺ (**Figure 41d,f**). Type C cells proliferate rapidly and the majority of type C cells express markers of cell cycle entry such as Ki67 and PCNA. CHD7 was expressed by the majority of proliferating (Ki67⁺) cells (**Figure 41g,h**) and most cells that expressed CHD7 were proliferating (**Figure 41g,i**). MASH1 also marks activated NSCs and type C cells. CHD7 was expressed by almost all MASH1⁺ cells (**Figure 41j,k**), and many CHD7⁺ cells expressed MASH1 (**Figure 41j,l**). CHD7 was expressed in many type A cells, as shown by its expression in the RMS where type A cells migrate to the OB (see **Figure 40e**), but this was at a much lower level than other cells in the SVZ. CHD7 was not expressed at high levels by PSA-NCAM⁺ neuroblasts (**Figure 41m,n**), and few highly-expressing CHD7⁺ cells also expressed PSA-NCAM (**Figure 41m,o**). These data show that CHD7 is expressed mainly in proliferating type C cells in the SVZ, and CHD7 expression is downregulated as cells proceed through the neurogenic lineage (**Figure 42**).

5: Results Part III

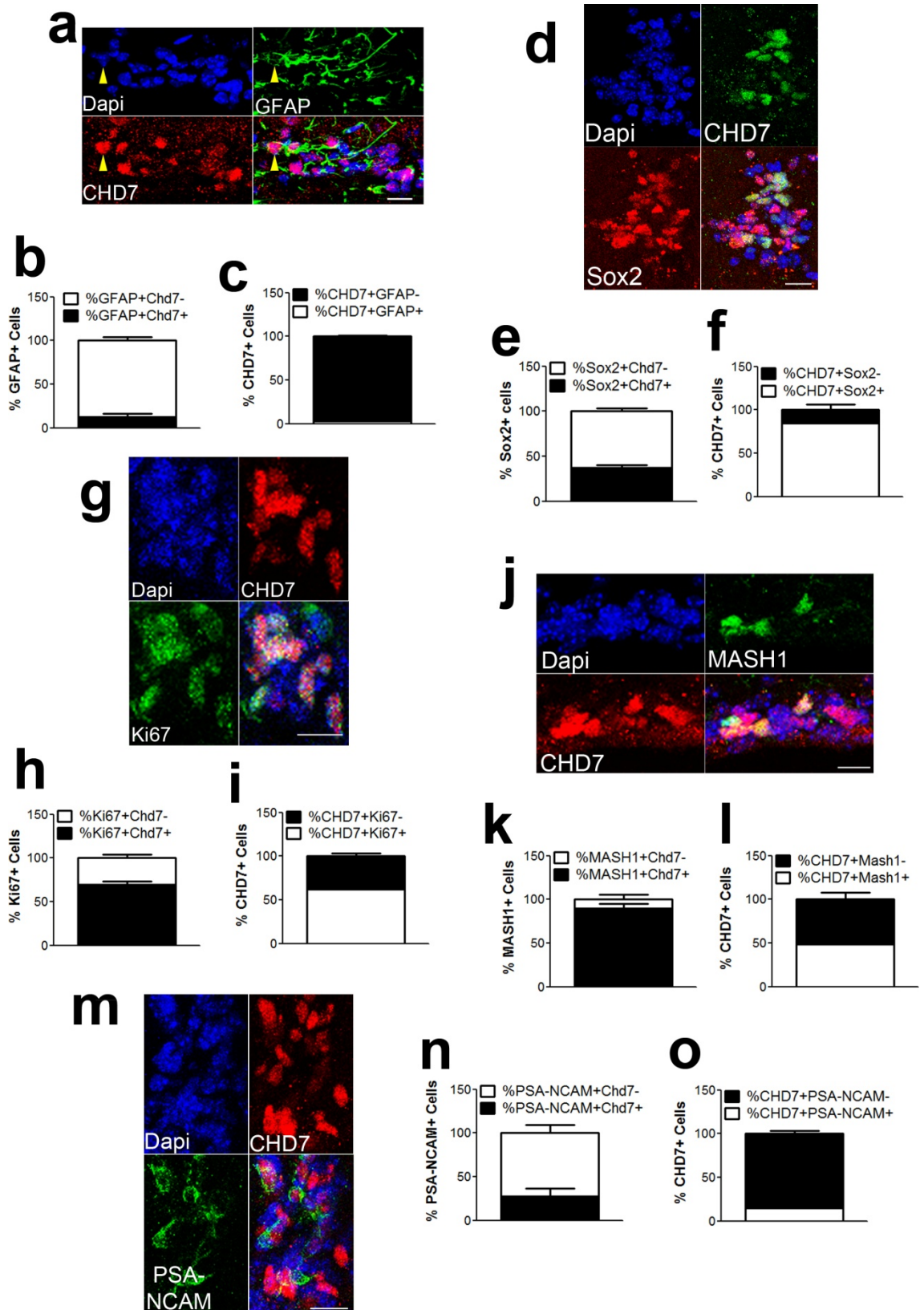


Figure 41 - CHD7 is expressed by proliferating cells and type C cells. **a**, Representative image of SVZ sections stained with antibodies raised against CHD7 and GFAP, Sox2 (**d**), Ki67 (**g**), MASH1 (**j**), and PSA-NCAM (**m**). The yellow arrow head shows a GFAP⁺CHD7⁺ cell. Scale bars, 20µm. **b**, Quantification of the percentage of GFAP⁺, Sox2⁺ (**e**), Ki67⁺ (**h**), MASH1⁺ (**k**), and PSA-NCAM⁺ (**n**) cells that also express CHD7. **c**, Quantification of the percentage of CHD7⁺ cells that also express GFAP, Sox2 (**f**), Ki67 (**h**), MASH1 (**l**), and PSA-NCAM (**o**). n = 100-150 cells analysed by confocal microscope. All data represented as mean ± s.e.m.

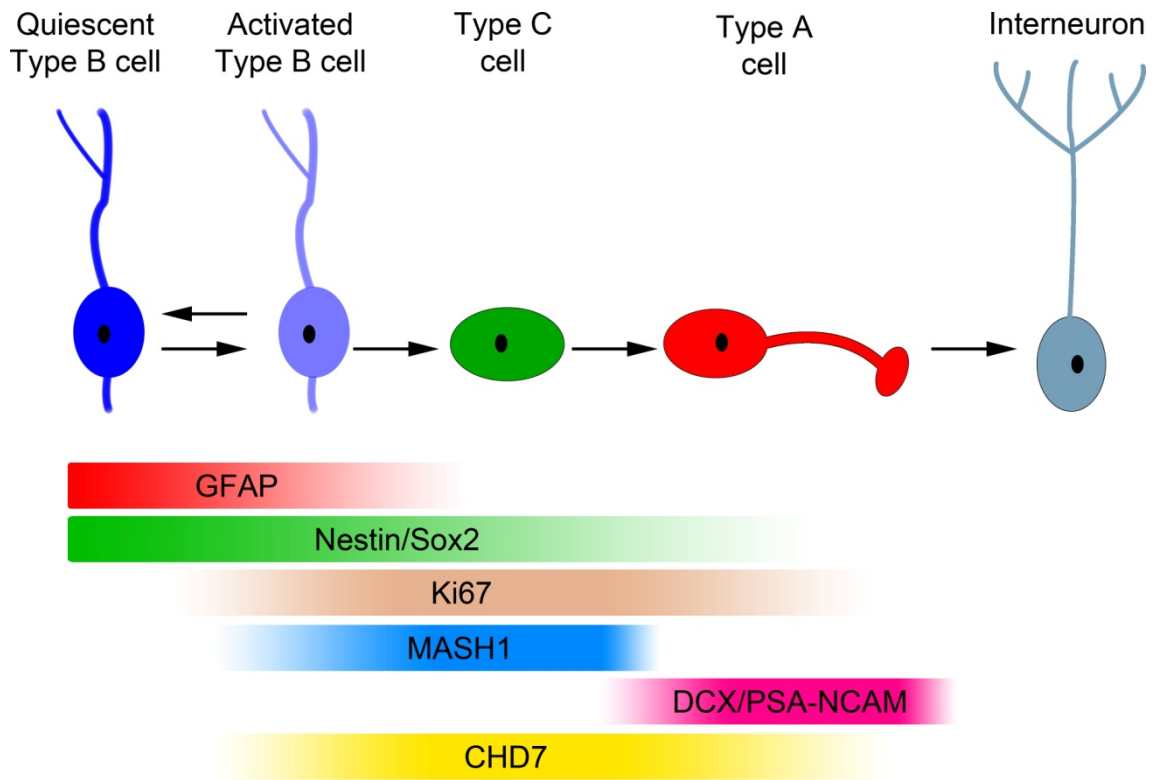


Figure 42 - Schematic of CHD7 expression in the SVZ. CHD7 is expressed mostly in type C cells and is expressed at much lower levels in type A cells. CHD7 is also expressed at low levels in interneurons in the glomerular cell layer of the OB (not shown).

5.4. Reduction in *Chd7* expression results in a decrease in immature neuron production in the subventricular zone

My data so far suggests that a reduction in *Chd7* expression causes a decrease in the number of TH⁺ OB interneurons (see **Section 5.2.**). CHD7 is expressed by transit amplifying cells in the area of SVZ associated with TH-interneuron production (see **Section 5.3.**), and therefore likely plays a role in fate decisions and the differentiation of SVZ cells. I therefore hypothesised that CHD7 regulates the generation of new neurons in SVZ-OB neurogenesis. To determine if a reduction in *Chd7* expression affects the generation of immature interneurons, sections of the SVZ of WT and *Chd7^{gt/+}* mice were stained with antibodies raised against DCX, a marker of immature neurons (type A cells; **Figure 43a**). *Chd7^{gt/+}* mice had fewer DCX⁺ cells specifically in the area of the lateral ventricle where CHD7 is expressed (**Figure 43b-d**). These data suggest that cells with reduced *Chd7* expression may have an impaired differentiation capability. Alternatively, there may be a defect in progenitor proliferation causing impaired formation of new immature neurons, or there may be an increase in the apoptosis of type A cells. To determine if the proliferation of SVZ cells was affected by a decrease in *Chd7* expression, sections of the SVZ of WT and *Chd7^{gt/+}* mice were stained with antibodies raised against PCNA to label proliferating cells, the majority of which are type C transit amplifying cells [183]. Interestingly, SVZ proliferation was increased in the lateral wall and RMS (**Figure 43e-g**). These data show that proliferation in the SVZ is not impaired and suggests that a decrease in immature neuron formation may instead be due to impaired differentiation. That the number of proliferating cells in the SVZ increases suggests that there is a block in differentiation which causes an accumulation of proliferating type C cells. To determine if a reduction in *Chd7* expression leads to changes in apoptosis, an activated caspase 3 stain will need to be performed (see **Section 6.11.6.**). Collectively, these data reveal a role for CHD7 in SVZ-OB neurogenesis, with *Chd7^{gt/+}* mice exhibiting a decrease in the generation of type A cells possibly due to a block in

differentiation which results in a decrease in the production of TH⁺ interneurons in the OB.

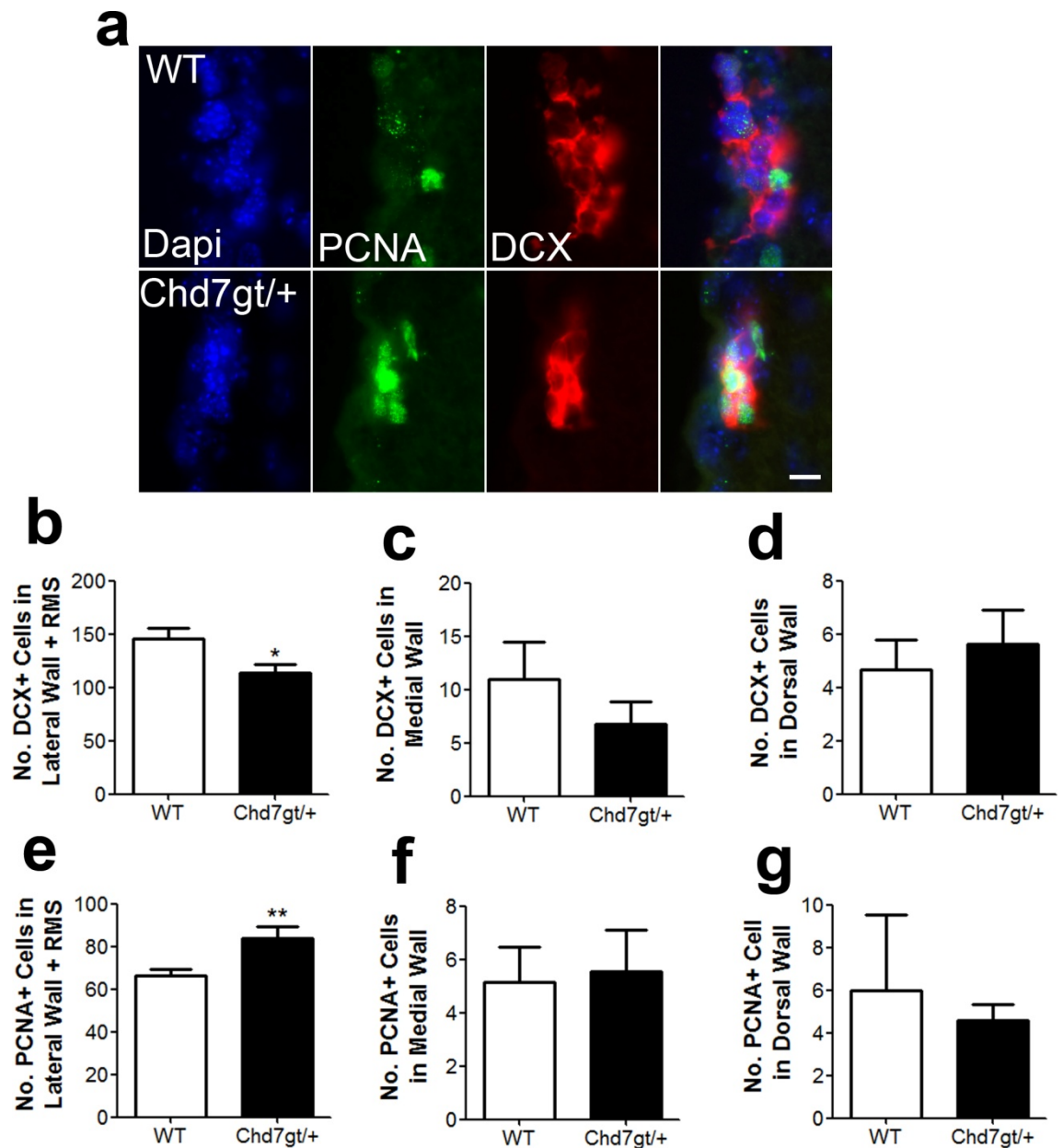


Figure 43 - Reduction in Chd7 expression affects SVZ neurogenesis. **a**, Representative image of the lateral wall of the SVZ of *Chd7^{gt/+}* and WT mice stained with antibodies raised against PCNA and DCX. Scale bar, 20 μ m. **b**, Quantification of the number of DCX⁺ cells in the lateral wall of the lateral ventricle and RMS, and in the medial wall (**c**), and dorsal wall (**d**) of the lateral ventricle of *Chd7^{gt/+}* and WT mice per 10 μ m section. Note, there is no change in the number of DCX⁺ cells in the medial and dorsal walls of the lateral ventricle as CHD7 is not expressed there. n=3 animals / condition. **e**, Quantification of the number of PCNA⁺ cells in the lateral wall of the lateral ventricle and RMS, and in the medial wall (**f**), and dorsal wall (**g**) of the lateral ventricle of *Chd7^{gt/+}* and WT mice per 10 μ m section. n=3 animals / condition. All data represented as mean \pm s.e.m.; *P<0.05 **P<0.01 student's t test.

5.4.1. Loss of *Chd7* in NSCs blocks their differentiation

Chd7^{gt/+} mice have reduced *Chd7* expression in all cell types, including in olfactory epithelial stem cells (OESCs), and so the phenotypes seen may be due to effects on cells other than those in the SVZ neural lineage. Therefore, to exclude the possibility that the reduction in the number of TH-expressing interneurons is due to effects on OESCs, I sought to delete *Chd7* specifically from adult NSCs using a GLAST::CreERT2 mouse line [253]. GLAST is expressed by NSCs and astrocytes and so upon tamoxifen injection Cre-mediated recombination should only take place in NSCs [253]. To first determine its efficiency in the SVZ, the GLAST::CreERT2 line was crossed to a RYFP reporter line to generate GLAST::CreERT2;RYFP/+ mice. Adult GLAST::CreERT2;RYFP/+ mice were given 5 injections of tamoxifen to induce recombination and expression of YFP and sacrificed 5 days after the last tamoxifen injection (**Figure 44a**). Sections of the SVZ were stained with antibodies raised against GFP along with GFAP to label NSCs (**Figure 44c**). YFP could be detected in around 75% of GFAP⁺ cells (**Figure 44b**), however, this is likely to be an underestimation due to the difficulty in seeing individual GFAP⁺ cells in these sections. YFP⁺GFAP⁻ cells were also present in the SVZ which are presumably type C daughter cells (**Figure 44c**). Therefore, my tamoxifen injection regime in GLAST::CreERT2 mice results in efficient recombination in SVZ cells.

To delete *Chd7* specifically from adult NSCs, GLAST::CreERT2 mice were crossed with a mouse line where exon 3 of *Chd7* is floxed (*Chd7^{fl/fl}*) [EUCOMM ID: 35714] to generate a GLAST::CreERT2;*Chd7^{fl/fl}* mouse line (**Figure 45a**). Tamoxifen injection causes Cre-mediated recombination and formation of a truncated, non-functional CHD7 protein specifically in NSCs and astrocytes (*Chd7^{null}*; see **Section 6.3.**). *Chd7^{null}* and Cre-negative control mice (WT) were treated with tamoxifen and sacrificed 11 weeks later (**Figure 45b**). BrdU was administered in the drinking water of mice in the last 3 weeks of life to label all newly generated cells (**Figure 45b**). The number of BrdU⁺ cells was reduced in the SVZ and RMS of *Chd7^{null}* mice compared to WT, suggesting that loss of

Chd7 from NSCs results in a decrease in the number of new cells formed (**Figure 45c,d**). These data are consistent with decrease in SVZ neurogenesis in *Chd7^{gt/+}* mice.

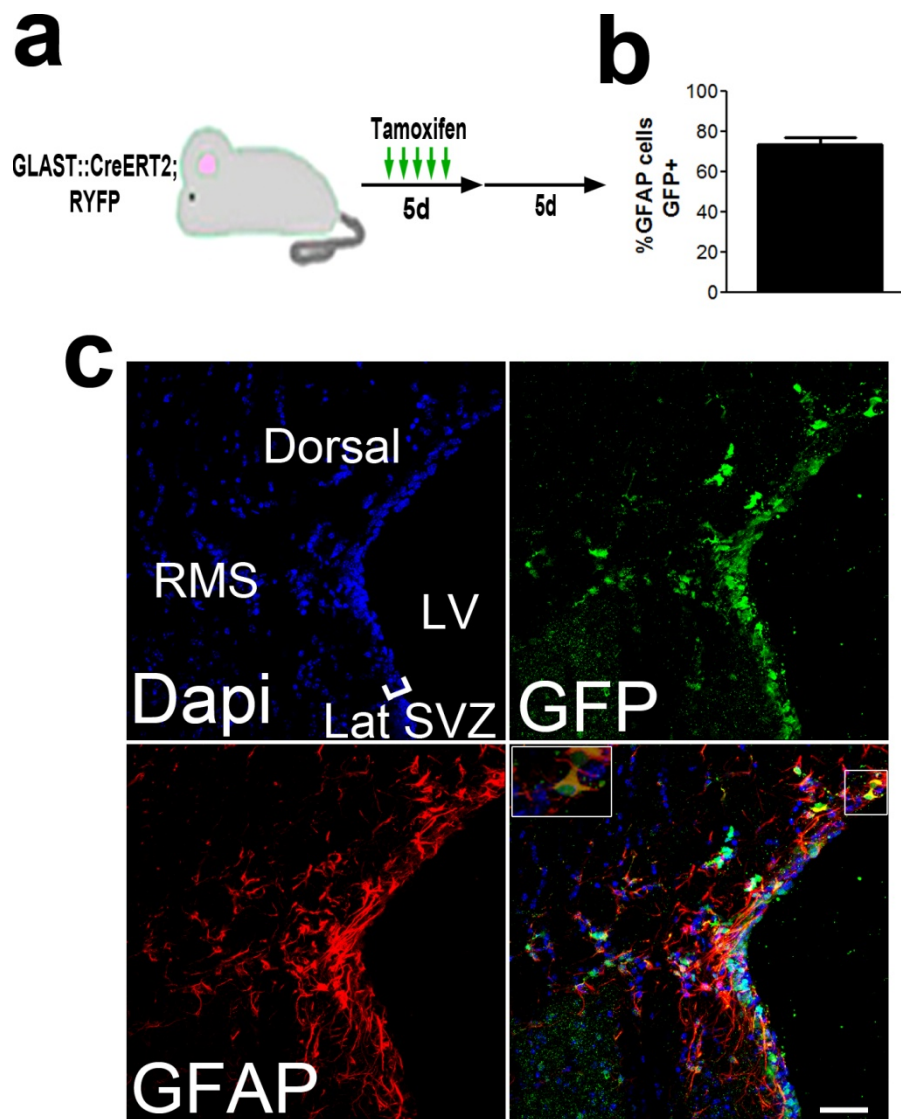


Figure 44 - Efficient recombination in the GLAST::CreERT2 mouse line. **a**, Schematic of the experimental strategy to induce recombination and YFP expression in SVZ NSCs. Adult GLAST::CreERT2;RYFP mice were given one injection of 80mg/kg tamoxifen a day for 5 days and sacrificed 5 days after the last tamoxifen injection. **b**, Quantification of the percentage of GFAP⁺ cells that were also GFP⁺. At least 60 GFAP⁺ cells were counted. n=2 animals. Data represented as mean \pm s.e.m. **c**, Representative image of a sagittal section of the lateral ventricle (LV) of GLAST::CreERT2;RYFP mice treated as in **a** stained with antibodies raised against GFP and GFAP. Note the large overlap between GFAP and GFP in the SVZ and RMS. The boxed area is enlarged in the merge and shows a GFP⁺GFAP⁺ cell. Lat SVZ, lateral wall of the SVZ. Scale bar, 100 μ m. n=2 animals.

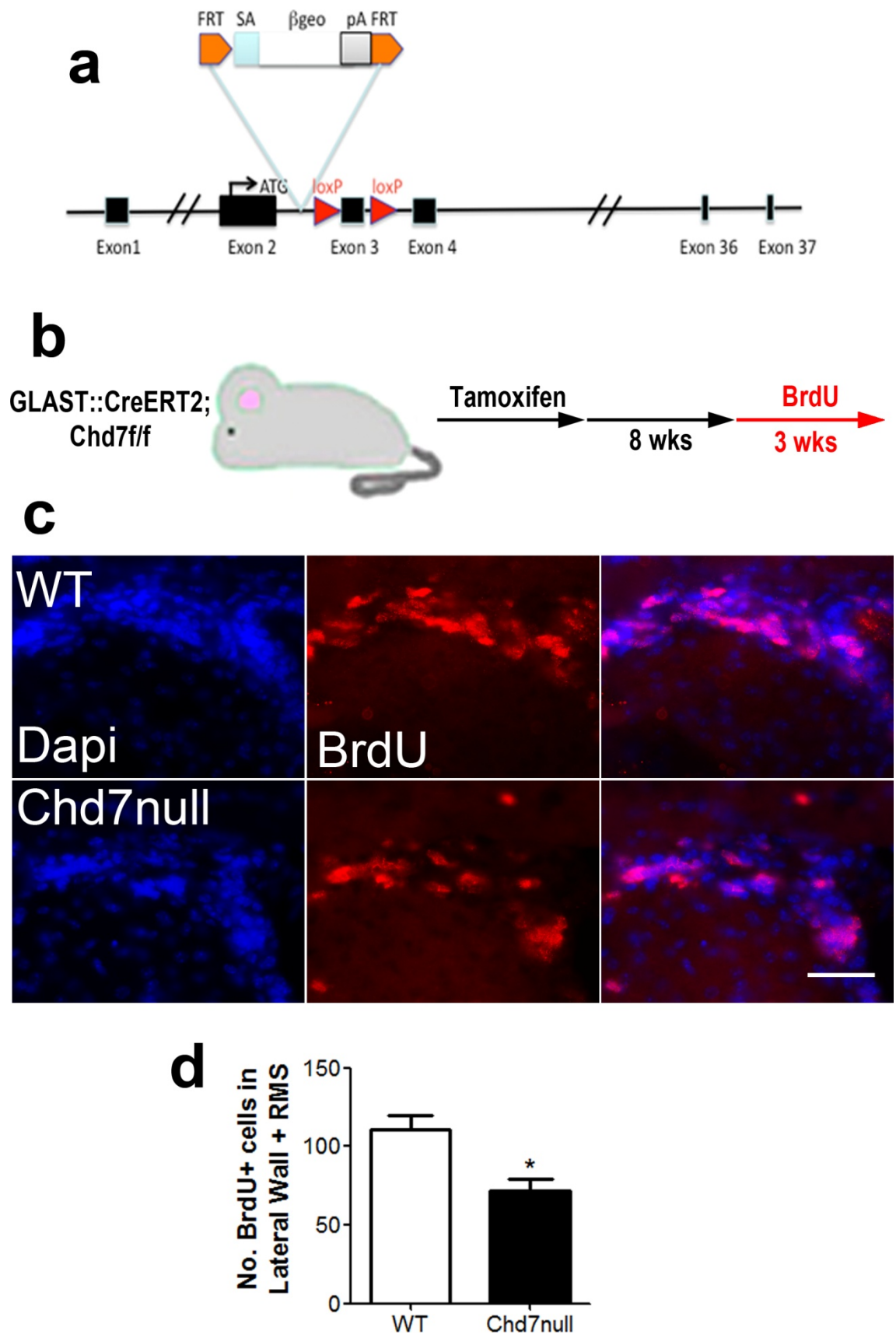


Figure 45 - Loss of *Chd7* in neural stem cells affects subventricular zone neurogenesis.

a, Schematic of the *Chd7* flox allele (EUCOMM ID: 35714). The selection cassette was removed by crossing with Flp deleter mice. Exon 3 is flanked by loxP sites to allow for conditional inactivation and the formation of a truncated, non-functional protein after Cre-mediated recombination. **b**, Schematic of the experimental strategy to delete *Chd7* from adult NSCs and label newly born cells by administering BrdU in the drinking water of mice. **c**, Representative image of a section of the SVZ and RMS of GLAST::CreERT2;*Chd7*^{fl/fl} mice treated with tamoxifen (*Chd7*null) and Cre-negative controls (WT) stained with antibodies raised against BrdU. Scale bar, 50µm. **d**, Quantification of the number of BrdU⁺ cells in the lateral wall and RMS of WT and *Chd7*null mice per 20µm section. n=2 animals / condition. Data represented as mean ± s.e.m.; *P<0.05 student's t test.

5.5. Restoration of *Chd7* function partially rescues the expression of tyrosine hydroxylase in the olfactory bulb

The data shown so far suggests that the reduction in TH expression in the OB likely reflects changes in SVZ-OB neurogenesis. I hypothesised that restoration of *Chd7* specifically in NSCs and their progeny could restore the number of TH-producing cells in the SVZ. To test this, *Chd7^{gt/+}* mice (which have 50% reduced *Chd7* expression (see **Figure 37b**)) were crossed to GLAST::CreERT2 mice to generate a GLAST::CreERT2;*Chd7^{gt/+}* mouse line. Injection of tamoxifen results in restoration of *Chd7* function specifically in NSCs and their progeny (GLAST::CreERT2;*Chd7^{+/+}* ; Rescue; **Figure 46a,b**), however, I did not have the mice to confirm by RT-qPCR to what extent the expression of *Chd7* is restored. GLAST::CreERT2 mice were used as controls (WT) (**Figure 46b**). Restoration of *Chd7* function in NSCs partially rescued the number of TH⁺ interneurons compared to GLAST::CreERT2;*Chd7^{gt/+}* mice (**Figure 46c,d**).

Collectively, these data show that CHD7 regulates TH⁺ interneuron production, and restoration of *Chd7* function specifically in NSCs can partly rescue the deficit of TH⁺ interneurons in the OB of *Chd7^{gt/+}* mice. Alternative explanations are possible and these will be discussed in **Section 5.6.2**.

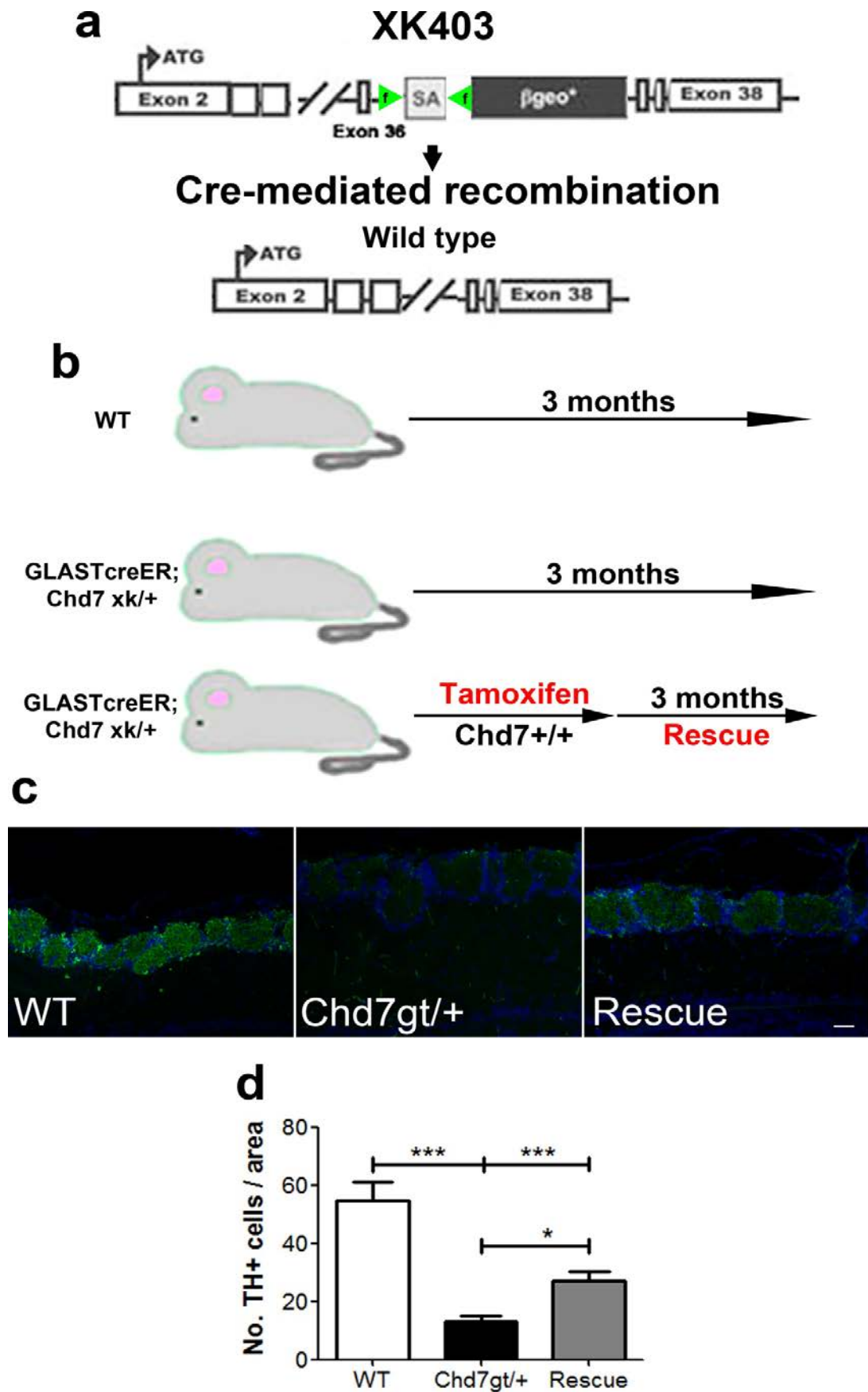


Figure 46 - Restoration of Chd7 function in neural stem cells partly rescues tyrosine hydroxylase production in the olfactory bulb. **a**, Schematic of the *Chd7*^{Δk403} allele before (top panel) and after (bottom panel) recombination. Cre-mediated recombination results in deletion of the splice acceptor (SA) site (green triangles flanking the SA) and loss of β-galactosidase activity, thereby allowing for the production of functional and stable CHD7 protein. Adapted from [356]. **b**, Schematic diagram of the strategy to assess the effect of restoration of *Chd7* function on OB neurogenesis. Three cohorts of adult mice were used: 1. GLAST::CreERT2 mice were used as controls (WT) and taken at 5 months of age (top panel); 2. GLAST::CreERT2;*Chd7*^{gt/+} mice (*Chd7*^{gt/+}) taken at 5 months of age (middle panel); 3. GLAST::CreERT2;*Chd7*^{gt/+} mice treated with tamoxifen at 2 months of age and sacrificed 3 months later (Rescue). **c**, Representative picture of OB glomerular sections stained with antibodies raised against TH (green), and Dapi (blue). Scale bar, 100μm. **d**, Quantification of the number of TH⁺ interneurons per area of WT, *Chd7*^{gt/+} and Rescue mice per 10μm section. n=3 animals / condition. Data represented as mean ± s.e.m.; *P<0.05 ***P<0.001 student's t test.

5.6. Discussion

I sought to investigate the role of the chromatin remodelling enzyme CHD7 in adult neurogenesis. The data presented here depict a specific role for CHD7 in the regulation of the production of TH⁺ interneurons from SVZ cells (**Figure 47**). These data show that CHD7 is expressed mainly by type C cells in the dorso-lateral aspect of the SVZ and in the RMS, the area associated with production of TH⁺ OB interneurons [207]. Reduction in *Chd7* expression results in a decrease in OB length whilst having very little effect on the size of other areas of the brain. My data suggests that *Chd7* is required for the formation of immature neurons of the TH-lineage (**Figure 47**). I have shown that loss of *Chd7* specifically in NSCs results in a loss of the formation of new cells in the SVZ and restoration of *Chd7* function specifically in adult NSCs results in an increase in TH⁺ interneurons in the OB compared to *Chd7^{fl/+}* mice. These results show that *Chd7* does indeed regulate adult neurogenesis.

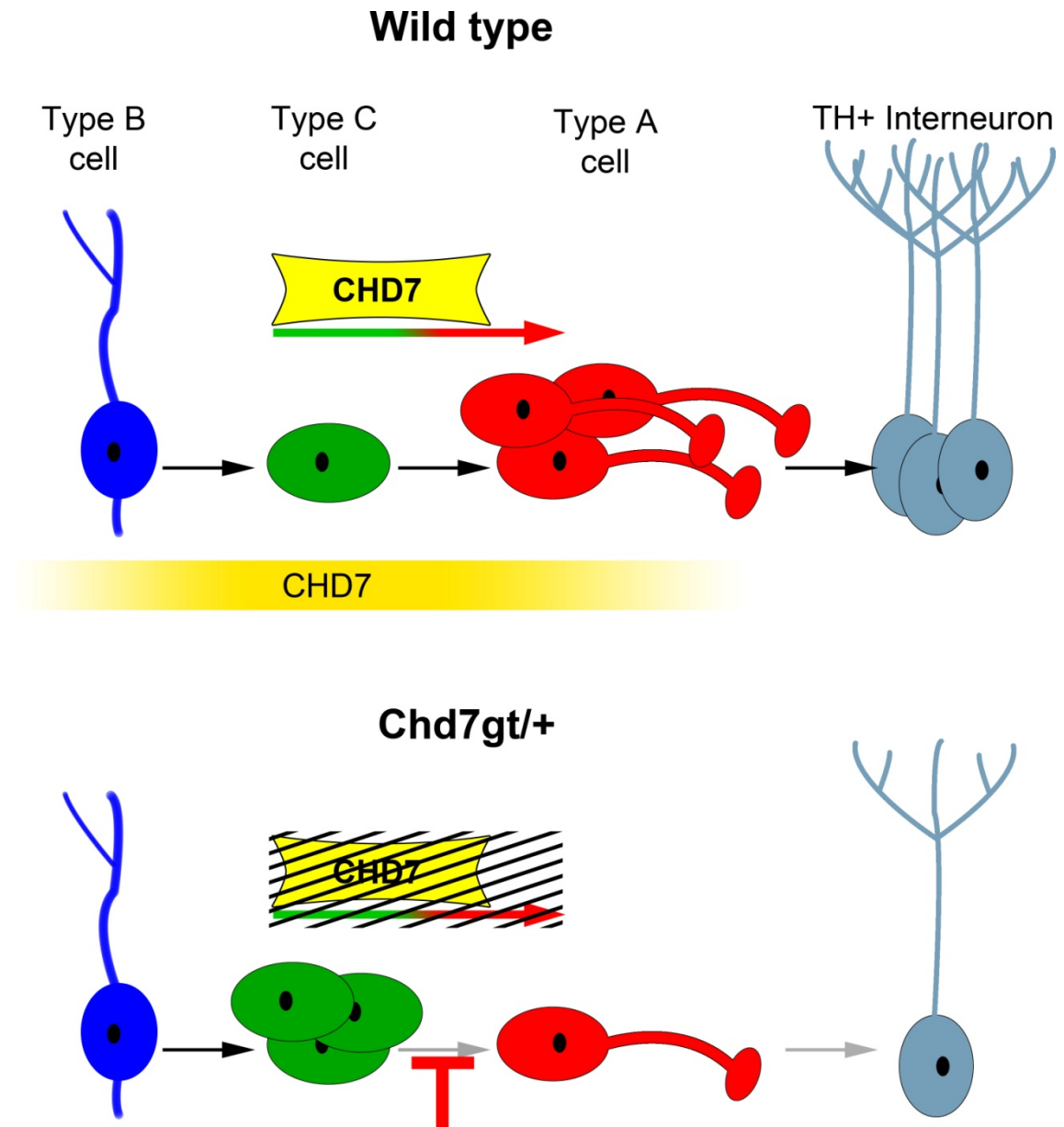


Figure 47 - Reduction in *Chd7* expression affects subventricular zone neurogenesis.

Under homeostatic conditions, SVZ neurogenesis is required for the formation of new OB interneurons (top panel). However, a reduction in *Chd7* expression results in a loss of TH⁺ interneurons and a decrease in the number of immature neurons (type A cells) (bottom panel). Additionally, a reduction in *Chd7* expression also leads to an increase in the number of proliferating cells in the SVZ, possibly due to a block in differentiation (red block).

5.6.1. The reduction in olfactory bulb size and number of tyrosine hydroxylase⁺ interneurons may be progressive with age

The OB length is around 10% shorter in P21 *Chd7^{gt/+}* mice compared to WT littermates (see **Figure 37e**). That the forebrain length of P21 *Chd7^{gt/+}* mice is not significantly shorter (see **Figure 37f**) argues that this is not due to a developmental delay, but instead reflects a specific effect of a reduction of *Chd7* expression on the formation of the OB. By adulthood the OB of *Chd7^{gt/+}* mice is 33% shorter than controls, suggesting that the decline in OB size is progressive with age (see **Figure 37d**). SVZ-OB neurogenesis is presumably required for maintenance of OB structure and size since the OB interneuron population is constantly turned over [210-212]. Furthermore, the decline in number of interneurons producing TH also appears to decline with age in *Chd7^{gt/+}* mice compared with controls (compare the number of TH⁺ interneurons in *Chd7^{gt/+}* mice in **Figure 38b** with **Figure 46d**). These data imply that a reduction in *Chd7* expression leads to a decline in the formation of TH⁺ interneurons that is progressive with age and further indicate that a reduction in *Chd7* leads to impaired SVZ-OB neurogenesis.

I have shown that restoration of *Chd7* function, specifically in NSCs, results in a significant increase in TH-expressing interneurons in just 3 months compared to *Chd7^{gt/+}* mice. If the reduction in TH⁺ interneurons is progressive with age in *Chd7^{gt/+}* mice, then the restoration of *Chd7* function may reinstate a normal level of OB neurogenesis and maintain the production of TH⁺ interneurons, whereas the number of TH⁺ interneurons would continue to decline in *Chd7^{gt/+}* mice. A fourth cohort of *Chd7^{gt/+}* mice taken at 2 months of age, at the very start of the experiments, would be needed to test this.

5.6.2. A reduction in *Chd7* expression may result in a loss of cells of the tyrosine hydroxylase lineage, or a loss of tyrosine hydroxylase production

I have shown that *Chd7^{gt/+}* mice display a reduction in *Er81* expression, which is an early marker for cells of the TH-lineage [390, 391]. However, *Er81* is also required for the expression of TH in cells [390, 391]. Hence, an alternative explanation for the loss of TH-producing cells in *Chd7^{gt/+}* mice could be that a reduction in *Chd7* expression results in decreased expression of TH from cells rather than a decrease in the formation of TH-expressing cells (**Figure 48**). These points can be addressed by staining OB sections of *Chd7^{gt/+}* and WT mice with markers to specifically label cells that would produce TH (such as dopamine decarboxylase (DDC), an enzyme involved in the production of TH). This would reveal if the TH-expressing interneurons are still present in *Chd7^{gt/+}* mice, but just not producing TH. However, preliminary experiments performed using DDC antibodies have shown them to be very non-specific and they do not overlap with TH expression. Therefore, other antibodies such as dopamine transporter (DAT) [392], will be required to distinguish between a reduction in TH-expression or a reduction in interneurons.

A reduction in *Chd7* expression causing a decreased expression of TH from cells (**Figure 48**), may also mean that restoration of *Chd7* function in NSCs results in a significant increase in TH-expressing interneurons due to restoration of *Chd7* function reinitiating the signalling programs required for the production of TH, such as expression of *Er81*. To determine if the reduction in TH⁺ interneurons in *Chd7^{gt/+}* mice was due to a reduction in neurogenesis, the number of type A cells would need to be counted in Rescue mice. If restoration of *Chd7* results in an increase in the number of type A cells compared to *Chd7^{gt/+}* mice it would suggest that CHD7 regulates the formation of TH⁺ interneurons. To fully conclude this, labelling newly born cells in Rescue mice through BrdU pulse-chase experiment would allow for the analysis of the number of newborn neurons that have integrated into the OB [228]. If CHD7 regulates the formation of TH⁺ interneurons, an increase in the number of BrdU⁺

cells would be seen in the OB in Rescue mice. Additionally, using a marker to specifically label cells that would produce TH would reveal if the TH-expressing interneurons are still present in *Chd7^{gt/+}* mice, but just not producing TH. To fully appreciate the role of CHD7 in dopaminergic OB neuron production, lineage tracing using a *GLAST::CreERT2;Chd7^{f/+};RYFP/+* would need to be performed. This would allow for the analysis of the contribution of cells with reduced *Chd7* expression to OB neurogenesis, and so the number of newly formed TH⁺ OB interneurons can be calculated.

To fully determine if the reduction in *Er81* expression seen in *Chd7^{gt/+}* mice is due to a decrease in its expression in immature neurons, the transcription of *Er81* would need to be determined in isolated type A cells.

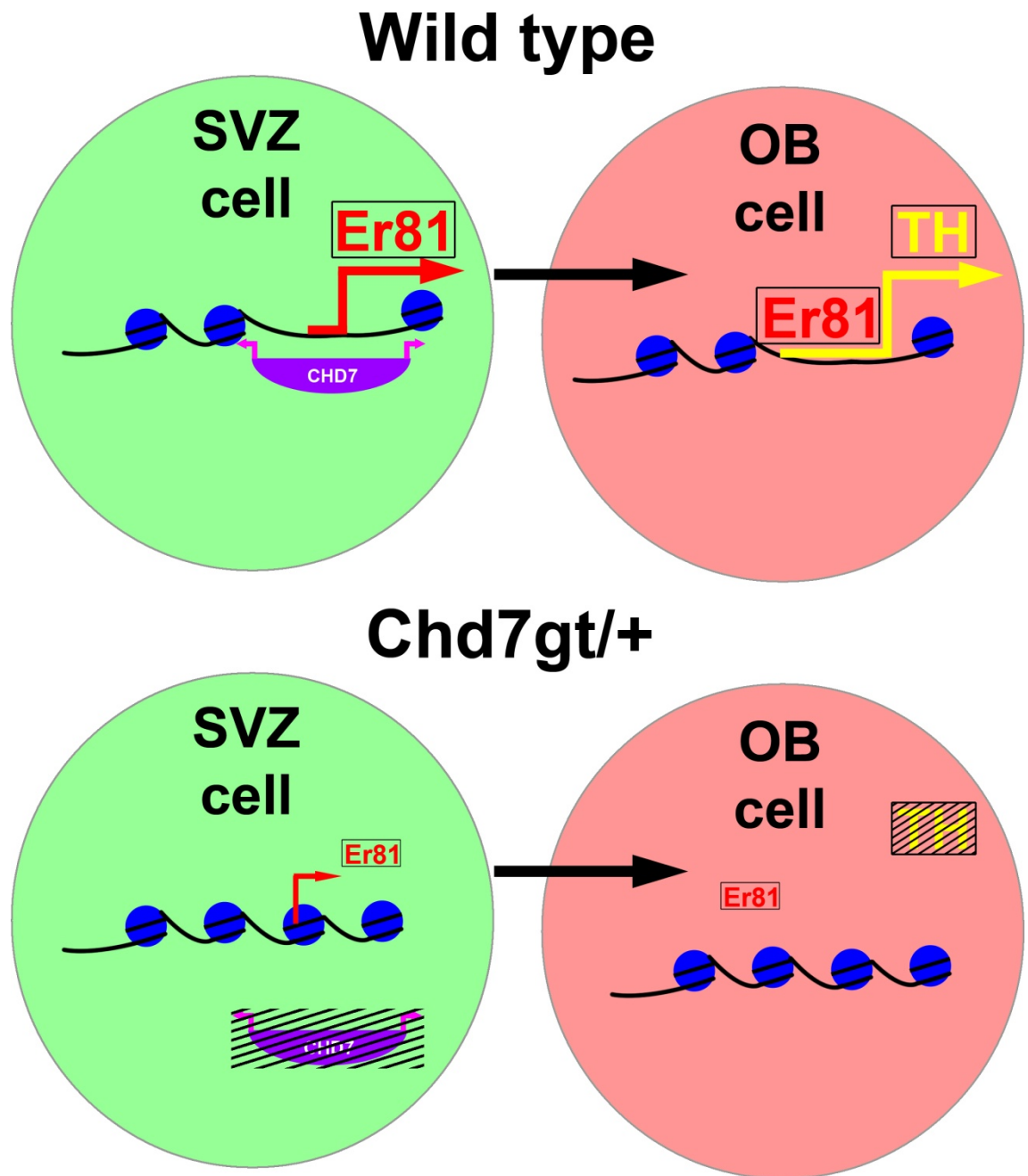


Figure 48 - Regulation of *Er81* expression by CHD7. CHD7 may bind to *Er81* promoter elements or distal enhancers to induce *Er81* expression in cells of the SVZ-OB neurogenic lineage. *Er81* then directly induces the expression of tyrosine hydroxylase in dopaminergic OB cells (top panel). In *Chd7*^{gt/+} mice, a reduction in *Chd7* expression may limit the expression of *Er81*, thereby causing a reduction in the expression of tyrosine hydroxylase from OB cells without affecting the production of cells (bottom panel).

5.6.3. CHD7 regulates subventricular zone - olfactory bulb neurogenesis

Studies by Layman et al. showed that CHD7 was expressed by MASH1⁺ stem cells in the olfactory epithelium [345]. The data presented here show that CHD7 is expressed in MASH1⁺ cells in the SVZ. It is interesting to speculate that CHD7 has a conserved role in MASH1⁺ cells to drive the neurogenic program. The authors also found that reduction in *Chd7* expression led to decreased proliferation of the epithelial stem cells [345]. Whilst I have not calculated the proliferation specifically of NSCs in the SVZ, my data indicate that proliferation in the SVZ is generally increased, perhaps suggesting differences in the role of *Chd7* in different stem cell populations. Layman et al. attributed a decline in TH expression in the OB of *Chd7*^{gt/+} mice to a decrease in the proliferation of olfactory epithelial stem cells and a loss of signalling to dopaminergic interneurons (see **Figure 35**) [345]. Restoration of *Chd7* function specifically in NSCs and astrocytes, partially rescued the deficiency in TH in the OB, and argues against a decrease in olfactory epithelial stem cell proliferation being the sole reason for a loss of TH in the OB. An alternative explanation to these findings is that CHD7 may affect GLAST⁺ mature astrocyte function, which may, in turn, regulate stem cells and their progeny in the olfactory epithelium. However, in preliminary studies using a GLAST::CreERT2;RYFP mouse line, I could not detect YFP expression in the olfactory epithelium 3 months after tamoxifen-induced recombination (data not shown). These data suggest that this Cre is not active in the olfactory epithelium, and therefore restoration of *Chd7* in GLAST⁺ cells does not directly affect the olfactory epithelium. Furthermore, the finding that very few GFAP-expressing cells also express CHD7 suggests that the regulation of mature astrocyte function by CHD7 is unlikely.

5.6.4. Loss of *Chd7* results in a large reduction in olfactory bulb neurogenesis

Recently, CHD7 was shown to play a role in adult SVZ-OB neurogenesis in mice. Feng et al. observed that CHD7 was expressed in few GFAP⁺ cells and also in the majority of proliferating cells as well as in neuroblast cells [386], which is in agreement with my data. The authors utilised NestinCreERT2;*Chd7*^{ff} and Tlx-CreERT2;*Chd7*^{ff} mouse lines to specifically delete *Chd7* from adult NSCs and progenitors [386]. Feng et al. saw that 8 weeks after tamoxifen injection, the OB of Tlx-CreERT2;*Chd7*^{ff} mice had a reduction in the number of TH⁺, CalR⁺, and CalB⁺ interneurons [386]. I have shown that a reduction in *Chd7* expression leads to a decrease in the number of TH⁺ OB interneurons without affecting other types of interneurons (see **Figure 38**). These data suggest that the effect of CHD7 on adult neurogenesis may be dependent on the level of *Chd7*. I have shown that the transcript of *Chd7* is reduced by 50% in *Chd7*^{gt/+} mice (see **Figure 37b**), whilst Feng et al. observed a complete absence of CHD7 protein in the SVZ of Tlx-CreERT2;*Chd7*^{ff} mice that had been injected with tamoxifen [386]. Therefore, a reduction in *Chd7* levels to 50% of WT levels may preferentially affect TH⁺ interneuron production, whereas ablation of *Chd7* may affect all types of OB interneuron production. These data suggest that cells of the TH-lineage may be more sensitive to the *Chd7* gene dosage. I have shown that loss of *Chd7* from adult NSCs using a GLAST::CreERT2;*Chd7*^{ff} mouse line leads to a reduction in the formation of newly formed cells (see **Figure 45d**), in agreement with Feng et al. [386], and so further analysis of neurogenesis in this mouse line will allow for greater comparisons to be made.

5.6.5. CHD7 in adult subventricular zone neurogenesis

Collectively, these data show that CHD7 plays a role in the neurogenic progression of SVZ cells, specifically affecting production of TH-expressing OB interneurons. In order to determine the full role of CHD7 in adult neurogenesis, I

sought to analyse the effect of loss of *Chd7* in hippocampal neurogenesis. This will allow for similarities and differences to be drawn between the role of CHD7 in the regulation of different NSC populations which serve different brain systems, revealing common themes in the regulation of NSCs and their progeny.

Chapter 6

Results Part IV

6.1. Quiescence of a somatic stem cell population is essential for maintenance of the stem cell pool

Quiescence is a property of somatic stem cell populations that is essential for the maintenance of stem cell number and function. In support of this, I have previously shown that loss of muscle stem cell quiescence can lead to a loss of stem cell number and function (see **Chapter 4**). In the SVZ and SGZ neurogenic niches NSCs are in a relatively quiescent state, which has been shown to be essential to prevent proliferative exhaustion and premature differentiation of the stem cell pool [201, 253].

6.1.1. Maintenance of neural stem cell quiescence

Notch signalling is a critical regulator of NSC quiescence. For example, NSCs express Notch receptor, and signalling from Notch ligand-expressing progenitors in the niche is crucial for preserving NSC quiescence and preventing their proliferative exhaustion [252, 253, 256, 260]. Deletion of *Rbpj*, the transcriptional activator of Notch signalling, specifically from adult NSCs results in the loss of NSC quiescence, a transient increase in neurogenesis, followed by an eventual loss of the NSC pool and a decline in neurogenesis [252, 256]. This was shown to be due to premature conversion of NSCs to transit-amplifying progeny, showing that a loss of quiescence coupled with differentiating (non-self-renewing) divisions can lead to depletion of the stem cell pool [252, 256]. These data are in contrast to what is seen in *p21* mutant mice. *p21*^{-/-} mice display an increase in NSC proliferation and initially exhibit an increase in NSC number, suggesting that a loss of NSC quiescence can also lead to an increase in the NSC pool if coupled with self-renewing divisions. In middle-aged *p21*^{-/-} mice however, NSCs also undergo proliferative exhaustion and neurogenesis declines [393]. Collectively, these data indicate that the maintenance of NSC quiescence and regulation of NSC fate decisions is critical for the maintenance of adult neurogenesis.

6.1.2. Neural stem cell proliferation and ageing

Low-level proliferation of hippocampal NSCs and the generation of new granule neurons is vital for specific types of hippocampal function [224-227].

Proliferative exhaustion of stem cells has been suggested to be the primary cause of ageing [18, 394]. Ageing is associated with reduced NSC proliferation and a decrease in newly generated neurons [187, 395-397], leading to cognitive decline [17, 398, 399]. Whether there is a decrease in the numbers of NSCs with age is largely disputed, with some studies reporting a strong reduction in cell numbers in the ageing hippocampus of rodents [400-402], and others reporting a change in their proliferative state, but not in their absolute numbers [253, 403]. The cell cycle entry and associated depletion of NSCs has been contested in two recent models. Encinas et al. proposed a 'disposable stem cell model' where quiescent NSCs enter the cell cycle, undergo a limited number of asymmetric cell divisions, and terminally differentiate into mature astrocytes, thus leading to depletion of the stem cell pool during life [404]. *In vivo* clonal analyses by Bonaguidi et al. by a low dose of tamoxifen injection in a NSC reporter mouse reported a diverse behavior of NSCs [196]. The authors observed some depletion of the NSC pool with time but also noted that some NSCs that had cycled did not terminally differentiate but instead persisted for long periods of time [196]. Therefore, investigating the mechanisms which regulate NSC quiescence and differentiation under homeostatic conditions in adults may help to better understand the signalling pathways which lead to proliferative exhaustion of stem cells and cognitive decline with ageing.

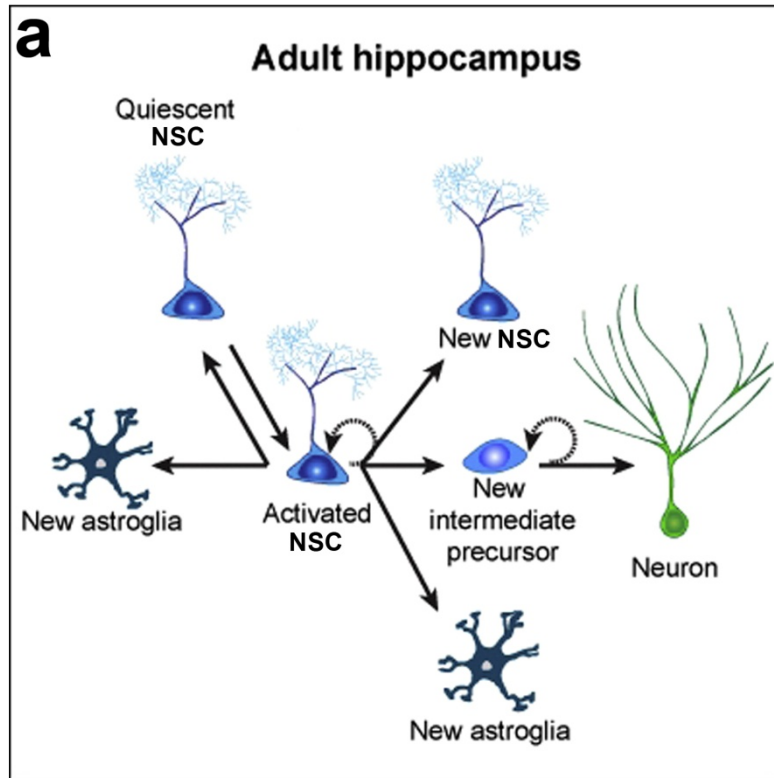
6.1.3. Regulation of neural stem cell fate decisions

In addition to proliferation, regulation of NSC fate decisions can modulate levels of neurogenesis in the adult forebrain. This can be achieved, for example, by changing the proportion of cells undergoing proliferative versus differentiative divisions, symmetric versus asymmetric divisions, and gliogenic versus neurogenic divisions (**Figure 49**).

With ageing, two opposing scenarios have been proposed with regards to changes in NSC fate decisions. Some studies have reported a decrease in the number of newborn neural cells with age [230, 405]. Other studies reported that the proportion of differentiated cell types generated from the pool of cycling NSCs is similar or only slightly changed, even if the number of proliferating NSCs and absolute number of newborn neurons decreases during aging [16, 406-408].

Nevertheless, before developing approaches to combat the age-related decline in NSC activity and possible changes in function, it is important to first identify the mechanisms involved in the regulation of NSC proliferation, maintenance, and cell fate decisions under homeostatic conditions in adults. I have shown that CHD7 plays a role in adult SVZ neurogenesis, by regulating the proliferation and differentiation of SVZ cells (see **Chapter 5**). However, the role of CHD7 and chromatin remodelling in hippocampal neurogenesis remains unknown. I hypothesised that, like in the SVZ, CHD7 plays a role in adult hippocampal neurogenesis and that loss of *Chd7* results in impaired formation or differentiation of SGZ cells. The aims for this chapter are to:

1. Determine the expression profile of CHD7 in SGZ cells.
2. Characterise of the effects of a loss of *Chd7* on adult hippocampal neurogenesis specifically examining the effects on neurogenesis and the NSCs themselves.
3. Use *in vitro* NSC cultures to model the phenotypes seen after loss of *Chd7 in vivo*.



b

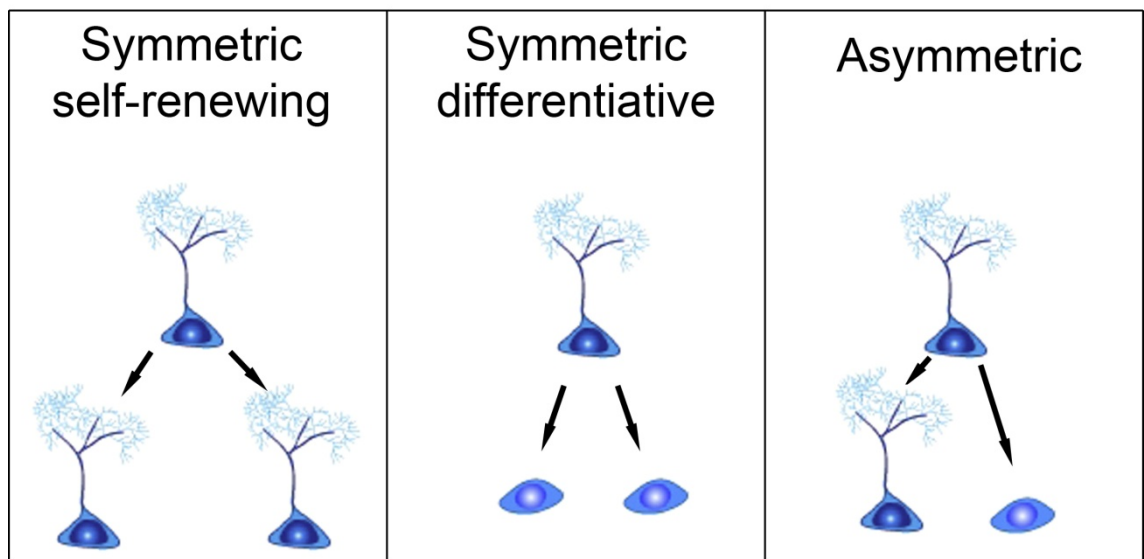


Figure 49 - Schematic diagram of the fate decisions of adult neural stem cells. **a**, *In vivo* clonal analysis has shown that neural stem cells (NSCs) can self-renew, differentiate into astroglia, or form precursor cells capable of expanding their population and differentiating into neurons. **b**, NSCs are capable of undergoing different types of division. Symmetric self-renewing divisions amplify the population of NSCs at the expense of forming differentiated cell types. Conversely, symmetric differentiative divisions lead to an increase in the progenitor pool but also lead to a depletion of the NSC pool. Asymmetric cell divisions allow for the maintenance of the NSC pool as well as the production of differentiated cell types. Adapted from [196].

6.2. CHD7 is expressed in transit amplifying cells in the subgranular zone

To first determine if *Chd7* was expressed in the hippocampus, *in situ* hybridisation using an anti-sense *Chd7* probe was performed on coronal sections of adult WT (CD1 mouse strain) brains. *Chd7* was expressed in the SGZ of the dentate gyrus (DG) where NSCs and progenitors reside (**Figure 50a**). This result was confirmed by antibody staining (**Figure 50b**). Of note, the expression of CHD7 was much lower in the SGZ than in the SVZ as determined by immunofluorescence intensity (data not shown).

To determine which cell types in the SGZ express CHD7, a series of co-localisation experiments were performed by staining hippocampal sections of adult WT mice with antibodies raised against CHD7 and various markers of cells in the neurogenic lineage (see **Figure 9**). NSCs in the SGZ can be readily identified based on GFAP immunoreactivity and the presence of GFAP⁺ processes extending through the granular layer of the DG. CHD7 was not detected in any GFAP⁺ NSCs in the SGZ (**Figure 51a-c**). Sox2 is a marker of NSCs and transit amplifying progeny (type 1 and type 2 cells; see **Figure 9**). CHD7 was expressed in 6% of Sox2⁺ cells (**Figure 51d,e**). However, the majority of cells which expressed CHD7 also expressed Sox2, meaning that most CHD7⁺ cells are Sox2⁺ (**Figure 51d,f**). MASH1 is a marker of type 2a cells (see **Figure 9**). CHD7 was expressed by around half of all MASH1⁺ cells in the SGZ (**Figure 51g,h**), but almost all cells which expressed CHD7 also expressed

MASH1 (**Figure 51g,i**). Therefore, most CHD7⁺ cells are Sox2⁺MASH1⁺, suggesting that CHD7 is present in transit amplifying type 2a cells (**Figure 52**). Furthermore, CHD7 was not detected in mature NeuN⁺ granule neurons in the dentate gyrus (**Figure 51j-l**), suggesting that CHD7 is downregulated as SGZ cells differentiate. Due to the low expression of CHD7 in the SGZ I have not yet analysed the expression of CHD7 in proliferating cells and type 3 cells. However, my data suggests that CHD7 will be expressed in proliferating cells since CHD7 is expressed in MASH1⁺ cells which are proliferative, and may be expressed in type 3 cells but at lower levels similar to in the SVZ (see **Figure 41**).

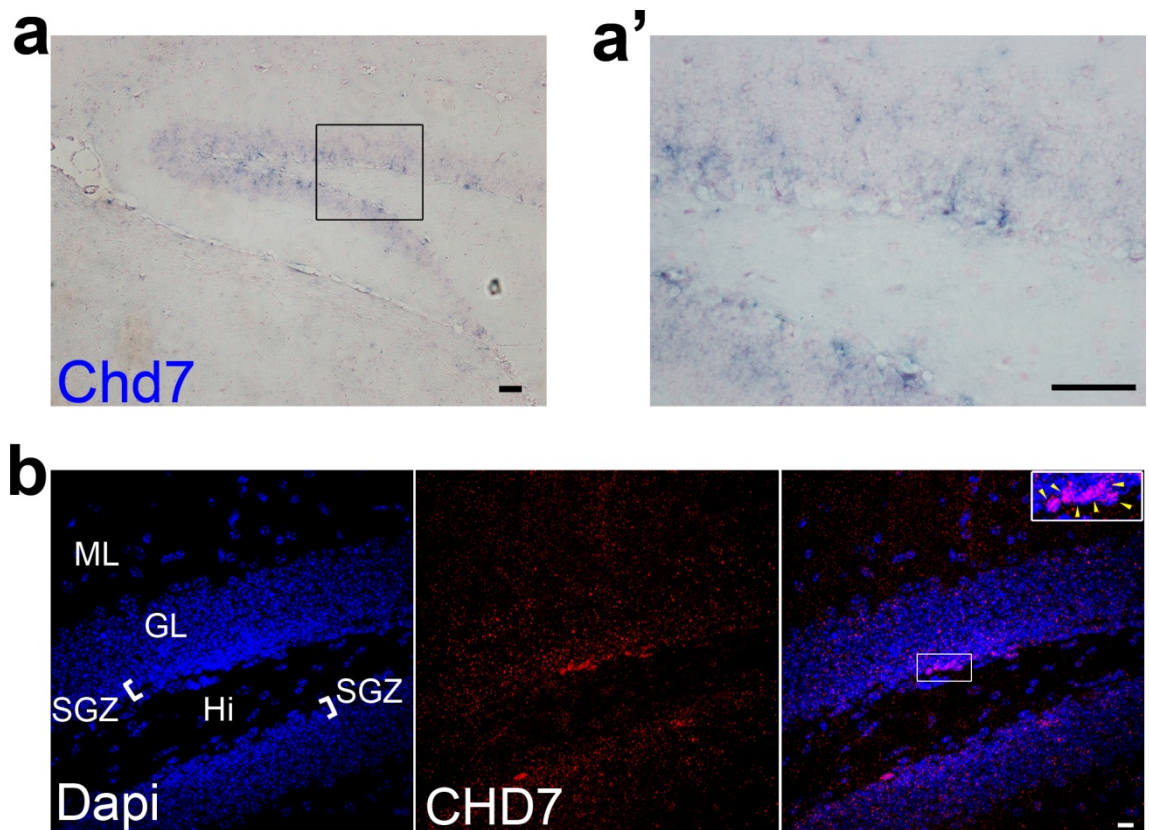


Figure 50 - CHD7 is expressed in the subgranular zone of the dentate gyurs. a, *In situ* hybridisation using an anti-sense *Chd7* probe (blue) in the SVZ. The boxed area is enlarged in **a'. Scale bars, 50 μ m. **b**, Coronal adult DG section stained with an anti-CHD7 antibody and Dapi. The boxed area is enlarged in the far right panel. Yellow arrow heads show CHD7⁺ cells with clear nuclear staining. SGZ, subgranular zone; Hi, hilus; GL, granular layer; ML, molecular layer. Scale bar, 20 μ m.**

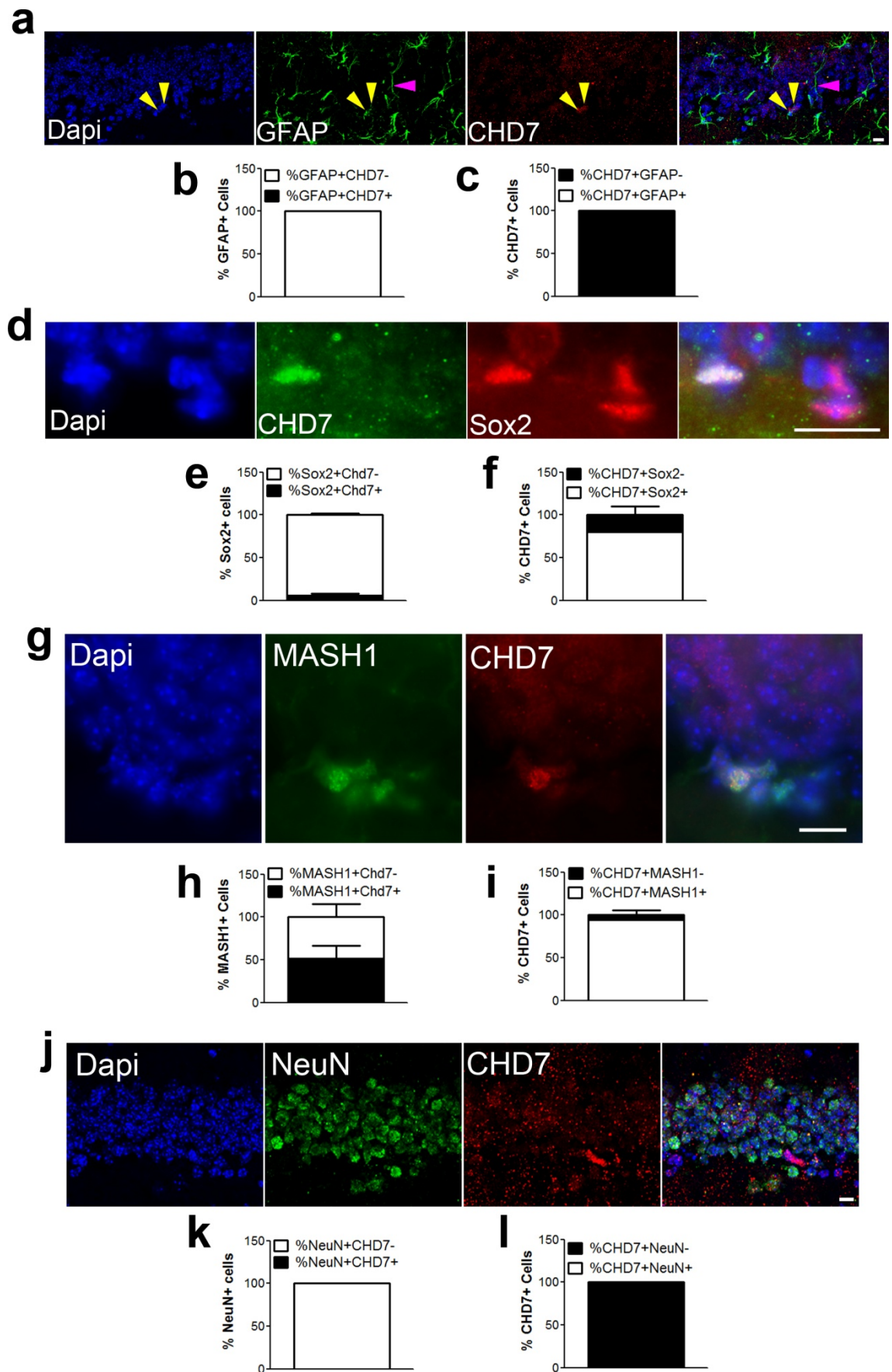


Figure 51 - CHD7 is expressed by a subset of type 2a cells. **a**, Representative image of dentate gyrus sections stained with antibodies raised against CHD7 and GFAP, Sox2 (**d**), MASH1 (**g**), and NeuN (**j**). Yellow arrow heads show CHD7⁺GFAP⁻ cells, purple arrow head shows a likely NSC with a GFAP⁺ process protruding through the granular layer of the dentate gyrus. A lower magnification image of (**a**) compared to other pictures was chosen to show GFAP⁺ processes through the dentate gyrus. Scale bars, 20µm. **b**, Quantification of the percentage of GFAP⁺, Sox2⁺ (**e**), MASH1⁺ (**h**) and NeuN⁺ (**k**) cells that also express CHD7. **c**, Quantification of the percentage of CHD7⁺ cells that also express GFAP, Sox2 (**f**), MASH1 (**h**) and NeuN (**l**). n = 100-150 cells analysed by confocal microscope. All data represented as mean ± s.e.m.

6: Results Part IV

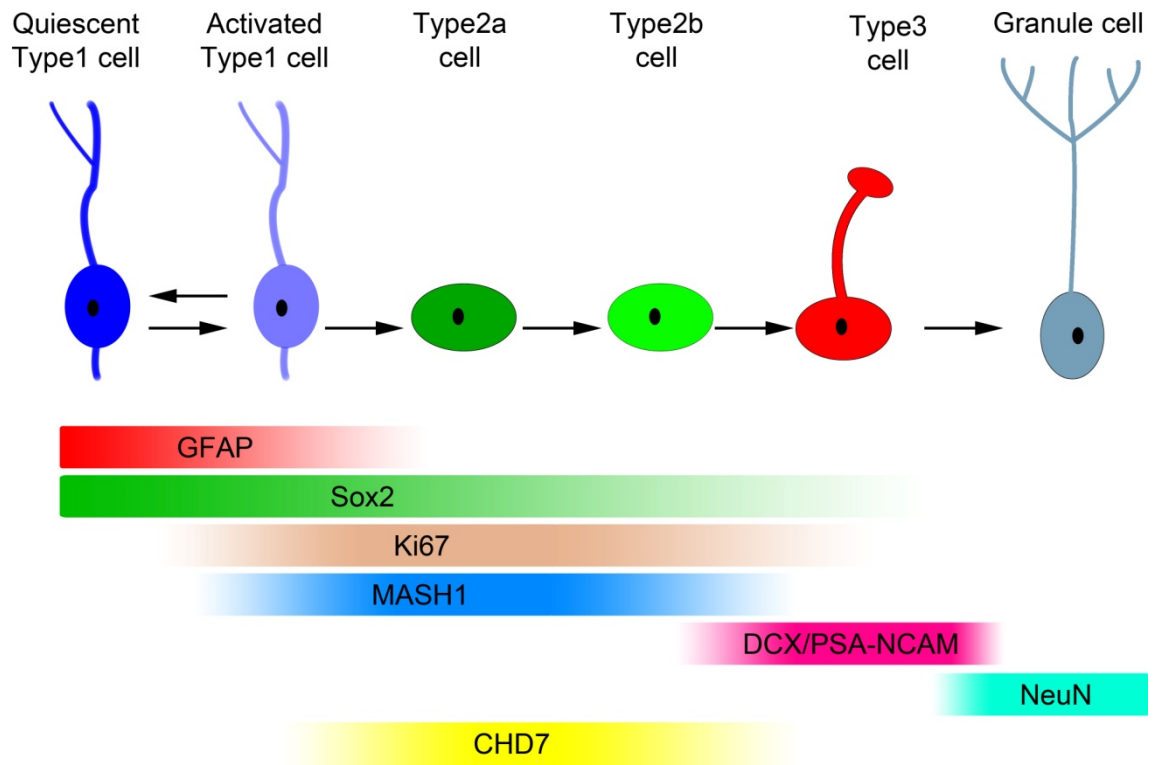


Figure 52 - Schematic of CHD7 expression in the dentate gyrus. CHD7 is expressed in a subset of type 2a cells.

6.3. The GLAST::CreERT2;Chd7^{ff} mouse line allows for efficient deletion of *Chd7* in the dentate gyrus

I have shown that CHD7 is expressed by transit amplifying cells in the SGZ (see **Figure 52**) and therefore CHD7 likely plays a role in hippocampal neurogenesis. To determine if CHD7 is an essential regulator of adult hippocampal neurogenesis, I sought to delete *Chd7* specifically from adult NSCs using a GLAST::CreERT2 mouse line [253]. GLAST is expressed by NSCs and astrocytes and so upon tamoxifen injection Cre-mediated recombination should only take place in NSCs [253]. To first determine its efficiency in the DG, the GLAST::CreERT2 line was crossed to a RYFP reporter line to generate GLAST::CreERT2;RYFP/+ mice. Adult GLAST::CreERT2;RYFP/+ mice were given 5 injections of tamoxifen to induce recombination and expression of YFP and sacrificed 7 days and 28 days after the last tamoxifen injection (**Figure 53a**). Sections of the SVZ were stained with antibodies raised against GFP along with GFAP to label NSCs (**Figure 53c,d**). 7 days after the last tamoxifen injection 86% of radial GFAP⁺ cells were YFP⁺, showing efficient recombination in NSCs (**Figure 53b**). Additionally, some YFP⁺ cells which were not GFAP⁺ were observed, and these are presumably NSC progeny (**Figure 53c**). 28 days after the last tamoxifen injection, YFP⁺ cells in the granular layer (GL) of the DG were visible (**Figure 53d**). As cells born in the SGZ differentiate they migrate to deeper layers of the granular layer, and so YFP⁺ cells in the GL are presumably new neurons formed from NSCs. Furthermore, at this time point many GFAP⁺ cells were still YFP⁺, showing that recombination is stable (**Figure 53d**). Therefore, my tamoxifen injection regime in GLAST::CreERT2 mice results in efficient recombination in SGZ cells.

To delete *Chd7* specifically from adult NSCs, GLAST::CreERT2 mice were crossed with Chd7^{ff} mice to generate a GLAST::CreERT2;Chd7^{ff} mouse line (see **Figure 45a**). Tamoxifen injection causes Cre-mediated recombination and the formation of a truncated, non-functional CHD7 protein specifically in NSCs and astrocytes (Chd7null). To test if the deletion of *Chd7* was efficient, the DG of GLAST::CreERT2;Chd7^{ff} (Chd7null) and Cre-negative control mice (WT) was

stained with antibodies raised against CHD7 and the number of CHD7⁺ cells was counted 1 week and 4 weeks after tamoxifen administration. Hardly any CHD7⁺ cells were detected in the DG of *Chd7* null mice both 1 weeks and 4 weeks after *Chd7* deletion, indicating that deletion of *Chd7* was efficient (**Figure 54a-d**). Therefore using the GLAST::CreERT2;*Chd7*^{f/f} mouse line allows for efficient deletion of *Chd7* and recombination in a large portion of NSCs.

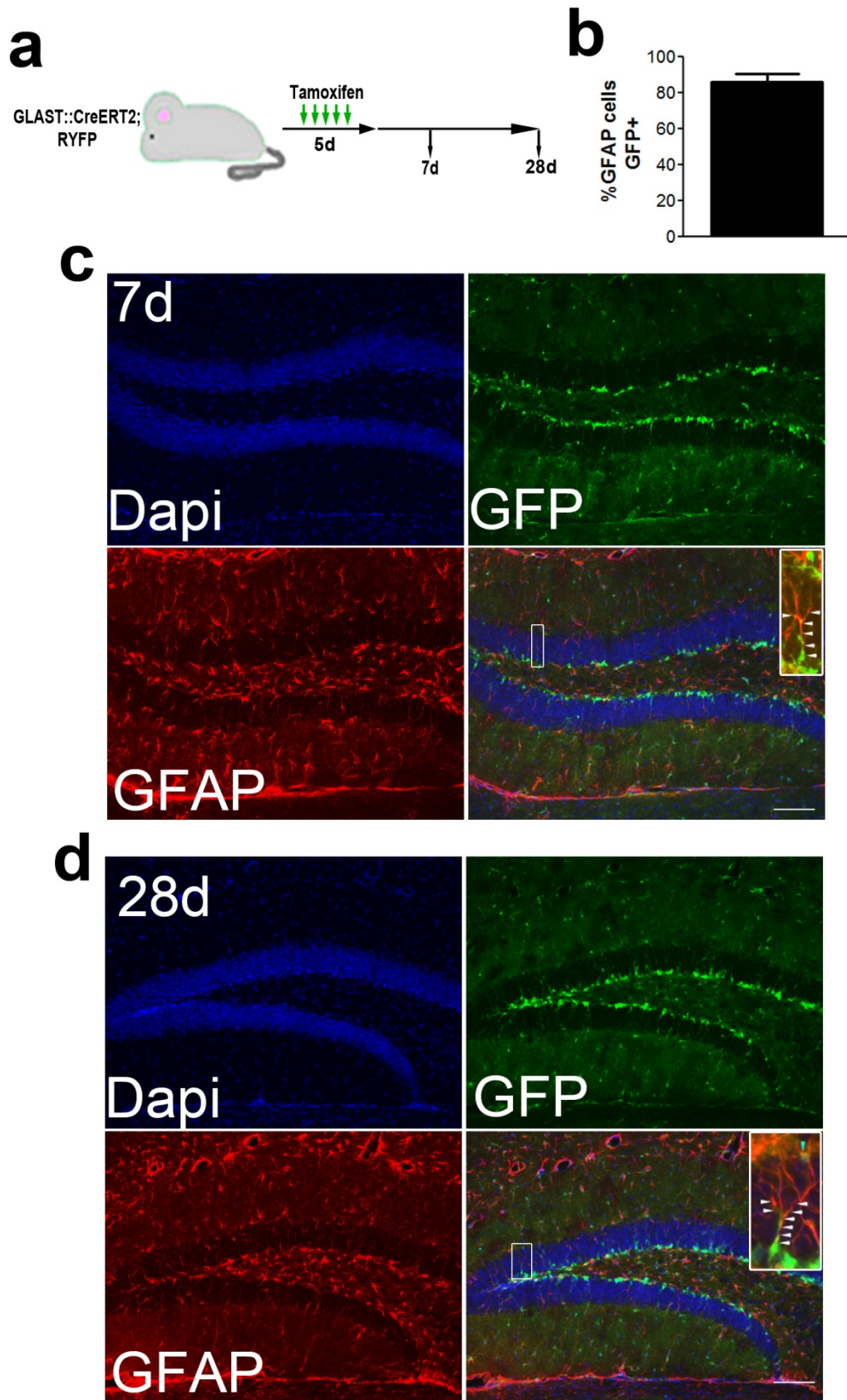


Figure 53 - Efficient recombination in the dentate gyrus of GLAST::CreERT2 mice. a, Schematic of the experimental strategy to induce recombination and YFP expression in SGZ NSCs. Adult GLAST::CreERT2;RYFP mice were given one injection of 80mg/kg tamoxifen a day for 5 days and sacrificed either 7 days or 28 days after the last tamoxifen injection. **b,** Quantification of the percentage of radial GFAP⁺ cells that were also GFP⁺ in the SGZ. At least 90 GFAP⁺ cells were counted. n=2 animals. Data represented as mean \pm s.e.m. **c,** Representative image of a coronal section of the dentate gyrus of GLAST::CreERT2;RYFP mice 7 days or 28 days **(d)** after tamoxifen injection stained with antibodies raised against GFP and GFAP. GFP antibodies recognise YFP protein. White arrow heads show GFAP⁺GFP⁺ astrocytic processes. Note the large overlap between GFAP and GFP. Also note the presence of YFP⁺ cells in the granular cell layer (light blue arrow head which is GFAP⁺) in **(c)**, indicating that recombined NSCs have produced new mature neurons. Scale bar, 100 μ m. n=2 animals / condition.

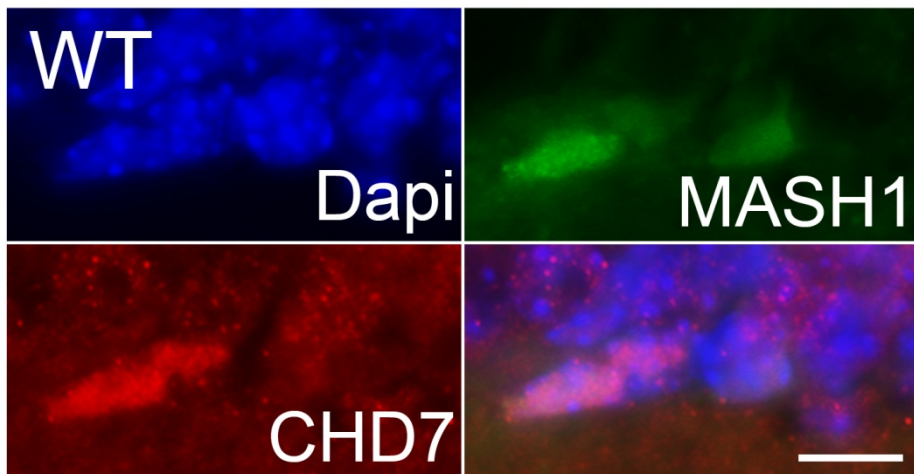
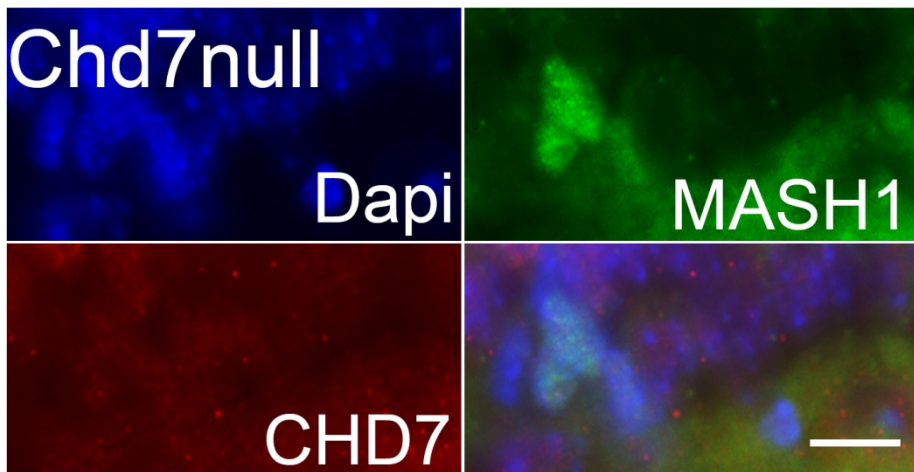
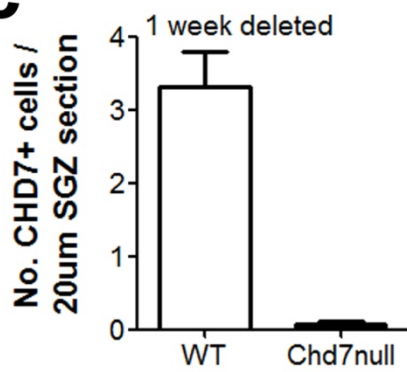
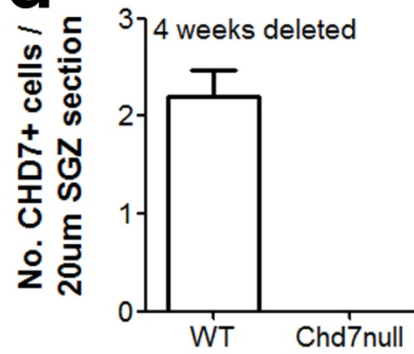
a**b****c****d**

Figure 54 - The GLAST::CreERT2;Chd7^{ff} mouse line allows for efficient deletion of Chd7.

a, Representative image of a section of the SGZ stained with antibodies raised against CHD7 and MASH1 in WT and Chd7null **(b)** adult brains 4 weeks after tamoxifen administration.

Sections were stained with antibodies raised against MASH1 to fully identify CHD7⁺ cells since the majority of CHD7⁺ cells also express MASH1. **c**, Quantification of the number of CHD7⁺ cells in the SGZ of WT and Chd7null mice 1 week and 4 weeks **(d)** after the last tamoxifen injection. n=2-4 animals / condition. All data represented as mean ± s.e.m.

6.4. Loss of *Chd7* in neural stem cells causes a reduction in neurogenesis

CHD7 is expressed in neurogenic SGZ cells and so I hypothesised that CHD7 likely plays a role in hippocampal neurogenesis. To analyse the effect of loss of *Chd7* on hippocampal neurogenesis, GLAST::CreERT2;Chd7^{ff} (Chd7null) and Cre-negative control mice (WT) were treated with tamoxifen and sacrificed 12 weeks later (**Figure 55a**). Sections of the hippocampus were stained with antibodies raised against DCX to label immature neurons (type 3 cells). Chd7null mice displayed a 45% reduction in the number of immature neurons in the DG compared to WT (**Figure 55b,c**), showing that CHD7 is a critical regulator of neurogenesis. A decrease in neurogenesis could be due to impaired differentiation of neuronal progenitors or impaired proliferation of cells in the SGZ. To determine if proliferation in the SGZ was altered after loss of *Chd7*, Chd7null and WT mice were treated with tamoxifen and sacrificed 12 weeks later. BrdU was injected 24 hours before sacrifice to label proliferating cells (**Figure 55a**). A 24 hour BrdU pulse labels the majority of progenitors without labelling a significant number of neurons [228]. Despite a large decrease in neurogenesis, the number of proliferating cells (BrdU⁺ or PCNA⁺) in the SGZ was not altered (**Figure 55d,e**). These data suggest that the formation and/or survival of DCX⁺ type 3 cells is impaired. Alternatively, it is possible that CHD7 may regulate DCX expression, and loss of *Chd7* results in the inability of cells to express DCX. This will be addressed in **Section 6.5**.

To determine if the formation of new mature neurons is affected after loss of *Chd7*, adult GLAST::CreERT2;Chd7^{ff} (Chd7null) and Cre-negative control (WT)

mice were injected with tamoxifen and sacrificed 11 weeks later, giving BrdU in their drinking water for the last 3 weeks of life to label newly born cells (**Figure 55f**). The number of newborn cells (BrdU⁺) in the DG was reduced by 55% in Chd7null mice (**Figure 55h**), showing that the formation of new cells is impaired in Chd7null mice. To fully determine if the formation of new neurons was impaired, sections of the DG of Chd7null and WT mice were stained with antibodies raised against BrdU and NeuN. Any cells which are BrdU⁺NeuN⁺ cells are new granule neurons [228]. The percentage of newly formed cells that were mature neurons (%BrdU⁺NeuN⁺) was reduced by 33% (**Figure 55g,i**). These data show that the production of newborn cells is decreased in Chd7null mice, and the percentage of newly formed cells that become neurons is adversely affected by the loss of *Chd7*.

A decrease in the percentage of newly formed cells that become neurons could be due to:

1. An increase in apoptosis (see **Section 6.11.6.**)
2. A delay or block in neurogenesis (see **Section 6.6.**)
3. Decreased expansions of neural progenitors (see **Section 6.5.**)
4. A fate change of SGZ cells (see **Section 6.8.**)

These possibilities will be discussed in the following sections.

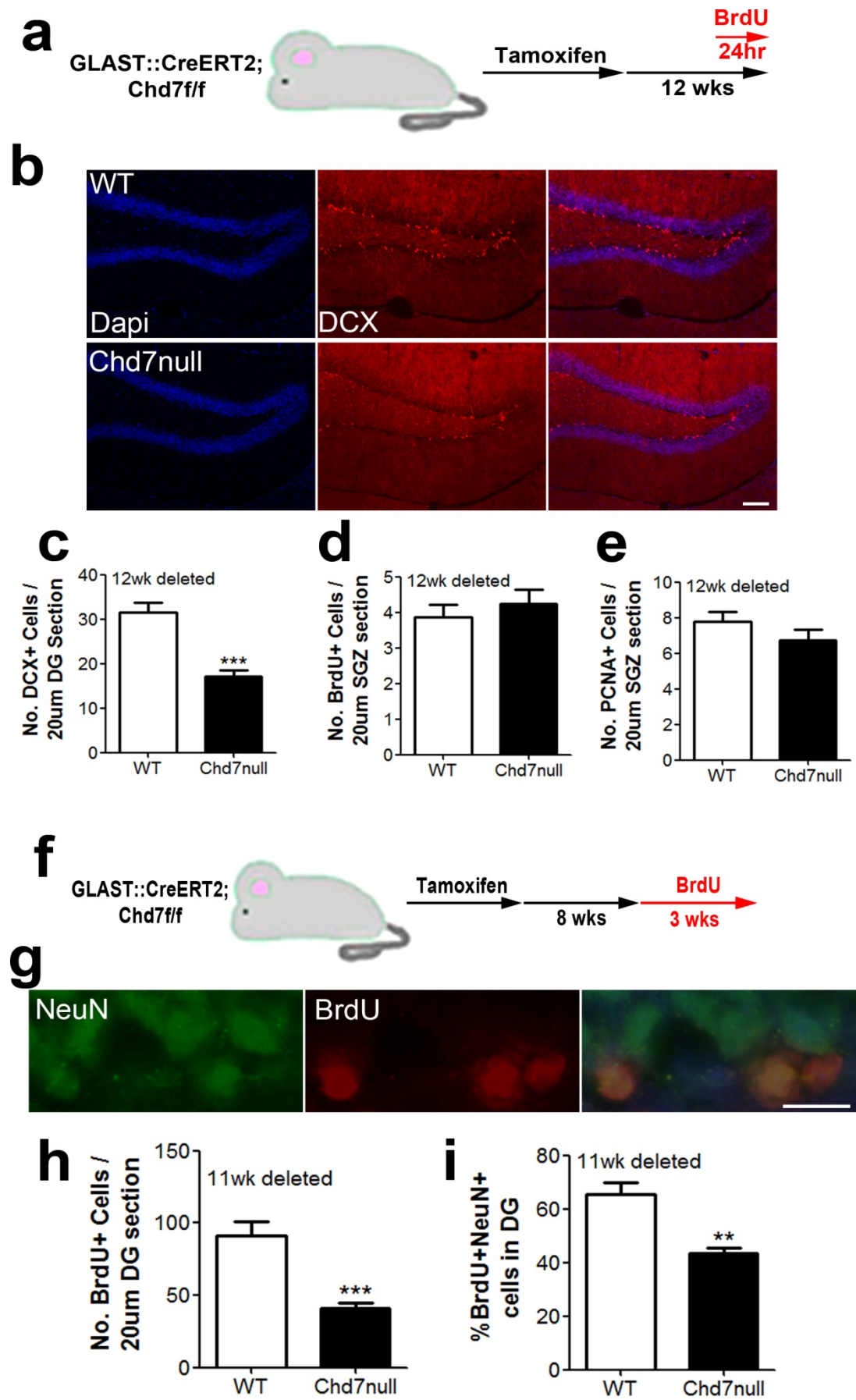


Figure 55 - *Chd7* regulates adult hippocampal neurogenesis. **a**, Schematic diagram of the experimental strategy to delete *Chd7* from adult NSCs for 12 weeks (long-term) and label proliferating cells by injecting BrdU 24 hours prior to sacrifice. **b**, Representative image of a section of the DG of GLAST::CreERT2;*Chd7*^{ff} mice treated with tamoxifen (*Chd7*null) and Cre-negative controls (WT) stained with antibodies raised against DCX. Scale bar, 100µm. **c**, Quantification of the number of DCX⁺ cells in the DG of *Chd7*null and WT mice per 20µm section. n=4 animals / condition. **d**, Quantification of the number of BrdU⁺ and PCNA⁺ (**e**) cells in the SGZ of *Chd7*null and WT mice per 20µm section. n=4 animals / condition. **f**, Schematic diagram of the experimental strategy to delete *Chd7* from adult NSCs and label newly born cells by administering BrdU in the drinking water of mice. **g**, Representative image of a section of the DG stained with antibodies raised against BrdU and NeuN. Scale bar, 20µm. **h**, Quantification of the number of BrdU⁺ cells and the percentage of BrdU⁺ cells that were NeuN⁺ (**i**) in the DG of *Chd7*null and WT mice per 20µm section. n=2 animals / condition. All data represented as mean ± s.e.m.; **P<0.01 ***P<0.001 student's t test.

6.5. Loss of *Chd7* leads to a transient increase in neurogenesis

I have shown that the loss of *Chd7* in NSCs leads to a decrease in the number of immature neurons in the dentate gyrus (see **Figure 55c**). One possible explanation is that the decrease in the number of DCX⁺ cells formed may indicate that CHD7 regulates DCX expression. Hence, a loss of *Chd7* expression would cause a loss of DCX⁺ cells. To test this, adult GLAST::CreERT2;*Chd7*^{ff} (*Chd7*null) and Cre-negative control (WT) mice were injected with tamoxifen and sacrificed 1 week later to determine if impaired DCX expression was a primary defect caused by the loss of *Chd7* (**Figure 56a**). At this time point there was no change in the number of DCX⁺ immature neurons in *Chd7*null mice compared to WT (**Figure 56b**), suggesting that the expression of DCX and formation of immature neurons is not impaired after the loss of *Chd7*. However, it could be argued that at this time point, only a very small percentage of recombined NSCs would not have formed type 3 cells, and so this is why no effect on immature neurons is seen in *Chd7*null cells [228]. To address this point, adult *Chd7*null and WT mice were injected with tamoxifen and sacrificed 4 weeks later (**Figure 56c**). At this time point many NSCs should have formed type 3 cells [228]. Furthermore, 4 weeks after tamoxifen injection in GLAST::CreERT2;RYFP/+ mice I have shown that recombined cells can be

observed in the granular layer of the DG, indicating that some SGZ NSCs have formed new mature neurons (see **Figure 53c**). Therefore, if CHD7 regulates the expression of DCX, abnormalities should be seen 4 weeks after *Chd7* deletion. Interestingly, 4 weeks after *Chd7* deletion, there was an increase in the number of DCX⁺ immature neurons (**Figure 56d**), showing that loss of *Chd7* does not lead to a loss of DCX⁺ cells. Collectively, these data show that loss of *Chd7* in NSCs leads to a transient increase in neurogenesis followed by a large decline in new neuron formation. This transient increase in neurogenesis could be explained by an increase in the number of progenitors in the SGZ, or by an increase in NSC proliferation leading to a general increase in formation of more DCX⁺ cells, or by a decrease in the apoptosis of DCX⁺ cells, or by a block in the differentiation of immature neurons. To determine if the number of progenitors was altered in the SGZ, adult *Chd7*null and WT mice were injected with tamoxifen and sacrificed 4 weeks later (**Figure 56c**). DG sections of *Chd7*null and WT mice were stained with antibodies raised against the transit amplifying type 2a cell type MASH1. Four weeks after loss of *Chd7* there was no change in the number of type 2a cells in the SGZ (**Figure 56f**), suggesting that the transient increase in neurogenesis was not due to an increase in the number of progenitors. These data also argue that the eventual loss in neurogenesis seen in *Chd7*null cells is not due to an impaired expansion of immature progenitors, since the number of MASH1⁺ cells is not altered.

A transient increase in neurogenesis due to a decrease in apoptosis seems unlikely as the loss of *Chd7* eventually leads to the depletion of DCX⁺ cells and a decreased number of newly born cells forming neurons, which may imply that there is possibly an increase in apoptosis at this time point. However, this will need further investigation (see **Section 6.11.6**).

Lastly, the hypothesis that an increase in NSC proliferation may lead to a transient increase in neurogenesis will be discussed in **Section 6.7**.

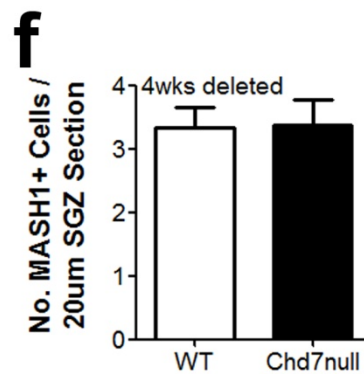
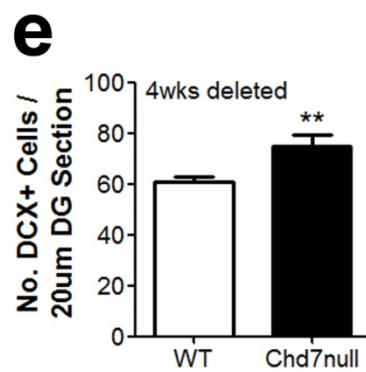
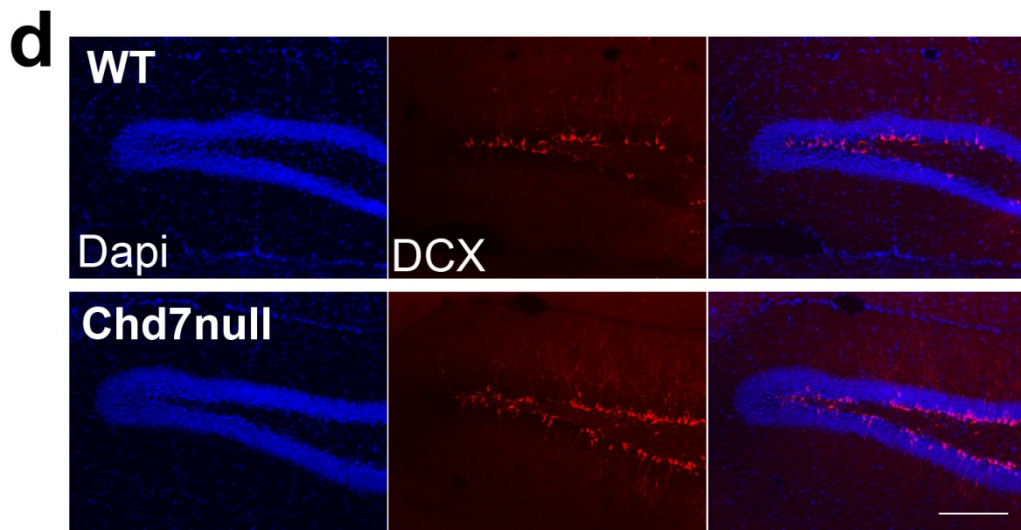
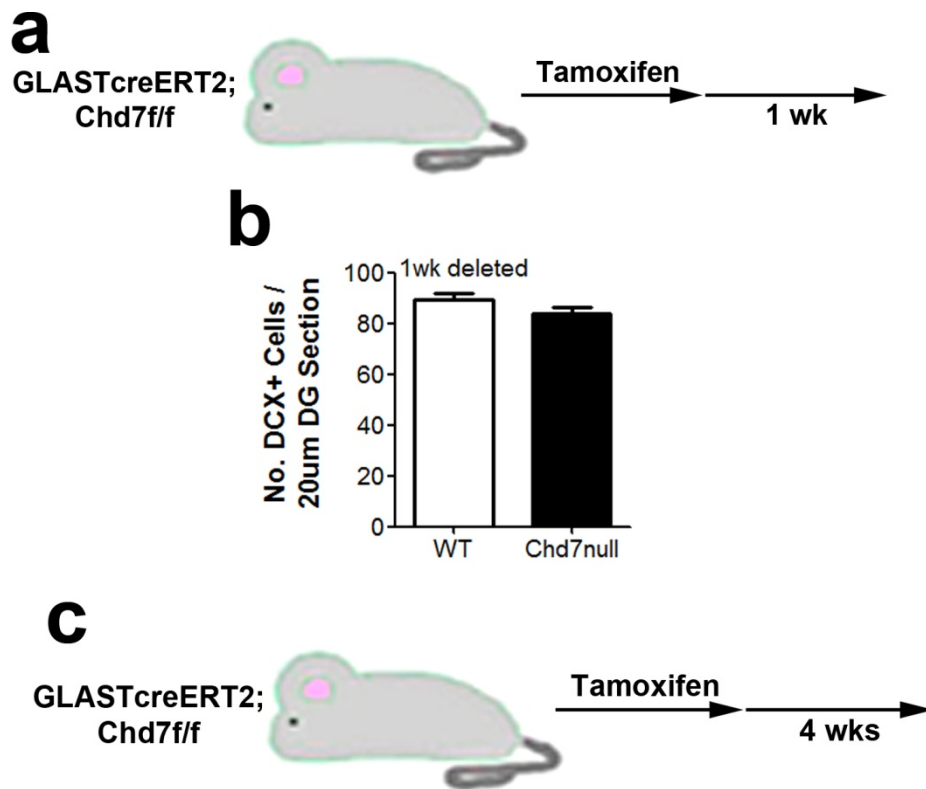


Figure 56 - Loss of *Chd7* results in a transient increase in neurogenesis. **a**, Schematic of the experimental strategy to delete *Chd7* from adult NSCs for 1 week (short-term). **b**, Quantification of the number of DCX⁺ cells in the DG of *Chd7* null and WT mice 1 week after the last tamoxifen injection per 20µm section. n=4 animals / condition. **c**, Schematic of the experimental strategy to delete *Chd7* from adult NSCs for 4 weeks (mid-term) and label proliferating cells by injecting BrdU 24 hours prior to sacrifice. **d**, Representative image of a section of the DG of GLAST::CreERT2;*Chd7*^{fl/fl} mice treated with tamoxifen (*Chd7* null) and Cre-negative controls (WT) 4 weeks after the last tamoxifen injection stained with antibodies raised against DCX. Scale bar, 100µm. **e**, Quantification of the number of DCX⁺ cells in the DG of *Chd7* null and WT mice per 20µm section. n=4 animals / condition. **f**, Quantification of the number of BrdU⁺ cells in the SGZ of *Chd7* null and WT mice 4 weeks after the last tamoxifen injection per 20µm section. n=4 animals / condition. **g**, Quantification of the number of MASH1⁺ cells in the DG of *Chd7* null and WT mice 4 weeks after the last tamoxifen injection per 20µm section. n=4 animals / condition. All data represented as mean ± s.e.m.; **P<0.01 student's t test.

6.6. Loss of *Chd7* impairs mature neuron formation

I have shown that the loss of *Chd7* lead to a transient increase in immature neuron formation followed by a large decline in neurogenesis. The data so far suggest that a block in neuronal differentiation occurs when immature neurons proceed to full maturation. To further confirm this I employed the use of an *in vitro* model of NSCs which allows for the analysis of cell proliferation and differentiation in defined conditions [365]. Cultured NSCs are therefore a good model for analysing if CHD7 is an essential regulator of neurogenesis. To obtain this cell line, foetal NSCs from the cortex and striatum of E16.5 NestinCre;*Chd7*^{δ/δ} (*Chd7* null) and Cre-negative embryos (WT) were isolated and cultured to form foetal-derived NSCs. These cells retain multi-lineage differentiation capacity after prolonged expansion [364] and give a high yield of neurons when put under certain conditions [365]. To determine if *Chd7* was expressed by cells in growth conditions and under differentiation conditions, RNA was extracted from *Chd7* null and WT cells and RT-qPCR for *Chd7* was performed. *Chd7* expression was upregulated as cells were put into differentiation conditions and expression was then downregulated as cells differentiated further (**Figure 57a**). These data show that in this *in vitro* culture

system, *Chd7* is expressed in more neuronally committed cells, which is consistent with *Chd7* being expressed in neuronally-committed type 2a cells *in vivo* (see **Figure 52**). These data suggest that the expression of *Chd7* in the *in vitro* culture of NSCs reflect that seen *in vivo*. Importantly, the expression of *Chd7* was completely absent in *Chd7*null cells (**Figure 57a**). To confirm that CHD7 protein expression was absent in *Chd7*null cells, a western blot of CHD7 in total cell lysates of *Chd7*null and WT cells after being placed in neuronal differentiation conditions for 3 days (where expression of *Chd7* was at its greatest) was performed. CHD7 protein was completely absent from *Chd7*null cells (**Figure 57b**), confirming that these mutant cells do not express CHD7.

To confirm that CHD7 is an essential regulator of neurogenesis, *Chd7*null and WT cells in growth medium, neuronal differentiation conditions for 3 days, or neuronal differentiation conditions for 6 days were stained using antibodies raised against the mature neuron marker MAP2. *Chd7*null cells displayed a decreased tendency to form mature neurons compared to WT cells (**Figure 57c**), showing that CHD7 regulates mature neuron formation.

I have previously shown that loss of *Chd7* results in a transient increase in neurogenesis and I have suggested that loss of *Chd7* expression leads to an inability of immature neurons to fully mature. To test this *in vitro*, *Chd7*null and WT cells in growth medium, neuronal differentiation conditions for 3 days, or neuronal differentiation conditions for 6 days were stained using antibodies raised against the immature neuron marker DCX. *Chd7*null cells displayed a large increase in the number of DCX⁺ cells (**Figure 57d,e**). These data show that loss of *Chd7* does not negatively affect DCX expression. Instead, these data suggest that impaired neurogenesis in *Chd7*null cells is a result of immature neurons being unable to fully differentiate. The block in the differentiation of DCX⁺ cells may lead to their accumulation before an increase in apoptosis leads to a decline in DCX⁺ cells

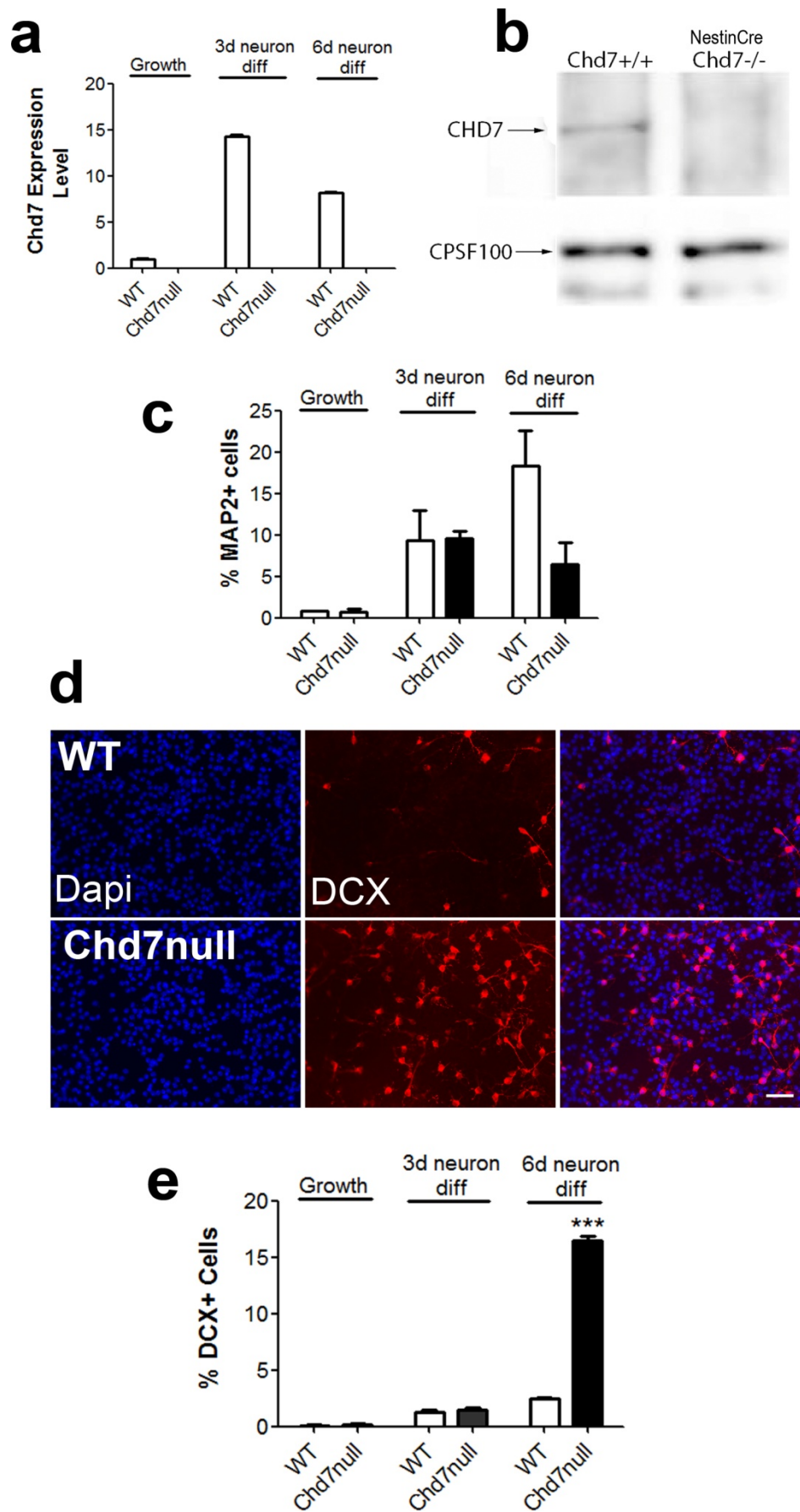


Figure 57 - CHD7 is essential for neurogenesis in vitro. **a**, RT-qPCR expression level of *Chd7* from cultured foetal-derived NSCs from NestinCre;*Chd7*^{Δ/Δ} (*Chd7*null) and Cre-negative (WT) E16.5 embryos under growth conditions (Growth), differentiation conditions for 3 days (3d neuron diff) and 6 days (6d neuron diff) relative to WT. Note *Chd7* expression is completely absent from *Chd7*null cells. n = 2 cultures performed in duplicate. **b**, Western blot for CHD7 on total cell lysates of cultured foetal-derived NSCs from *Chd7*null (NestinCre *Chd7*^{-/-}) and WT (*Chd7*^{+/+}) cells under differentiation conditions for 3 days. Cleavage and polyadenylation specificity factor 100 (CPSF100) was used as a loading control. **c**, Quantification of the number of MAP2⁺ mature neurons formed from *Chd7*null and WT cells under growth conditions (Growth), differentiation conditions for 3 days (3d neuron diff) and 6 days (6d neuron diff). n = 2 cultures performed in duplicate. **d**, Representative image of cultured foetal-derived NSCs from *Chd7*null and WT E16.5 embryos under differentiation conditions for 6 days stained with antibodies raised against DCX. Scale bar, 50μm. **e**, Quantification of the number of DCX⁺ immature neurons formed from *Chd7*null and WT cells under growth conditions (Growth), differentiation conditions for 3 days (3d neuron diff) and 6 days (6d neuron diff). n = 2 cultures performed in duplicate. All data represented as mean ± s.e.m.; ***P<0.001 student's t test.

6.7. CHD7 regulates neural stem cell quiescence

I have shown that CHD7 is a critical regulator of adult neurogenesis. Loss of *Chd7* leads to a transient increase in neurogenesis followed by a large decline in neuron formation. I have shown that the number of MASH1⁺ cells is unaffected after the loss of *Chd7* (see **Figure 56f**), suggesting that changes in progenitor number are not the cause of the transient increase in the number of DCX⁺ cells. I have suggested that the accumulation of DCX⁺ cells may be due to a block in differentiation before their numbers are reduced by an increase in apoptosis. One remaining possibility for the transient increase in neurogenesis is that an increase in NSC proliferation may cause an increase in the number of immature neurons formed. To first determine if the numbers of proliferating cells was altered shortly after loss of *Chd7*, adult GLAST::CreERT2;*Chd7*^{fl/fl} (*Chd7*null) and Cre-negative control (WT) mice were injected with tamoxifen and sacrificed 1 week later. BrdU was injected 24 hours before sacrifice to label proliferating cells (**Figure 58a**). The number of proliferating cells (BrdU⁺) was over 2-fold greater in the SGZ of *Chd7*null mice compared to WT (**Figure 58b,c**). These data show that loss of *Chd7* initially causes an increase in the

number of proliferating cells in the SGZ. To determine if an increase in proliferation in the SGZ leads to an alteration in the total number of NSCs and progenitors after a short-term deletion of *Chd7*, sections of the DG were stained with antibodies raised against Sox2 to label type1 and type2 cells. There was no change in the number of Sox2⁺ cells in *Chd7*null mice compared to WT (**Figure 58d**). These data suggest that the total number of NSCs and progenitors was not altered, meaning that the increase in the proliferation of SGZ cells was not due to changes in the cellular composition of the niche. However, analysing the number of NSCs and progenitors separately is needed to fully conclude if there is a change in these cell populations. Collectively, these results show that loss of *Chd7* initially affects proliferation in the SGZ.

An increase in the number of proliferating cells in the SGZ could reflect a loss of NSC quiescence or an increase in progenitor proliferation. To determine which cell types are proliferating, DG sections of mice treated as in **Figure 58a** were stained with antibodies raised against BrdU, Sox2 and GFAP to determine the number of NSCs (GFAP⁺Sox2⁺ SGZ cells with a radial morphology) and progenitors (GFAP⁻Sox2⁺ SGZ cells) that had cycled in the 24 hour period (BrdU⁺; **Figure 59a**). The number of BrdU⁺ radial NSCs was over 2.5 fold greater in *Chd7*null mice compared to WT (**Figure 59b**). Interestingly, the number of cycling progenitors (GFAP⁻Sox2⁺) was no different between *Chd7*null and WT mice (**Figure 59c**), suggesting that the primary effect of loss of *Chd7* is a loss of NSC quiescence, with no effect on progenitor cycling. These data show that loss of *Chd7* in NSCs leads to a loss of NSC quiescence. Further experiments to investigate if there are any changes in the number of type 1 and type 2 cell populations separately at this stage will be useful in determining if a loss of NSC quiescence results in an increase in NSC number or progenitor number.

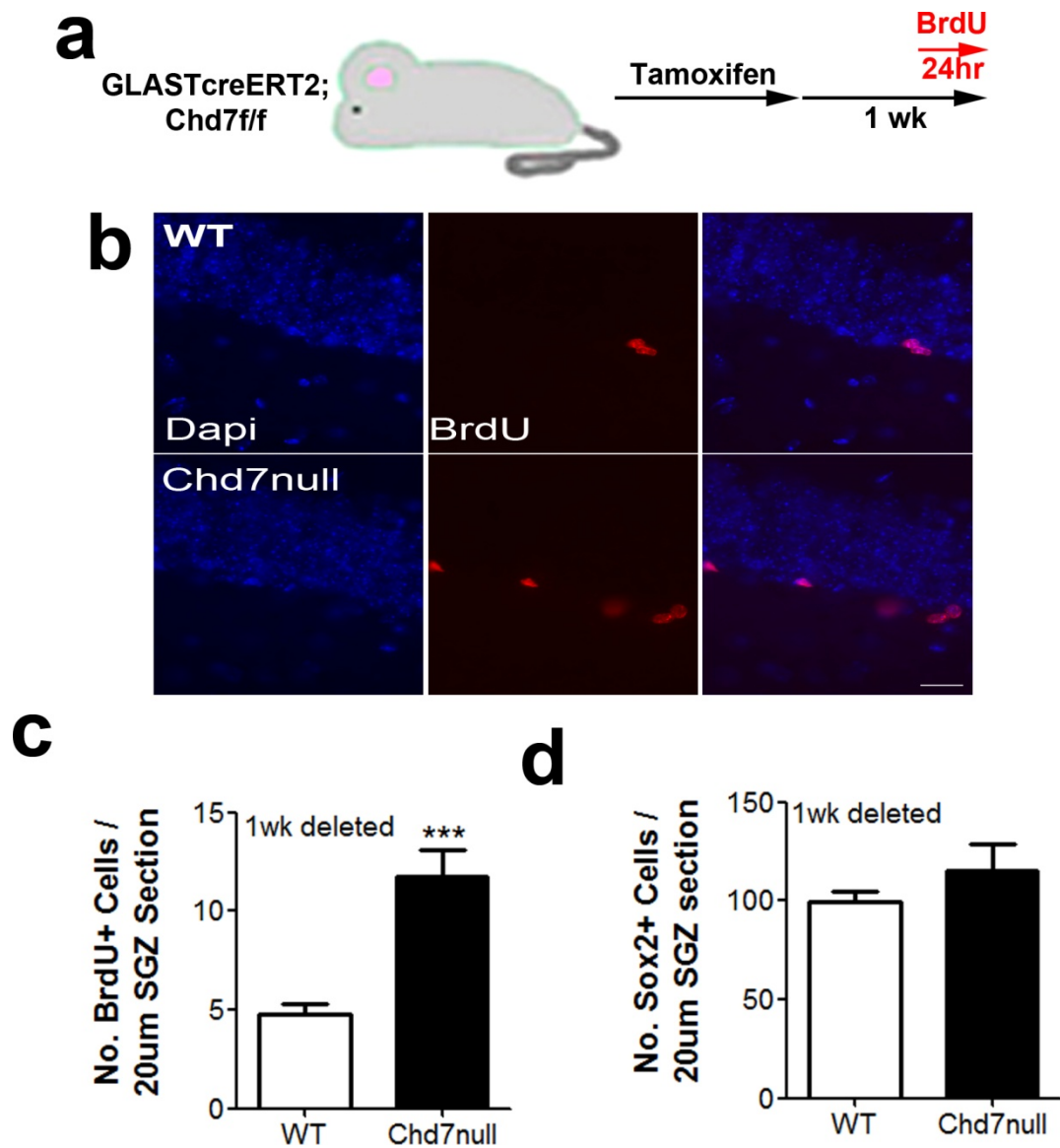


Figure 58 - Loss of *Chd7* initially results in increased subgranular zone proliferation. a, Schematic diagram of the experimental strategy to delete *Chd7* from adult NSCs for 1 week (short-term) and label proliferating cells by injecting BrdU 24 hours prior to sacrifice. **b,** Representative image of a section of the DG of GLAST::CreERT2;*Chd7*^{f/f} mice treated with tamoxifen (*Chd7*null) and Cre-negative controls (WT) stained with antibodies raised against BrdU. Scale bar, 20µm. **c,** Quantification of the total number of BrdU⁺ cells and Sox2⁺ cells (**d**) in the SGZ of *Chd7*null and WT mice per 20µm section. n=2-3 animals / condition. All data represented as mean ± s.e.m.; ***P<0.001 student's t test.

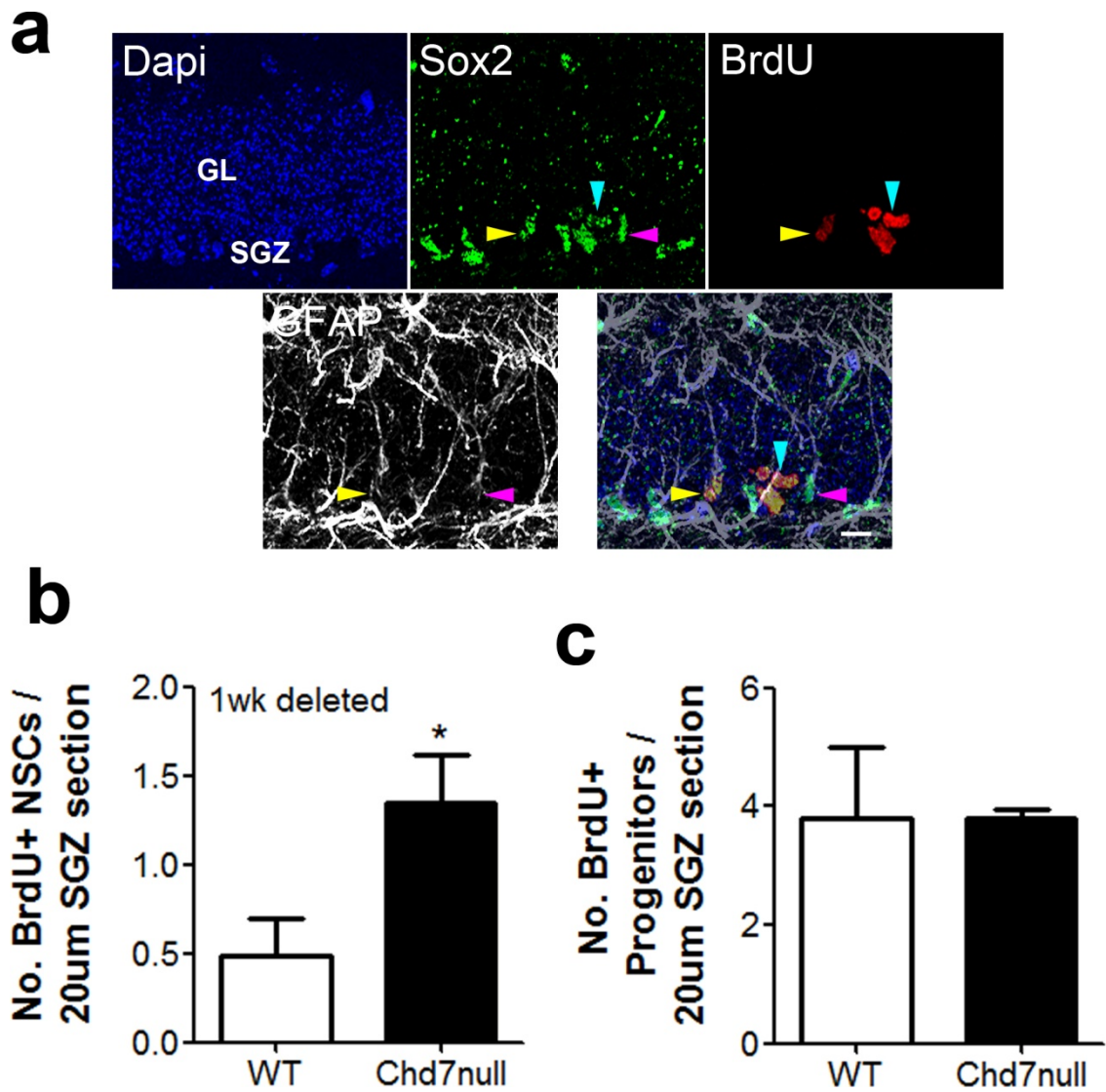


Figure 59 - CHD7 regulates neural stem cell quiescence. **a**, Representative image of a section of the DG stained with antibodies raised against BrdU, Sox2, and GFAP with Dapi. Yellow arrow heads shows a BrdU⁺ NSC (BrdU⁺Sox2⁺GFAP⁺ cells in the SGZ), purple arrow heads shows a BrdU⁻ NSCs, light blue arrow heads show a BrdU⁺ progenitor (BrdU⁺Sox2⁺GFAP⁻). Scale bar, 20 μ m. **b**, Quantification of the percentage of BrdU⁺ NSCs and progenitors (**c**) in the SGZ of Chd7null and WT mice. n=4 animals / condition. All data represented as mean \pm s.e.m.; *P<0.05 student's t test.

6.8. Loss of *Chd7* results in an increase in the number of neural stem cells

I have shown that the loss of *Chd7* in NSCs results in the loss of stem cell quiescence, followed by a transient increase in neurogenesis and then a large decrease in neurogenesis in the long-term. One remaining possibility for the eventual loss of neurogenesis and decreased tendency for SGZ to form neurons is that there may be a fate change of NSCs. For example, NSCs may have an increased tendency to self renew or form glial cells in *Chd7* null mice, and immature neurons may have an impaired differentiation capacity, leading to a transient increase in immature neuron formation and a decrease in mature neuron formation. Alternatively, loss of stem cell quiescence may lead to depletion of the NSC pool due to proliferative exhaustion and differentiation of NSCs [259, 393]. To distinguish between these possibilities, GLAST::CreERT2;*Chd7*^{fl/fl} (*Chd7* null) and Cre-negative control (WT) mice were treated with tamoxifen and sacrificed 12 weeks later (**Figure 60a**). Sections of the dentate gyrus were stained with antibodies raised against Sox2 and GFAP and the number of non-neurogenic, non-radial radial astrocytes (GFAP⁺Sox2⁻) were counted to determine if there was a fate change to glial cells. There was no change in the number of mature astrocytes in the DG of *Chd7* null compared to WT mice, indicating that loss of *Chd7* does not result in a fate change to glial cells. To further confirm this, a S100 β stain, to mark only mature astrocytes, would be needed.

To determine if the loss of *Chd7* leads to an increase in self-renewal or a decrease in the number of NSCs, sections of the dentate gyrus were stained with antibodies raised against Sox2 and GFAP and the number of radial NSCs (GFAP⁺Sox2⁺ cells with a cell body in the SGZ and astrocytic processes through the GL) in the SGZ were counted. Surprisingly, the number of NSCs present in *Chd7* null SGZ was increased by over 20% (**Figure 60b,d**), and the number of Sox2⁺GFAP⁻ progenitors was decreased compared to WT (**Figure 60e**). These data suggest that pool of NSCs has expanded due to increased symmetric divisions forming more NSCs. Alternatively, it may be possible that

the pool of NSCs has been maintained over a 12 week period in Chd7null mice, whereas the pool of NSCs in WT mice has undergone division-coupled astrocytic differentiation (**Figure 61**). This mechanism of NSC loss in WT mice has been proposed to be the reason for the loss of NSCs with age and states that NSCs only undergo limited rounds of division before differentiating into post-mitotic astrocytes [404]. This possibility will be addressed in **Section 6.11.4**.

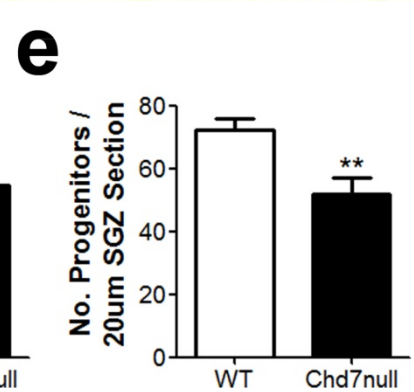
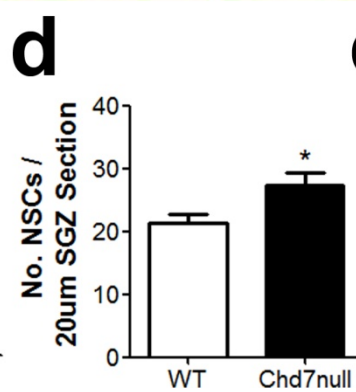
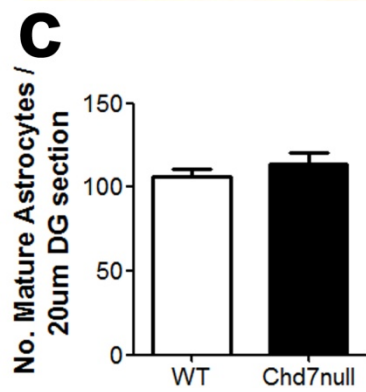
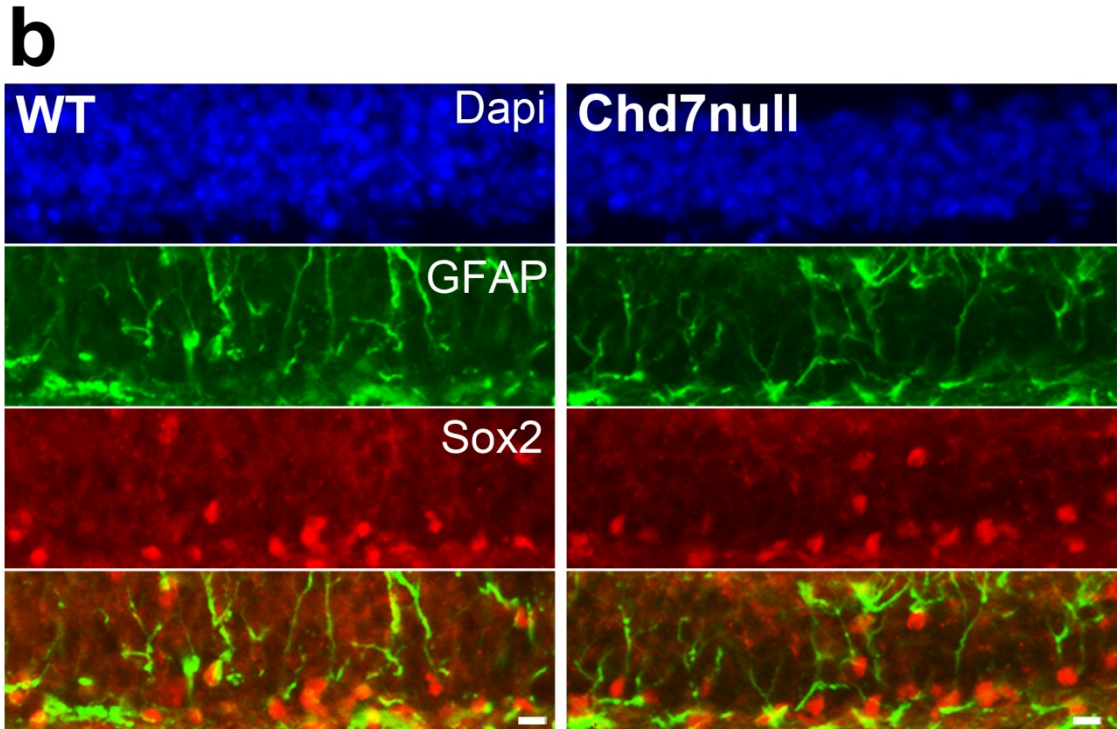


Figure 60 - Loss of *Chd7* results in an increase in the number of neural stem cells. a, Schematic diagram of the experimental strategy to delete *Chd7* from adult NSCs for 12 weeks (long-term). **b,** Representative image of a section of the DG of GLAST::CreERT2;*Chd7*^{fl/fl} mice treated with tamoxifen (*Chd7*null) and Cre-negative controls (WT) stained with antibodies raised against GFAP and Sox2 with Dapi 12 weeks after *Chd7* deletion. Scale bar, 10µm. **c,** Quantification of the number of GFAP⁺Sox2⁻ non-radial cells (mature astrocytes) in the DG of *Chd7*null and WT mice per 20µm section. n = 4 animals / condition. **d,** Quantification of the number of GFAP⁺Sox2⁺ radial NSCs and GFAP⁻Sox2⁺ progenitors (**e**) in the SGZ of *Chd7*null and WT mice per 20µm section. n = 4 animals / condition. All data represented as mean ± s.e.m.; *P<0.05 **P<0.01 student's t test.

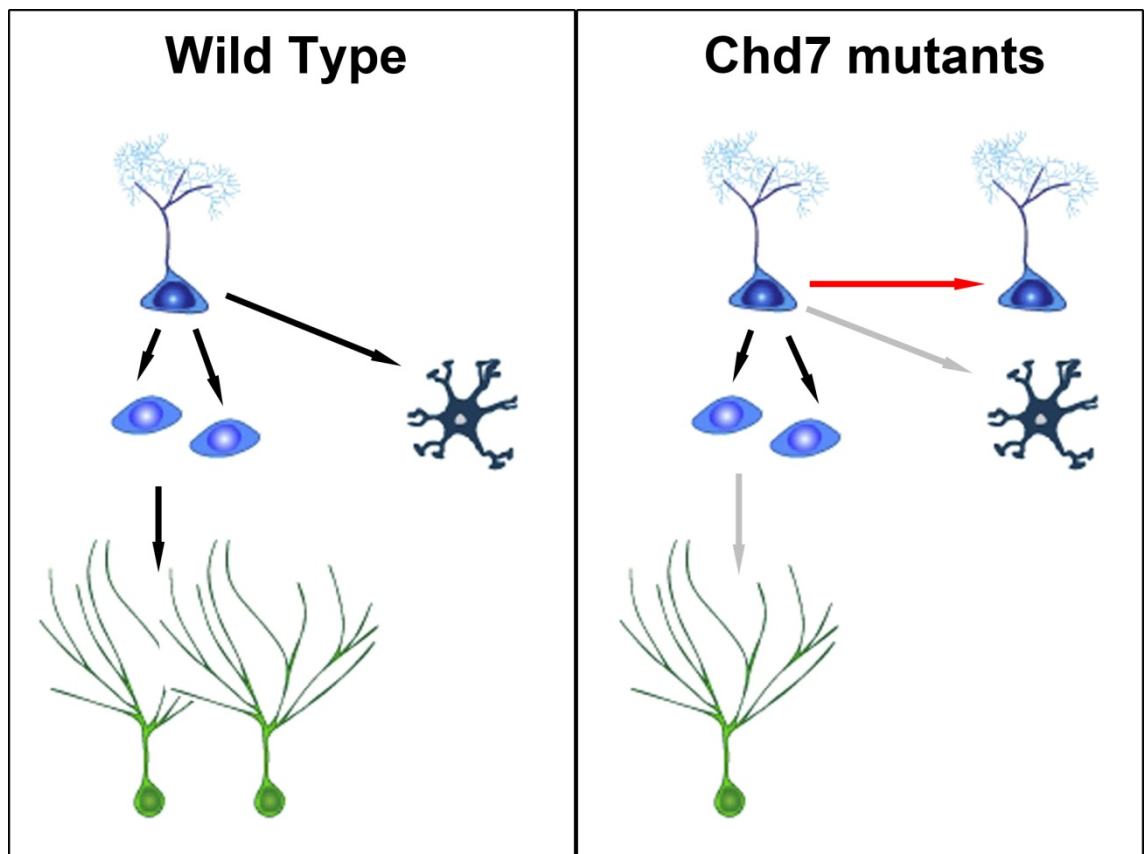


Figure 61 - The disposable stem cell hypothesis may account for an increase in the number of neural stem cells in Chd7 mutants over time. The disposable stem cell hypothesis states that NSCs, once activated, undergo a few rapid rounds of division to generate progenitors before differentiating into post-mitotic astrocytes (left panel) [404]. In the Chd7null dentate gyrus, it is possible that instead of undergoing differentiation into post-mitotic astrocytes, the NSCs are instead maintained, leading to a relative increase in the number of NSCs over time compared to wild type (right panel).

6.9. Loss of neural stem cell quiescence may be due to loss of Notch signalling

Notch signalling is a conserved regulator of NSC quiescence in the SVZ and SGZ [252, 253, 256, 260]. Loss of Notch signalling is associated with loss of NSC quiescence [252, 253, 256, 260]. Therefore, it may be possible that altered Notch signalling is responsible for a loss of NSC quiescence. To test this hypothesis, GLAST::CreERT2;Chd7^{fl/fl} (Chd7null) and Cre-negative control (WT) mice were treated with tamoxifen and the DG was then microdissected three weeks later and RNA was extracted (**Figure 62a**). A three week time point was chosen because CHD7 is predominantly expressed in MASH1⁺ type 2 cells, and so by three weeks after recombination a sufficient number of GLAST⁺ NSCs should have formed type 2 daughter cells [196, 233]. RT-qPCR analysis for the downstream effector of Notch signalling, *Hes5* was performed to determine if Notch signalling was altered in Chd7null mice *in vivo*. Interestingly, the expression of *Hes5* tended to be decreased by around 50% (**Figure 62b**), suggesting that loss of Notch signalling may be the reason for a loss in NSC quiescence.

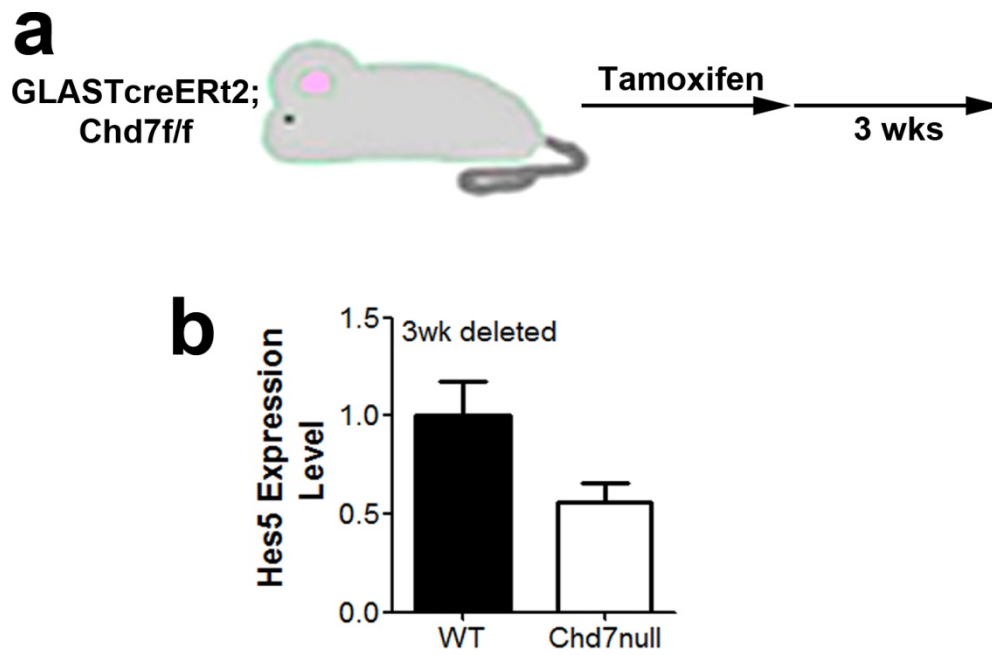


Figure 62 - Loss of *Chd7* leads to a decrease in Notch signalling. **a**, Schematic of the experimental strategy to delete *Chd7* from adult NSCs for 3 weeks. **b**, RT-qPCR expression level of *Hes5* from dissected DG of GLAST::CreERT2;*Chd7*^{f/f} (*Chd7*null) and Cre-negative control (WT) mice treated with tamoxifen and sacrificed 3 weeks later. n=2-3 animals / condition. Data are from 2 reactions conducted in duplicate. Data represented as mean ± s.e.m.

6.10. A decrease in *Chd7* expression may be linked to intellectual disability in CHARGE syndrome

De novo mutations in *CHD7* is one of the leading causes of CHARGE syndrome, a congenital defect characterised by coloboma of the eye, heart defects, atresia of the nasal choanae, retardation of growth, genital and ear abnormalities and deafness [330]. 90% of patients with CHARGE syndrome also present with intellectual disability [330], suggesting that *CHD7* is a key regulator of brain development and neurogenesis in humans.

Neurogenesis in the adult hippocampus plays an important role in certain types of learning tasks, memory formation, and pattern separation [224-227]. Therefore, defects in adult hippocampal neurogenesis likely contribute to intellectual disability [17, 398, 399]. I have shown that *CHD7* is an essential regulator of adult neurogenesis and loss of *Chd7* in NSCs results in a loss of neurogenesis (see **Section 6.4.**). Therefore, I hypothesised that a loss of *CHD7* and a decrease in hippocampal neurogenesis is at least partly responsible for the intellectual disability phenotypes seen in CHARGE syndrome patients. However, CHARGE syndrome is caused by heterozygous mutations and deletions of the *CHD7* gene [330], and so a complete loss of *Chd7* does not model the syndrome accurately. To address this point, I utilised a mouse line heterozygous for a genetrapped *Chd7* allele (*Chd7^{gt/+}*). This genetrapped allele presumably results in the translation of an unstable, truncated, non-functional protein which is rapidly degraded (see **Figure 37a**). Mice carrying the *Chd7^{gt}* allele have been previously shown to display phenotypes associated with *Chd7* haploinsufficiency such as abnormalities in pharyngeal arch arteries and other phenotypes associated with CHARGE syndrome [356]. I have previously shown that *Chd7^{gt/+}* mice have a 50% reduction in *Chd7* expression in the olfactory bulb (OB) compared to WT (see **Figure 37b**), and so *Chd7^{gt/+}* mice presumably have decreased *Chd7* expression in all brain regions.

To determine if a reduction in *Chd7* expression affects the generation of immature interneurons in the DG, sections of the DG of adult WT and *Chd7^{gt/+}* mice were stained with antibodies raised against DCX (**Figure 63a**). *Chd7^{gt/+}*

mice had fewer DCX⁺ cells compared to WT, suggesting that hippocampal neurogenesis is impaired (**Figure 63b**). To determine if the number of proliferating cells in the SGZ is altered in *Chd7^{gt/+}* mice, sections of the DG of adult WT and *Chd7^{gt/+}* mice were stained with antibodies raised against PCNA (**Figure 63a**). A reduction in *Chd7* expression had no effect on the number of proliferating cells in the SGZ of *Chd7^{gt/+}* mice (**Figure 63c**), suggesting that the main phenotype of decrease in *Chd7* expression is a reduction in neurogenesis. Further experiments subjecting *Chd7^{gt/+}* mice to hippocampal-dependent learning tasks would show if a decrease in *Chd7* expression causes impaired learning and memory.

Collectively, these data indicate that impaired hippocampal neurogenesis in *Chd7^{gt/+}* mice may reflect the intellectual disability associated with in CHARGE syndrome.

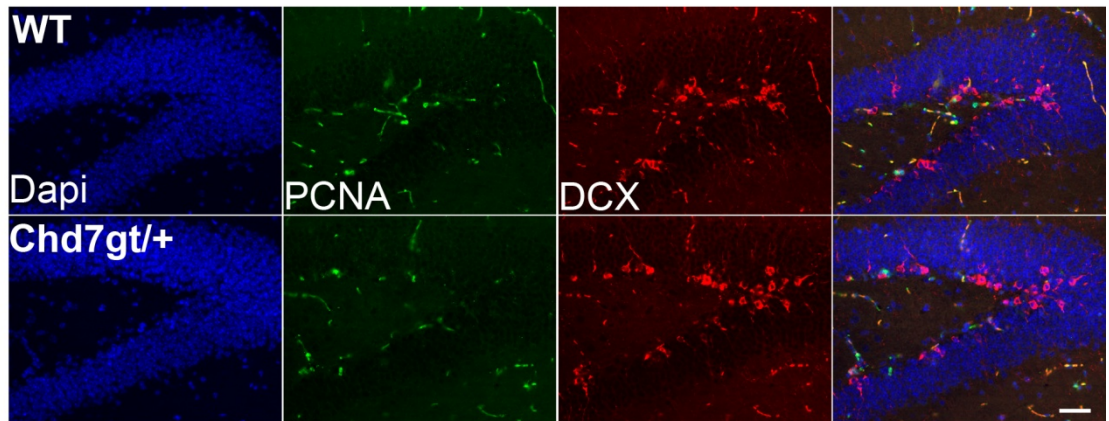
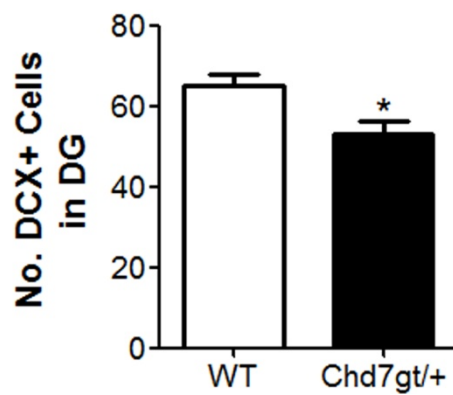
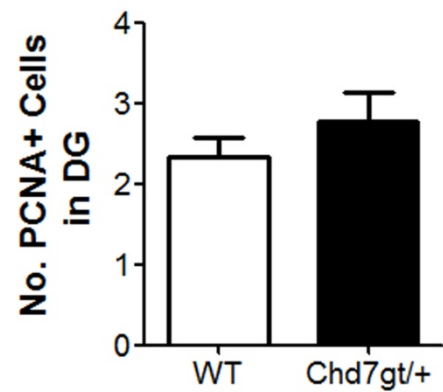
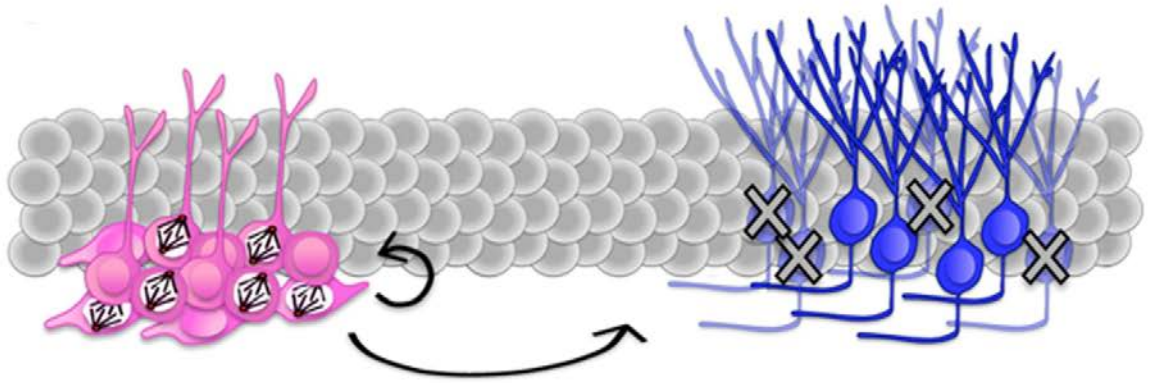
a**b****c**

Figure 63 - Reduction in *Chd7* expression affects hippocampal neurogenesis. a, Representative picture of the DG of adult *Chd7gt/+* and WT mice stained with antibodies raised against PCNA and DCX. Scale bar, 50 μ m. **b,** Quantification of the number of DCX+ and PCNA+ (c) cells in the DG of WT and *Chd7gt/+* mice per 10 μ m section. n=3 animals / condition. All data represented as mean \pm s.e.m.; *P<0.05 student's t test.

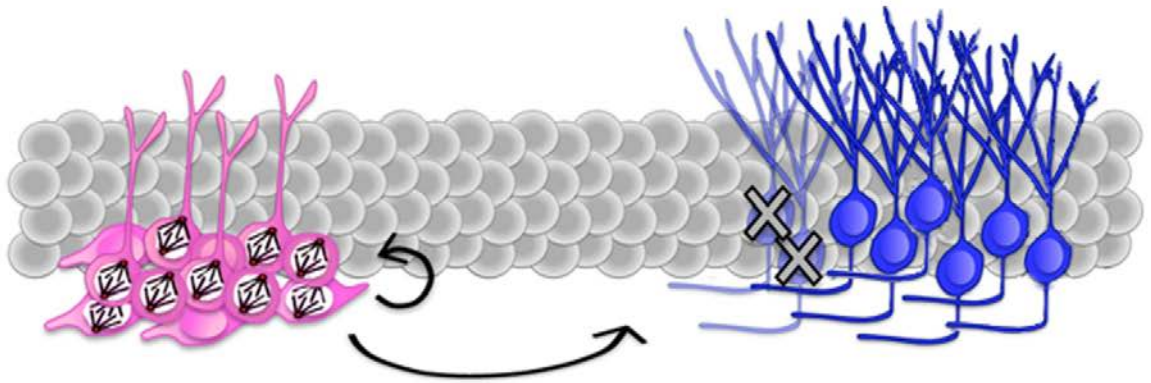
6.11. Discussion

I sought to investigate the role of the chromatin remodelling enzyme CHD7 on adult hippocampal neurogenesis. The data presented here show that CHD7 is a key regulator of the maintenance and differentiation of hippocampal NSCs. These data show that upon *Chd7* loss, NSC quiescence is disrupted and this leads to a transient increase in neurogenesis. In addition, a long-term loss of *Chd7* results in a large decline in neurogenesis and an increase in the number of NSCs, consistent with an increase in self-renewing divisions and a block in neurogenesis (**Figure 64**).

Adult hippocampus



Short-mid-term *Chd7* deletion



Long-term *Chd7* deletion

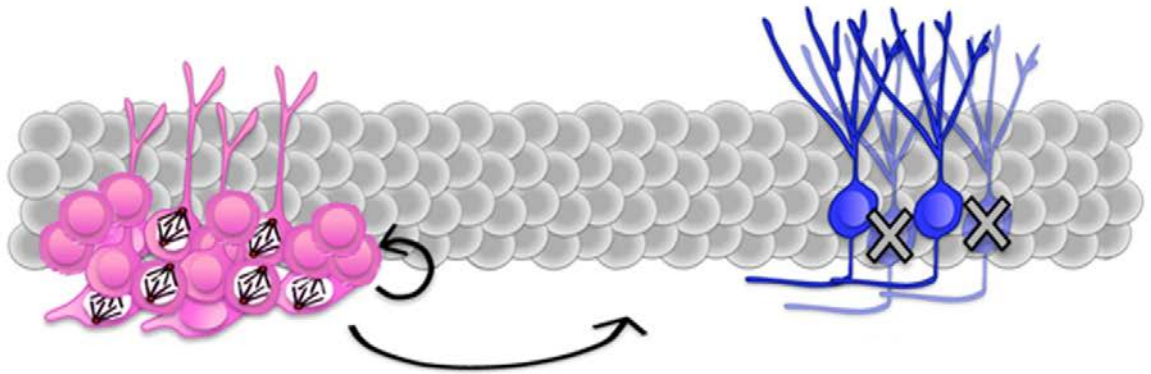


Figure 64 - Schematic diagram of the role of CHD7 in adult hippocampal neurogenesis.

Under homeostatic conditions, adult hippocampal neurogenesis depends on the balance between NSC (pink) activation (mitotic spindles) and daughter cell differentiation to form immature neurons (blue; top panel). Proliferating NSCs can generate additional NSCs or new neurons (arrows). During maturation, many neurons undergo apoptosis (crosses). 1-4 weeks after the deletion of *Chd7* from NSCs, NSCs lose quiescence and neurogenesis is transiently increased (middle panel). This may be due to the inhibition of apoptosis of cells, or their increased formation. 12 weeks after deletion of *Chd7* the number of NSCs is increased and the number of immature and mature neurons formed is decreased (bottom panel). Adapted from [184].

6.11.1. Chd7 may regulate neural stem cell quiescence cell autonomously or non-cell autonomously

I have shown that CHD7 could not be detected in GFAP⁺ NSCs in the SGZ (see **Section 6.2**). However, the expression of CHD7 in the SGZ is much lower than in the SVZ, and so it is possible that SGZ NSCs may express a low level of CHD7. Furthermore, a subset of MASH1⁺ cells also display NSC properties and are capable of producing differentiated progeny as well as maintaining their own pool by self-renewal [409]. Since CHD7 was mostly detected in MASH1⁺ cells, it is possible that CHD7 is expressed by MASH1⁺ NSCs. Therefore, a loss of NSC quiescence after *Chd7* deletion may be a cell-autonomous effect. However, the niche also largely regulates NSC quiescence [410]. I have shown that the total number of Sox2⁺ cells does not change initially after loss of *Chd7* in NSCs (see **Figure 58d**), thus a loss of NSC quiescence is unlikely to be due to a change in the cellular composition of the niche. It is possible, however, that intrinsic changes in progenitors may induce a loss of NSC quiescence. For example, type 2 cells in the dentate gyrus express Notch ligand such as Jag1 and Dll1 and signal to NSCs which express Notch receptor such as Notch 1 [259]. Notch signalling is a crucial regulator of NSC quiescence [259]. I have shown that Notch signalling is reduced in *Chd7* null mice (see **Figure 62b**), and this may be due to changes in the expression of Notch ligands on type 2 cells, or changes in the expression of Notch receptors on type 1 cells. RT-qPCR analysis of Notch

receptors and ligands will show if Notch signalling is altered due to the expression of receptors on type 1 cells or ligands on type 2 cells.

6.11.2. Decreased Notch signalling only accounts for some of the phenotypes seen after the loss of Chd7

A loss of Notch signalling has been shown to cause a loss of NSC quiescence and a transient increase in neurogenesis followed by a large decline in neurogenesis and depletion of the stem cell pool due to proliferative exhaustion [252]. I have shown that in *Chd7* null mice, loss of NSC quiescence leads to a transient increase in neurogenesis followed by a large decline in neurogenesis and maintenance of the stem cell pool, possibly through an increase in self-renewal (see **Figure 64**). Therefore, a decrease in Notch signalling only accounts for some of the phenotypes seen in *Chd7* null mice. However, it is possible that CHD7 regulates different aspects of neurogenesis by regulating the expression of genes associated with self-renewal and lineage priming in NSCs. In agreement with this concept, the CHD family member CHD4 has been shown to regulate the expression of genes associated with self-renewal and cell fate decisions in HSCs [385]. Alternatively, CHD7 may have separate roles in NSCs and differentiating progeny.

6.11.3. Chd7 may have separate roles in the self-renewal, maintenance of quiescence, and differentiation of neural stem cells

I have shown that the loss of *Chd7* specifically in NSCs results in the loss of NSC quiescence, an increase in the NSC pool, and a decrease in the formation of new neurons (see **Figure 64**). I hypothesise that these phenotypes are not all regulated by one single mechanism, but instead CHD7 has different effects on NSCs and their differentiating progeny (**Figure 65**). Therefore, analysing the role of CHD7 in different aspects of neurogenesis would reveal the full role of CHD7 in adult neurogenesis.

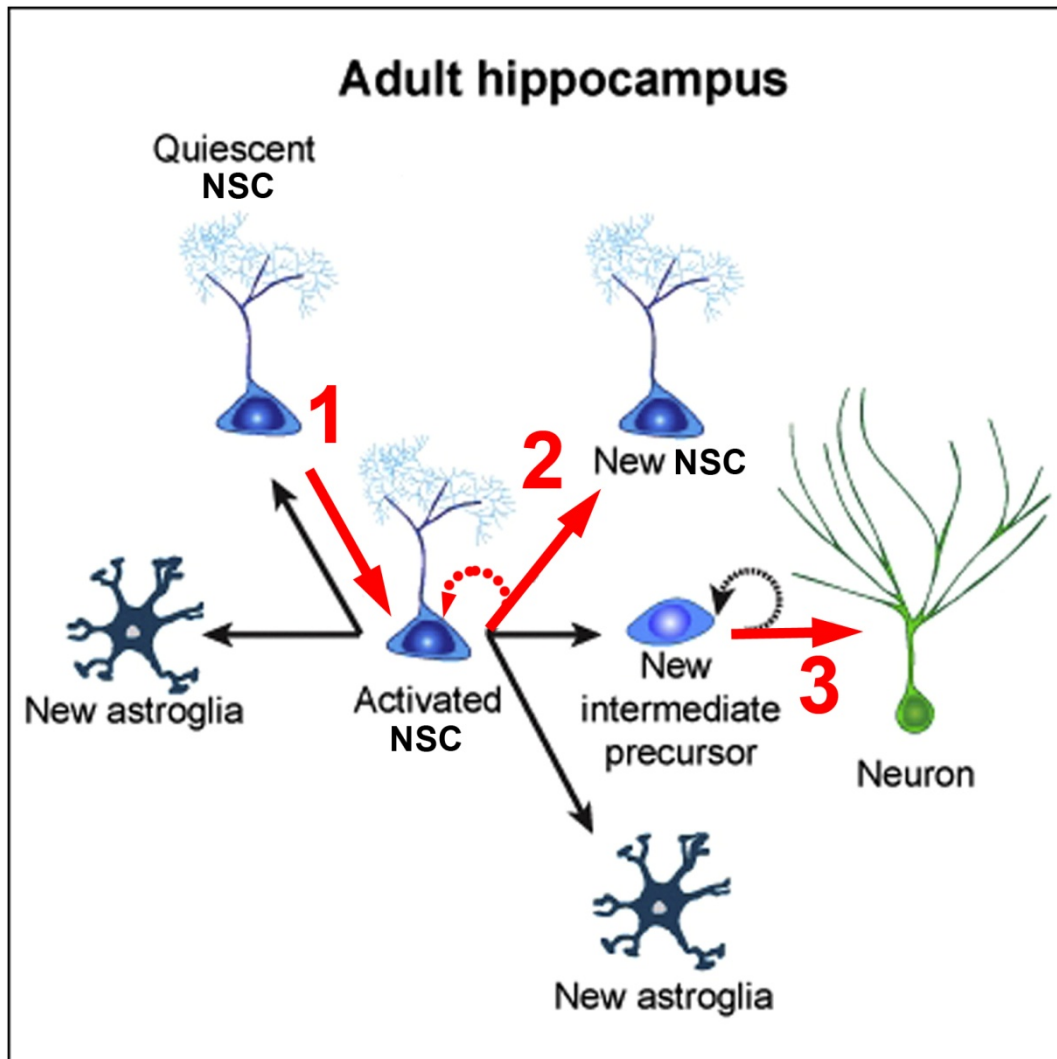


Figure 65 - The role of CHD7 in adult hippocampal neurogenesis. CHD7 can regulate NSC quiescence (1), the self-renewal of NSCs (2), and the differentiation of daughter cells (3). Adapted from [196].

6.11.3.1. CHD7 regulates the differentiation of immature neurons

My data show that a loss of *Chd7* in NSCs leads to a decrease in mature neuron formation and an increase in immature neuron formation *in vitro* (see **Section 6.6**). Therefore, I hypothesise that CHD7 plays a role specifically in immature neurons to regulate their differentiation into mature neurons. This could be addressed by deleting NSCs specifically from more differentiated cells and analysing the differentiation potential of recombined cells.

6.11.3.2. CHD7 regulates NSC quiescence

I hypothesise that CHD7 regulates NSC quiescence independently of the role of CHD7 on progenitor cell differentiation and NSC self-renewal. Although I have not been able to detect CHD7 in GFAP⁺ NSCs in the dentate gyrus, CHD7 is expressed in MASH1⁺ cells, a subpopulation of which is capable of long-term neurogenic potential [409]. Therefore, CHD7 may regulate NSC quiescence cell-autonomously. This possibility can be directly tested *in vitro* by inducing cells into quiescence by adding BMP4 to the culture media [411], and then deleting *Chd7*. I have generated CreERT2;*Chd7*^{fl/fl};RYFP/+ foetal-derived NSCs, and so addition of 4-hydroxy-tamoxifen to the culture should result in deletion of *Chd7* within all cells. Utilising this cell line, it will be possible to examine whether *Chd7* null cells are capable of returning to quiescence in this assay. This assay provides a powerful tool for the analysis of the role of CHD7 in quiescent and activating NSCs.

6.11.3.3. CHD7 regulates NSC self-renewal

I hypothesise that the self-renewal of NSCs is regulated by CHD7 independently of the effects of CHD7 on the formation of new neurons. The signalling pathways which regulate adult NSC self-renewal *in vivo* are not well understood, and so analysis of direct CHD7 targets may reveal novel pathways required for the maintenance of the stem cell pool. *In vivo* clonal analysis (described below) can be performed to address this.

6.11.4. *In vivo* clonal analysis of adult neural stem cells

I have demonstrated that CHD7 is expressed in 50% of MASH1⁺ cells (see **Figure 51**). This may reflect a unique subset of type 2a cells that require CHD7, or it may reflect a stage in the cell cycle or the degree of differentiation of type 2 cells (i.e. CHD7 may just be expressed by MASH1⁺ cells that are cycling or less differentiated MASH1⁺ cells for example). It is tempting to speculate that CHD7 is required by a subset of MASH1⁺ cells to activate the neurogenic differentiation program and, without CHD7, cells instead revert to a more stem cell-like state, leading to an increase in NSC number in the long-term (see **Figure 64**). *In vivo* clonal analysis of NSCs after *Chd7* deletion is needed to test this hypothesis. This involves injection of a small amount of tamoxifen in GLAST::CreERT2;*Chd7*^{fl/fl};RYFP/+ mice to label only a few cells in the SGZ and analysing the fate of recombined cells [196].

6.11.5. Neural stem cell quiescence and maintenance of the stem cell pool

The data presented here describes a unique scenario where loss of NSC quiescence is not coupled to a depletion of the stem cell pool. I have shown that the neural stem cell pool is increased 3 months after loss of *Chd7* (see **Figure 64**). However, it is possible that this time point is not long enough to see proliferative exhaustion of NSCs and a loss of the stem cell pool. In agreement with this, loss of cell cycle regulators, such as p21, also leads to the loss of NSC quiescence and an increase in NSC self-renewal followed by depletion of the stem cell pool [393]. *p21*^{-/-} mice display a greater number of NSCs up to 5 months of age compared to WT mice due to increased NSC proliferation [393]. Thereafter, however, the number of NSCs in *p21*^{-/-} mice decline and are reduced at 16 months of age relative to WT mice [393]. *p21*^{-/-} NSCs initially display an increased self-renewal capacity *in vitro* [393]. However, the self-renewal of *p21*^{-/-} NSCs eventually becomes limited and cells only survive a few passages [393]. Interestingly, foetal-derived NSCs from NestinCre;*Chd7*^{δ/δ} embryos are able to be passaged for many months (data not shown),

suggesting that *in vitro*, NSC self-renewal potential is not affected, or, at least, not reduced. However, *in vitro*, cells are grown in high amounts of FGF2 and EGF, and so small changes in self-renewal may be masked by the culture conditions. These data show that *Chd7* null and *p21*^{-/-} mice share many similarities in changes in neurogenesis. Therefore, it will be interesting to examine and changes in the expression of p21 in the DG of *Chd7* null mice. Furthermore, I am preparing to determine the number of NSCs present in the SGZ of *Chd7* null mice over 6 months after deletion to determine if NSCs without *Chd7* eventually succumb to proliferative exhaustion.

6.11.6. CHD7 and the regulation of apoptosis

I have shown that the loss of *Chd7* results in a transient increase in immature neuron formation, followed by a large decrease in the number of immature neurons compared to wild type (see **Figure 64**). It is possible that apoptosis is employed as a mechanism to attenuate the accumulation of immature neurons, resulting in an eventual decline in the number of DCX⁺ cells. In the DG, programmed cell death is largely responsible for the numbers of new neurons formed and it has been shown that less than 30% of newborn cells in the hippocampus survive to be mature neurons [229, 233, 264]. There are two critical periods of survival of precursors and neurons, with most apoptosis taking place at the transit-amplifying to neuroblast stage, where newly born cells are between 2 and 4 days old, and a second at the stage of maturation of immature neurons, where cells are between 1 and 3 weeks old [264]. Therefore, an increase in apoptosis may be responsible for a decrease in neurogenesis. I hypothesise that the eventual reduction in DCX⁺ cells in *Chd7* null mice is due to increased apoptosis in the second stage of maturation of immature neurons due to the inability of cells to form new mature neurons. To test this, sections of the DG of *Chd7* null and WT mice would need to be stained with an antibody such as cleaved caspase-3 along with markers of cells in the neurogenic lineage to determine if the apoptosis of certain populations is altered. All sections for this experiment have been prepared but not completed in time for writing this thesis.

6.11.7. CHD7 may regulate adult hippocampal and olfactory bulb neurogenesis in a similar fashion

My data suggests that CHD7 plays a similar role in the SGZ and SVZ. The reduction in the number of newly formed cells after the loss of *Chd7*, and the reduction in immature neuron formation in the SVZ and dentate gyrus of *Chd7* heterozygous mice, indicates that CHD7 may regulate hippocampal neurogenesis and SVZ-OB neurogenesis in a similar fashion. These findings may be surprising considering that NSCs in the hippocampus and SVZ serve different purposes and brain systems, and are regulated by different mechanisms [412, 413]. It would also be interesting to see if CHD7 is a conserved regulator of adult somatic stem cell function in niches outside of the brain. In support of this idea, it has been observed that CHD7 is widely expressed in many tissue-specific stem cell niches like hair follicles and bronchioles in the adult lung [414].

6.11.8. CHD7 and human disease

I have suggested that a decrease in *Chd7* expression and a consequent reduction in hippocampal neurogenesis may be responsible for a part of the intellectual disability observed in CHARGE syndrome. This shows that analysing the effect of CHD7 on hippocampal NSCs and the differentiation of daughter cells may help to better understand CHARGE syndrome. Additionally, CHD7 may also be involved in other syndromes. Batsukh et al. recently showed that CHD7 directly interacts with CHD8 [348]. *De novo* mutations in *CHD8* has been heavily implicated in autism spectrum disorder [327, 415], a disorder of neural development characterised by impaired social interaction, communication, and repetitive behaviour. Mouse models of autism exhibit defects in learning and memory and synaptic plasticity [416]. Since SGZ neurogenesis is important for certain types of hippocampal-dependent learning tasks [224-227], these findings indicate that interactions between CHD7 and CHD8 may play a role in hippocampal neurogenesis and autism spectrum disorder.

6.11.9. CHD7 regulates adult hippocampal neurogenesis via SoxC transcription factors

Recently, CHD7 has been shown to play an important role in adult hippocampal neurogenesis through the regulation of the chromatin structure around SoxC transcription factors [414]. In agreement with the data shown here, Feng et al. showed that CHD7 was expressed by type 2 and type 3 cells but was not conclusively shown to be present in NSCs [414].

After deletion of *Chd7*, Feng et al. showed that there was a decrease in the number of newly formed neurons along with a slight increase in the number of Ki67⁺ cells in the DG [414]. The authors suggested that there was an accumulation of proliferating cells due to a blockage in neuronal differentiation [414]. Twelve weeks after deletion of *Chd7* I see no change in the number of proliferating cells in the SGZ (see **Figure 55**). Furthermore, I show that there is in fact a decrease in the number of progenitors in the SGZ (see **Figure 60e**). The increase in proliferation seen by Feng et al. may be increased proliferation of NSCs, but the authors have not analysed specifically which cells are proliferating. Alternatively, the phenotypes seen by Feng et al. may be different to the phenotypes I see because of the different time points at which the mice were taken. Of note, Feng et al. do not show that loss of neurogenesis is a primary phenotype after loss of *Chd7* in adult NSCs since a decrease in type 3 cells was only observed 14 weeks after the loss of *Chd7*, and the authors did not examine any earlier time points [414].

6.11.9.1. CHD7 regulates the chromatin state around the promoter of Sox4 and Sox11

From the Cancer Genome Atlas project, focusing specifically on gliomas, the SoxC transcription factors, Sox4 and Sox11, were greatly downregulated with *Chd7* [414]. Sox4 and Sox11 have been previously shown to play an essential role in adult neurogenesis by binding directly to the *Dcx* promoter and inducing its expression [417]. Feng et al. showed that loss of *Chd7* from the adult

neurogenic lineage was associated with decreased expression of *Sox4* and *Sox11* [414]. Transfection of cells lacking *Chd7* with *Sox4* or *Sox11* expression constructs rescued the impairment in neuronal differentiation in cells lacking *Chd7* [414]. Importantly, *Sox4* and *Sox11* function to increase the expression of *Dcx* [417]. My data suggest that the number of DCX⁺ cells is not impaired immediately after loss of *Chd7*, and is even increased slightly 4 weeks after *Chd7* deletion, suggesting that the effect of CHD7 on *Sox4* and *Sox11* may not be crucial for neurogenesis *in vivo*. Despite this, it may be possible that *Sox4* and *Sox11* activate other transcriptional programs required for proper neuronal differentiation, and so further investigation into the role of *Sox4* and *Sox11* in adult neurogenesis is needed.

6.11.9.3. *Notch1* expression is correlated with *Chd7* expression

Feng et al. found that *Notch1* was highly positively correlated with CHD7, meaning that a decrease in *Chd7* expression is found with a decrease in *Notch1* expression [414]. These data suggest that loss of NSC quiescence in *Chd7* null mice could be due to a decrease in the expression of *Notch1* on NSCs. These data also suggest that overexpression of *Chd7* would lead to an increase in *Notch1* expression and increased NSC quiescence. These points can be addressed by examining the expression of Notch ligands and receptors on NSCs and their progeny. Furthermore, I have access to a *Chd7* overexpression construct, and so transfection of foetal-derived NSCs with the construct would show if overexpression of *Chd7* results in an increase in quiescence *in vitro*.

6.12. CHD7 regulates different aspects of adult neurogenesis

The data presented here indicate a role for CHD7 in the maintenance of the NSC pool, regulation of NSC quiescence, and regulation of the terminal differentiation of daughter cells. Furthermore, I have suggested that a decline in neurogenesis in mice heterozygous for *Chd7* may be responsible for the intellectual disability associated with CHARGE syndrome. Although a recent

study has shown a role for CHD7 in the differentiation of NSC progeny [414], I have identified a novel role for CHD7 in the regulation of NSC quiescence and cell fate decisions. This suggests that CHD7 may potentially regulate the transcription of diverse sets of genes, and so further investigation into the targets of CHD7 would give an insight into the role of CHD7 in adult neurogenesis.

Chapter 7

Discussion

7.1. Discussion

Ageing is a physiological process whereby the composition of many somatic stem cell niches is disrupted and the stem cells display intrinsic changes [9]. Ageing leads to alterations in stem cell number and function, often having a negative impact on tissue homeostasis. In addition, the numbers of stem cells present in various tissues generally declines with age [17-20]. Still very little is known about age-related changes in mammalian stem cell niches and how this impacts on stem cell number. Furthermore, the mechanisms controlling stem cell quiescence and fate decisions are not completely understood. In this thesis I attempted to examine intrinsic and niche influences on stem cell quiescence and differentiation using skeletal muscle SCs and adult NSCs.

7.1.1. Quiescence is a property of many somatic stem cells essential for stem cell function and maintenance of the stem cell pool

As ageing progresses, the regenerative ability of skeletal muscle declines due, at least in part, to impaired SC function [146, 147]. The physiological changes which lead to impaired SC function in aged animals have been intensely investigated [10, 148, 150, 164, 169]. However, the changes which lead to a decline in the number of SCs, and the relevance of a loss of SCs, with ageing, were unknown. Here, I have identified a specific and functionally important change in the molecular composition of the aged stem cell niche. Upregulation of FGF2 by the muscle fibre drives a subset of SCs to break quiescence and lose self-renewal capacity under homeostatic conditions in aged animals. This results in an increased tendency of SCs to differentiate or apoptose (see **Figure 33**).

Chakalakal et al. have shown that two pools of SCs exist in adult skeletal muscle; a label retaining cell (LRC) population, and a non-LRC population [418]. Upon transplantation, aged LRCs seeded approximately threefold more SCs and differentiated myonuclei than did non-LRC transplant recipients [418], showing that maintenance of quiescence is essential for regeneration and stem

cell function. These data also indicate that the quiescent, label-retaining population may represent the true regenerative stem cell population.

As ageing progresses in adult skeletal muscle there is a diminution of highly functioning LRCs and a gain of committed non-LRCs [418]. That non-LRCs self renew poorly and tend to differentiate, suggests that the relative increase of non-LRCs in aged muscle occurs through proliferation of LRCs [418]. These data indicate that the transition of LRCs into the non-LRC compartment due to a loss of quiescence is responsible for impaired regeneration in aged animals. However, these studies show that in aged animals there still exists a subset of SCs with great regenerative capacity, but the decline in SC number may limit full regeneration.

Label retention is a characteristic which allows for the identification of adult stem cells in other tissue systems, such as NSCs in the adult forebrain, hair follicle bulge cells, and HSCs [419-422]. Interestingly, like in the SC niche, quiescent HSCs and NSCs are often found alongside more proliferative tissue-specific stem cells [253, 423], suggesting that heterogeneity based on proliferative history within adult stem cell populations may be a common feature in adult stem cell niches. Investigating whether the more proliferative tissue-specific stem cells are formed from the quiescent population, or whether they represent a completely different population of cells, independent of the quiescent stem cell lineage, would give a better insight into the role of heterogeneity within adult tissue-specific stem cells.

Interestingly, quiescence is not a feature of SCs in all muscles. Satellite cells in the extraocular muscles remain proliferative under homeostatic conditions and add myonuclei to the uninjured myofibre [116] and these muscles are unaffected in Duchenne muscular dystrophy [117]. These studies indicate that SCs of the extraocular muscles may display mechanisms to prevent proliferative exhaustion of the stem cell population which are not present in SCs of the limb, perhaps reflecting their different ontogeny from limb muscles. Indeed, quiescence is not a universal feature of all adult somatic stem cells. Actively proliferating Lgr5⁺ stem cells have been described in the stomach,

small intestine and colon, with these cells displaying self-renewal ability and the capacity to generate differentiated cell types [424, 425]. These studies suggest that quiescence is not an obligatory feature of stemness.

The incorporation and retention of DNA analogues, such as BrdU, is often used to study cell-cycle kinetics. However, these DNA labels can only be visualised in fixed and permeabilised cells. Furthermore, in many tissues, fully differentiated cells often retain label [422, 426]. Therefore, as an alternative strategy, we have labelled chromatin *in vivo* using a doxycycline-inducible transgenically expressed EGFP-tagged histone 2B (H2B-GFP) [418, 420]. This approach enables fractionation of live LRC and non-LRC populations by FACS and has been used in several tissues [420-422]. This technique allows for additional identification of different stem cell populations based on proliferative history and will give a better understanding of the differences between quiescent and proliferative stem cell populations.

7.1.2. Maintenance of the stem cell pool is essential for tissue function

Loss of tissue-specific stem cells and their impaired function has been proposed to be one of the primary causes of ageing [18, 394]. This has been suggested to be due to a combination of heritable intrinsic events, such as DNA damage, as well as extrinsic influences, such as changes in the stem cell niches. These events collectively lead to a decline in tissue function under homeostatic and regenerative conditions. Several effects of ageing on the brain, skeletal muscle and blood organ have been described in humans, and have been suggested to be due to, in part, impaired stem cell function. Impaired HSC function has been suggested to contribute to decreased immunity [427], increased incidence of bone marrow failure [428], and moderate anaemia [429, 430], whereas impaired NSC function with age has been suggested to contribute to cognitive decline [17, 398, 399], and impaired SC function has been proposed to be the main cause of age-related sarcopenia [146].

My data shows that increasing the sensitivity of aged SCs to niche-derived FGF2 leads to increased depletion of the SC pool (see **Section 4.3**). Chakalakal et al. have shown that further diminution of the aged SC pool, achieved by long-term *Spry1* deletion in aged SCs, impairs muscle regenerative capacity and further exacerbates ageing [418]. Conversely, muscle injury after a short-term (10 day) deletion of *Spry1* in aged mice, when the number of Pax7⁺ cells had increased owing to the initial loss of quiescence (see **Section 4.2**), led to a greater regenerated muscle fibre size compared to aged controls [418]. These data show that the exacerbated loss of the SC pool, due to a long-term increase in FGF signalling in aged uninjured muscle, becomes limiting on regeneration. Therefore, strategies to maintain the quiescence of SCs under homeostatic conditions should result in maintenance of the SC pool and allow for efficient regeneration. These data also show that increasing the SC pool in aged animals such as through transplantation should also allow for efficient regeneration.

I have shown that inhibition of FGF signalling led to decreased cycling of the aged SC pool and a decreased tendency to apoptose (see **Section 4.4**). Chakalakal et al. tested whether long-term inhibition of FGF-signalling would improve SC regenerative capacity by injuring adult and aged mice after six weeks of FGFR inhibition [418]. After injury, muscle fibre size was 30% smaller in FGFR-inhibited mice compared with controls, suggesting that repression of FGF signalling inhibits myofibre repair [418]. This is in agreement with data showing that FGF signalling is important for efficient skeletal muscle regeneration [113, 114]. In contrast, the number of self-renewing SCs was greater in aged FGFR-inhibited mice than in controls [418]. This result demonstrates that repressing FGF-signalling during ageing improves the self-renewal capacity of satellite cells during regeneration. Therefore, investigating changes in stem cell niches with age, and their effects on resident stem cells, will give an insight into the reasons behind altered stem cell number and function with age.

7.1.3. Upregulation of FGF2 in the aged satellite cell niche may be due to accumulated myofibre damage

I hypothesised that upregulation of FGF2 with age may be due to the accumulation of chronic myotrauma over time (see **Section 3.4**). Under homeostatic conditions there is no turnover of skeletal muscle, and so low-level myotrauma, which may not elicit a regenerative response, may accumulate on the myofibre throughout life. The promoter region of *Fgf2* has binding sites for many transcription factors, including AP1, c-Jun, and p53 (as predicted by SABiosciences' Text Mining Application). The transcription factor with the greatest number of predicted binding sites on the *Fgf2* promoter is Signal Transducer And Activator Of Transcription 1 (STAT1). STAT1 is a transcription factor upregulated in stress and is involved in interferon signalling. Interestingly, *Stat1* expression increases in aged single fibres compared to adult (data not shown), suggesting that accumulated myofibre damage may cause the fibre to upregulate STAT1 which then induces the transcription of *Fgf2*. It is important to note that STAT1 is only active as a transcription factor in its phosphorylated form, so an upregulation of *Stat1* does not necessarily mean an upregulation in its activity. It would be interesting to further investigate the role of STAT1 in aged skeletal muscle.

7.1.4. Ageing in the hippocampus is associated with altered neural stem cell function and cognitive decline

The hippocampus is one of the areas in the brain that is most susceptible to functional and structural alterations in ageing, which are often accompanied by learning and memory problems [431]. It has been proposed that an age-related decline in neurogenesis may underlie age-associated learning and memory declines [395, 406, 432] and may contribute to pathological conditions such as Alzheimer's disease [433-435]. Decreased neurogenesis has been correlated with decreased proliferation of neural precursors in the DG [395], but the reasons for this decrease in proliferation, and exactly which cells are affected, remains largely unexplored. Even in the data presented here, a reduction in

immature neuron production can be seen in WT mice with age (compare the number of DCX⁺ cells in the WT DG from **Figure 55c** to **Figure 56bd**) as well as a slight reduction in the number of proliferating cells (compare the number of BrdU⁺ cells in the WT SGZ from **Figure 55d** to **Figure 58c**). Furthermore, It is generally accepted that the number of NSCs declines with age [196, 404] and decreased dentate neurogenesis has been proposed to be a result of increased quiescence of NSCs [403]. Therefore, strategies to increase NSC number and their proliferation may ameliorate age-related phenotypes to a certain extent. Increased progenitor proliferation in aged rats has been achieved through infusion of IGF1[436] and exposure to environmental enrichment, which has been associated with improved performance in spatial learning tasks [15, 230, 437]. Physical exercise can increase progenitor proliferation and neurogenesis in adult animals and has a similar effect in the aged DG [405, 438]. I have shown that loss of *Chd7* specifically in NSCs results in an increase in NSC proliferation and an increase in the NSC pool (see **Figure 64**). These results suggest that a loss of *Chd7* in aged animals may temporary ameliorate age-related phenotypes. However, loss of *Chd7* also results in a decrease in neurogenesis. Dissecting out the pathways by which CHD7 regulates aspects of neurogenesis, from NSC proliferation, to stem cell self-renewal, to daughter cell differentiation may give a better insight into how to reverse age-related changes in NSCs and their daughter cells.

7.1.5. Ageing in the hippocampus is associated with changes in the chromatin landscape

Changes in the structure of chromatin has been proposed to be one of the reasons for the age-related changes to biological functions in cells and the increased incidence of disease [439]. During ageing, somatic stem cells display decreased chromatin stability and extensive chromatin remodelling which occurs with changes in cellular gene expression profiles [440]. These changes have been shown to impair stem cell function [441, 442].

In contrast to stable genetic changes to the DNA sequence, epigenetic changes are reversible and, therefore, are an interesting therapeutic target for the treatment of age-related diseases. Individuals with Hutchinson-Gilford progeria syndrome (HGPS) display characteristics of premature ageing. Aged individuals and HGPS patients exhibit disrupted cellular chromatin structure and nuclear organisation, suggesting that there may be a link between altered chromatin structure and ageing [443]. Furthermore, the spacing of nucleosomes may become more irregular with age in mammalian cells, and chromatin fibres in ageing fibroblasts become less dense, suggesting a loosening of chromatin structure with age [444, 445]. Aged mice generally have a decreased ability to maintain heterochromatin, as shown by less efficient X-inactivation [446]. Collectively these data suggest that changes in chromatin structure may lead to aberrant age-related changes in cells. Further evidence for this came from analysis of chromatin remodelling complexes with age. Nucleosome Remodelling Deacetylase (NURD) is a protein complex with ATP-dependent chromatin remodelling activity and histone-deacetylase activity [447]. HGPS cells exhibit decreased levels of NURD subunits, which has been proposed to cause a loss of H3K9me₃, associated with heterochromatic regions, and elevated levels of DNA damage foci [448]. Healthy aged cells also demonstrate a decline in levels of NURD subunits, such as retinoblastoma binding protein 4 (RBBP4) and RBBP7 [449]. It is not known how decreased NURD activity causes ageing phenotypes, but these studies highlight the importance of chromatin modifications in ageing. It would be interesting to see if the expression of *Chd7* changes with age. It is tempting to speculate that a gradual loss of *Chd7* expression may lead to decreased formation and impaired maturation of neurons with age. Indeed, mice heterozygous for *Chd7* display a decreased formation of immature neurons in the dentate gyrus (see **Section 6.10**), and newly formed neurons from NSCs lacking *Chd7* display abnormal dendrite morphology [414], which may cause an increased incidence of age-related neurodegenerative disorders.

7.1.6. CHD7 and the regulation of bHLH factors in neurogenesis and myogenesis

I have shown that CHD7 is highly expressed in a subset of MASH1⁺ cells in the SGZ and suggest that CHD7 may be required to allow for proper differentiation and self-renewal of these cells (see **Figure 65**). CHD7 is also highly expressed in proliferating cells in the SVZ and SGZ [414]. From preliminary experiments in adult myogenic cells, *Chd7* is expressed at very low levels in quiescent SCs and RSCs, greatly increases in proliferative myoblasts, and is then downregulated as myoblasts fuse to form myotubes (data not shown). This suggests that CHD7 may have a similar role in myogenesis and neurogenesis as they are expressed in bHLH-expressing progenitors. However, *Chd7*^{gt/+} mice do not show any changes in myofibre diameter, indicating that a decrease in *Chd7* expression does affect developmental myogenesis at least (data not shown). *CHD7* loss of function mutations have been associated with CHARGE syndrome [330]. CHARGE syndrome patients generally do not display gross muscle abnormalities, but do have a low muscle tone with muscles unable to maintain a contraction for as long as normal tone muscles [450]. It has not been shown that CHARGE syndrome patients with *CHD7* mutations have decreased muscle tone, but it is tempting to speculate that, like in neurogenesis, loss of *Chd7* results in impaired maturation of newly formed cells, leading to impaired contractile properties in skeletal muscle. Crossing a *Chd7*^{ff} mouse line with a *Pax7*^{CreERT2/+} mouse line would allow for deletion of *Chd7* specifically in SCs. Analysing muscle regeneration in these mice would show whether CHD7 is involved in SC or daughter cell function.

7.1.7. CHD proteins in adult neurogenesis

Recently, CHD5 has been shown to play a similar role in neurogenesis as CHD7 [451]. CHD5 was shown to be expressed in type2b, type3, and mature neurons in the DG [451]. shRNA-mediated knockdown of *Chd5 in vitro* led to impaired neuronal differentiation, suggesting that CHD5 plays a critical role in adult neurogenesis, specifically in neuronal differentiation [451]. GO analysis of

Chd5-depleted cells showed that mutant cells were unable to activate many genes involved in late-stage neuronal differentiation, including genes with roles in the regulation of synapse development and neuron projections [451]. Furthermore, the authors showed that a cohort of PcG target genes characteristic of non-neuronal lineages were upregulated in mutant cells, suggesting that proper neuronal differentiation is dependent on the capacity of CHD5 to facilitate the activation of pro-neurogenic genes and maintain the repression of Polycomb-repressed genes [451]. Considering that CHD7 is expressed predominantly by type2a cells (see **Figure 52**), CHD5 is expressed by type2b, type3, and mature cells [451], and CHD8 appears to be expressed by mature neurons in the DG (data not shown), it is tempting to speculate that CHD proteins act in a temporal manner to regulate neurogenesis and proper neuron formation. Interestingly, overexpression of CHD5 failed to promote neurogenesis, suggesting that it lacks the inductive capacity of proneural factors such as MASH1. Whether CHD7 also lacks inductive capacity for neurogenesis remains to be determined. Together, these results show that CHD proteins play important roles in neurogenesis and neuronal maturation.

7.1.8. CHD7 may play a role in autism spectrum disorder and neurodegenerative disorders

Adult neurogenesis has been shown to play a significant role in various neurological disorders and diseases, including epilepsy and depression [452]. Furthermore, neurodegenerative disorders such as Huntington's disease and Parkinson's disease exhibit specific alterations in neurogenic areas leading to changes in dendrite morphology and synaptic plasticity.

I have shown that a reduction in *Chd7* expression results in a decrease in immature neuron formation and suggested that impaired neurogenesis in these mutants may be responsible for the intellectual disability seen in CHARGE syndrome patients (see **Section 6.10**). Preliminary data from a microarray of misregulated transcripts from *Chd7*null and wild type dentate gyrus shows many transcripts involved in synapse formation, plasticity, and ion channel formation

are altered in *Chd7* null mice compared to controls (data not shown). These data are consistent with an involvement of CHD7 in the efficient differentiation of neural progenitors. Additionally, pathway analysis showed that misregulated transcripts were involved in Huntington's, Alzheimer's, and Parkinson's diseases (data not shown), implicating a role for *Chd7* in the regulation of many neurodegenerative diseases and neuron maturation.

Recently, impaired neuronal maturation and misregulation of ion channels has been implicated in some of the phenotypes associated with ASD [453, 454]. For example, *MARK1* (microtubule affinity-regulating kinase 1), which is upregulated in the DG of *Chd7* null mice (data not shown), has been found to be overexpressed in the prefrontal cortex of patients with autism and causes changes in the function of cortical dendrites [455]. *AUTS2* (Autism susceptibility candidate 2) has been found to be disrupted in patients with ASD and a loss of *AUTS2* function has been implicated in intellectual disability [456, 457]. *Auts2* is downregulated in the DG of *Chd7* null mice (data not shown). *Shank3* is a postsynaptic protein found to be downregulated in the DG of *Chd7* null mice (data not shown) and haploinsufficiency of *Shank3* leads to deficits in synaptic function, social interaction, and social communication [458]. These data implicate a role for CHD7 in ASD. Recently, mutations in another CHD family member, *CHD8*, have been shown to play a role in autism spectrum disorder, and may account for up to 0.4% of cases [327]. It is tempting to speculate that CHD7 may play a role in ASD through interactions with CHD8. Examining the binding partners and direct targets of CHD7 would be useful for uncovering the role of CHD7 in ASD.

7.1.9. Intrinsic and extrinsic changes affect somatic cell function

In this thesis I set out to examine the fundamental properties of somatic stem cells and explore the mechanisms regulating stem cell quiescence and differentiation. The data presented in this thesis display the necessity for strict control of the intrinsic chromatin landscape and the extrinsic niche environment on somatic cell function. I have shown that alterations in the niche lead to a loss

of SC quiescence and depletion of the SC pool. I have shown that loss of the chromatin remodelling enzyme CHD7 leads to a loss of NSC quiescence and a loss of neurogenesis. Both changes lead to alterations in the tissue associated with ageing, such as impaired regenerative capability in skeletal muscle, and a decrease in neurogenesis in the hippocampus. Furthermore, based on expression profiles, I have suggested that CHD7 may play a similar role in myogenesis as it does in neurogenesis. Collectively, these data help to better understand the regulation of stem cell quiescence and cell fate decisions, two fundamental properties of somatic stem cells which allow for the maintenance of a functional stem cell pool throughout life.

7.2. Future work

The data presented in this thesis establish a role for CHD7 in the regulation of NSC quiescence, self-renewal, and differentiation. However, how CHD7 regulates these separate events is not completely understood. Recently, CHD7 has been shown to be essential for the differentiation of neural progenitors through the regulation of SoxC transcription factors [414], but the role of CHD7 in NSCs remains largely unexplored. Future experiments aim to examine how CHD7 regulates NSC quiescence and self-renewal, and the long-term effects of the loss of *Chd7* from NSCs.

7.2.1. In vivo clonal lineage analysis

I have shown that the loss of *Chd7* results in an increase in the number of NSCs compared to WT (see **Figure 64**). To fully determine whether this is due to an increase in NSC self-renewal, an *in vivo* clonal analysis assay can be performed [196]. This involves injecting GLAST::CreERT2;*Chd7*^{fl/fl};RYFP/+ and Cre-negative (WT) mice with a small amount of tamoxifen to induce recombination in only a small number of cells. Sacrificing mice 3 months after tamoxifen injection will allow for clonal analysis of recombined cells through use

of the *YFP* allele. If the loss of *Chd7* is associated with increased NSC self-renewal, I would expect to see two or more RYFP⁺ cells with a radial glia morphology next to each other in the SGZ. I have generated GLAST::CreERT2;*Chd7*^{ff};RYFP/+ and Cre-negative control mice to begin *in vivo* lineage tracing. These experiments will also show the exact extent of the decrease in neurogenesis in *Chd7*null mice at the single cell level. Due to the complexity of generating these mice, I have not been able to complete this experiment before writing my thesis.

7.2.2. The long-term effect of a loss of *Chd7* on the neural stem cell pool

I have shown that there is an increase in the number of NSCs 3 months after deletion of *Chd7* compared to WT (see **Figure 64**). However, it is possible that this increase in the stem cell pool may only be temporary, and NSCs eventually succumb to proliferative exhaustion and the pool is depleted. Therefore, analysing the number of NSCs present in *Chd7*null and WT mice longer than 3 months after deletion is necessary to fully understand the role of CHD7 in adult neurogenesis. Due to the length of time needed for this experiment, I have not yet been able to collect the samples. However, I have planned to take GLAST::CreERT2;*Chd7*^{ff} and Cre-negative control mice 8 months after tamoxifen injection and count the number of stem cells present in the hippocampus.

7.2.3. The role of CHD7 on neural stem cell quiescence

I have shown that the loss of *Chd7* in NSCs results in a loss of NSC quiescence (see **Figure 64**). It has been recently shown that NSCs in culture can be induced into a state of reversible quiescence through the replacement of EGF with BMP4 in the culture media [411]. Using this technique, I plan to examine if *Chd7*null cells display any defects in quiescence induction by staining for markers of cell cycle entry such as Ki67 after addition of BMP4 to the culture

media. Furthermore, I have generated foetal-derived NSCs from CreER^{T2};Chd7^{ff};RYFP/+ mice to delete *Chd7* after quiescence induction and examine any inability to remain quiescent. These experiments will determine the role of CHD7 in the maintenance of NSC quiescence.

7.2.4. Chromatin immunoprecipitation of CHD7 in cultured neural stem cells

Chromatin immunoprecipitation (ChIP) with massively parallel DNA sequencing (ChIP-Seq) can be used to determine the binding sites of DNA-binding proteins across the genome. ChIP-seq analysis of CHD7 binding sites in cultured ES-cells showed that CHD7 binds to areas associated with genes involved in Notch signalling and progression through the neurogenic lineage, including *Hes1*, *Hes5*, *Mash1* and *NeuroD1* [341]. Therefore ChIP-Seq analysis of Chd7null (negative control) and WT cells cultured under growth conditions and differentiation conditions, will suggest possible direct targets of CHD7 and show how the distribution of CHD7 across the genome changes as cells are induced to differentiate. Furthermore, this technique can also be used in combination with the *in vitro* quiescence assay, as detailed in **Section 7.2.3**, to determine if CHD7 associates with regulatory regions that control the expression of genes important for the maintenance of NSC quiescence. The chromatin state around identified CHD7 binding sites can then be analysed by micrococcal nuclease digestion, which examines the density of chromatin. These experiments will help to identify primary changes caused by loss of *Chd7* and will also identify direct targets of CHD7.

Bibliography

1. Keller, G., *Embryonic stem cell differentiation: emergence of a new era in biology and medicine*. *Genes Dev*, 2005. **19**(10): p. 1129-55.
2. Jahagirdar, B.N. and C.M. Verfaillie, *Multipotent adult progenitor cell and stem cell plasticity*. *Stem Cell Rev*, 2005. **1**(1): p. 53-9.
3. Lensch, M.W., L. Daheron, and T.M. Schlaeger, *Pluripotent stem cells and their niches*. *Stem Cell Rev*, 2006. **2**(3): p. 185-201.
4. Li, L. and R. Bhatia, *Stem cell quiescence*. *Clin Cancer Res*, 2011. **17**(15): p. 4936-41.
5. Pietras, E.M., M.R. Warr, and E. Passegue, *Cell cycle regulation in hematopoietic stem cells*. *J Cell Biol*, 2011. **195**(5): p. 709-20.
6. Conover, J.C. and R.Q. Notti, *The neural stem cell niche*. *Cell Tissue Res*, 2008. **331**(1): p. 211-24.
7. Kenyon, J. and S.L. Gerson, *The role of DNA damage repair in aging of adult stem cells*. *Nucleic Acids Res*, 2007. **35**(22): p. 7557-65.
8. Gopinath, S.D. and T.A. Rando, *Stem cell review series: aging of the skeletal muscle stem cell niche*. *Aging Cell*, 2008. **7**(4): p. 590-598.
9. Smith, J.A. and R. Daniel, *Stem cells and aging: a chicken-or-the-egg issue?* *Aging Dis*, 2012. **3**(3): p. 260-8.
10. Conboy, I.M., et al., *Rejuvenation of aged progenitor cells by exposure to a young systemic environment*. *Nature*, 2005. **433**(7027): p. 760-764.
11. Brooks, S.V. and J.A. Faulkner, *Contractile properties of skeletal muscles from young, adult and aged mice*. *J Physiol*, 1988. **404**: p. 71-82.
12. Bouab, M., et al., *Aging of the subventricular zone neural stem cell niche: evidence for quiescence-associated changes between early and mid-adulthood*. *Neuroscience*, 2011. **173**: p. 135-49.
13. Molofsky, A.V., et al., *Increasing p16INK4a expression decreases forebrain progenitors and neurogenesis during ageing*. *Nature*, 2006. **443**(7110): p. 448-52.
14. Jarrard, L.E., *What does the hippocampus really do?* *Behav Brain Res*, 1995. **71**(1-2): p. 1-10.
15. Drapeau, E., et al., *Spatial memory performances of aged rats in the water maze predict levels of hippocampal neurogenesis*. *Proc Natl Acad Sci U S A*, 2003. **100**(24): p. 14385-90.
16. Bizon, J.L., H.J. Lee, and M. Gallagher, *Neurogenesis in a rat model of age-related cognitive decline*. *Aging Cell*, 2004. **3**(4): p. 227-34.
17. Bishop, N.A., T. Lu, and B.A. Yankner, *Neural mechanisms of ageing and cognitive decline*. *Nature*, 2010. **464**(7288): p. 529-35.
18. Sharpless, N.E. and R.A. DePinho, *How stem cells age and why this makes us grow old*. *Nat Rev Mol Cell Biol*, 2007. **8**(9): p. 703-13.
19. Drummond-Barbosa, D., *Stem cells, their niches and the systemic environment: an aging network*. *Genetics*, 2008. **180**(4): p. 1787-97.
20. Voog, J. and D.L. Jones, *Stem cells and the niche: a dynamic duo*. *Cell Stem Cell*, 2010. **6**(2): p. 103-15.
21. Geiger, H., G. de Haan, and M.C. Florian, *The ageing haematopoietic stem cell compartment*. *Nat Rev Immunol*, 2013. **13**(5): p. 376-89.

Bibliography

22. Issa, J.P., *Age-related epigenetic changes and the immune system*. Clin Immunol, 2003. **109**(1): p. 103-8.
23. Gonzalo, S., *Epigenetic alterations in aging*. J Appl Physiol, 2010. **109**(2): p. 586-97.
24. Conover, J.C. and B.A. Shook, *Aging of the subventricular zone neural stem cell niche*. Aging Dis, 2011. **2**(1): p. 49-63.
25. Grefte, S., et al., *Skeletal muscle development and regeneration*. Stem Cells Dev, 2007. **16**(5): p. 857-68.
26. Armand, O., et al., *Origin of satellite cells in avian skeletal muscles*. Arch Anat Microsc Morphol Exp, 1983. **72**(2): p. 163-81.
27. Tajbakhsh, S. and M.E. Buckingham, *Mouse limb muscle is determined in the absence of the earliest myogenic factor myf-5*. Proc Natl Acad Sci U S A, 1994. **91**(2): p. 747-51.
28. Ontell, M. and K. Kozeka, *Organogenesis of the mouse extensor digitorum logus muscle: a quantitative study*. Am J Anat, 1984. **171**(2): p. 149-61.
29. Ontell, M., et al., *Myosatellite cells, growth, and regeneration in murine dystrophic muscle: a quantitative study*. Anat Rec, 1984. **208**(2): p. 159-74.
30. Zammit, P.S., T.A. Partridge, and Z. Yablonka-Reuveni, *The skeletal muscle satellite cell: the stem cell that came in from the cold*. J.Histochem.Cytochem., 2006. **54**(11): p. 1177-1191.
31. Trainor, P.A., S.S. Tan, and P.P. Tam, *Cranial paraxial mesoderm: regionalisation of cell fate and impact on craniofacial development in mouse embryos*. Development, 1994. **120**(9): p. 2397-408.
32. Hacker, A. and S. Guthrie, *A distinct developmental programme for the cranial paraxial mesoderm in the chick embryo*. Development, 1998. **125**(17): p. 3461-72.
33. Noden, D.M., *The embryonic origins of avian cephalic and cervical muscles and associated connective tissues*. Am J Anat, 1983. **168**(3): p. 257-76.
34. Seale, P., et al., *Pax7 is required for the specification of myogenic satellite cells*. Cell, 2000. **102**(6): p. 777-786.
35. McGeachie, J.K. and M.D. Grounds, *The timing between skeletal muscle myoblast replication and fusion into myotubes, and the stability of regenerated dystrophic myofibres: an autoradiographic study in mdx mice*. J Anat, 1999. **194** (Pt 2): p. 287-95.
36. Schultz, E., *Changes in the satellite cells of growing muscle following denervation*. Anat.Rec., 1978. **190**(2): p. 299-311.
37. Schmalbruch, H. and D.M. Lewis, *Dynamics of nuclei of muscle fibers and connective tissue cells in normal and denervated rat muscles* 7. Muscle Nerve, 2000. **23**(4): p. 617-626.
38. Reznik, M., *Thymidine-3H uptake by satellite cells of regenerating skeletal muscle*. J Cell Biol, 1969. **40**(2): p. 568-71.
39. Shafiq, S.A. and M.A. Gorycki, *Regeneration in skeletal muscle of mouse: some electron-microscope observations*. J Pathol Bacteriol, 1965. **90**(1): p. 123-7.
40. Bischoff, R., *Regeneration of single skeletal muscle fibers in vitro*. Anat.Rec., 1975. **182**(2): p. 215-235.
41. Konigsberg, U.R.L., B. H. Konigsberg, I. R., *The regenerative response of single mature muscle fibers isolated in vitro*. Dev.Biol., 1975(45): p. 260-275.
42. Shea, K.L., et al., *Sprouty1 regulates reversible quiescence of a self-renewing adult muscle stem cell pool during regeneration*. Cell Stem Cell, 2010. **6**(2): p. 117-129.
43. Lepper, C., S.J. Conway, and C.M. Fan, *Adult satellite cells and embryonic muscle progenitors have distinct genetic requirements*. Nature, 2009. **460**(7255): p. 627-631.

Bibliography

44. Blaveri, K., et al., *Patterns of repair of dystrophic mouse muscle: studies on isolated fibers*. Dev.Dyn., 1999. **216**(3): p. 244-256.
45. Heslop, L., et al., *Transplanted primary neonatal myoblasts can give rise to functional satellite cells as identified using the Myf5nlacZ⁺ mouse*. Gene Ther., 2001. **8**(10): p. 778-783.
46. Watt, D.J., et al., *The movement of muscle precursor cells between adjacent regenerating muscles in the mouse*. Anat.Embryol.(Berl), 1987. **175**(4): p. 527-536.
47. Partridge, T.A., et al., *Conversion of mdx myofibres from dystrophin-negative to -positive by injection of normal myoblasts*. Nature, 1989. **337**(6203): p. 176-9.
48. Yao, S.N. and K. Kurachi, *Implanted myoblasts not only fuse with myofibers but also survive as muscle precursor cells*. J Cell Sci, 1993. **105 (Pt 4)**: p. 957-63.
49. Morgan, J.E., et al., *Myogenic cell lines derived from transgenic mice carrying a thermolabile T antigen: a model system for the derivation of tissue-specific and mutation-specific cell lines*. Dev Biol, 1994. **162**(2): p. 486-98.
50. Gross, J.G. and J.E. Morgan, *Muscle precursor cells injected into irradiated mdx mouse muscle persist after serial injury*. Muscle Nerve, 1999. **22**(2): p. 174-85.
51. Cousins, J.C., et al., *Regeneration of skeletal muscle from transplanted immortalised myoblasts is oligoclonal*. J Cell Sci, 2004. **117**(Pt 15): p. 3259-69.
52. Rocheteau, P., et al., *A subpopulation of adult skeletal muscle stem cells retains all template DNA strands after cell division*. Cell, 2012. **148**(1-2): p. 112-25.
53. Collins, C.A., et al., *Stem cell function, self-renewal, and behavioral heterogeneity of cells from the adult muscle satellite cell niche*. Cell, 2005. **122**(2): p. 289-301.
54. Sacco, A., et al., *Self-renewal and expansion of single transplanted muscle stem cells*. Nature, 2008. **456**(7221): p. 502-506.
55. Rosenblatt, J.D. and D.J. Parry, *Gamma irradiation prevents compensatory hypertrophy of overloaded mouse extensor digitorum longus muscle*. J Appl Physiol, 1992. **73**(6): p. 2538-43.
56. Ten Broek, R.W., S. Grefte, and J.W. Von den Hoff, *Regulatory factors and cell populations involved in skeletal muscle regeneration*. J.Cell Physiol, 2010. **224**(1): p. 7-16.
57. Ivanova, A., et al., *In vivo genetic ablation by Cre-mediated expression of diphtheria toxin fragment A*. Genesis., 2005. **43**(3): p. 129-135.
58. Lepper, C., T.A. Partridge, and C.M. Fan, *An absolute requirement for Pax7-positive satellite cells in acute injury-induced skeletal muscle regeneration*. Development, 2011. **138**(17): p. 3639-46.
59. Murphy, M.M., et al., *Satellite cells, connective tissue fibroblasts and their interactions are crucial for muscle regeneration*. Development, 2011. **138**(17): p. 3625-37.
60. McCarthy, J.J., et al., *Effective fiber hypertrophy in satellite cell-depleted skeletal muscle*. Development, 2011. **138**(17): p. 3657-66.
61. Sambasivan, R., et al., *Pax7-expressing satellite cells are indispensable for adult skeletal muscle regeneration*. Development, 2011. **138**(17): p. 3647-56.
62. Hayashi, S., et al., *Expression patterns of Xenopus FGF receptor-like 1/nou-darake in early Xenopus development resemble those of planarian nou-darake and Xenopus FGF8*. Dev.Dyn., 2004. **230**(4): p. 700-707.
63. Sheehan, S.M., et al., *HGF is an autocrine growth factor for skeletal muscle satellite cells in vitro*. Muscle Nerve, 2000. **23**(2): p. 239-245.
64. Engert, J.C., E.B. Berglund, and N. Rosenthal, *Proliferation precedes differentiation in IGF-I-stimulated myogenesis*. J Cell Biol, 1996. **135**(2): p. 431-40.

Bibliography

65. Chakravarthy, M.V., B.S. Davis, and F.W. Booth, *IGF-I restores satellite cell proliferative potential in immobilized old skeletal muscle*. J Appl Physiol, 2000. **89**(4): p. 1365-79.
66. Philippou, A., et al., *Type I insulin-like growth factor receptor signaling in skeletal muscle regeneration and hypertrophy*. J Musculoskelet Neuronal Interact, 2007. **7**(3): p. 208-18.
67. Florini, J.R., D.Z. Ewton, and S.L. Roof, *Insulin-like growth factor-I stimulates terminal myogenic differentiation by induction of myogenin gene expression*. Mol Endocrinol, 1991. **5**(5): p. 718-24.
68. Husmann, I., et al., *Growth factors in skeletal muscle regeneration*. Cytokine Growth Factor Rev, 1996. **7**(3): p. 249-58.
69. Allen, R.E. and L.K. Boxhorn, *Inhibition of skeletal muscle satellite cell differentiation by transforming growth factor-beta*. J Cell Physiol, 1987. **133**(3): p. 567-572.
70. McLennan, I.S. and K. Koishi, *The transforming growth factor-betas: multifaceted regulators of the development and maintenance of skeletal muscles, motoneurons and Schwann cells*. Int J Dev Biol, 2002. **46**(4): p. 559-67.
71. Florini, J.R., D.Z. Ewton, and S.A. Coolican, *Growth hormone and the insulin-like growth factor system in myogenesis*. Endocr Rev, 1996. **17**(5): p. 481-517.
72. Collins, R.A. and M.D. Grounds, *The role of tumor necrosis factor-alpha (TNF-alpha) in skeletal muscle regeneration. Studies in TNF-alpha(-/-) and TNF-alpha(-/-)/LT-alpha(-/-) mice*. J Histochem Cytochem, 2001. **49**(8): p. 989-1001.
73. Warren, G.L., et al., *Physiological role of tumor necrosis factor alpha in traumatic muscle injury*. FASEB J, 2002. **16**(12): p. 1630-2.
74. Li, Y.P., *TNF-alpha is a mitogen in skeletal muscle*. Am J Physiol Cell Physiol, 2003. **285**(2): p. C370-6.
75. Reid, M.B. and Y.P. Li, *Tumor necrosis factor-alpha and muscle wasting: a cellular perspective*. Respir Res, 2001. **2**(5): p. 269-72.
76. Luo, G., et al., *IL-1beta stimulates IL-6 production in cultured skeletal muscle cells through activation of MAP kinase signaling pathway and NF-kappa B*. Am J Physiol Regul Integr Comp Physiol, 2003. **284**(5): p. R1249-54.
77. Doumit, M.E., D.R. Cook, and R.A. Merkel, *Fibroblast growth factor, epidermal growth factor, insulin-like growth factors, and platelet-derived growth factor-BB stimulate proliferation of clonally derived porcine myogenic satellite cells*. J Cell Physiol, 1993. **157**(2): p. 326-32.
78. Wrobel, E., E. Brzoska, and J. Moraczewski, *M-cadherin and beta-catenin participate in differentiation of rat satellite cells*. Eur J Cell Biol, 2007. **86**(2): p. 99-109.
79. Otto, A., et al., *Canonical Wnt signalling induces satellite-cell proliferation during adult skeletal muscle regeneration*. J Cell Sci, 2008. **121**(Pt 17): p. 2939-50.
80. Goichberg, P., et al., *Recruitment of beta-catenin to cadherin-mediated intercellular adhesions is involved in myogenic induction*. J Cell Sci, 2001. **114**(Pt 7): p. 1309-19.
81. Gavard, J., et al., *N-cadherin activation substitutes for the cell contact control in cell cycle arrest and myogenic differentiation: involvement of p120 and beta-catenin*. J Biol Chem, 2004. **279**(35): p. 36795-802.
82. Ishido, M., et al., *Alterations of M-cadherin, neural cell adhesion molecule and beta-catenin expression in satellite cells during overload-induced skeletal muscle hypertrophy*. Acta Physiol (Oxf), 2006. **187**(3): p. 407-18.
83. Brack, A.S., et al., *BCL9 is an essential component of canonical Wnt signaling that mediates the differentiation of myogenic progenitors during muscle regeneration*. Dev Biol, 2009.

Bibliography

84. Kim, C.H., et al., *Beta-catenin interacts with MyoD and regulates its transcription activity*. Mol Cell Biol, 2008. **28**(9): p. 2941-51.
85. Brohl, D., et al., *Colonization of the satellite cell niche by skeletal muscle progenitor cells depends on Notch signals*. Dev Cell, 2012. **23**(3): p. 469-81.
86. Vasyutina, E., et al., *RBP-J (Rbpsiuh) is essential to maintain muscle progenitor cells and to generate satellite cells*. Proc Natl Acad Sci U S A, 2007. **104**(11): p. 4443-8.
87. Schuster-Gossler, K., R. Cordes, and A. Gossler, *Premature myogenic differentiation and depletion of progenitor cells cause severe muscle hypotrophy in Delta1 mutants*. Proc Natl Acad Sci U S A, 2007. **104**(2): p. 537-42.
88. Conboy, I.M. and T.A. Rando, *The regulation of Notch signaling controls satellite cell activation and cell fate determination in postnatal myogenesis*. Dev.Cell, 2002. **3**(3): p. 397-409.
89. Fukada, S., et al., *Molecular signature of quiescent satellite cells in adult skeletal muscle*. Stem Cells, 2007. **25**(10): p. 2448-2459.
90. Sun, H., et al., *Stra13 regulates satellite cell activation by antagonizing Notch signaling*. J Cell Biol, 2007. **177**(4): p. 647-57.
91. Mourikis, P., et al., *A critical requirement for notch signaling in maintenance of the quiescent skeletal muscle stem cell state*. Stem Cells, 2012. **30**(2): p. 243-52.
92. Brack, A.S., et al., *A temporal switch from notch to Wnt signaling in muscle stem cells is necessary for normal adult myogenesis*. Cell Stem Cell, 2008. **2**(1): p. 50-59.
93. Shinin, V., et al., *Asymmetric division and cosegregation of template DNA strands in adult muscle satellite cells*. Nat Cell Biol, 2006. **8**(7): p. 677-87.
94. Knox, S., et al., *Not all perlecanans are created equal: interactions with fibroblast growth factor (FGF) 2 and FGF receptors*. J Biol Chem, 2002. **277**(17): p. 14657-65.
95. Kiselyov, V.V., et al., *Structural basis for a direct interaction between FGFR1 and NCAM and evidence for a regulatory role of ATP*. Structure, 2003. **11**(6): p. 691-701.
96. Sanchez-Heras, E., et al., *The fibroblast growth factor receptor acid box is essential for interactions with N-cadherin and all of the major isoforms of neural cell adhesion molecule*. J Biol Chem, 2006. **281**(46): p. 35208-16.
97. Kastner, S., et al., *Gene expression patterns of the fibroblast growth factors and their receptors during myogenesis of rat satellite cells*. J.Histochem.Cytochem., 2000. **48**(8): p. 1079-1096.
98. Sheehan, S.M. and R.E. Allen, *Skeletal muscle satellite cell proliferation in response to members of the fibroblast growth factor family and hepatocyte growth factor*. J.Cell Physiol, 1999. **181**(3): p. 499-506.
99. Zhao, P., et al., *Fgfr4 is required for effective muscle regeneration in vivo. Delineation of a MyoD-Tead2-Fgfr4 transcriptional pathway*. J Biol Chem, 2006. **281**(1): p. 429-38.
100. Yablonka-Reuveni, Z. and A.J. Rivera, *Temporal expression of regulatory and structural muscle proteins during myogenesis of satellite cells on isolated adult rat fibers*. Dev.Biol., 1994. **164**(2): p. 588-603.
101. Yablonka-Reuveni, Z., R. Seger, and A.J. Rivera, *Fibroblast growth factor promotes recruitment of skeletal muscle satellite cells in young and old rats*. J.Histochem.Cytochem., 1999. **47**(1): p. 23-42.
102. Clegg, C.H., et al., *Growth factor control of skeletal muscle differentiation: commitment to terminal differentiation occurs in G1 phase and is repressed by fibroblast growth factor*. J Cell Biol, 1987. **105**(2): p. 949-56.

Bibliography

103. Alterio, J., et al., *Acidic and basic fibroblast growth factor mRNAs are expressed by skeletal muscle satellite cells*. *Biochem Biophys Res Commun*, 1990. **166**(3): p. 1205-12.
104. Groux-Muscatelli, B., et al., *Proliferating satellite cells express acidic fibroblast growth factor during in vitro myogenesis*. *Dev Biol*, 1990. **142**(2): p. 380-5.
105. Rosenthal, S.M., et al., *Fibroblast growth factor inhibits insulin-like growth factor-II (IGF-II) gene expression and increases IGF-I receptor abundance in BC3H-1 muscle cells*. *Mol Endocrinol*, 1991. **5**(5): p. 678-84.
106. Emoto, N., et al., *Basic fibroblast growth factor (FGF) in the central nervous system: identification of specific loci of basic FGF expression in the rat brain*. *Growth Factors*, 1989. **2**(1): p. 21-9.
107. Anderson, J.E., L. Liu, and E. Kardami, *Distinctive patterns of basic fibroblast growth factor (bFGF) distribution in degenerating and regenerating areas of dystrophic (mdx) striated muscles*. *Dev Biol*, 1991. **147**(1): p. 96-109.
108. Grounds, M.D., *Towards understanding skeletal muscle regeneration*. *Pathol Res Pract*, 1991. **187**(1): p. 1-22.
109. Flanagan-Steet, H., et al., *Loss of FGF receptor 1 signaling reduces skeletal muscle mass and disrupts myofiber organization in the developing limb*. *Dev.Biol.*, 2000. **218**(1): p. 21-37.
110. Itoh, N., T. Mima, and T. Mikawa, *Loss of fibroblast growth factor receptors is necessary for terminal differentiation of embryonic limb muscle*. *Development*, 1996. **122**(1): p. 291-300.
111. Marics, I., et al., *FGFR4 signaling is a necessary step in limb muscle differentiation*. *Development*, 2002. **129**(19): p. 4559-69.
112. Lagha, M., et al., *Pax3 regulation of FGF signaling affects the progression of embryonic progenitor cells into the myogenic program*. *Genes Dev.*, 2008. **22**(13): p. 1828-1837.
113. Lefaucheur, J.P. and A. Sebille, *Muscle regeneration following injury can be modified in vivo by immune neutralization of basic fibroblast growth factor, transforming growth factor beta 1 or insulin-like growth factor I*. *J Neuroimmunol*, 1995. **57**(1-2): p. 85-91.
114. Floss, T., H.H. Arnold, and T. Braun, *A role for FGF-6 in skeletal muscle regeneration*. *Genes Dev*, 1997. **11**(16): p. 2040-51.
115. Neuhaus, P., et al., *Reduced mobility of fibroblast growth factor (FGF)-deficient myoblasts might contribute to dystrophic changes in the musculature of FGF2/FGF6/mdx triple-mutant mice*. *Mol Cell Biol*, 2003. **23**(17): p. 6037-48.
116. McLoon, L.K., et al., *Continuous myofiber remodeling in uninjured extraocular myofibers: myonuclear turnover and evidence for apoptosis*. *Muscle Nerve*, 2004. **29**(5): p. 707-15.
117. Porter, J.D., et al., *Constitutive properties, not molecular adaptations, mediate extraocular muscle sparing in dystrophic mdx mice*. *FASEB J*, 2003. **17**(8): p. 893-5.
118. Lagord, C., et al., *Differential myogenicity of satellite cells isolated from extensor digitorum longus (EDL) and soleus rat muscles revealed in vitro*. *Cell Tissue Res*, 1998. **291**(3): p. 455-68.
119. Day, K., et al., *Nestin-GFP reporter expression defines the quiescent state of skeletal muscle satellite cells*. *Dev.Biol.*, 2007. **304**(1): p. 246-259.
120. Nagata, Y., et al., *Sphingomyelin levels in the plasma membrane correlate with the activation state of muscle satellite cells*. *J.Histochem.Cytochem.*, 2006. **54**(4): p. 375-384.
121. Kuang, S., et al., *Asymmetric self-renewal and commitment of satellite stem cells in muscle*. *Cell*, 2007. **129**(5): p. 999-1010.

Bibliography

122. Gayraud-Morel, B., et al., *Myf5 haploinsufficiency reveals distinct cell fate potentials for adult skeletal muscle stem cells*. J Cell Sci, 2012. **125**(Pt 7): p. 1738-49.
123. Conboy, M.J., A.O. Karasov, and T.A. Rando, *High incidence of non-random template strand segregation and asymmetric fate determination in dividing stem cells and their progeny*. PLoS.Biol., 2007. **5**(5): p. e102.
124. Shinin, V., B. Gayraud-Morel, and S. Tajbakhsh, *Template DNA-strand co-segregation and asymmetric cell division in skeletal muscle stem cells*. Methods Mol.Biol., 2009. **482**: p. 295-317.
125. Kanisicak, O., et al., *Progenitors of skeletal muscle satellite cells express the muscle determination gene, MyoD*. Dev.Biol., 2009.
126. Schultz, E., *Satellite cell proliferative compartments in growing skeletal muscles*. Dev Biol, 1996. **175**(1): p. 84-94.
127. Ono, Y., et al., *Slow-dividing satellite cells retain long-term self-renewal ability in adult muscle*. J Cell Sci, 2012. **125**(Pt 5): p. 1309-17.
128. Bischoff, R., *Interaction between satellite cells and skeletal muscle fibers*. Development, 1990. **109**(4): p. 943-952.
129. Ratajczak, M.Z., et al., *Expression of functional CXCR4 by muscle satellite cells and secretion of SDF-1 by muscle-derived fibroblasts is associated with the presence of both muscle progenitors in bone marrow and hematopoietic stem/progenitor cells in muscles*. Stem Cells, 2003. **21**(3): p. 363-71.
130. Conboy, I.M., et al., *Notch-mediated restoration of regenerative potential to aged muscle*. Science, 2003. **302**(5650): p. 1575-1577.
131. Langsdorf, A., et al., *Sulfs are regulators of growth factor signaling for satellite cell differentiation and muscle regeneration*. Dev Biol, 2007. **311**(2): p. 464-77.
132. Olwin, B.B. and A. Rapraeger, *Repression of myogenic differentiation by aFGF, bFGF, and K-FGF is dependent on cellular heparan sulfate*. J Cell Biol, 1992. **118**(3): p. 631-9.
133. Tatsumi, R., et al., *HGF/SF is present in normal adult skeletal muscle and is capable of activating satellite cells*. Dev.Biol., 1998. **194**(1): p. 114-128.
134. Yamada, M., et al., *Matrix metalloproteinases are involved in mechanical stretch-induced activation of skeletal muscle satellite cells*. Muscle Nerve, 2006. **34**(3): p. 313-319.
135. Mathew, S.J., et al., *Connective tissue fibroblasts and Tcf4 regulate myogenesis*. Development, 2011. **138**(2): p. 371-84.
136. Schmalbruch, H., *The morphology of regeneration of skeletal muscles in the rat*. Tissue Cell, 1976. **8**(4): p. 673-92.
137. Christov, C., et al., *Muscle satellite cells and endothelial cells: close neighbors and privileged partners*. Mol Biol Cell, 2007. **18**(4): p. 1397-409.
138. Abou-Khalil, R., et al., *Autocrine and paracrine angiopoietin 1/Tie-2 signaling promotes muscle satellite cell self-renewal*. Cell Stem Cell, 2009. **5**(3): p. 298-309.
139. Yin, H., F. Price, and M.A. Rudnicki, *Satellite cells and the muscle stem cell niche*. Physiol Rev, 2013. **93**(1): p. 23-67.
140. Schultz, E., *Changes in the satellite cells of growing muscle following denervation*. Anat Rec, 1978. **190**(2): p. 299-311.
141. Rodrigues, A.C. and H. Schmalbruch, *Satellite cells and myonuclei in long-term denervated rat muscles 19*. Anat.Rec., 1995. **243**(4): p. 430-437.
142. Viguie, C.A., et al., *Quantitative study of the effects of long-term denervation on the extensor digitorum longus muscle of the rat*. Anat Rec, 1997. **248**(3): p. 346-54.

Bibliography

143. Kuschel, R., Z. Yablonka-Reuveni, and A. Bornemann, *Satellite cells on isolated myofibers from normal and denervated adult rat muscle*. *J Histochem Cytochem*, 1999. **47**(11): p. 1375-84.
144. Jejurikar, S.S., C.L. Marcelo, and W.M. Kuzon, Jr., *Skeletal muscle denervation increases satellite cell susceptibility to apoptosis*. *Plast Reconstr Surg*, 2002. **110**(1): p. 160-8.
145. Hermanson, J.W., M.C. Moschella, and M. Ontell, *Effect of neonatal denervation-reinnervation on the functional capacity of a 129ReJ dy/dy murine dystrophic muscle*. *Exp Neurol*, 1988. **102**(2): p. 210-6.
146. Brack, A.S. and T.A. Rando, *Intrinsic changes and extrinsic influences of myogenic stem cell function during aging*. *Stem Cell Rev.*, 2007. **3**(3): p. 226-237.
147. Conboy, I.M. and T.A. Rando, *Aging, stem cells and tissue regeneration: lessons from muscle*. *Cell Cycle*, 2005. **4**(3): p. 407-10.
148. Shavlakadze, T., J. McGeachie, and M.D. Grounds, *Delayed but excellent myogenic stem cell response of regenerating geriatric skeletal muscles in mice*. *Biogerontology*, 2010. **11**(3): p. 363-76.
149. Brack, A.S., H. Bildsoe, and S.M. Hughes, *Evidence that satellite cell decrement contributes to preferential decline in nuclear number from large fibres during murine age-related muscle atrophy*. *J Cell Sci*, 2005. **118**(Pt 20): p. 4813-21.
150. Collins, C.A., et al., *A population of myogenic stem cells that survives skeletal muscle aging*. *Stem Cells*, 2007. **25**(4): p. 885-894.
151. Shefer, G., et al., *Satellite-cell pool size does matter: defining the myogenic potency of aging skeletal muscle*. *Dev.Biol.*, 2006. **294**(1): p. 50-66.
152. Sacco, A., et al., *Short telomeres and stem cell exhaustion model Duchenne muscular dystrophy in mdx/mTR mice*. *Cell*, 2010. **143**(7): p. 1059-1071.
153. Decary, S., et al., *Replicative potential and telomere length in human skeletal muscle: implications for satellite cell-mediated gene therapy*. *Hum Gene Ther*, 1997. **8**(12): p. 1429-38.
154. Harley, C.B. and B. Villeponteau, *Telomeres and telomerase in aging and cancer*. *Curr Opin Genet Dev*, 1995. **5**(2): p. 249-55.
155. Renault, V., et al., *Skeletal muscle regeneration and the mitotic clock*. *Exp Gerontol*, 2000. **35**(6-7): p. 711-9.
156. Decary, S., et al., *Shorter telomeres in dystrophic muscle consistent with extensive regeneration in young children*. *Neuromuscul Disord*, 2000. **10**(2): p. 113-20.
157. Gardner, J.P., et al., *Telomere dynamics in macaques and humans*. *J Gerontol A Biol Sci Med Sci*, 2007. **62**(4): p. 367-74.
158. Bortoli, S., et al., *Gene expression profiling of human satellite cells during muscular aging using cDNA arrays*. *Gene*, 2003. **321**: p. 145-54.
159. Schultz, E. and B.H. Lipton, *Skeletal muscle satellite cells: changes in proliferation potential as a function of age*. *Mech Ageing Dev*, 1982. **20**(4): p. 377-83.
160. Barani, A.E., et al., *Age-related changes in the mitotic and metabolic characteristics of muscle-derived cells*. *J Appl Physiol*, 2003. **95**(5): p. 2089-98.
161. Asakura, A., M. Komaki, and M. Rudnicki, *Muscle satellite cells are multipotential stem cells that exhibit myogenic, osteogenic, and adipogenic differentiation*. *Differentiation*, 2001. **68**(4-5): p. 245-53.
162. Wada, M.R., et al., *Generation of different fates from multipotent muscle stem cells*. *Development*, 2002. **129**(12): p. 2987-95.

Bibliography

163. Shefer, G., M. Wleklinski-Lee, and Z. Yablonka-Reuveni, *Skeletal muscle satellite cells can spontaneously enter an alternative mesenchymal pathway*. J Cell Sci, 2004. **117**(Pt 22): p. 5393-404.
164. Brack, A.S., et al., *Increased Wnt signaling during aging alters muscle stem cell fate and increases fibrosis*. Science, 2007. **317**(5839): p. 807-810.
165. Naito, A.T., et al., *Complement C1q activates canonical Wnt signaling and promotes aging-related phenotypes*. Cell, 2012. **149**(6): p. 1298-313.
166. Charge, S.B., A.S. Brack, and S.M. Hughes, *Aging-related satellite cell differentiation defect occurs prematurely after Ski-induced muscle hypertrophy*. Am.J.Physiol Cell Physiol, 2002. **283**(4): p. C1228-C1241.
167. Pan, L., et al., *Stem cell aging is controlled both intrinsically and extrinsically in the Drosophila ovary*. Cell Stem Cell, 2007. **1**(4): p. 458-69.
168. Boyle, M., et al., *Decline in self-renewal factors contributes to aging of the stem cell niche in the Drosophila testis*. Cell Stem Cell, 2007. **1**(4): p. 470-8.
169. Carlson, B.M. and J.A. Faulkner, *Muscle transplantation between young and old rats: age of host determines recovery*. Am.J.Physiol, 1989. **256**(6 Pt 1): p. C1262-C1266.
170. Ryan, N.A., et al., *Lower skeletal muscle capillarization and VEGF expression in aged vs. young men*. J.Appl.Physiol, 2006. **100**(1): p. 178-185.
171. Snow, M.H., *The effects of aging on satellite cells in skeletal muscles of mice and rats*. Cell Tissue Res., 1977. **185**(3): p. 399-408.
172. Goldspink, G., et al., *Age-related changes in collagen gene expression in the muscles of mdx dystrophic and normal mice*. Neuromuscul Disord, 1994. **4**(3): p. 183-91.
173. Alexakis, C., T. Partridge, and G. Bou-Gharios, *Implication of the satellite cell in dystrophic muscle fibrosis: a self perpetuating mechanism of collagen over-production*. Am.J.Physiol Cell Physiol, 2007.
174. Carlson, M.E., M. Hsu, and I.M. Conboy, *Imbalance between pSmad3 and Notch induces CDK inhibitors in old muscle stem cells*. Nature, 2008. **454**(7203): p. 528-532.
175. Carlson, M.E., et al., *Relative roles of TGF-beta1 and Wnt in the systemic regulation and aging of satellite cell responses*. Aging Cell, 2009. **8**(6): p. 676-689.
176. Beggs, M.L., et al., *Alterations in the TGFbeta signaling pathway in myogenic progenitors with age*. Aging Cell, 2004. **3**(6): p. 353-361.
177. Burks, T.N., et al., *Losartan restores skeletal muscle remodeling and protects against disuse atrophy in sarcopenia*. Sci Transl Med, 2011. **3**(82): p. 82ra37.
178. Lorts, A., et al., *Deletion of periostin reduces muscular dystrophy and fibrosis in mice by modulating the transforming growth factor-beta pathway*. Proc Natl Acad Sci U S A, 2012. **109**(27): p. 10978-83.
179. Ashcroft, G.S., S.J. Mills, and J.J. Ashworth, *Ageing and wound healing*. Biogerontology, 2002. **3**(6): p. 337-45.
180. Fahim, M.A. and N. Robbins, *Ultrastructural studies of young and old mouse neuromuscular junctions*. J Neurocytol, 1982. **11**(4): p. 641-56.
181. Jejurikar, S.S., et al., *Aging increases the susceptibility of skeletal muscle derived satellite cells to apoptosis*. Exp.Gerontol., 2006. **41**(9): p. 828-836.
182. Zammit, P.S., T.A. Partridge, and Z. Yablonka-Reuveni, *The skeletal muscle satellite cell: the stem cell that came in from the cold*. J Histochem Cytochem, 2006. **54**(11): p. 1177-91.
183. Doetsch, F., *A niche for adult neural stem cells*. Curr Opin Genet Dev, 2003. **13**(5): p. 543-50.

Bibliography

184. Artegiani, B. and F. Calegari, *Age-related cognitive decline: can neural stem cells help us?* Aging (Albany NY), 2012. **4**(3): p. 176-86.
185. Anthony, T.E., et al., *Radial glia serve as neuronal progenitors in all regions of the central nervous system.* Neuron, 2004. **41**(6): p. 881-90.
186. Kriegstein, A. and A. Alvarez-Buylla, *The glial nature of embryonic and adult neural stem cells.* Annu Rev Neurosci, 2009. **32**: p. 149-84.
187. Altman, J. and G.D. Das, *Autoradiographic and histological evidence of postnatal hippocampal neurogenesis in rats.* J Comp Neurol, 1965. **124**(3): p. 319-35.
188. Goldman, S.A. and F. Nottebohm, *Neuronal production, migration, and differentiation in a vocal control nucleus of the adult female canary brain.* Proc Natl Acad Sci U S A, 1983. **80**(8): p. 2390-4.
189. Spalding, K.L., et al., *Dynamics of hippocampal neurogenesis in adult humans.* Cell, 2013. **153**(6): p. 1219-27.
190. Seri, B., et al., *Astrocytes give rise to new neurons in the adult mammalian hippocampus.* J Neurosci, 2001. **21**(18): p. 7153-60.
191. Imura, T., H.I. Kornblum, and M.V. Sofroniew, *The predominant neural stem cell isolated from postnatal and adult forebrain but not early embryonic forebrain expresses GFAP.* J Neurosci, 2003. **23**(7): p. 2824-32.
192. Morshead, C.M., et al., *The ablation of glial fibrillary acidic protein-positive cells from the adult central nervous system results in the loss of forebrain neural stem cells but not retinal stem cells.* Eur J Neurosci, 2003. **18**(1): p. 76-84.
193. Mu, Y., S.W. Lee, and F.H. Gage, *Signaling in adult neurogenesis.* Curr Opin Neurobiol, 2010. **20**(4): p. 416-23.
194. Gross, R.E., et al., *Bone morphogenetic proteins promote astroglial lineage commitment by mammalian subventricular zone progenitor cells.* Neuron, 1996. **17**(4): p. 595-606.
195. Gage, F.H., *Mammalian neural stem cells.* Science, 2000. **287**(5457): p. 1433-8.
196. Bonaguidi, M.A., et al., *In vivo clonal analysis reveals self-renewing and multipotent adult neural stem cell characteristics.* Cell, 2011. **145**(7): p. 1142-55.
197. Eriksson, P.S., et al., *Neurogenesis in the adult human hippocampus.* Nat Med, 1998. **4**(11): p. 1313-7.
198. Bergmann, O., et al., *The age of olfactory bulb neurons in humans.* Neuron, 2012. **74**(4): p. 634-9.
199. Ray, J., et al., *Proliferation, differentiation, and long-term culture of primary hippocampal neurons.* Proc Natl Acad Sci U S A, 1993. **90**(8): p. 3602-6.
200. Reynolds, B.A. and S. Weiss, *Generation of neurons and astrocytes from isolated cells of the adult mammalian central nervous system.* Science, 1992. **255**(5052): p. 1707-10.
201. Doetsch, F., et al., *Subventricular zone astrocytes are neural stem cells in the adult mammalian brain.* Cell, 1999. **97**(6): p. 703-16.
202. Lazarini, F. and P.M. Lledo, *Is adult neurogenesis essential for olfaction?* Trends Neurosci, 2011. **34**(1): p. 20-30.
203. Ming, G.L. and H. Song, *Adult neurogenesis in the mammalian brain: significant answers and significant questions.* Neuron, 2011. **70**(4): p. 687-702.
204. Sakamoto, M., et al., *Continuous neurogenesis in the adult forebrain is required for innate olfactory responses.* Proc Natl Acad Sci U S A, 2011. **108**(20): p. 8479-84.
205. Alvarez-Buylla, A. and J.M. Garcia-Verdugo, *Neurogenesis in adult subventricular zone.* J Neurosci, 2002. **22**(3): p. 629-34.

Bibliography

206. Lledo, P.M., M. Alonso, and M.S. Grubb, *Adult neurogenesis and functional plasticity in neuronal circuits*. Nat Rev Neurosci, 2006. **7**(3): p. 179-93.
207. Lledo, P.M., F.T. Merkle, and A. Alvarez-Buylla, *Origin and function of olfactory bulb interneuron diversity*. Trends Neurosci, 2008. **31**(8): p. 392-400.
208. Lois, C. and A. Alvarez-Buylla, *Proliferating subventricular zone cells in the adult mammalian forebrain can differentiate into neurons and glia*. Proc Natl Acad Sci U S A, 1993. **90**(5): p. 2074-7.
209. Kaplan, M.S., N.A. McNelly, and J.W. Hinds, *Population dynamics of adult-formed granule neurons of the rat olfactory bulb*. J Comp Neurol, 1985. **239**(1): p. 117-25.
210. Biebl, M., et al., *Analysis of neurogenesis and programmed cell death reveals a self-renewing capacity in the adult rat brain*. Neurosci Lett, 2000. **291**(1): p. 17-20.
211. Petreanu, L. and A. Alvarez-Buylla, *Maturation and death of adult-born olfactory bulb granule neurons: role of olfaction*. J Neurosci, 2002. **22**(14): p. 6106-13.
212. Rosselli-Austin, L. and J. Altman, *The postnatal development of the main olfactory bulb of the rat*. J Dev Physiol, 1979. **1**(4): p. 295-313.
213. Alvarez-Buylla, A. and D.A. Lim, *For the long run: maintaining germinal niches in the adult brain*. Neuron, 2004. **41**(5): p. 683-6.
214. Khodosevich, K., J. Alfonso, and H. Monyer, *Dynamic changes in the transcriptional profile of subventricular zone-derived postnatally born neuroblasts*. Mech Dev, 2013. **130**(6-8): p. 424-32.
215. Belluzzi, O., et al., *Electrophysiological differentiation of new neurons in the olfactory bulb*. J Neurosci, 2003. **23**(32): p. 10411-8.
216. Basak, O. and V. Taylor, *Stem cells of the adult mammalian brain and their niche*. Cell Mol Life Sci, 2009. **66**(6): p. 1057-72.
217. Luskin, M.B., *Restricted proliferation and migration of postnatally generated neurons derived from the forebrain subventricular zone*. Neuron, 1993. **11**(1): p. 173-89.
218. Kato, T., et al., *Continual replacement of newly-generated olfactory neurons in adult rats*. Neurosci Lett, 2001. **307**(1): p. 17-20.
219. Winner, B., et al., *Long-term survival and cell death of newly generated neurons in the adult rat olfactory bulb*. Eur J Neurosci, 2002. **16**(9): p. 1681-9.
220. Lledo, P.M. and A. Saghatelian, *Integrating new neurons into the adult olfactory bulb: joining the network, life-death decisions, and the effects of sensory experience*. Trends Neurosci, 2005. **28**(5): p. 248-54.
221. Brill, M.S., et al., *Adult generation of glutamatergic olfactory bulb interneurons*. Nat Neurosci, 2009. **12**(12): p. 1524-33.
222. Gritti, A., et al., *Multipotent neural stem cells reside into the rostral extension and olfactory bulb of adult rodents*. J Neurosci, 2002. **22**(2): p. 437-45.
223. Merkle, F.T., Z. Mirzadeh, and A. Alvarez-Buylla, *Mosaic organization of neural stem cells in the adult brain*. Science, 2007. **317**(5836): p. 381-4.
224. Imayoshi, I., et al., *Roles of continuous neurogenesis in the structural and functional integrity of the adult forebrain*. Nat Neurosci, 2008. **11**(10): p. 1153-61.
225. Saxe, M.D., et al., *Ablation of hippocampal neurogenesis impairs contextual fear conditioning and synaptic plasticity in the dentate gyrus*. Proc Natl Acad Sci U S A, 2006. **103**(46): p. 17501-6.
226. Sahay, A., et al., *Increasing adult hippocampal neurogenesis is sufficient to improve pattern separation*. Nature, 2011. **472**(7344): p. 466-70.

Bibliography

227. Jessberger, S., et al., *Dentate gyrus-specific knockdown of adult neurogenesis impairs spatial and object recognition memory in adult rats*. Learn Mem, 2009. **16**(2): p. 147-54.
228. Kempermann, G., et al., *Milestones of neuronal development in the adult hippocampus*. Trends Neurosci, 2004. **27**(8): p. 447-52.
229. Steiner, B., et al., *Differential regulation of gliogenesis in the context of adult hippocampal neurogenesis in mice*. Glia, 2004. **46**(1): p. 41-52.
230. Kempermann, G., H.G. Kuhn, and F.H. Gage, *Experience-induced neurogenesis in the senescent dentate gyrus*. J Neurosci, 1998. **18**(9): p. 3206-12.
231. Jessberger, S., et al., *Directed differentiation of hippocampal stem/progenitor cells in the adult brain*. Nat Neurosci, 2008. **11**(8): p. 888-93.
232. Cameron, H.A., et al., *Differentiation of newly born neurons and glia in the dentate gyrus of the adult rat*. Neuroscience, 1993. **56**(2): p. 337-44.
233. Seri, B., et al., *Cell types, lineage, and architecture of the germinal zone in the adult dentate gyrus*. J Comp Neurol, 2004. **478**(4): p. 359-78.
234. Alvarez-Buylla, A., J.M. Garcia-Verdugo, and A.D. Tramontin, *A unified hypothesis on the lineage of neural stem cells*. Nat Rev Neurosci, 2001. **2**(4): p. 287-93.
235. Kempermann, G., H.G. Kuhn, and F.H. Gage, *More hippocampal neurons in adult mice living in an enriched environment*. Nature, 1997. **386**(6624): p. 493-5.
236. Bayer, S.A., J.W. Yackel, and P.S. Puri, *Neurons in the rat dentate gyrus granular layer substantially increase during juvenile and adult life*. Science, 1982. **216**(4548): p. 890-2.
237. Crespo, D., B.B. Stanfield, and W.M. Cowan, *Evidence that late-generated granule cells do not simply replace earlier formed neurons in the rat dentate gyrus*. Exp Brain Res, 1986. **62**(3): p. 541-8.
238. Herrera, D.G., J.M. Garcia-Verdugo, and A. Alvarez-Buylla, *Adult-derived neural precursors transplanted into multiple regions in the adult brain*. Ann Neurol, 1999. **46**(6): p. 867-77.
239. Lim, D.A., et al., *Noggin antagonizes BMP signaling to create a niche for adult neurogenesis*. Neuron, 2000. **28**(3): p. 713-26.
240. Ihrie, R.A. and A. Alvarez-Buylla, *Cells in the astroglial lineage are neural stem cells*. Cell Tissue Res, 2008. **331**(1): p. 179-91.
241. Shihabuddin, L.S., et al., *Adult spinal cord stem cells generate neurons after transplantation in the adult dentate gyrus*. J Neurosci, 2000. **20**(23): p. 8727-35.
242. Barkho, B.Z., et al., *Identification of astrocyte-expressed factors that modulate neural stem/progenitor cell differentiation*. Stem Cells Dev, 2006. **15**(3): p. 407-21.
243. Buckwalter, M.S., et al., *Chronically increased transforming growth factor-beta1 strongly inhibits hippocampal neurogenesis in aged mice*. Am J Pathol, 2006. **169**(1): p. 154-64.
244. Jiao, J. and D.F. Chen, *Induction of neurogenesis in nonconventional neurogenic regions of the adult central nervous system by niche astrocyte-produced signals*. Stem Cells, 2008. **26**(5): p. 1221-30.
245. Song, H., C.F. Stevens, and F.H. Gage, *Astroglia induce neurogenesis from adult neural stem cells*. Nature, 2002. **417**(6884): p. 39-44.
246. Bath, K.G., et al., *Variant brain-derived neurotrophic factor (Val66Met) alters adult olfactory bulb neurogenesis and spontaneous olfactory discrimination*. J Neurosci, 2008. **28**(10): p. 2383-93.
247. Ma, D.K., et al., *Neuronal activity-induced Gadd45b promotes epigenetic DNA demethylation and adult neurogenesis*. Science, 2009. **323**(5917): p. 1074-7.

Bibliography

248. Yang, P., et al., *Ciliary neurotrophic factor mediates dopamine D2 receptor-induced CNS neurogenesis in adult mice*. J Neurosci, 2008. **28**(9): p. 2231-41.
249. Palmer, T.D., A.R. Willhoite, and F.H. Gage, *Vascular niche for adult hippocampal neurogenesis*. J Comp Neurol, 2000. **425**(4): p. 479-94.
250. Tavazoie, M., et al., *A specialized vascular niche for adult neural stem cells*. Cell Stem Cell, 2008. **3**(3): p. 279-88.
251. Shen, Q., et al., *Adult SVZ stem cells lie in a vascular niche: a quantitative analysis of niche cell-cell interactions*. Cell Stem Cell, 2008. **3**(3): p. 289-300.
252. Ehm, O., et al., *RBPJkappa-dependent signaling is essential for long-term maintenance of neural stem cells in the adult hippocampus*. J Neurosci, 2010. **30**(41): p. 13794-807.
253. Lugert, S., et al., *Quiescent and active hippocampal neural stem cells with distinct morphologies respond selectively to physiological and pathological stimuli and aging*. Cell Stem Cell, 2010. **6**(5): p. 445-56.
254. Ohtsuka, T., et al., *Visualization of embryonic neural stem cells using Hes promoters in transgenic mice*. Mol Cell Neurosci, 2006. **31**(1): p. 109-22.
255. Stump, G., et al., *Notch1 and its ligands Delta-like and Jagged are expressed and active in distinct cell populations in the postnatal mouse brain*. Mech Dev, 2002. **114**(1-2): p. 153-9.
256. Imayoshi, I., et al., *Essential roles of Notch signaling in maintenance of neural stem cells in developing and adult brains*. J Neurosci, 2010. **30**(9): p. 3489-98.
257. Bertrand, N., D.S. Castro, and F. Guillemot, *Proneural genes and the specification of neural cell types*. Nat Rev Neurosci, 2002. **3**(7): p. 517-30.
258. Kopan, R. and M.X. Ilagan, *The canonical Notch signaling pathway: unfolding the activation mechanism*. Cell, 2009. **137**(2): p. 216-33.
259. Imayoshi, I. and R. Kageyama, *The role of Notch signaling in adult neurogenesis*. Mol Neurobiol, 2011. **44**(1): p. 7-12.
260. Ables, J.L., et al., *Notch1 is required for maintenance of the reservoir of adult hippocampal stem cells*. J Neurosci, 2010. **30**(31): p. 10484-92.
261. Breunig, J.J., et al., *Notch regulates cell fate and dendrite morphology of newborn neurons in the postnatal dentate gyrus*. Proc Natl Acad Sci U S A, 2007. **104**(51): p. 20558-63.
262. Androutsellis-Theotokis, A., et al., *Notch signalling regulates stem cell numbers in vitro and in vivo*. Nature, 2006. **442**(7104): p. 823-6.
263. Gridley, T., *Notch signaling in vascular development and physiology*. Development, 2007. **134**(15): p. 2709-18.
264. Sierra, A., et al., *Microglia shape adult hippocampal neurogenesis through apoptosis-coupled phagocytosis*. Cell Stem Cell, 2010. **7**(4): p. 483-95.
265. Tashiro, A., et al., *NMDA-receptor-mediated, cell-specific integration of new neurons in adult dentate gyrus*. Nature, 2006. **442**(7105): p. 929-33.
266. Kempermann, G., et al., *Early determination and long-term persistence of adult-generated new neurons in the hippocampus of mice*. Development, 2003. **130**(2): p. 391-9.
267. Epp, J.R., M.D. Spritzer, and L.A. Galea, *Hippocampus-dependent learning promotes survival of new neurons in the dentate gyrus at a specific time during cell maturation*. Neuroscience, 2007. **149**(2): p. 273-85.
268. Dalla, C., et al., *Neurogenesis and learning: acquisition and asymptotic performance predict how many new cells survive in the hippocampus*. Neurobiol Learn Mem, 2007. **88**(1): p. 143-8.

Bibliography

269. van Praag, H., G. Kempermann, and F.H. Gage, *Running increases cell proliferation and neurogenesis in the adult mouse dentate gyrus*. *Nat Neurosci*, 1999. **2**(3): p. 266-70.
270. van Praag, H., et al., *Running enhances neurogenesis, learning, and long-term potentiation in mice*. *Proc Natl Acad Sci U S A*, 1999. **96**(23): p. 13427-31.
271. Anderson, M.F., et al., *Insulin-like growth factor-I and neurogenesis in the adult mammalian brain*. *Brain Res Dev Brain Res*, 2002. **134**(1-2): p. 115-22.
272. Mandairon, N., F. Jourdan, and A. Didier, *Deprivation of sensory inputs to the olfactory bulb up-regulates cell death and proliferation in the subventricular zone of adult mice*. *Neuroscience*, 2003. **119**(2): p. 507-16.
273. Mandairon, N., et al., *Long-term fate and distribution of newborn cells in the adult mouse olfactory bulb: Influences of olfactory deprivation*. *Neuroscience*, 2006. **141**(1): p. 443-51.
274. Alonso, M., et al., *Olfactory discrimination learning increases the survival of adult-born neurons in the olfactory bulb*. *J Neurosci*, 2006. **26**(41): p. 10508-13.
275. Alonso, M., et al., *Turning astrocytes from the rostral migratory stream into neurons: a role for the olfactory sensory organ*. *J Neurosci*, 2008. **28**(43): p. 11089-102.
276. Yamaguchi, M. and K. Mori, *Critical period for sensory experience-dependent survival of newly generated granule cells in the adult mouse olfactory bulb*. *Proc Natl Acad Sci U S A*, 2005. **102**(27): p. 9697-702.
277. Doetsch, F., et al., *EGF converts transit-amplifying neurogenic precursors in the adult brain into multipotent stem cells*. *Neuron*, 2002. **36**(6): p. 1021-34.
278. Merkle, F.T., et al., *Radial glia give rise to adult neural stem cells in the subventricular zone*. *Proc Natl Acad Sci U S A*, 2004. **101**(50): p. 17528-32.
279. Hack, M.A., et al., *Neuronal fate determinants of adult olfactory bulb neurogenesis*. *Nat Neurosci*, 2005. **8**(7): p. 865-72.
280. Kohwi, M., et al., *Pax6 is required for making specific subpopulations of granule and periglomerular neurons in the olfactory bulb*. *J Neurosci*, 2005. **25**(30): p. 6997-7003.
281. Waclaw, R.R., et al., *The zinc finger transcription factor Sp8 regulates the generation and diversity of olfactory bulb interneurons*. *Neuron*, 2006. **49**(4): p. 503-16.
282. Young, K.M., et al., *Subventricular zone stem cells are heterogeneous with respect to their embryonic origins and neurogenic fates in the adult olfactory bulb*. *J Neurosci*, 2007. **27**(31): p. 8286-96.
283. Kelsch, W., et al., *Distinct mammalian precursors are committed to generate neurons with defined dendritic projection patterns*. *PLoS Biol*, 2007. **5**(11): p. e300.
284. Filippov, V., et al., *Subpopulation of nestin-expressing progenitor cells in the adult murine hippocampus shows electrophysiological and morphological characteristics of astrocytes*. *Mol Cell Neurosci*, 2003. **23**(3): p. 373-82.
285. Ma, D.K., et al., *Epigenetic choreographers of neurogenesis in the adult mammalian brain*. *Nat Neurosci*, 2010. **13**(11): p. 1338-44.
286. Jobe, E.M., A.L. McQuate, and X. Zhao, *Crosstalk among Epigenetic Pathways Regulates Neurogenesis*. *Front Neurosci*, 2012. **6**: p. 59.
287. Lim, D.A., et al., *In vivo transcriptional profile analysis reveals RNA splicing and chromatin remodeling as prominent processes for adult neurogenesis*. *Mol Cell Neurosci*, 2006. **31**(1): p. 131-48.
288. Fasano, C.A., et al., *shRNA knockdown of Bmi-1 reveals a critical role for p21-Rb pathway in NSC self-renewal during development*. *Cell Stem Cell*, 2007. **1**(1): p. 87-99.

Bibliography

289. Schuettengruber, B., et al., *Trithorax group proteins: switching genes on and keeping them active*. Nat Rev Mol Cell Biol, 2011. **12**(12): p. 799-814.
290. Ringrose, L. and R. Paro, *Polycomb/Trithorax response elements and epigenetic memory of cell identity*. Development, 2007. **134**(2): p. 223-32.
291. Wang, H., et al., *Role of histone H2A ubiquitination in Polycomb silencing*. Nature, 2004. **431**(7010): p. 873-8.
292. de Napoles, M., et al., *Polycomb group proteins Ring1A/B link ubiquitylation of histone H2A to heritable gene silencing and X inactivation*. Dev Cell, 2004. **7**(5): p. 663-76.
293. Schuettengruber, B., et al., *Genome regulation by polycomb and trithorax proteins*. Cell, 2007. **128**(4): p. 735-45.
294. Sparmann, A. and M. van Lohuizen, *Polycomb silencers control cell fate, development and cancer*. Nat Rev Cancer, 2006. **6**(11): p. 846-56.
295. Zhou, W., et al., *Histone H2A monoubiquitination represses transcription by inhibiting RNA polymerase II transcriptional elongation*. Mol Cell, 2008. **29**(1): p. 69-80.
296. Stock, J.K., et al., *Ring1-mediated ubiquitination of H2A restrains poised RNA polymerase II at bivalent genes in mouse ES cells*. Nat Cell Biol, 2007. **9**(12): p. 1428-35.
297. Schuettengruber, B. and G. Cavalli, *Recruitment of polycomb group complexes and their role in the dynamic regulation of cell fate choice*. Development, 2009. **136**(21): p. 3531-42.
298. Winston, F. and M. Carlson, *Yeast SNF/SWI transcriptional activators and the SPT/SIN chromatin connection*. Trends Genet, 1992. **8**(11): p. 387-91.
299. Ho, L. and G.R. Crabtree, *Chromatin remodelling during development*. Nature, 2010. **463**(7280): p. 474-84.
300. Hassan, A.H., et al., *Function and selectivity of bromodomains in anchoring chromatin-modifying complexes to promoter nucleosomes*. Cell, 2002. **111**(3): p. 369-79.
301. Boyer, L.A., R.R. Latek, and C.L. Peterson, *The SANT domain: a unique histone-tail-binding module?* Nat Rev Mol Cell Biol, 2004. **5**(2): p. 158-63.
302. Lusser, A. and J.T. Kadonaga, *Chromatin remodeling by ATP-dependent molecular machines*. Bioessays, 2003. **25**(12): p. 1192-200.
303. Delmas, V., D.G. Stokes, and R.P. Perry, *A mammalian DNA-binding protein that contains a chromodomain and an SNF2/SWI2-like helicase domain*. Proc Natl Acad Sci U S A, 1993. **90**(6): p. 2414-8.
304. Azuara, V., et al., *Chromatin signatures of pluripotent cell lines*. Nat Cell Biol, 2006. **8**(5): p. 532-8.
305. Bernstein, B.E., et al., *A bivalent chromatin structure marks key developmental genes in embryonic stem cells*. Cell, 2006. **125**(2): p. 315-26.
306. Mikkelsen, T.S., et al., *Genome-wide maps of chromatin state in pluripotent and lineage-committed cells*. Nature, 2007. **448**(7153): p. 553-60.
307. Cao, R., Y. Tsukada, and Y. Zhang, *Role of Bmi-1 and Ring1A in H2A ubiquitylation and Hox gene silencing*. Mol Cell, 2005. **20**(6): p. 845-54.
308. Molofsky, A.V., et al., *Bmi-1 dependence distinguishes neural stem cell self-renewal from progenitor proliferation*. Nature, 2003. **425**(6961): p. 962-7.
309. Bruggeman, S.W., et al., *Ink4a and Arf differentially affect cell proliferation and neural stem cell self-renewal in Bmi1-deficient mice*. Genes Dev, 2005. **19**(12): p. 1438-43.
310. Zencak, D., et al., *Bmi1 loss produces an increase in astroglial cells and a decrease in neural stem cell population and proliferation*. J Neurosci, 2005. **25**(24): p. 5774-83.

Bibliography

311. van der Lugt, N.M., et al., *Posterior transformation, neurological abnormalities, and severe hematopoietic defects in mice with a targeted deletion of the bmi-1 proto-oncogene*. *Genes Dev*, 1994. **8**(7): p. 757-69.
312. Fasano, C.A., et al., *Bmi-1 cooperates with Foxg1 to maintain neural stem cell self-renewal in the forebrain*. *Genes Dev*, 2009. **23**(5): p. 561-74.
313. Cui, H., et al., *Bmi-1 is essential for the tumorigenicity of neuroblastoma cells*. *Am J Pathol*, 2007. **170**(4): p. 1370-8.
314. He, S., et al., *Bmi-1 over-expression in neural stem/progenitor cells increases proliferation and neurogenesis in culture but has little effect on these functions in vivo*. *Dev Biol*, 2009. **328**(2): p. 257-72.
315. Wu, M., et al., *Molecular regulation of H3K4 trimethylation by Wdr82, a component of human Set1/COMPASS*. *Mol Cell Biol*, 2008. **28**(24): p. 7337-44.
316. Lim, D.A., et al., *Chromatin remodelling factor Mll1 is essential for neurogenesis from postnatal neural stem cells*. *Nature*, 2009. **458**(7237): p. 529-33.
317. Matsumoto, S., et al., *Brg1 is required for murine neural stem cell maintenance and gliogenesis*. *Dev Biol*, 2006. **289**(2): p. 372-83.
318. Hirabayashi, Y., et al., *Polycomb limits the neurogenic competence of neural precursor cells to promote astrogenic fate transition*. *Neuron*, 2009. **63**(5): p. 600-13.
319. Fong, A.P., et al., *Genetic and epigenetic determinants of neurogenesis and myogenesis*. *Dev Cell*, 2012. **22**(4): p. 721-35.
320. Jones, H., *Genetics: Analysis of Genes and Genomes, 6th Edition, Chap. 11*. 2005.
321. Marfella, C.G. and A.N. Imbalzano, *The Chd family of chromatin remodelers*. *Mutat Res*, 2007. **618**(1-2): p. 30-40.
322. Bouazoune, K. and R.E. Kingston, *Chromatin remodeling by the CHD7 protein is impaired by mutations that cause human developmental disorders*. *Proc Natl Acad Sci U S A*, 2012. **109**(47): p. 19238-43.
323. Bienz, M., *The PHD finger, a nuclear protein-interaction domain*. *Trends Biochem Sci*, 2006. **31**(1): p. 35-40.
324. Shur, I. and D. Benayahu, *Characterization and functional analysis of CReMM, a novel chromodomain helicase DNA-binding protein*. *J Mol Biol*, 2005. **352**(3): p. 646-55.
325. Schuster, E.F. and R. Stoger, *CHD5 defines a new subfamily of chromodomain-SWI2/SNF2-like helicases*. *Mamm Genome*, 2002. **13**(2): p. 117-9.
326. Chiba, H., et al., *Two human homologues of Saccharomyces cerevisiae SWI2/SNF2 and Drosophila brahma are transcriptional coactivators cooperating with the estrogen receptor and the retinoic acid receptor*. *Nucleic Acids Res*, 1994. **22**(10): p. 1815-20.
327. O'Roak, B.J., et al., *Multiplex targeted sequencing identifies recurrently mutated genes in autism spectrum disorders*. *Science*, 2012. **338**(6114): p. 1619-22.
328. Law, M.E., et al., *Molecular cytogenetic analysis of chromosomes 1 and 19 in glioma cell lines*. *Cancer Genet Cytogenet*, 2005. **160**(1): p. 1-14.
329. White, P.S., et al., *Definition and characterization of a region of 1p36.3 consistently deleted in neuroblastoma*. *Oncogene*, 2005. **24**(16): p. 2684-94.
330. Vissers, L.E., et al., *Mutations in a new member of the chromodomain gene family cause CHARGE syndrome*. *Nat Genet*, 2004. **36**(9): p. 955-7.
331. Kim, H.G., et al., *Mutations in CHD7, encoding a chromatin-remodeling protein, cause idiopathic hypogonadotropic hypogonadism and Kallmann syndrome*. *Am J Hum Genet*, 2008. **83**(4): p. 511-9.

Bibliography

332. Schnetz, M.P., et al., *CHD7 targets active gene enhancer elements to modulate ES cell-specific gene expression*. PLoS Genet, 2010. **6**(7): p. e1001023.
333. Schnetz, M.P., et al., *Genomic distribution of CHD7 on chromatin tracks H3K4 methylation patterns*. Genome Res, 2009. **19**(4): p. 590-601.
334. Heintzman, N.D., et al., *Histone modifications at human enhancers reflect global cell-type-specific gene expression*. Nature, 2009. **459**(7243): p. 108-12.
335. Heintzman, N.D., et al., *Distinct and predictive chromatin signatures of transcriptional promoters and enhancers in the human genome*. Nat Genet, 2007. **39**(3): p. 311-8.
336. Kennison, J.A. and J.W. Tamkun, *Dosage-dependent modifiers of polycomb and antennapedia mutations in Drosophila*. Proc Natl Acad Sci U S A, 1988. **85**(21): p. 8136-40.
337. Daubresse, G., et al., *The Drosophila kismet gene is related to chromatin-remodeling factors and is required for both segmentation and segment identity*. Development, 1999. **126**(6): p. 1175-87.
338. Therrien, M., et al., *A genetic screen for modifiers of a kinase suppressor of Ras-dependent rough eye phenotype in Drosophila*. Genetics, 2000. **156**(3): p. 1231-42.
339. Srinivasan, S., K.M. Dorigi, and J.W. Tamkun, *Drosophila Kismet regulates histone H3 lysine 27 methylation and early elongation by RNA polymerase II*. PLoS Genet, 2008. **4**(10): p. e1000217.
340. Melicharek, D.J., et al., *Kismet/CHD7 regulates axon morphology, memory and locomotion in a Drosophila model of CHARGE syndrome*. Hum Mol Genet, 2010. **19**(21): p. 4253-64.
341. Engelen, E., et al., *Sox2 cooperates with Chd7 to regulate genes that are mutated in human syndromes*. Nat Genet, 2011. **43**(6): p. 607-11.
342. Takada, I., et al., *A histone lysine methyltransferase activated by non-canonical Wnt signalling suppresses PPAR-gamma transactivation*. Nat Cell Biol, 2007. **9**(11): p. 1273-85.
343. Bajpai, R., et al., *CHD7 cooperates with PBAF to control multipotent neural crest formation*. Nature, 2010. **463**(7283): p. 958-62.
344. Hurd, E.A., et al., *Loss of Chd7 function in gene-trapped reporter mice is embryonic lethal and associated with severe defects in multiple developing tissues*. Mamm Genome, 2007. **18**(2): p. 94-104.
345. Layman, W.S., et al., *Defects in neural stem cell proliferation and olfaction in Chd7 deficient mice indicate a mechanism for hyposmia in human CHARGE syndrome*. Hum Mol Genet, 2009. **18**(11): p. 1909-23.
346. Bergman, J.E., et al., *Study of smell and reproductive organs in a mouse model for CHARGE syndrome*. Eur J Hum Genet, 2010. **18**(2): p. 171-7.
347. Allen, M.D., et al., *Solution structure of the BRK domains from CHD7*. J Mol Biol, 2007. **371**(5): p. 1135-40.
348. Batsukh, T., et al., *CHD8 interacts with CHD7, a protein which is mutated in CHARGE syndrome*. Hum Mol Genet, 2010. **19**(14): p. 2858-66.
349. Nishijo, K., et al., *Biomarker system for studying muscle, stem cells, and cancer in vivo*. FASEB J, 2009. **23**(8): p. 2681-90.
350. Basson, M.A., et al., *Sprouty1 is a critical regulator of GDNF/RET-mediated kidney induction*. Dev Cell, 2005. **8**(2): p. 229-39.
351. Yang, X., et al., *Overexpression of Spry1 in chondrocytes causes attenuated FGFR ubiquitination and sustained ERK activation resulting in chondrodysplasia*. Dev Biol, 2008. **321**(1): p. 64-76.

Bibliography

352. Yu, K., et al., *Conditional inactivation of FGF receptor 2 reveals an essential role for FGF signaling in the regulation of osteoblast function and bone growth*. *Development*, 2003. **130**(13): p. 3063-74.
353. Trokovic, R., et al., *FGFR1 is independently required in both developing mid- and hindbrain for sustained response to isthmic signals*. *EMBO J*, 2003. **22**(8): p. 1811-23.
354. Slezak, M., et al., *Transgenic mice for conditional gene manipulation in astroglial cells*. *Glia*, 2007. **55**(15): p. 1565-76.
355. Stryke, D., et al., *BayGenomics: a resource of insertional mutations in mouse embryonic stem cells*. *Nucleic Acids Res*, 2003. **31**(1): p. 278-81.
356. Randall, V., et al., *Great vessel development requires biallelic expression of Chd7 and Tbx1 in pharyngeal ectoderm in mice*. *J Clin Invest*, 2009. **119**(11): p. 3301-10.
357. Tronche, F., et al., *Disruption of the glucocorticoid receptor gene in the nervous system results in reduced anxiety*. *Nat Genet*, 1999. **23**(1): p. 99-103.
358. Buono, M., et al., *Sulfatase modifying factor 1-mediated fibroblast growth factor signaling primes hematopoietic multilineage development*. *J Exp Med*, 2010. **207**(8): p. 1647-60.
359. Umemori, H., et al., *FGF22 and its close relatives are presynaptic organizing molecules in the mammalian brain*. *Cell*, 2004. **118**(2): p. 257-70.
360. Rosenblatt, J.D., et al., *Culturing satellite cells from living single muscle fiber explants*. *In Vitro Cell Dev Biol Anim*, 1995. **31**(10): p. 773-9.
361. Yoshida, N., et al., *Cell heterogeneity upon myogenic differentiation: down-regulation of MyoD and Myf-5 generates 'reserve cells'*. *J Cell Sci*, 1998. **111** (Pt 6): p. 769-79.
362. Schulte-Merker, S., et al., *The protein product of the zebrafish homologue of the mouse T gene is expressed in nuclei of the germ ring and the notochord of the early embryo*. *Development*, 1992. **116**(4): p. 1021-32.
363. Yaguchi, Y., et al., *Fibroblast growth factor (FGF) gene expression in the developing cerebellum suggests multiple roles for FGF signaling during cerebellar morphogenesis and development*. *Dev Dyn*, 2009. **238**(8): p. 2058-72.
364. Conti, L., et al., *Niche-independent symmetrical self-renewal of a mammalian tissue stem cell*. *PLoS Biol*, 2005. **3**(9): p. e283.
365. Spiliotopoulos, D., et al., *An optimized experimental strategy for efficient conversion of embryonic stem (ES)-derived mouse neural stem (NS) cells into a nearly homogeneous mature neuronal population*. *Neurobiol Dis*, 2009. **34**(2): p. 320-31.
366. Morrison, S.J. and A.C. Spradling, *Stem cells and niches: mechanisms that promote stem cell maintenance throughout life*. *Cell*, 2008. **132**(4): p. 598-611.
367. Orford, K.W. and D.T. Scadden, *Deconstructing stem cell self-renewal: genetic insights into cell-cycle regulation*. *Nat Rev Genet*, 2008. **9**(2): p. 115-28.
368. Morrison, S.J., et al., *The aging of hematopoietic stem cells*. *Nat Med*, 1996. **2**(9): p. 1011-6.
369. Sudo, K., et al., *Age-associated characteristics of murine hematopoietic stem cells*. *J Exp Med*, 2000. **192**(9): p. 1273-80.
370. Lagha, M., et al., *Pax3 regulation of FGF signaling affects the progression of embryonic progenitor cells into the myogenic program*. *Genes Dev*, 2008. **22**(13): p. 1828-37.
371. Groves, J.A., C.L. Hammond, and S.M. Hughes, *Fgf8 drives myogenic progression of a novel lateral fast muscle fibre population in zebrafish*. *Development*, 2005. **132**(19): p. 4211-22.
372. Kudla, A.J., et al., *The FGF receptor-1 tyrosine kinase domain regulates myogenesis but is not sufficient to stimulate proliferation*. *J Cell Biol*, 1998. **142**(1): p. 241-50.

Bibliography

373. Hannon, K., et al., *Differentially expressed fibroblast growth factors regulate skeletal muscle development through autocrine and paracrine mechanisms*. J Cell Biol, 1996. **132**(6): p. 1151-9.
374. Gross, I., et al., *Mammalian sprouty proteins inhibit cell growth and differentiation by preventing ras activation*. J Biol Chem, 2001. **276**(49): p. 46460-8.
375. Yusoff, P., et al., *Sprouty2 inhibits the Ras/MAP kinase pathway by inhibiting the activation of Raf*. J Biol Chem, 2002. **277**(5): p. 3195-201.
376. Mason, J.M., et al., *Sprouty proteins: multifaceted negative-feedback regulators of receptor tyrosine kinase signaling*. Trends Cell Biol, 2006. **16**(1): p. 45-54.
377. Impagnatiello, M.A., et al., *Mammalian sprouty-1 and -2 are membrane-anchored phosphoprotein inhibitors of growth factor signaling in endothelial cells*. J Cell Biol, 2001. **152**(5): p. 1087-98.
378. Gross, I., et al., *The receptor tyrosine kinase regulator Sprouty1 is a target of the tumor suppressor WT1 and important for kidney development*. J Biol Chem, 2003. **278**(42): p. 41420-30.
379. Fiedler, U. and H.G. Augustin, *Angiopoietins: a link between angiogenesis and inflammation*. Trends Immunol, 2006. **27**(12): p. 552-8.
380. Shim, W.S., I.A. Ho, and P.E. Wong, *Angiopoietin: a TIE(d) balance in tumor angiogenesis*. Mol Cancer Res, 2007. **5**(7): p. 655-65.
381. Mikkelsen, T.S., et al., *Dissecting direct reprogramming through integrative genomic analysis*. Nature, 2008. **454**(7200): p. 49-55.
382. Meshorer, E., et al., *Hyperdynamic plasticity of chromatin proteins in pluripotent embryonic stem cells*. Dev Cell, 2006. **10**(1): p. 105-16.
383. Efroni, S., et al., *Global transcription in pluripotent embryonic stem cells*. Cell Stem Cell, 2008. **2**(5): p. 437-47.
384. Gaspar-Maia, A., et al., *Chd1 regulates open chromatin and pluripotency of embryonic stem cells*. Nature, 2009. **460**(7257): p. 863-8.
385. Yoshida, T., et al., *The role of the chromatin remodeler Mi-2beta in hematopoietic stem cell self-renewal and multilineage differentiation*. Genes Dev, 2008. **22**(9): p. 1174-89.
386. Feng, R., et al., *Sox2 protects neural stem cells from apoptosis via up-regulating survivin expression*. Biochem J, 2013. **450**(3): p. 459-68.
387. Favaro, R., et al., *Hippocampal development and neural stem cell maintenance require Sox2-dependent regulation of Shh*. Nat Neurosci, 2009. **12**(10): p. 1248-56.
388. Ferri, A.L., et al., *Sox2 deficiency causes neurodegeneration and impaired neurogenesis in the adult mouse brain*. Development, 2004. **131**(15): p. 3805-19.
389. Cavallaro, M., et al., *Impaired generation of mature neurons by neural stem cells from hypomorphic Sox2 mutants*. Development, 2008. **135**(3): p. 541-57.
390. Saino-Saito, S., et al., *ER81 and CaMKIV identify anatomically and phenotypically defined subsets of mouse olfactory bulb interneurons*. J Comp Neurol, 2007. **502**(4): p. 485-96.
391. Cave, J.W., et al., *Differential regulation of dopaminergic gene expression by Er81*. J Neurosci, 2010. **30**(13): p. 4717-24.
392. Cossette, M., D. Levesque, and A. Parent, *Neurochemical characterization of dopaminergic neurons in human striatum*. Parkinsonism Relat Disord, 2005. **11**(5): p. 277-86.
393. Kippin, T.E., D.J. Martens, and D. van der Kooy, *p21 loss compromises the relative quiescence of forebrain stem cell proliferation leading to exhaustion of their proliferation capacity*. Genes Dev, 2005. **19**(6): p. 756-67.

Bibliography

394. Sahin, E. and R.A. Depinho, *Linking functional decline of telomeres, mitochondria and stem cells during ageing*. Nature, 2010. **464**(7288): p. 520-8.
395. Kuhn, H.G., H. Dickinson-Anson, and F.H. Gage, *Neurogenesis in the dentate gyrus of the adult rat: age-related decrease of neuronal progenitor proliferation*. J Neurosci, 1996. **16**(6): p. 2027-33.
396. Seki, T. and Y. Arai, *Age-related production of new granule cells in the adult dentate gyrus*. Neuroreport, 1995. **6**(18): p. 2479-82.
397. Leuner, B., et al., *Diminished adult neurogenesis in the marmoset brain precedes old age*. Proc Natl Acad Sci U S A, 2007. **104**(43): p. 17169-73.
398. Gage, F.H., P.A. Kelly, and A. Bjorklund, *Regional changes in brain glucose metabolism reflect cognitive impairments in aged rats*. J Neurosci, 1984. **4**(11): p. 2856-65.
399. Lazarov, O., et al., *When neurogenesis encounters aging and disease*. Trends Neurosci, 2010. **33**(12): p. 569-79.
400. Walter, J., et al., *Age-related effects on hippocampal precursor cell subpopulations and neurogenesis*. Neurobiol Aging, 2011. **32**(10): p. 1906-14.
401. Jinno, S., *Decline in adult neurogenesis during aging follows a topographic pattern in the mouse hippocampus*. J Comp Neurol, 2011. **519**(3): p. 451-66.
402. Alonso, G., *Proliferation of progenitor cells in the adult rat brain correlates with the presence of vimentin-expressing astrocytes*. Glia, 2001. **34**(4): p. 253-66.
403. Hattiangady, B. and A.K. Shetty, *Ageing does not alter the number or phenotype of putative stem/progenitor cells in the neurogenic region of the hippocampus*. Neurobiol Aging, 2008. **29**(1): p. 129-47.
404. Encinas, J.M., et al., *Division-coupled astrocytic differentiation and age-related depletion of neural stem cells in the adult hippocampus*. Cell Stem Cell, 2011. **8**(5): p. 566-79.
405. van Praag, H., et al., *Exercise enhances learning and hippocampal neurogenesis in aged mice*. J Neurosci, 2005. **25**(38): p. 8680-5.
406. Rao, M.S., et al., *Newly born cells in the ageing dentate gyrus display normal migration, survival and neuronal fate choice but endure retarded early maturation*. Eur J Neurosci, 2005. **21**(2): p. 464-76.
407. Rao, M.S., B. Hattiangady, and A.K. Shetty, *The window and mechanisms of major age-related decline in the production of new neurons within the dentate gyrus of the hippocampus*. Aging Cell, 2006. **5**(6): p. 545-58.
408. McDonald, H.Y. and J.M. Wojtowicz, *Dynamics of neurogenesis in the dentate gyrus of adult rats*. Neurosci Lett, 2005. **385**(1): p. 70-5.
409. Kim, E.J., et al., *Ascl1 (Mash1) defines cells with long-term neurogenic potential in subgranular and subventricular zones in adult mouse brain*. PLoS One, 2011. **6**(3): p. e18472.
410. Suh, H., W. Deng, and F.H. Gage, *Signaling in adult neurogenesis*. Annu Rev Cell Dev Biol, 2009. **25**: p. 253-75.
411. Martynoga, B., et al., *Epigenomic enhancer annotation reveals a key role for NFIX in neural stem cell quiescence*. Genes Dev, 2013. **27**(16): p. 1769-86.
412. Kuhn, H.G., et al., *Epidermal growth factor and fibroblast growth factor-2 have different effects on neural progenitors in the adult rat brain*. J Neurosci, 1997. **17**(15): p. 5820-9.
413. Jin, K., et al., *Neurogenesis in dentate subgranular zone and rostral subventricular zone after focal cerebral ischemia in the rat*. Proc Natl Acad Sci U S A, 2001. **98**(8): p. 4710-5.

414. Feng, W., et al., *The Chromatin Remodeler CHD7 Regulates Adult Neurogenesis via Activation of SoxC Transcription Factors*. Cell Stem Cell, 2013. **13**(1): p. 62-72.
415. Neale, B.M., et al., *Patterns and rates of exonic de novo mutations in autism spectrum disorders*. Nature, 2012. **485**(7397): p. 242-5.
416. Moretti, P., et al., *Learning and memory and synaptic plasticity are impaired in a mouse model of Rett syndrome*. J Neurosci, 2006. **26**(1): p. 319-27.
417. Mu, L., et al., *SoxC transcription factors are required for neuronal differentiation in adult hippocampal neurogenesis*. J Neurosci, 2012. **32**(9): p. 3067-80.
418. Chakkalakal, J.V., et al., *The aged niche disrupts muscle stem cell quiescence*. Nature, 2012. **490**(7420): p. 355-60.
419. Cotsarelis, G., T.T. Sun, and R.M. Lavker, *Label-retaining cells reside in the bulge area of pilosebaceous unit: implications for follicular stem cells, hair cycle, and skin carcinogenesis*. Cell, 1990. **61**(7): p. 1329-37.
420. Tumber, T., et al., *Defining the epithelial stem cell niche in skin*. Science, 2004. **303**(5656): p. 359-63.
421. Wilson, A., et al., *Hematopoietic stem cells reversibly switch from dormancy to self-renewal during homeostasis and repair*. Cell, 2008. **135**(6): p. 1118-29.
422. Foudi, A., et al., *Analysis of histone 2B-GFP retention reveals slowly cycling hematopoietic stem cells*. Nat Biotechnol, 2009. **27**(1): p. 84-90.
423. Kiel, M.J., et al., *SLAM family receptors distinguish hematopoietic stem and progenitor cells and reveal endothelial niches for stem cells*. Cell, 2005. **121**(7): p. 1109-21.
424. Barker, N., et al., *Identification of stem cells in small intestine and colon by marker gene Lgr5*. Nature, 2007. **449**(7165): p. 1003-7.
425. Barker, N., et al., *Lgr5(+ve) stem cells drive self-renewal in the stomach and build long-lived gastric units in vitro*. Cell Stem Cell, 2010. **6**(1): p. 25-36.
426. Kiel, M.J., et al., *Haematopoietic stem cells do not asymmetrically segregate chromosomes or retain BrdU*. Nature, 2007. **449**(7159): p. 238-42.
427. Linton, P.J. and K. Dorshkind, *Age-related changes in lymphocyte development and function*. Nat Immunol, 2004. **5**(2): p. 133-9.
428. Lichtman, M.A. and J.M. Rowe, *The relationship of patient age to the pathobiology of the clonal myeloid diseases*. Semin Oncol, 2004. **31**(2): p. 185-97.
429. Guralnik, J.M., et al., *Prevalence of anemia in persons 65 years and older in the United States: evidence for a high rate of unexplained anemia*. Blood, 2004. **104**(8): p. 2263-8.
430. Beghe, C., A. Wilson, and W.B. Ershler, *Prevalence and outcomes of anemia in geriatrics: a systematic review of the literature*. Am J Med, 2004. **116 Suppl 7A**: p. 3S-10S.
431. Driscoll, I., et al., *The aging hippocampus: cognitive, biochemical and structural findings*. Cereb Cortex, 2003. **13**(12): p. 1344-51.
432. Nacher, J., et al., *NMDA receptor antagonist treatment increases the production of new neurons in the aged rat hippocampus*. Neurobiol Aging, 2003. **24**(2): p. 273-84.
433. Haughey, N.J., et al., *Disruption of neurogenesis in the subventricular zone of adult mice, and in human cortical neuronal precursor cells in culture, by amyloid beta-peptide: implications for the pathogenesis of Alzheimer's disease*. Neuromolecular Med, 2002. **1**(2): p. 125-35.
434. Haughey, N.J., et al., *Disruption of neurogenesis by amyloid beta-peptide, and perturbed neural progenitor cell homeostasis, in models of Alzheimer's disease*. J Neurochem, 2002. **83**(6): p. 1509-24.

Bibliography

435. Donovan, M.H., et al., *Decreased adult hippocampal neurogenesis in the PDAPP mouse model of Alzheimer's disease*. J Comp Neurol, 2006. **495**(1): p. 70-83.
436. Lichtenwalner, R.J., et al., *Intracerebroventricular infusion of insulin-like growth factor-I ameliorates the age-related decline in hippocampal neurogenesis*. Neuroscience, 2001. **107**(4): p. 603-13.
437. Kempermann, G., D. Gast, and F.H. Gage, *Neuroplasticity in old age: sustained fivefold induction of hippocampal neurogenesis by long-term environmental enrichment*. Ann Neurol, 2002. **52**(2): p. 135-43.
438. Kronenberg, G., et al., *Physical exercise prevents age-related decline in precursor cell activity in the mouse dentate gyrus*. Neurobiol Aging, 2006. **27**(10): p. 1505-13.
439. Feser, J. and J. Tyler, *Chromatin structure as a mediator of aging*. FEBS Lett, 2011. **585**(13): p. 2041-8.
440. Pollina, E.A. and A. Brunet, *Epigenetic regulation of aging stem cells*. Oncogene, 2011. **30**(28): p. 3105-26.
441. Chouliaras, L., et al., *Caloric restriction attenuates age-related changes of DNA methyltransferase 3a in mouse hippocampus*. Brain Behav Immun, 2011. **25**(4): p. 616-23.
442. Bondolfi, L., et al., *Impact of age and caloric restriction on neurogenesis in the dentate gyrus of C57BL/6 mice*. Neurobiol Aging, 2004. **25**(3): p. 333-40.
443. Hennekam, R.C., *Hutchinson-Gilford progeria syndrome: review of the phenotype*. Am J Med Genet A, 2006. **140**(23): p. 2603-24.
444. Ishimi, Y., et al., *Changes in chromatin structure during aging of human skin fibroblasts*. Exp Cell Res, 1987. **169**(2): p. 458-67.
445. Macieira-Coelho, A. and F. Puvion-Dutilleul, *Evaluation of the reorganization in the high-order structure of DNA occurring during cell senescence*. Mutat Res, 1989. **219**(3): p. 165-70.
446. Cattanaach, B.M., *Position effect variegation in the mouse*. Genet Res, 1974. **23**(3): p. 291-306.
447. Xue, Y., et al., *NURD, a novel complex with both ATP-dependent chromatin-remodeling and histone deacetylase activities*. Mol Cell, 1998. **2**(6): p. 851-61.
448. Pegoraro, G., et al., *Ageing-related chromatin defects through loss of the NURD complex*. Nat Cell Biol, 2009. **11**(10): p. 1261-7.
449. Pegoraro, G. and T. Misteli, *The central role of chromatin maintenance in aging*. Aging (Albany NY), 2009. **1**(12): p. 1017-22.
450. Lalani, S.R., et al., *CHARGE Syndrome*, in *GeneReviews*, R.A. Pagon, et al., Editors. 1993, University of Washington, Seattle: Seattle WA.
451. Egan, C.M., et al., *CHD5 Is Required for Neurogenesis and Has a Dual Role in Facilitating Gene Expression and Polycomb Gene Repression*. Dev Cell, 2013. **26**(3): p. 223-36.
452. Danzer, S.C., *Depression, stress, epilepsy and adult neurogenesis*. Exp Neurol, 2012. **233**(1): p. 22-32.
453. Wegiel, J., et al., *The neuropathology of autism: defects of neurogenesis and neuronal migration, and dysplastic changes*. Acta Neuropathol, 2010. **119**(6): p. 755-70.
454. Thatcher, K.N. and J.M. LaSalle, *Dynamic changes in Histone H3 lysine 9 acetylation localization patterns during neuronal maturation require MeCP2*. Epigenetics, 2006. **1**(1): p. 24-31.

Bibliography

455. Maussion, G., et al., *Convergent evidence identifying MAP/microtubule affinity-regulating kinase 1 (MARK1) as a susceptibility gene for autism*. Hum Mol Genet, 2008. **17**(16): p. 2541-51.
456. Jolley, A., et al., *De novo intragenic deletion of the autism susceptibility candidate 2 (AUTS2) gene in a patient with developmental delay: a case report and literature review*. Am J Med Genet A, 2013. **161**(6): p. 1508-12.
457. Kalscheuer, V.M., et al., *Mutations in autism susceptibility candidate 2 (AUTS2) in patients with mental retardation*. Hum Genet, 2007. **121**(3-4): p. 501-9.
458. Bozdagi, O., et al., *Haploinsufficiency of the autism-associated Shank3 gene leads to deficits in synaptic function, social interaction, and social communication*. Mol Autism, 2010. **1**(1): p. 15.